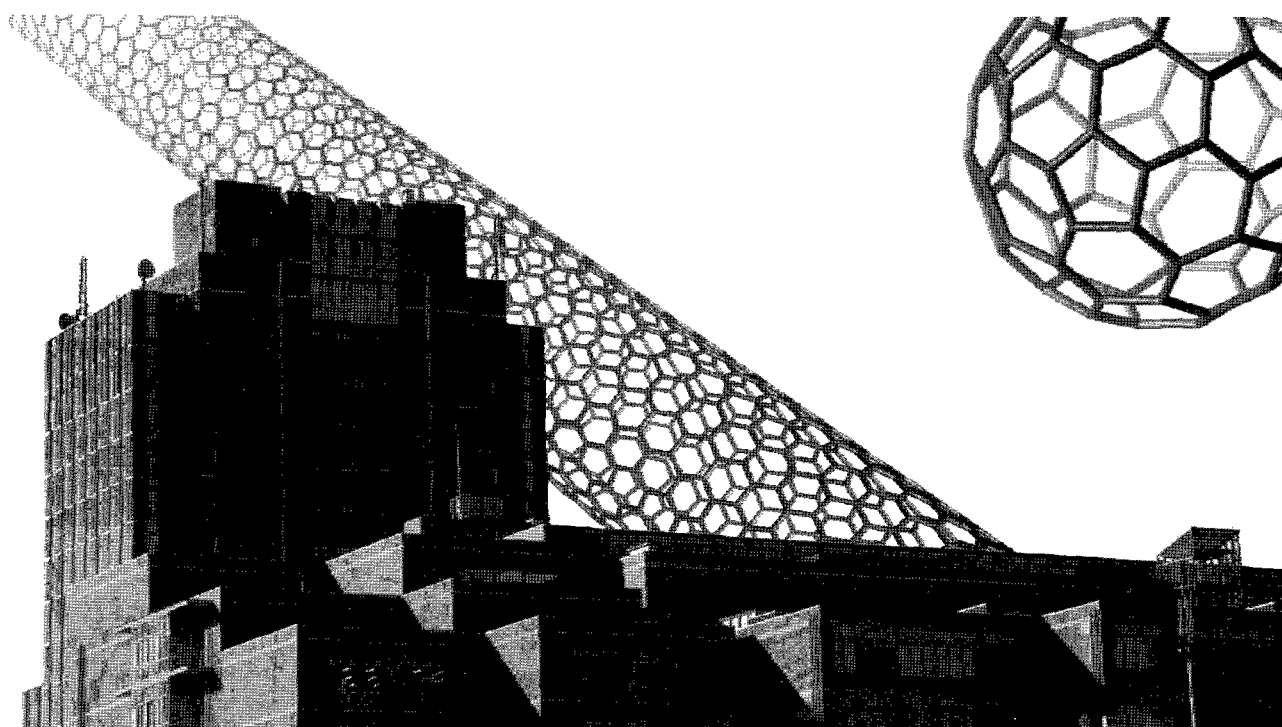


Abstract
The 36th Fullerene-Nanotubes General Symposium

第36回フラーレン・ナノチューブ
総合シンポジウム

講演要旨集



March 2-4, 2009 Nagoya, Aichi
平成21年3月2日～4日 名城大学

The Fullerenes and Nanotubes Research Society
フラーレン・ナノチューブ学会

材料科学研究でお困りのことはございませんか？

Material Matters™

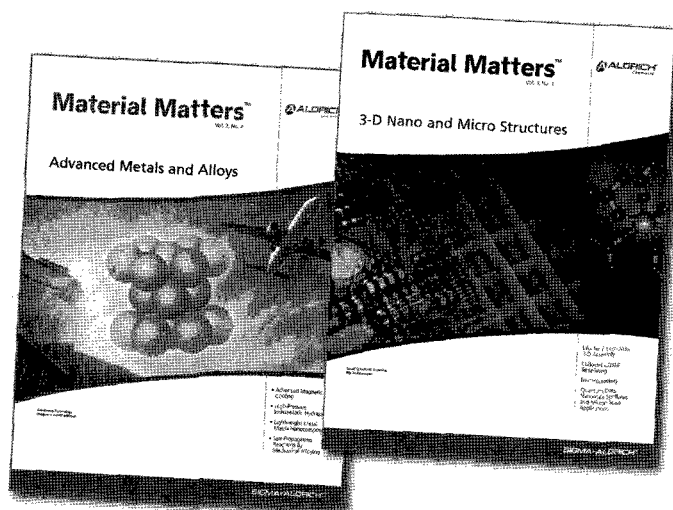
新規登録
募集中！

Aldrich がお届けする材料科学分野の季刊テクニカルニュースレターです。

各号毎のテーマにもとづいて、世界各国の第一線の研究者が研究結果やその分野の最新情報を執筆します。

既刊特集内容(カッコ内は号数)

- ナノ材料の応用最前線 (2-1)
- 水素貯蔵材料 (2-2)
- 有機エレクトロニクス (2-3)
- 先端金属および合金 (2-4)
- 3次元ナノおよびマイクロ構造 (3-1)
- ナノ規模表面改質 (3-2)
- 生体材料 (3-3)



定期送付のご登録は右記 URL から

<http://www.sigma-aldrich.co.jp/aldrich/mscatalog>



Materials Science 2008-2010 カタログ (英語)

材料科学研究に関する約 4,000 品目の製品を掲載しています。
研究室に 1 冊！ ご活用ください。

〈掲載項目〉

- ナノ材料
- 有機エレクトロニクス
- 高分子化学
- 代替エネルギー
- 金属およびセラミック科学
- マイクロ・ナノエレクトロニクス
- 書籍、実験器具類

SIGMA-ALDRICH®

シグマ アルドリッチ ジャパン株式会社
〒140-0002 東京都品川区東品川2-2-24
天王洲セントラルタワー4階

■ 製品に関するお問い合わせは、弊社テクニカルサポートへ
TEL : 03-5796-7330 FAX : 03-5796-7335
E-mail : sialjpts@sial.com

■ 在庫照会・ご注文方法に関するお問い合わせは、弊社カスタマーサービスへ
TEL : 03-5796-7320 FAX : 03-5796-7325
E-mail : sialjpcs@sial.com

<http://www.sigma-aldrich.com/japan>

Abstract
The 36th Fullerene-Nanotubes General Symposium

第 36 回 フラーレン・ナノチューブ
総合シンポジウム

講演要旨集

The Fullerenes and Nanotubes Research Society

The Chemical Society of Japan

The Japan Society of Applied Physics

The Physical Society of Japan

The Electrochemical Society of Japan

The Society of Polymer Science, Japan

主催：フラーレン・ナノチューブ学会

共催：日本化学会

協賛：日本物理学会・応用物理学会・電気化学会・高分子学会

Date: March 2nd(Mon)–4th(Wed), 2009

Place: Meijo University

1-501 Shiogamaguchi, Tempaku-ku, Nagoya 468-8502

TEL: 052-832-1151

Presentation: Special Lecture (25 min presentation, 5 min discussion)

General Lecture (10 min presentation, 5 min discussion)

Poster Preview (1 min presentation, no discussion)

日時：平成 21 年 3 月 2 日(月)～4 日(水)

場所：名城大学

〒468-8502 愛知県名古屋市天白区塩釜口 1-501

TEL：052-832-1151

発表時間：特別講演 (発表 25 分・質疑応答 5 分)

一般講演 (発表 10 分・質疑応答 5 分)

ポスタープレビュー (発表 1 分・質疑応答 なし)

展示団体御芳名(アイウエオ順、敬称略)

IOP英国物理学会出版局
アイクストロン(株)
エスケーバイオ・インターナショナル(株)
NPGネイチャーアジア・パシフィック
コスモ・バイオ(株)
(株)島津製作所
(株)セントラル科学貿易
東京ダイレック(株)
東洋炭素(株)
ナカライテスク(株)
日本電子(株)
(株)堀場製作所

広告掲載団体御芳名(アイウエオ順、敬称略)

アイクストロン(株)
(株)ATR
エクセルソフト(株)
エスケーバイオ・インターナショナル(株)
コスモ・バイオ(株)
シグマ アルドリッチ ジャパン(株)
(株)島津製作所
スペクトラ・フィジックス(株)
(株)セントラル科学貿易
東京ダイレック(株)
東洋炭素(株)
ナカライテスク(株)
日本電子(株)
日本分光(株)
日本分析工業(株)
(有)菱田商店
日立工機(株)
ブルカー・ダルトニクス(株)
フロンティアカーボン(株)
(株)フロンティア出版
(株)マシナックス
(株)UBE科学分析センター

Contents

Time Table	i
Chairperson	iii
Program	Japanese	iv
	English	xvi
Abstracts	Special Lecture	1
	General Lecture	7
	Poster Presentation	51
Author Index	171

目次

早見表	i
座長一覽	iii
プログラム	和文	iv
	英文	xvi
講演予稿	特別講演	1
	一般講演	7
	ポスター発表	51
発表索引	171

プログラム早見表

各項目敬称略

	3月2日(月)	3月3日(火)	3月4日(水)	
9:00	特別講演1(野田 優) 9:00~9:30	特別講演2(宮澤 薫一) 9:00~9:30	特別講演4(今堀 博) 9:00~9:30	9:00
9:30	一般講演4件 (ナノチューブの物性) 9:30~10:30	一般講演4件 (フラーレンの環境と安全評価・金属内包フラーレン) 9:30~10:30	一般講演4件 (ナノチューブの生成と精製) 9:30~10:30	9:30
10:30	休憩 10:30~10:45			10:30
10:45	一般講演4件 (ナノチューブの物性) 10:45~11:45	一般講演4件 (フラーレン固体とフラーレンの化学) 10:45~11:45	特別講演5(亘理 文夫) 10:45~11:15	10:45
11:45	昼食 11:45~13:00		一般講演5件 (ナノチューブの生成と精製) 11:15~12:30	11:15
13:00	一般講演5件 (ナノチューブの物性) 13:00~14:15	授賞式 13:00~13:30 特別講演3(山名 修一) 13:30~14:00	昼食 12:30~13:45 特別講演6(湯田坂 雅子) 13:45~14:15	12:30
14:15	休憩 14:15~14:30	一般講演4件 (ナノワイヤー) 14:00~15:00	ポスタープレビュー 1分×40件 14:15~14:55	13:45
14:30	一般講演5件 (ナノチューブの応用) 14:30~15:45	休憩 15:00~15:15	ポスターセッション 14:55~16:15	14:15
15:45	ポスタープレビュー 1分×40件 15:45~16:25	一般講演4件 (グラフェン・ナノ炭素粒子) 15:15~16:15		14:55
16:25	ポスターセッション 16:25~17:45	ポスタープレビュー 1分×40件 16:15~16:55	ポスターセッション 16:55~18:15	16:15
17:45				16:15

18:30~懇親会

特別講演 発表25分 質疑5分
一般講演 発表10分 質疑5分
ポスタープレビュー
発表1分 質疑なし

3月2日(月)
チュートリアル 103講義室
15:00~16:30
講師 丸山茂夫先生
東京大学大学院
工学系研究科 教授

TIME TABLE

	Mon. Mar. 2	Tue. Mar. 3	Wed. Mar. 4	
9:00	Special Lecture (S. Noda) 9:00~9:30	Special Lecture (K. Miyazawa) 9:00~9:30	Special Lecture (H. Imahori) 9:00~9:30	9:00
9:30	General Lecture[4] (Properties of Nanotubes) 9:30~10:30	General Lecture[4] (Environmental/Safety Characterization of Fullerenes and Endohedral Metallofullerenes) 9:30~10:30	General Lecture[4] (Formation and Purification of Nanotubes) 9:30~10:30	9:30
10:30	Break 10:30~10:45			10:30
10:45	General Lecture[4] (Properties of Nanotubes) 10:45~11:45	General Lecture[4] (Fullerene Solids and Chemistry of Fullerenes) 10:45~11:45	Special Lecture (F. Watari) 10:45~11:15	10:45
11:45	Lunch 11:45~13:00		General Lecture[5] (Formation and Purification of Nanotubes) 11:15~12:30	11:15
13:00	General Lecture[5] (Properties of Nanotubes) 13:00~14:15	Awards Ceremony 13:00~13:30	Lunch 12:30-13:45	12:30
14:15	Break 14:15~14:30	Special Lecture (S. Yamana) 13:30~14:00	Special Lecture (M. Yudasaka) 13:45~14:15	13:45
14:30	General Lecture[5] (Applications of Nanotubes) 14:30~15:45	General Lecture[4] (Nanowires) 14:00~15:00	Poster Preview 1min x [40] 14:15~14:55	14:15
15:45	Poster Preview 1min x [40] 15:45~16:25	Break 15:00~15:15	Poster Session 14:55-16:15	14:55
16:25	Poster Session 16:25~17:45	General Lecture[4] (Graphene and Carbon Nanoparticles) 15:15~16:15		16:15
17:45		Poster Preview 1min x [40] 16:15~16:55		16:15
		Poster Session 16:55~18:15		

18:30~ Banquet

Mon. Mar. 2
Tutorial Room103
15:00~16:30
Prof. Shigeo Maruyama

Special Lectures: 25min Presentation, 5min Discussion
 General Lectures: 10min Presentation, 5min Discussion
 Poster Previews: 1min Presentation, No Discussion

座長一覧

3月2日(月)

(敬称略)

	時 間	座 長
特 別 講 演(野田)	9:00 ~ 9:30	丸山 茂夫
一 般 講 演	9:30 ~ 10:30	岡崎 俊也
一 般 講 演	10:45 ~ 11:45	宮本 良之
一 般 講 演	13:00 ~ 14:15	齋藤 晋
一 般 講 演	14:30 ~ 15:45	大野 雄高
ポスターレビュー	15:45 ~ 16:25	北浦 良
ポスターセッション	16:25 ~ 17:45	藤ヶ谷 剛彦

3月3日(火)

	時 間	座 長
特 別 講 演(宮澤)	9:00 ~ 9:30	湯田坂 雅子
一 般 講 演	9:30 ~ 10:30	大澤 映二
一 般 講 演	10:45 ~ 11:45	若林 知成
特 別 講 演(山名)	13:30 ~ 14:00	篠原 久典
一 般 講 演	14:00 ~ 15:00	阿知波 洋次
一 般 講 演	15:15 ~ 16:15	河合 孝純
ポスターレビュー	16:15 ~ 16:55	前田 優
ポスターセッション	16:55 ~ 18:15	村上 陽一

3月4日(水)

	時 間	座 長
特 別 講 演(今堀)	9:00 ~ 9:30	中嶋 直敏
一 般 講 演	9:30 ~ 10:30	菅井 俊樹
特 別 講 演(亙理)	10:45 ~ 11:15	宮澤 薫一
一 般 講 演	11:15 ~ 12:30	齋藤 毅
特 別 講 演(湯田坂)	13:45 ~ 14:15	坂東 俊治
ポスターレビュー	14:15 ~ 14:55	小塩 明
ポスターセッション	14:55 ~ 16:15	田中 倫子

3月2日(月)

特別講演 発表25分・質疑応答5分
一般講演 発表10分・質疑応答5分
ポスタープレビュー 発表1分・質疑応答なし

特別講演(9:00-9:30)

- IS-1 コンビナトリアル手法による単層カーボンナノチューブ基板上成長の研究 1
○野田優

一般講演(9:30-10:30)

ナノチューブの物性

- 1-1 水分子内包単層カーボンナノチューブからの近赤外蛍光スペクトル 7
○千足昇平、花島干城、水戸部涼太、本間芳和
- 1-2 単層カーボンナノチューブの励起子遷移エネルギーの環境効果 8
○齋藤理一郎、佐藤健太郎、塩見淳一郎、丸山茂夫
- 1-3 単一カーボンナノチューブの低温磁気光学分光 9
○松永隆佑、松田一成、金光義彦
- 1-4 紫外領域における単層カーボンナノチューブの光学的性質 10
○高木祥光、岡田晋

☆☆☆☆☆☆ 休憩 (10:30-10:45) ☆☆☆☆☆☆

一般講演(10:45-11:45)

ナノチューブの物性

- 1-5 ドライブプロセスでフレキシブル基板上に作製したSWCNT超薄膜の電気・光学特性評価 11
○齋藤毅、ピカウシュクラ、湯村守雄、飯島澄男
- 1-6 ボロンドープ単層ナノチューブ薄膜における超伝導の圧力依存性 12
松平将治、○春山純志、中村仁、清水台生、江口豊明、西尾隆宏、長谷川幸雄、佐野浩孝、
家泰弘、J.Reppert、A.M.Rao
- 1-7 室温におけるカーボンナノチューブの電流-電圧特性評価 13
○東城友都、原智子、村本祥隆、横前拓也、林卓哉、金隆岩、遠藤守信
- 1-8 リモートプラズマCVDに合成された低温成長CNTのナノサイズビアにおける電気特性評価 14
○飯塚正知、石丸研太郎、横山大輔、岩崎孝之、由比藤勇、竹内輝明、佐藤信太郎、二瓶瑞久、
栗野祐二、川原田洋

☆☆☆☆☆☆ 昼食 (11:45-13:00) ☆☆☆☆☆☆

一般講演(13:00-14:15)

ナノチューブの物性

- 1-9 垂直配向単層カーボンナノチューブの熱伝導率の特性 15
○石川桂、田中三郎、宮崎康次、塩見淳一郎、丸山茂夫
- 1-10 ピーポッド構造と多層カーボンナノチューブの熱伝導における分子動力学シミュレーション 16
○西村史生、渡辺一之、山本貴博
- 1-11 分光電気化学測定による単層カーボンナノチューブの電子準位の直接決定 17
○田中泰彦、平兮康彦、中嶋直敏
- 1-12 非開口ナノチューブにおける自発分極 18
○大谷実、岡田晋
- 1-13 張力下におけるカーボンナノチューブへの水素吸着特性 19
○河合孝純、宮本良之

3月2日(月)

☆☆☆☆☆☆ 休憩 (14:15-14:30) ☆☆☆☆☆☆

一般講演(14:30-15:45)

ナノチューブの応用

- 1-14 低温下でのアザフラーレンC₅₉N内包単層カーボンナノチューブにおける光誘起電流の観測 20
○李永峰、金子俊郎、畠山力三
- 1-15 高純度半導体単層カーボンナノチューブを用いた薄膜トランジスタの性能向上 21
○藤井俊治郎、田中丈士、金赫華、宮田耕充、菅洋志、内藤泰久、三成剛生、宮寺哲彦、塚越一仁、片浦弘道
- 1-16 カーボンナノチューブ黒体：垂直配向SWNTによる高効率光吸収体 22
○水野耕平、石井順太郎、岸田英夫、早水祐平、保田諭、二葉ドン、湯村守雄、畠賢治
- 1-17 共鳴ラマン分光法によるカーボンナノチューブ/UV硬化性樹脂ナノコンポジットの分散性評価 23
○福丸貴弘、藤ヶ谷剛彦、中嶋直敏
- 1-18 カーボンナノチューブ/高分子ゲル複合体の近赤外光誘起相転移 24
○森本達郎、藤ヶ谷剛彦、中嶋直敏

ポスタープレビュー(15:45-16:25)

ポスターセッション(16:25-17:45)

ナノチューブの物性

- 1P-1 Molecular Geometry and Electronic Structure of Single Wall Carbon Nanotube in Non-equilibrium States 51
Somphob Thompho、Oraphan Saengsawang、Uthumporn Arsawang and ○Supot Hannongbua
- 1P-2 STMを用いた単層カーボンナノチューブの欠陥エンジニアリング 52
○海老根裕太、Maxime Berthe、吉田昭二、谷中淳、鈴木哲、住友弘二、武内修、重川秀実
- 1P-3 不純物置換したカーボンナノチューブの第一原理計算 53
○是常隆、斎藤晋
- 1P-4 圧力一定分子動力学法による直径の細い単層カーボンナノチューブの相転移研究 54
○櫻井誠大、斎藤晋
- 1P-5 ボロンドープカーボンナノチューブのマイクロ波CVD法による合成と評価 55
○渡邊徹、水口佳一、津田俊輔、山口尚秀、高野義彦
- 1P-6 多層カーボンナノチューブの低温磁気伝導における位相緩和現象の観測 56
○M. Kida、T. Hatori、Y. Nakamura、Y. Togashi、N. Aoki、J. P. Bird、Y. Ochiai
- 1P-7 二層カーボンナノチューブにおけるブリージングモードの温度依存性 57
○寛仁志、内藤亮治、蓮池紀幸、木曾田賢治、西尾弘司、一色俊之、播磨弘
- 1P-8 カーボンナノチューブの仕事関数 58
○加藤幸一郎、斎藤晋
- 1P-9 ボロンドープ単層カーボンナノチューブFETの電気特性 59
○清水台生、春山純志、佐野浩孝、家泰弘、江口豊明、西尾隆宏、長谷川幸雄、Jason Reppert、Aooarao Rao
- 1P-10 ラマン分光法によるCoMoCATナノチューブのレーザー照射と熱酸化の評価 60
○袴塚麻里、姜東哲、小島謙一、橘勝
- 1P-11 C₆₀(OH)_nによる単層カーボンナノチューブの分散 61
○前田優、加藤敬明、肥後淳基、長谷川正、土屋敬広、赤阪健、Jing Lu、永瀬茂

3月2日(月)

1P-12	温度勾配をもつカーボンナノチューブにおける質量輸送 ○志賀拓磨、高橋徹、E.R.Hernandez、渡辺一之	62
1P-13	半導体単層ナノチューブにおける欠陥状態のエネルギー準位 ○佐々木健一、若林克法、齋藤理一郎	63
1P-14	多層ナノチューブ断面における波状変形の機構解明 ○佐藤太裕、島弘幸	64
1P-15	電解質プラズマ中におけるイオン液体照射単層カーボンナノチューブの電気特性 ○廣津佑、金子俊郎、畠山力三	65
1P-16	トリフェニレン誘導体により溶液・固体中で安定に孤立分散した単層カーボンナノチューブの調製 ○山本竜広、加藤大	66
1P-17	単層カーボンナノチューブのラマン共鳴分光におけるGバンドスペクトル ○朴珍成、佐々木健一、齋藤理一郎、Gene Dresselhaus、Mildred S. Dresselhaus	67
1P-18	多層ナノチューブ・酸化ボロン混合体の水素雰囲気高温処理により作製される磁性多層ナノチューブ ○遠藤宏紀、坂東俊治、飯島澄男	68
1P-19	局所ゲート顕微鏡によるCNT-FETの電気特性評価 ○沖川侑揮、岸本茂、大野雄高、水谷孝	69
1P-20	ボロンドープ単層ナノチューブ薄膜におけるマイスナー効果の圧力依存性 ○中村仁、松平将治、春山純志、清水台生、江口豊明、西尾隆宏、長谷川幸雄、佐野浩孝、冢泰弘、J.Reppert、A.M.Rao	70
1P-21	カーボンナノチューブ・フォノンファイバーに関する分子動力学計算 ○山本貴博、西村史生、高橋徹、渡辺一之	71
1P-22	炭素ナノワイヤのエネルギー論と電子構造 ○岡田晋	72
内包ナノチューブ		
1P-23	ナノチューブとピーポッドのバルク構造解析のための実験室高分解能X線回折計 ○青柳忍、西堀英治、北浦良、澤博、坂田誠、篠原久典	73
1P-24	ナノチューブ内部での単層ナノチューブ成長 ○伊豆好史、塩見淳一郎、丸山茂夫	74
1P-25	第一原理計算による酸素内包単層カーボンナノチューブの電子状態予測 ○原田啓太郎、松田和之、真庭豊、手島正吾、中村壽	75
1P-26	単層カーボンナノチューブ内における水クラスターの誘電特性 ○三上史記、松田和之、真庭豊	76
1P-27	金属内包フラーレンピーポッド($Gd@C_{82}$) _n @SWCNTのSTM/STS測定 ○大橋一範、飯島祐樹、今津直樹、北浦良、篠原久典	77
1P-28	カルシウム原子内包による大気安定n型単層カーボンナノチューブトランジスタの作製 ○清水哲弘、加藤俊顕、大原渡、畠山力三	78
1P-29	Encapsulation of Room Temperature Ionic Liquid inside Single-Wall Carbon Nanotubes ○Shimou Chen、Ryo Kitaura、and Hisanori Shinohara	79

3月2日(月)

炭素ナノ粒子

- 1P-30 気相におけるポリイン類の電子スペクトルおよびフラグメンテーション 80
○山田武史、和田資子、若林知成、奥田晃史、生方正章
- 1P-31 溶液中におけるポリイン-ヨウ素錯体の形成 81
○和田資子、若林知成、長田良一、加藤立久
- 1P-32 熱処理によりランタンカーバイドを生成するフラーレン煤のキャラクタリゼーション 82
○山本和典、赤阪健
- 1P-33 アルコール蒸気を用いた高密度炭素アーク放電法による多面体グラファイト粒子の形成 83
○片桐洋次、小塩明、小海文夫

その他

- 1P-34 C₆₀-PANIとC₆₀-PTFE 複合フィルムの合成特性、構造と形状 84
ビクトル カザチェンコ、三重野哲、○イハル ラザナウ
- 1P-35 発煙硝酸を用いた新規SWNT官能基化 85
○北村啓、関戸大、竹内久人、大野正富
- 1P-36 鉄電極によるオリゴアセンへのスピン注入の理論研究 86
○加藤良隆、笛野博之、田中一義
- 1P-37 Density-functional tight-binding molecular dynamics simulations of the self-capping process in open-ended 87
(n,n) SWCNTs (n=3 to 10)
○Hironori Hara、Stephan Irle
- 1P-38 アルカリ土類金属-黒鉛層間化合物の作製と超伝導探索 88
○平郡諭、木全希、小林本忠
- 1P-39 イオン移動度測定のためのイオンRFデバイスの特性評価 89
○菅井俊樹
- 1P-40 グラファイトコーンの一次元配列を有する垂直配向カーボンナノファイバーの成長 90
○山崎貴之、小塩明、丹後佑太、今井智仁、小海文夫

3月3日(火)

特別講演 発表25分・質疑応答5分
一般講演 発表10分・質疑応答5分
ポスタープレビュー 発表1分・質疑応答なし

特別講演 (9:00-9:30)

- 2S-2 フラーレンナノマテリアルの合成と評価 2
○宮澤薫一

一般講演 (9:30-10:30)

フラーレンの環境と安全評価・金属内包フラーレン

- 2-1 フラーレンC₆₀のin vitro評価における影響要因の検討 25
○堀江祐範、西尾敬子、篠原直秀、加藤晴久、中村文子、藤田克英、衣笠晋一、遠藤茂寿、岩橋均、吉田康一、中西準子
- 2-2 フラーレンC₆₀のキャラクタリゼーションと細胞応答に関する検討 26
○西尾敬子、堀江祐範、篠原直秀、加藤晴久、中村文子、藤田克英、衣笠晋一、遠藤茂寿、岩橋均、吉田康一、中西準子
- 2-3 Sc₂C₈₂の構造決定と分子変換 27
○栗原広樹、山崎裕子、溝呂木直美、生沼みどり、土屋敬広、永瀬茂、赤阪健
- 2-4 Sc₂C₂@C₈₂ (II) の紫外光電子分光 28
○宮崎隆文、青木雄祐、徳本頌治、隅井良平、沖本治哉、梅本久、伊藤靖浩、篠原久典、日野照純

☆☆☆☆☆☆ 休憩 (10:30-10:45) ☆☆☆☆☆☆

一般講演 (10:45-11:45)

フラーレン固体とフラーレンの化学

- 2-5 PCBMに関連した界面における電子準位接続:PCBM/Ag基板・PCBM/フタロシアニン界面 29
○赤池幸紀、金井要、大内幸雄、関一彦
- 2-6 1次元ピーナツ型C₆₀ポリマーの朝永-Luttinger状態における幾何曲率効果 30
○島弘幸、吉岡英生、尾上順
- 2-7 水素分子内包C₆₀の物性 31
○熊代良太郎、良知健、村田靖次郎、小松紘一、澤博、小濱芳允、川路均、阿竹徹、谷垣勝己
- 2-8 カーボンオニオンからフラーレンへの簡単な生成機構 32
○尾形照彦、豊谷仁男

☆☆☆☆☆☆ 昼食 (11:45-13:00) ☆☆☆☆☆☆

授賞式 (13:00-13:30)

特別講演 (13:30-14:00)

- 2S-3 ライフサイエンス分野におけるフラーレンの事業展開 3
○山名修一

一般講演 (14:00-15:00)

ナノワイヤー

- 2-9 有機溶媒中における炭素粉末のレーザーアブレーションによるポリイン分子の生成機構 33
○若林知成、才川真央、和田資子
- 2-10 金ナノワイヤー内包単層カーボンナノチューブの合成とキャラクタリゼーション 34
○小林慶太、北浦良、篠原久典

3月3日(火)

- 2-11 半金属分子ナノワイヤ: 酸素分子内包カーボンナノチューブ 35
○田中倫子、河合孝純、岡田晋
- 2-12 高充填・長尺銅ナノワイヤー内包カーボンナノチューブ 36
○小塩明、鬼頭大信、中野寛之、藤原裕司、佐藤英樹、小海文夫

☆☆☆☆☆☆ 休憩 (15:00-15:15) ☆☆☆☆☆☆

一般講演 (15:15-16:15)

グラフェン・ナノ炭素粒子

- 2-13 ナノグラフェンの作製と化学修飾 37
○高井和之、西村康寛、榎敏明
- 2-14 ハーフメタリックなアームチェアグラフェンナノリボン 38
○澤田啓介、石井史之、斎藤峯雄
- 2-15 触媒膜厚制御によるカーボンナノチューブと多層グラフェンの選択成長 39
○近藤大雄、佐藤信太郎、二瓶瑞久、栗野祐二
- 2-16 一桁ナノバッキーダイヤモンド(SNBD)粒子表面上の多極静電ポテンシャル場が与える影響について 40
○大澤映二、何鼎、黄Houjin、コロボフ・ミハイル、ロシュコバ・ナタリア

ポスタープレビュー (16:15-16:55)

ポスターセッション (16:55-18:15)

ナノチューブの応用

- 2P-1 SiCの表面分解により合成された高配向CNTの電気二重層キャパシタへの応用 91
○加藤治夫、楠美智子、杉本重幸、杉原邦浩、山本信幸、藤田秀紀、柴田典義
- 2P-2 カーボンナノチューブ表面でのチトクロムcの電気化学的挙動 92
富永昌人、○山口裕之、坂本伸悟、西村敏史、金子詩織、谷口功
- 2P-3 In-situラマン分光電気化学測定法を用いたカーボンナノチューブの界面挙動解析 93
富永昌人、○坂本伸悟、西村敏史、谷口功
- 2P-4 NaClによる直径に依存しない単層カーボンナノチューブの酸化効果 94
小林雄樹、○佐野正人
- 2P-5 電界放出のためのカーボンファイバー上のカーボンナノチューブの成長 95
○張奉鎔、伊藤陽一、林靖彦、岸直希、徳永智春、松本英俊、福菌一幸、種村眞幸、谷岡明彦
- 2P-6 Direct Growth of Single-walled Carbon Nanotubes Films and Their Opto-electric Properties 96
○Huafeng Wang、Kaushik Ghosh、Zhenhua Li、Takahiro Maruyama、Sakae Inoue、Yoshinori Ando
- 2P-7 Optical properties of single-wall carbon nanotube-P3HT composites 97
○Ye Feng、Yasumitsu Miyata、Kiyoto Matsuishi、Hiromichi Kataura
- 2P-8 Ionization Vacuum Gauge with a Carbon Nanotube Field Electron Emitter Combined with a Shield Electrode 98
○劉華榮、中原仁、上村佐四郎、齋藤弥八
- 2P-9 アルキル鎖をコアに持つポリアミドアミンデンドリマーを用いた単層カーボンナノチューブの可分散化 99
○池内亮太、内田哲也、藤井達生、高田潤、高口豊

3月3日(火)

2P-10	電子顕微鏡用に向けたカーボンナノチューブ電界エミッタの電界放出特性 ○草野賢和、安坂幸師、中原仁、齋藤弥八	100
2P-11	フラロデンドロンを利用した炭酸カルシウム/単層カーボンナノチューブ複合体の作製 ○筒井徹、高口豊	101
2P-12	非定常短細線法によるCNTナノ流体の熱伝導率測定 ○森松武史、諸江将吾、高田保之、藤井丕夫、鈴木信三、河野正道	102
2P-13	単層カーボンナノチューブからの電界発光におけるゲート電圧依存性 ○日比野訓士、牧英之、佐藤徹哉、鈴木哲、小林慶裕	103
2P-14	カーボンナノチューブからの電界電子放出に及ぼす炭化水素ガス吸着の効果 ○山下徹也、安坂幸師、中原仁、齋藤弥八	104
2P-15	垂直配向SWNT膜の色素増感型太陽電池対極への応用 ○大川潤、エイナルソンエリック、塩見淳一郎、丸山茂夫	105
2P-16	Carbon nanotube growth on atomic force microscope cantilever by using liquid Co catalyst ○邱建超、吉村雅満、上田一之	106
2P-17	SWNTへの金属蒸着の分子動力学 ○松尾哲平、塩見淳一郎、丸山茂夫	107
2P-18	ラインパターンカーボンナノチューブ冷陰極の作製および特性評価 ○白鳥洋介、古市考次、野田優	108
2P-19	ポリベンズイミダゾール被覆化カーボンナノチューブからなる新規燃料電池触媒の開発 岡本稔、○藤ヶ谷剛彦、中嶋直敏	109
2P-20	単層カーボンナノチューブ膜の透明導電特性とその膜厚依存性 ○羽場英介、野田優	110
2P-21	Defects on Multi-walled Carbon Nanotubes by Cobalt Oxide ○金度賢、脇慶子	111
金属内包フラーレン		
2P-22	La@C ₈₂ 第三の異性体 ○久我秀徳、二川秀史、溝呂木直美、土屋敬広、生沼みどり、ズデネクスラニナ、赤阪健、与座健治、永瀬茂	112
2P-23	Molecular and Electronic Structures of Di-erbium and Di-erbium-carbide Metallofullerenes Er ₂ (C ₂)@C ₈₂ : Density Functional Theory Calculations ○Jian Wang、Stephan Irlle、Keiji Morokuma	113
2P-24	電子ビーム衝突電離生成イオン性異種フラーレンの選択照射 ○英洋平、金子俊郎、畠山力三、表研次、笠間泰彦	114
2P-25	走査型トンネル顕微鏡によるオクタンチオール自己組織化単分子膜上のLu@C ₈₂ の分子配向変化の観察 ○岩本全央、安武裕輔、梅本久、伊藤靖浩、沖本治哉、泉乃里子、篠原久典、真島豊	115
2P-26	金属内包フラーレンの保存方法の検討 ○菊地陽介、大場琢磨、山下冬子、高林康裕、小野吉弘、河地和彦、表研次、笠間泰彦、久保園芳博	116
フラーレンの化学		
2P-27	アミノフラーレン誘導体の合成及びナノコンポジットへの応用 ○関戸大、大野克磨、大山恭之、齋藤大介、熊谷進、武田光博、北村啓、大野正富	117

3月3日(火)

2P-28	Ultrasound-Assisted Cycloadditions of [70]Fullerene with Various 2-Azidoethyl per-O-Acetyl Glycosides Shinsook Yoon、Sung Ho Hwang、Sung Kyu Hong、○Jeong Ho Lee and Weon Bae Ko	118
2P-29	ジアステレオ選択的Diels-Alder反応により生成したフラロデンドロンのエナンチオマー分離 ○津川直樹、高橋宜大、高口豊	119
2P-30	カルバゾール五重付加型[60]フラーレン誘導体の合成と電気化学的および光電変換特性 ○中原勝正、松尾豊、中村栄一	120
2P-31	発光性および液晶性を示す十重付加型[60]フラーレン ○李昌治、松尾豊、中村栄一	121
2P-32	光スイッチング可能なナノキャパシタとしてのフラーレン自己組織化単分子膜 ○セバスチャンラッヒャー、坂本和子、松尾敬子、松尾豊、中村栄一	122
2P-33	パラジウム触媒によるフラーレンの分子変換 ○南保正和、森進、伊丹健一郎	123
フラーレンの応用		
2P-34	フラーレン誘導体C ₆₀ X ₂ の電子輸送特性 ○徳永健	124
2P-35	Preparation of Self-Assembled of α -D-Mannosyl Fullerene[C ₆₀] - Gold Nanoparticle Films Shinsook Yoon、Sung Ho Hwang、○Sung Kyu Hong、Jeong Ho Lee、Jung Mi Kim and Weon Bae Ko	125
フラーレンの生成、高次フラーレン		
2P-36	Synthesis and Structural Characterization of Nano-Peapods Encapsulating Higher Fullerenes by High-Resolution TEM ○Teguh Endah Saraswati、Naoki Imazu、Kazunori Ohashi、Yasuhiro Ito、Ryo Kitaura and Hisanori Shinohara	126
2P-37	シアノポリイン類NC ₇ HおよびNC ₉ HのNMRによるキャラクタリゼーション ○才川真央、若林知成	127
2P-38	イオン照射による窒素原子内包フラーレンN@C ₆₀ の製作 ○木下雅仁、若林知成	128
2P-39	Computational Study on the Stone-Wales Transformation of non-IPR C ₆₀ Fullerenes Jun Li、Ting Ren、○Xiang Zhao	129
2P-40	静電リングに蓄積したC ₆₀ ⁻ のレーザー合流実験 ○城丸春夫、後藤基、兒玉健、松本淳、阿知波洋次、間嶋拓也、田沼肇、東俊行、A.E.K. Sunden、K.Hansen	130

3月4日(水)

特別講演 発表25分・質疑応答5分
一般講演 発表10分・質疑応答5分
ポスタープレビュー 発表1分・質疑応答なし

特別講演 (9:00-9:30)

- 3S-4 フラーレン・カーボンナノチューブを用いた人工光合成系の構築 4
○今堀博

一般講演 (9:30-10:30)

ナノチューブの生成と精製

- 3-1 カーボンナノチューブの密度勾配遠心によるカイラリティ分離 41
○加藤雄一、新留康郎、中嶋直敏
- 3-2 ゼオライト表面から合成された単層カーボンナノチューブの直径・カイラリティ分布 42
○村上陽一、茂木堯彦、野田優、大久保達也、丸山茂夫
- 3-3 カイラリティ選択性の高い単層カーボンナノチューブの作成とその同定 43
○阿知波洋次、中山崇、井上亮人、大西侑気、児玉健、岡崎俊也
- 3-4 単層カーボンナノチューブのCVD合成における炭素源の分子構造の影響 44
○ピカウシユクラ、斎藤毅、湯村守雄、飯島澄男

☆☆☆☆☆☆ 休憩 (10:30-10:45) ☆☆☆☆☆☆

特別講演 (10:45-11:15)

- 3S-5 ナノチューブ・ナノパーティクルの生体反応性：機能性とリスクアセス 5
○亙理文夫

一般講演 (11:15-12:30)

ナノチューブの生成と精製

- 3-5 ウェット法による垂直配向単層SWNTのパターン合成 45
○項榮、エリック エイナルソン、塩見淳一郎、丸山茂夫
- 3-6 トップダウン・アプローチによるシリコン基板上での単層カーボンナノチューブの配向成長 46
○カルロ・オロフェオ、吾郷浩樹、吉原直記、辻正治
- 3-7 サブミリメートル長・単層カーボンナノチューブの流動層合成 47
○金 東榮、深井尋史、杉目恒志、長谷川馨、大沢利男、野田優
- 3-8 ラマン分光法による単層カーボンナノチューブの純度評価 48
○西出大亮、宮田耕充、柳和宏、田中丈士、片浦弘道
- 3-9 金属/半導体単層カーボンナノチューブ上ドデシル硫酸ナトリウム(SDS)の第一原理エネルギー計算 49
○大淵真理

☆☆☆☆☆☆ 昼食 (12:30-13:45) ☆☆☆☆☆☆

特別講演 (13:45-14:15)

- 3S-6 カーボンナノホーンを用いたドラッグデリバリー 6
○湯田坂雅子

ポスタープレビュー (14:15-14:55)

ポスターセッション (14:55-16:15)

3月4日(水)

ナノチューブの生成と精製

- 3P-1 高密度・高配向CNT膜へのSiドーピング 131
○丸山雄大、吉田健太、乗松航、楠美智子
- 3P-2 垂直配向単層カーボンナノチューブの分光評価 132
○エリック エイナルソン、項 榮、ティーラボン テウラキットセーリー、張 正宜、村上陽一、塩見淳一郎、丸山茂夫
- 3P-3 高真空ACCVD法を用いた単層カーボンナノチューブの低温合成 133
○山本洋平、岡部寛人、井上泰輝、エイナルソンエリック、渡辺誠、丸山茂夫
- 3P-4 密度勾配超遠心分離法による(6,5)ナノチューブの選択分離 134
○趙沛、村上陽一、項榮、エリック エイナルソン、塩見淳一郎、丸山茂夫
- 3P-5 孤立分散SWNTのカイラリティー特性に及ぼすOPOパルスレーザー照射のフルエンス効果 135
○田島勇、熊沢明、内田勝美、石井忠浩、矢島博文
- 3P-6 アセチレンからのカーボンナノチューブの低温成長 136
○白井聖、野田優
- 3P-7 アガロースゲルを用いた金属・半導体カーボンナノチューブの分離の進展 137
○田中丈士、金赫華、宮田耕充、藤井俊治郎、菅洋志、内藤泰久、三成剛生、宮寺哲彦、塚越一仁、片浦弘道
- 3P-8 レーザーアブレーションによるSWNT生成に対するレーザーパワーの影響 138
○手柴雅臣、若林知成
- 3P-9 ゼオライトに担持したFe-Sn触媒からの細線カーボンナノコイルの合成 139
○横田真志、須田善行、桶真一郎、滝川浩史、藤村洋平、山浦辰雄、伊藤茂生、植仁志、盛興昌勝
- 3P-10 密度勾配超遠心法を用いた単層カーボンナノチューブのカイラリティー分離 140
○上之菌佳也、内田勝美、石井忠浩、矢島博文
- 3P-11 水分添加の単層カーボンナノチューブの構造への影響 141
○吉原直記、吾郷浩樹、辻正治
- 3P-12 ディップペンナノリソグラフィーを用いたカーボンナノチューブ配線の作製法の開拓 142
○家弓尚子、藤ヶ谷剛彦、中嶋直敏
- 3P-13 多層グラフェンとナノチューブから成るカーボン複合構造体と金属電極界面でのTiC形成 143
○近藤大雄、佐藤信太郎、二瓶瑞久、池永英司、小島雅明、金正鎮、小林啓介、栗野祐二
- 3P-14 単層カーボンナノチューブ成長に関する理論計算 144
Jingshuang Dang、Weiwei Wang、○Xiang Zhao
- 3P-15 メスバウアー分光によるAl/SiO₂/Si基板上Fe触媒の挙動解析 145
○大島久純、島津智寛、シリーミラン、壬生攻
- 3P-16 拡散プラズマCVDによる単層カーボンナノチューブの直径制御 146
○黒田峻介、加藤俊顕、金子俊郎、畠山力三
- 3P-17 非磁性ナノ粒子からの単層カーボンナノチューブ成長における熱CVDとプラズマCVDの比較 147
○ゴラネビスゾーレ、加藤俊顕、金子俊郎、畠山力三
- 3P-18 高真空アルコールガスソース法による単層カーボンナノチューブ低温成長における酸化アルミニウムバッファ層の効果 148
○水谷芳裕、佐藤一徳、丸山隆浩、成塚重弥

3月4日(水)

- 3P-19 ガス圧調整によるアーク放電を用いたDWNTsの合成 149
○加藤勝弘、汪華鋒、趙新洛、井上栄、安藤義則
- 3P-20 孤立分散法を利用した、アーク放電法により作製された単層カーボンナノチューブの精製 150
○鈴木信三、原和人、藤田琢也、水澤崇志、岡崎俊也、阿知波洋次
- 3P-21 ナノチューブの無重力アーク合成におけるクラスター凝集過程のミー散乱測定 151
○三重野哲、譚国棟、薄葉州、古閑一憲、白谷正治

グラフェン

- 3P-22 Open and Closed Edges of Graphene Layers 152
○劉崢、末永和知、Peter J. F. Harris、飯島澄男
- 3P-23 高温加熱したYSZ (111)上でのC₆₀の熱分解によるカーボン系薄膜の作製 153
○野口卓也、島田敏宏、半澤明範、長谷川哲也
- 3P-24 微傾斜6H-SiC上エピタキシャル数層グラフェンの高温ラマン測定 154
○内藤亮治、鴨井督、笥仁志、蓮池紀幸、木曾田賢治、播磨弘、森田康平、田中悟、橋本明弘
- 3P-25 2層グラフェンにおける電極界面キャリア注入機構の観測 155
○氏家洋平、本岡正太郎、森本崇宏、デイビッド・K・フェリー、ジョナサン・P・バード、落合勇一
- 3P-26 ボロンナイトジェンナノリボンのエッジ状態 156
○Fawei Zheng、Ken-ichi Sasaki、Riichiro Saito、Wenhui Duan、Bing-Lin Gu
- 3P-27 ナノグラファイトリボンのエッジフォノンについて 157
○古川大、Zheng Fawei、齋藤理一郎
- 3P-28 パルス光照射によるグラファイト表面上の超高速構造変化: 第一原理時間依存計算によるアプローチ 158
○宮本良之

ナノホーン

- 3P-29 ナノホーン構造の詳細研究 159
入江路子、弓削亮太、飯島澄男、○湯田坂雅子
- 3P-30 集合体からの単一カーボンナノホーンの分離 160
○張民芳、飯島澄男、湯田坂雅子
- 3P-31 Plugs Formed by Hydrogen Peroxide Treatment at Holes of Carbon Nanohorns 161
○Jianxun Xu、Minfang Zhang、Sumio Iijima、Masako Yudasaka

フラーレン固体

- 3P-32 MgドープC₆₀のエピタキシャル成長と電気的特性評価 162
○名取雅人、小島信晃、鈴木秀俊、山口真史
- 3P-33 固体C₆₀の圧力誘起構造相転移 163
○山上雄一郎、斎藤晋
- 3P-34 光を照射したC₆₀の電気伝導特性 164
○千葉康人、都司一、上野岬、陳仕任、青木伸之、落合勇一
- 3P-35 脂肪族アミン類による[70]フラーレンの組織化挙動 165
○松岡健一、秋山毅、山田淳
- 3P-36 C₆₀ナノウィスカーの成長観察 166
○堀田賀洋子、宮澤薫一

3月4日(水)

- 3P-37 PMA 誘導した THP-1 細胞によるフラーレンナノウィスカーの取込み 167
○棚島真一、宮澤薫一、奥田順子、谷口彰良
- 3P-38 水分散性フラーレンウィスカー 168
○藤田泰彦、高口豊
- 3P-39 C₆₀ ナノファイバーの断面電子顕微鏡観察 169
○加藤良栄、宮澤薫一
- 3P-40 Cs₃C₆₀ の常温常圧下における光反射率測定 170
○高野琢、Alexey Y. Ganin、高林康裕、Matthew J. Rosseinsky、Kosmas Prassides、岩佐義宏

Monday, March 2nd

Special Lectures: 25 min (Presentation) + 5 min (Discussion)
General Lectures: 10 min (Presentation) + 5 min (Discussion)
Poster Previews: 1 min (Presentation), No Discussion

Special Lecture (9:00-9:30)

- 1S-1 SWCNT Growth on Substrates Studied by a Combinatorial Method 1
○*Suguru NODA*

General Lecture (9:30-10:30)

Properties of Nanotubes

- 1-1 Photoluminescence Spectra from SWNTs Encapsulating Water Molecules 7
○*Shohei Chiashi, Tateki Hanashima, Ryota Mitobe, Yoshikazu Homma*
- 1-2 Environmental effect on the exciton transition energy of single wall carbon nanotubes 8
○*Riichiro Saito, Kentaro Sato, Junichiro Shiomi, Shigeo Maruyama*
- 1-3 Low-Temperature Magneto-Optical Spectroscopy for Single SWNTs 9
○*Ryusuke Matsunaga, Kazunari Matsuda, Yoshihiko Kanemitsu*
- 1-4 Optical Properties of Single-Walled Carbon Nanotube in the UV Region 10
○*Yoshiteru Takagi, Susumu Okada*

☆☆☆☆☆☆ Coffee Break (10:30-10:45) ☆☆☆☆☆☆

General Lecture (10:45-11:45)

Properties of Nanotubes

- 1-5 Electronic and Optical Properties of SWCNT Thin Films Deposited on Flexible Substrates by Dry-Process 11
○*Takeshi Saito, Bikau Shukla, Motoo Yumura, Sumio Iijima*
- 1-6 Pressure dependence of superconductivity in thin films of boron-doped carbon nanotubes 12
M. Matsudaira, J. Haruyama, J. Nakamura, T. Shimizu, T. Eguchi, T. Nishio, Y. Hasegawa, H. Sano, Y. Iye, J. Reppert, A. M. Rao
- 1-7 Current-voltage Property Analysis of Carbon Nanotube at Room Temperature on Substrate 13
○*Tomohiro TOJO, Tomoko HARA, Yoshitaka MURAMOTO, Takuya YOKOMAE, Takuya HAYASHI, Yoong-Ahm KIM, Morinobu ENDO*
- 1-8 Electric characterization of CNTs grown in nanosized via interconnects at low temperatures by remote plasma CVD 14
○*M. Iizuka, K. Ishimaru, D. Yokoyama, T. Iwasaki, I. Yuito, T. Takeuchi, S. Sato, M. Nihei, Y. Awano, H. Kawarada*

☆☆☆☆☆☆ Lunch Time (11:45-13:00) ☆☆☆☆☆☆

General Lecture (13:00-14:15)

Properties of Nanotubes

- 1-9 Characterizing thermal conductivity of vertically-aligned single-walled carbon nanotube films 15
○*Kei Ishikawa, Saburo Tanaka, Koji Miyazaki, Junichiro Shiomi, Shigeo Maruyama*
- 1-10 Molecular-Dynamics Simulations on Thermal Transport in Peapod and Multi-Walled Carbon Nanotube 16
○*Fumio Nishimura, Kazuyuki Watanabe, Yamamoto Takahiro*
- 1-11 Direct Determined Precise Electronic States of Single-Walled Carbon Nanotubes 17
○*Yasuhiko Tanaka, Yasuhiko Hirana, Naotoshi Nakashima*
- 1-12 Intrinsic Electron Dipoles in Capped Carbon Nanotubes 18
○*Minoru Otani, Susumu Okada*

Monday, March 2nd

- 1-13 Hydrogen Adsorption on Carbon Nanotubes under Tensile Strains 19
○Takazumi Kawai, Yoshiyuki Miyamoto

☆☆☆☆☆☆ Coffee Break (14:15-14:30) ☆☆☆☆☆☆

General Lecture (14:30-15:45)

Applications of Nanotubes

- 1-14 Observation of Photoinduced Current in Azafullerene C₅₉N Encapsulated Single-Walled Carbon Nanotubes at Low Temperatures 20
○Yongfeng Li, Toshiro Kaneko, Rikizo Hatakeyama
- 1-15 Improvement of the performance of CNT thin-film transistor by using high purity semiconducting SWCNTs 21
○Shunjiro Fujii, Takeshi Tanaka, Hehua Jin, Yasumitsu Miyata, Hiroshi Suga, Yasuhisa Naitoh, Takeo Minari, Tetsuhiko Miyadera, Kazuhito Tsukagoshi, Hiromichi Kataura
- 1-16 Carbon Nanotube Black Body: Highly Efficient Light Absorber by Vertically Aligned Single Walled Carbon Nanotubes 22
○Kohei Mizuno, Juntaro Ishii, Hideo Kishida, Yuhei Hayamizu, Satoshi Yasuda, Don N Futaba, Motoo Yumura, Kenji Hata
- 1-17 Evaluation of dispersion state of carbon nanotubes/UV-curable resin nanocomposites by resonance Raman spectroscopy 23
○Takahiro Fukumaru, Tsuyohiko Fujigaya, Naotoshi Nakashima
- 1-18 NIR-Triggered Volume Phase Transition of Carbon Nanotubes / Polymer Gel Composite 24
○Tatsuro Morimoto, Tsuyohiko Fujigaya, Naotoshi Nakashima

Poster Preview (15:45-16:25)

Poster Session (16:25-17:45)

Properties of Nanotubes

- 1P-1 Molecular Geometry and Electronic Structure of Single Wall Carbon Nanotube in Non-equilibrium States 51
Somphob Thompho, Oraphan Saengsawang, Uthumporn Arsawang and ○Supot Hannongbua
- 1P-2 Defect creation and annihilation of Single-Walled Carbon Nanotubes with Scanning Tunneling Microscopy 52
○Yuta Ebine, Maxime Berthe, Shoji Yoshida, Atsushi Taninaka, Satoru Suzuki, Koji Sumitomo, Osamu Takeuchi, Hidemi Shigekawa
- 1P-3 First principles study of substitutional impurities in carbon nanotubes 53
○Takashi Koretsune, Susumu Saito
- 1P-4 Constant-Pressure Molecular Dynamics Study of Single-Walled Carbon Nanotubes with a Small Diameter 54
○Masahiro Sakurai and Susumu Saito
- 1P-5 Microwave plasma CVD synthesis and characterization of boron-doped carbon nanotubes 55
○Tohru Watanabe, Yoshikazu Mizuguchi, Shunsuke Tsuda, Takahide Yamaguchi, Yoshihiko Takano
- 1P-6 Phase Breaking in Low Temperature Magneto-resistance of Thin Multi-Walled Carbon Nanotubes 56
○M. Kida, T. Hatori, Y. Nakamura, Y. Togashi, N. Aoki, J. P. Bird, Y. Ochiai
- 1P-7 Temperature dependence of radial breathing modes in double walled carbon nanotubes 57
○Hitoshi Kakehi, Ryoji Naito, Noriyuki Hasuike, Kenji Kisoda, Koji Nishio, Toshiyuki Issiki, Hiroshi Harima
- 1P-8 Work Function of Single-Walled Carbon Nanotube 58
○Koichiro Kato, Susumu Saito
- 1P-9 Electrical features of FETs using boron-doped single-walled carbon nanotubes 59
○T. Shimizu, J. Haruyama, H. Sano, Y. Iye, T. Eguchi, T. Nishio, Y. Hasegawa, J. Reppert, A. M. Rao

Monday, March 2nd

1P-10	Effects of laser irradiation and thermal oxidation on CoMoCAT nanotubes Probed by Raman spectroscopy ○ <i>Mari Hakamatsuka, Dongchul Kang, Kenichi Kojima, Masaru Tachibana</i>	60
1P-11	$C_{60}(OH)_n$ Assisted Dispersion of Single-walled Carbon Nanotubes ○ <i>Yutaka Maeda, Takaaki Kato, Junki Higo, Tadashi Hasegawa, Takahiro Tsuchiya, Takeshi Akasaka, Jing Lu, Shigeru Nagase</i>	61
1P-12	Molecular-Dynamics Simulations on Phonon-Assisted Mass Transport in Carbon Nanotubes ○ <i>Takuma Shiga, Toru Takahashi, Eduardo R. Hernandez and Kazuyuki Watanabe</i>	62
1P-13	Energy level of defect-induced state in semiconducting single wall carbon nanotube ○ <i>Ken-ichi Sasaki, Katsunori Wakabayashi, Riichiro Saito</i>	63
1P-14	Mechanism of Radial Corrugation in Many-Walled Carbon Nanotubes ○ <i>Motohiro Sato, Hiroyuki Shima</i>	64
1P-15	Electrical Characteristics of Single-Walled Carbon Nanotubes Irradiated with Ionic Liquids in Electrolyte Plasmas ○ <i>Yu Hirotsu, Toshiro Kaneko, Rikizo Hatakeyama</i>	65
1P-16	Individually dispersed single-walled carbon nanotubes in both liquid and dried solid states using a new dispersant ○ <i>Tatsuhiko Yamamoto, Masaru Kato</i>	66
1P-17	G band resonance Raman spectra of single-wall carbon nanotubes ○ <i>Jin Sung Park, Kenich Sasaki, Riichiro Saito, Gene Dresselhaus, Mildred S. Dresselhaus</i>	67
1P-18	Magnetic attractive multiwalled carbon nanotubes formed by high temperature treatment of multiwalled carbon nanotube/boric-oxide composite in hydrogen environment ○ <i>Hiroki Endo, Shunji Bandow, Sumio Iijima</i>	68
1P-19	Characterization of CNT-FET by Scanning Gate Microscopy ○ <i>Yuki Okigawa, Shigeru Kishimoto, Yutaka Ohno, Takashi Mizutani</i>	69
1P-20	Pressure dependence of Meissner effect in thin films of boron-doped carbon nanotubes ○ <i>J. Nakamura, M. Matsudaira, J. Haruyama, T. Shimizu, T. Eguchi, T. Nishio, Y. Hasegawa, H. Sano, Y. Iye, J. Reppert, A. M. Rao</i>	70
1P-21	Molecular-Dynamics Simulations on Carbon-Nanotube Phonon Fiber ○ <i>Takahiro Yamamoto, Fumio Nishimura, Toru Takahashi, Kazuyuki Watanabe</i>	71
1P-22	Energetics and Electronic Structures of Carbon Nanowires ○ <i>Susumu Okada</i>	72
Endohedral Nanotubes		
1P-23	A high-resolution laboratory x-ray diffractometer for the bulk structure analysis of nanotubes and peapods ○ <i>Shinobu Aoyagi, Eiji Nishibori, Ryo Kitaura, Hiroshi Sawa, Makoto Sakata and Hisanori Shinohara</i>	73
1P-24	Nucleation of an SWNT inside a carbon nanotube ○ <i>Yoshifumi Izu, Junichiro Shiomi and Shigeo Maruyama</i>	74
1P-25	First principles calculations of electronic states in SWCNTs encapsulating oxygen molecules ○ <i>Keitaro Harada, Kazuyuki Matsuda, Yutaka Maniwa, Syogo Tejima, Hisashi Nakamura</i>	75
1P-26	Dielectric properties of water clusters inside SWCNTs ○ <i>Fuminori Mikmai, Kazuyuki Matuda, Yutaka Maniwa</i>	76

Monday, March 2nd

- 1P-27 Scanning Tunneling Microscopy/Spectroscopy on the Electronic Structure of Metallofullerene Peapods (Gd@C₈₂)_n@SWCNTs 77
○Kazunori Ohashi, Yuki Iijima, Naoki Imazu, Ryo Kitaura, Hisanori Shinohara
- 1P-28 Fabrication of the air stable n-type single-walled carbon nanotube transistor based on calcium atoms encapsulation 78
○Tetsuhiro Shimizu, Toshiaki Kato, Wataru Oohara, Rikizo Hatakeyama
- 1P-29 Encapsulation of Room Temperature Ionic Liquid inside Single-Wall Carbon Nanotubes 79
○Shimou Chen, Ryo Kitaura, and Hisanori Shinohara

Carbon nanoparticles

- 1P-30 Electronic spectra and fragmentation of polyynes in the gas phase 80
○Takeshi Yamada, Yoriko Wada, Tomonari Wakabayashi, Koji Okuda, Masa-aki Ubukata
- 1P-31 Formation of polyyne-iodine complexes in solutions 81
○Yoriko Wada, Tomonari Wakabayashi, Ryoichi Osada, Tatsuhisa Kato
- 1P-32 Characterization of La fullerene soot and formation of LaC₂ containing multi-shell carbon nanocapsules by heat treatment 82
○Kazunori Yamamoto, Takeshi Akasaka
- 1P-33 Formation of Polyhedral Graphite Particles by High-density Carbon Arc Discharge with Alcohol Vapor 83
○Yoji Katagiri, Akira Koshio, Fumio Kokai

Miscellaneous

- 1P-34 Formation Peculiarities, Structure and Morphology of C₆₀-PANI and C₆₀-PTFE Thin Composite Films 84
Victor Kazachenko, Tetsu Mieno, ○Ihar Razanau
- 1P-35 New Method of Sidewall Functionalization of SWNT with Fuming Nitric Acid 85
○Hiroshi Kitamura, Masaru Sekido, Hisato Takeuchi, Masatomi Ohno
- 1P-36 Theoretical Study of Spin Injection from Fe into Oligoacene 86
○Yoshitaka Kato, Hiroyuki Fueno, Kazuyoshi Tanaka
- 1P-37 Density-functional tight-binding molecular dynamics simulations of the self-capping process in open-ended (n,n) SWCNTs (n=3 to 10) 87
○Hironori Hara, Stephan Irle
- 1P-38 Synthesis and Search for Superconductivity of Alkaline Earth Graphite Intercalation Compounds 88
○Satoshi Heguri, Kimata Nozomu, Mototada Kobayashi
- 1P-39 Studies on Ion RF Devices for Ion Mobility Measurement 89
○Toshiki Sugai
- 1P-40 Growth of One-dimensional Array of Graphitic Cones in Vertically Aligned Carbon Nanofibers 90
○Takayuki Yamasaki, Akira Koshio, Yuta Tango, Tomohito Imai, Fumio Kokai

Tuesday, March 3rd

Special Lectures: 25 min (Presentation) + 5 min (Discussion)
General Lectures: 10 min (Presentation) + 5 min (Discussion)
Poster Previews: 1 min (Presentation), No Discussion

Special Lecture (9:00-9:30)

- 2S-2 Synthesis and properties of fullerene nanowhiskers and related fullerene nanomaterials 2
○*Kun'ichi Miyazawa*

General Lecture (9:30-10:30)

Environmental/Safety Characterization of Fullerenes and Endohedral

- 2-1 Examination of the factors affecting in vitro evaluation of cellular responses induced by fullerene C₆₀ 25
○*Masanori Horie, Keiko Nishio, Naohide Shinohara, Haruhisa Kato, Ayako Nakamura, Katsuhide Fujita, Shinichi Kinugasa, Shigehisa Endoh, Hitoshi Iwahashi, Yasukazu Yoshida and Junko Nakanishi*
- 2-2 Detailed characterization of cellular responses induced by fullerene C₆₀ 26
○*Keiko Nishio, Masanori Horie, Naohide Shinohara, Haruhisa Kato, Ayako Nakamura, Katsuhide Fujita, Shinichi Kinugasa, Shigehisa Endoh, Hitoshi Iwahashi, Yasukazu Yoshida, Junko Nakanishi*
- 2-3 Structure determination and chemical functionalization of metallofullerene Sc₂C₈₂ 27
○*Hiroki Kurihara, Yuko Yamazaki, Naomi Mizorogi, Midori O. Ishitsuka, Takahiro Tsuchiya, Shigeru Nagase, Takeshi Akasaka*
- 2-4 Ultraviolet Photoelectron Spectroscopy of Sc₂C₂@C₈₂ (II) 28
○*Takafumi Miyazaki, Yuusuke Aoki, Youji Tokumoto, Ryohei Sumii, Haruya Okimoto, Hisashi Umemoto, Yasuhiro Ito, Hisanori Shinohara, Shojun Hino*

☆☆☆☆☆☆ Coffee Break (10:30-10:45) ☆☆☆☆☆☆

General Lecture (10:45-11:45)

Fullerene solids and Chemistry of Fullerenes

- 2-5 Energy Level Alignment of Interfaces Related to PCBM: PCBM/Ag Substrate, PCBM/Phthalocyanines 29
○*Kouki Akaike, Kaname Kanai, Yukio Ouchi, Kazuhiko Seki*
- 2-6 Geometric curvature effects on Tomonaga-Luttinger states of one-dimensional peanut-shaped C₆₀ polymers 30
○*Hiroyuki Shima, Hideo Yoshioka, Jun Onoe*
- 2-7 Physical Properties of Hydrogen-molecule Endohedral C₆₀ 31
○*Ryotaro Kumashiro, Takeshi Rachi, Yasujiro Murata, Koichi Komatsu, Hiroshi Sawa, Yoshimitsu Kohama, Hitoshi Kawaji, Tooru Atake, Katsumi Tanigaki*
- 2-8 A Simple Formation Mechanism of a Fullerene from a Carbon Onion 32
○*Terihiko Ogata, Yoshio Tatamitani*

☆☆☆☆☆☆ Lunch Time (11:45-13:00) ☆☆☆☆☆☆

Awards Ceremony (13:00-13:30)

Special Lecture (13:30-14:00)

- 2S-3 Business Development of Fullerenes in Life Science Applications 3
○*Shuichi Yamana*

General Lecture (14:00-15:00)

Nanowires

- 2-9 Formation mechanism of polyyne molecules upon laser ablation of carbon particles in organic solvents 33
○*Tomonari Wakabayashi, Mao Saikawa, Yoriko Wada*

Tuesday, March 3rd

- 2-10 Synthesis and Characterization of Crystalline Gold Nanowires encapsulated within Single-Wall Carbon Nanotubes 34
○Keita Kobayashi, Ryo Kitaura, Hisanori Shinohara
- 2-11 Semimetallic Molecular Nanowire: Oxygen Molecules Encapsulated into Carbon Nanotubes 35
○Michiko Tanaka, Takazumi Kawai, Susumu Okada
- 2-12 Long Continuous Copper Nanowires Encapsulated in Carbon Nanotubes 36
○Akira Koshio, Hironobu Kito, Hiroyuki Nakano, Yuji Fujiwara, Hideki Sato, Fumio Kokai

☆☆☆☆☆☆ Coffee Break (15:00-15:15) ☆☆☆☆☆☆

General Lecture(15:15-16:15)

Graphene and Carbon Nanoparticles

- 2-13 Fabrication and Chemical modification of Nanographene 37
○Kazuyuki Takai, Yasuhiro Nishimura, Toshiaki Enoki
- 2-14 Half-metallic Armchair Graphene Nanoribbon 38
○Keisuke Sawada, Fumiyuki Ishii, Mineo Saito
- 2-15 Selective synthesis of carbon nanotubes and graphene multi-layers by controlling catalyst thickness 39
○Daiyu Kondo, Shintaro Sato, Mizuhisa Nihei, Yuji Awano
- 2-16 Cosequences of multi-pole electrostatic potential fields on the surface of single-nano buckydiamond (SNBD) particles 40
○Eiji Osawa, Dean Ho, Houjin Huang, Michail Korobov, Natalia Rozhkova

Poster Preview(16:15-16:55)

Poster Session(16:55-18:15)

Applications of Nanotubes

- 2P-1 Application of vertically well-aligned CNT films to capacitors 91
○Haruo Kato, Michiko Kusunoki, Shigeyuki Sugimoto, Kunihiro Sugihara, Nobuyuki Yamamoto, Hideki Hujita, Noriyoshi Shibata
- 2P-2 Electrochemical Behaviors of Cytochrome c at Carbon Nanotube Surfaces 92
Masato Tominaga, ○Hiroyuki Yamaguchi, Shingo Sakamoto, Toshifumi Nishimura, Shiori Kaneko, Isao Taniguchi
- 2P-3 Analysis of interfacial behaviors of carbon nanotubes using in-situ Raman spectroelectrochemistry 93
Masato Tominaga, ○Shingo Sakamoto, Toshifumi Nishimura, Isao Taniguchi
- 2P-4 Diameter-Independent Thermal Oxidation of Single-Walled Carbon Nanotubes with NaCl under Microwave Heating 94
Yuki Kobayashi, ○Masahito Sano
- 2P-5 Growth of Carbon Nanotubes on Flexible Carbon Fiber Sheet for Field Emitter 95
○Bongyong Jang, Yoichi Ito, Yasuhiko Hayashi, Naoki Kishi, Tomoharu Tokunaga, Hidetoshi Matsumoto, Kazuyuki Fukuzono, Masaki Tanemura, Akihiko Tanioka, Gehan A.J. Amaratunga
- 2P-6 Direct Growth of Single-walled Carbon Nanotubes Films and Their Opto-electric Properties 96
○Huaqiang Wang, Kaushik Ghosh, Zhenhua Li, Takahiro Maruyama, Sakae Inoue, Yoshinori Ando
- 2P-7 Optical properties of single-wall carbon nanotube-P3HT composites 97
○Ye Feng, Yasumitsu Miyata, Kiyoto Matsuishi, Hiromichi Kataura
- 2P-8 Ionization Vacuum Gauge with a Carbon Nanotube Field Electron Emitter Combined with a Shield Electrode 98
○Huarong Liu, Hitoshi Nakahara, Sashiro Uemura, Yahachi Saito

Tuesday, March 3rd

2P-9	Dispersion of Single-Walled Carbon Nanotubes Using Poly(amidoamine) Dendrimer Having Alkyl Chain at the Core ○Ryouta Ikeuchi, Tetsuya Uchida, Tatsuo Fujii, Jun Takada, Yutaka Takaguchi	99
2P-10	Field Emission of Carbon Nanotubes for Electron Microscopes ○Yoshikazu Kusano, Koji Asaka, Hitoshi Nakahara, Yahachi Saito	100
2P-11	Fabrication of CaCO ₃ /SWNT Nanocomposite Using Fullerodendron-Assisted Approach ○Akira Tsutsui, Yutaka Takaguchi	101
2P-12	Measurement of Thermal Conductivity of CNT-nanofluids by Transient Short-Wire Method ○Takeshi Morimatsu, Shogo Moroe, Yasuyuki Takata, Motoo Fujii, Shinzo Suzuki, Masamichi Kohno	102
2P-13	Gate voltage dependence of electroluminescence from single-walled carbon nanotubes ○Norihito Hibino, Hideyuki Maki, Tetsuya Sato, Satoru Suzuki, Yoshihiro Kobayashi	103
2P-14	Study on Hydrocarbon Adsorption on MWNTs Using Field Emission Microscopy (FEM) ○Tetsuya Yamashita, Koji Asaka, Hitoshi Nakahara, Yahachi Saito	104
2P-15	Application of Vertically-Aligned SWNT Films to the Counter Electrode of Dye-Sensitized Solar Cells ○Jun Okawa, Erik Einarsson, Junichiro Shiomi, Shigeo Maruyama	105
2P-16	Carbon nanotube growth on atomic force microscope cantilever by using liquid Co catalyst ○Chien-Chao Chiu, Masamichi Yoshimura, Kazuyuki Ueda	106
2P-17	A molecular dynamics study of metal coating on SWNT ○Tepei Matsuo, Junichiro Shiomi, Shigeo Maruyama	107
2P-18	Line-Patterned Carbon Nanotube Cold Cathodes ○Yosuke Shiratori, Koji Furuichi, Suguru Noda	108
2P-19	New electrocatalyst for PEFC based on carbon nanotubes wrapped by polybenzimidazole Minoru Okamoto, ○Tsuyohiko Fujigaya, Naotoshi Nakashima	109
2P-20	Transparent conducting properties of SWCNT films at a range of thickness ○Eisuke Haba, Suguru Noda	110
2P-21	Defects on Multi-walled Carbon Nanotubes by Cobalt Oxide ○Do-Hyun Kim, Keiko Waki	111
Endohedral Metallofullerenes		
2P-22	Third Isomer of La@C ₈₂ ○Hidenori Kuga, Hidehumi Nikawa, Naomi Mizorogi, Takahiro Tuchiya, Midori Oinuma, Slanina Zdenek, Takeshi Akasaka, Kenji Yoza, Shigeru Nagase	112
2P-23	Molecular and Electronic Structures of Di-erbium and Di-erbium-carbide Metallofullerenes Er ₂ (C ₂)@C ₈₂ : Density Functional Theory Calculations ○Jian Wang, Stephan Irle, Keiji Morokuma	113
2P-24	Selective Irradiation of Ionic Heterogeneous Fullerenes Generated by Electron Beam Impact Ionization ○Yohei Hanabusa, Toshiro Kaneko, Rikizo Hatakeyama, Kennji Omote, Yasuhiko Kasama	114
2P-25	Change in Molecular Orientation of Individual Lu@C ₈₂ on Octanethiol Self Assembled Monolayer Observed by Scanning Tunneling Microscopy ○Masachika Iwamoto, Yuhsuke Yasutake, Hisashi Umemoto, Yasuhiro Ito, Haruya Okimoto, Noriko Izumi, Hisanori Shinohara, Yutaka Majima	115

Tuesday, March 3rd

- 2P-26 Storage Condition of Metallofullerene 116
○Yosuke Kikuchi, Takuma Ooba, Fuyuko Yamashita, Yasuhiro Takabayashi, Yoshihiro Ono, Kazuhiko Kawachi, Kenji Omote, Yasuhko Kasama, Yoshihiro Kubozono

Chemistry of Fullerenes

- 2P-27 Synthesis of Amino Fullerene Derivative and its Application for PA-6 Nanocomposites 117
○Masaru Sekido, Katsuma Ohno, Yasuyuki Ohyama, Daisuke Saitou, Susumu Kumagai, Mitsuhiro Takeda, Hiroshi Kitamura, Masatomi Ohno
- 2P-28 Ultrasound-Assisted Cycloadditions of [70]Fullerene with Various 2-Azidoethyl per-O-Acetyl Glycosides 118
Shinsook Yoon, Sung Ho Hwang, Sung Kyu Hong, ○Jeong Ho Lee and Weon Bae Ko
- 2P-29 Enantiomeric Separation of Fulleredendron Formed by Diastereoselective Diels-Alder Reaction 119
○Naoki Tsugawa, Nobuhiro Takahashi, Yutaka Takaguchi
- 2P-30 Syntheses, Electrochemical and Photocurrent-Generating Properties of Penta(carbazolyl)[60]fullerene Derivatives 120
○Katsumasa Nakahara, Yutaka Matsuo, Eiichi Nakamura
- 2P-31 Luminescent and Liquid Crystalline Deca(organo)[60]Fullerenes 121
○Chang-Zhi Li, Yutaka Matsuo, Eiichi Nakamura
- 2P-32 Fullerene Self-Assembled Monolayer as a Nano Capacitor Switchable by Light 122
○Sebastian Lacher, Aiko Sakamoto, Keiko Matsuo, Yutaka Matsuo, Eiichi Nakamura
- 2P-33 Fullerene Functionalization through Palladium Catalysis 123
○Masakazu Nambo, Susumu Mori, Kenichiro Itami

Function and Applications of Fullerenes

- 2P-34 Electron-Transport Property of Fullerene Derivatives $C_{60}X_2$ 124
○Ken Tokunaga
- 2P-35 Preparation of Self-Assembled of α -D-Mannosyl Fullerene[C_{60}] - Gold Nanoparticle Films 125
Shinsook Yoon, Sung Ho Hwang, ○Sung Kyu Hong, Jeong Ho Lee, Jung Mi Kim and Weon Bae Ko

Fullerene Formation, Higher Fullerenes

- 2P-36 Synthesis and Structural Characterization of Nano-Peapods Encapsulating Higher Fullerenes by High-Resolution TEM 126
○Teguh Endah Saraswati, Naoki Imazu, Kazunori Ohashi, Yasuhiro Ito, Ryo Kitaura and Hisanori Shinohara
- 2P-37 NMR characterization of cyanopolyynes NC_7H and NC_9H 127
○Mao Saikawa, Tomonari Wakabayashi
- 2P-38 Production of atomic nitrogen-doped fullerene $N@C_{60}$ by ion bombardment 128
○Masahito Kinoshita, Tomonari Wakabayashi
- 2P-39 Computational Study on the Stone-Wales Transformation of non-IPR C_{60} Fullerenes 129
Jun Li, Ting Ren, ○Xiang Zhao
- 2P-40 Laser-merging experiments of C_{60}^- stored in an electrostatic ion storage ring 130
○H. Shiromaru, M. Goto, T. Kodama, J. Matsumoto, Y. Achiba, T. Majima, H. Tanuma, T. Azuma, A.E.K. Sunden, K. Hansen

Wednesday, March 4th

Special Lectures: 25 min (Presentation) + 5 min (Discussion)

General Lectures: 10 min (Presentation) + 5 min (Discussion)

Poster Previews: 1 min (Presentation), No Discussion

Special Lecture (9:00-9:30)

- 3S-4 Creation of Fullerene- and Carbon Nanotube-Based Artificial Photosynthetic Systems 4
○Hiroshi Imahori

General Lecture (9:30-10:30)

Formation and Purification of Nanotubes

- 3-1 Chirality Sorting of Single-Walled Carbon Nanotubes Using Density Gradients Centrifugation 41
○Yuichi Kato, Yasuro Niidome, Naotoshi Nakashima
- 3-2 Diameter and Chirality Distribution of SWNTs Grown from Zeolite Surfaces 42
○Yoichi Murakami, Takahiko Moteki, Suguru Noda, Tatsuya Okubo, Shigeo Maruyama
- 3-3 Highly selective production of single-wall carbon nanotubes by laser vaporization method 43
○Yohji Achiba, Takashi Nakayama, Akihito Inoue, Yuki Onishi, Takeshi Kodama, Toshiya Okazaki
- 3-4 Impact of Molecular Structure of Carbon Source in CVD Growth of SWCNTs 44
○Bikau Shukla, Takeshi Saito, Motoo Yumura, Sumio Iijima

☆☆☆☆☆☆ **Coffee Break (10:30-10:45)** ☆☆☆☆☆☆

Special Lecture (10:45-11:15)

- 3S-5 Biological Reaction of Nanotubes and Nanoparticles : Functions and Risk Assessment 5
○Fumio Watari

General Lecture (11:15-12:30)

Formation and Purification of Nanotubes

- 3-5 Patterned Growth of Vertically Aligned SWNTs through Liquid-based Catalyst Manipulation 45
○Rong Xiang, Erik Einarsson, Junichiro Shiomi, Shigeo Maruyama
- 3-6 Top-Down Approach to Align Single-Walled Carbon Nanotubes on Silicon Substrate 46
○Carlo M. Orofeo, Hiroki Ago, Naoki Yoshihara, Masaharu Tsuji
- 3-7 Fluidized Bed Synthesis of Sub-Millimeter-Long Single-Walled Carbon Nanotubes 47
○Dong Young Kim, Hirofumi Fukai, Hisashi Sugime, Kei Hasegawa, Toshio Osawa, Suguru Noda
- 3-8 Purity Evaluation of Single Wall Carbon Nanotubes based on Raman Spectroscopy 48
○Daisuke Nishide, Yasumitsu Miyata, Kazuhiro Yanagi, Takeshi Tanaka, Hiromichi Kataura
- 3-9 *Ab Initio* Energetics of Sodium Dodecyl Sulfate on Metallic and Semiconducting Single-Wall Carbon Nanotubes 49
○Mari Ohfuchi

☆☆☆☆☆☆ **Lunch Time (12:30-13:45)** ☆☆☆☆☆☆

Special Lecture (13:45-14:15)

- 3S-6 Application of carbon nanohorns to anti-cancer drug carriers 6
○Masako Yudasaka

Poster Preview (14:15-14:55)

Poster Session (14:55-16:15)

Wednesday, March 4th

Formation and Purification of Nanotubes

- 3P-1 Si Doping into Densely-Aligned Carbon Nanotube Films on SiC 131
○Takehiro Maruyama, Kenta Yoshida, Wataru Norimatsu, Michiko Kusunoki
- 3P-2 Optical spectroscopic characterization of vertically aligned single-walled carbon nanotubes 132
○Erik Einarsson, Rong Xiang, Theerapol Thurakitserree, Zhengyi Zhang, Yoichi Murakami, Junichiro Shiomi, Shigeo Maruyama
- 3P-3 Low Temperature Growth of Single-Walled Carbon Nanotubes by High Vacuum ACCVD Method 133
○Yohei Yamamoto, Hiroto Okabe, Taiki Inoue, Erik Einarsson, Makoto Watanabe, Shigeo Maruyama
- 3P-4 Selective Isolation of (6,5) Carbon Nanotubes by Density Gradient Ultracentrifugation 134
○Pei Zhao, Yoichi Murakami, Rong Xiang, Erik Einarsson, Junichiro Shiomi, Shigeo Maruyama
- 3P-5 Laser Fluence Effect on the Chirality Characteristics of Individually Dispersed Single-walled Carbon Nanotube in Aqueous Solution with Pulsed OPO Laser Irradiation 135
○Isamu Tajima, Akira Kumazawa, Katsumi Uchida, Tadahiro Ishii, Hirofumi Yajima
- 3P-6 Low temperature growth of carbon nanotubes from acetylene 136
○Takashi Shirai, Suguru Noda
- 3P-7 Progress in Separation of Metallic and Semiconducting Carbon Nanotubes Using Agarose Gel 137
○Takeshi Tanaka, Hehua Jin, Yasumitsu Miyata, Shunjiro Fujii, Hiroshi Suga, Yasuhisa Naitoh, Takeo Minari, Tetsuhiko Miyadera, Kazuhito Tsukagoshi, Hiromichi Kataura
- 3P-8 Influence of laser power on the formation of SWNTs by laser ablation 138
○Masaomi Teshiba, Tomonari Wakabayashi
- 3P-9 Synthesis of Thin Carbon Nanocoils by Fe-Sn Catalyst Supported on Zeolite 139
○Masashi Yokota, Yoshiyuki Suda, Shinichiro Oke, Hirofumi Takikawa, Youhei Fujumura, Tatsuo Yamaura, Shigeo Ito, Hitoshi Ue, Masakatsu Morioki
- 3P-10 Chirality Selective Separation for Single-walled Carbon Nanotube with Density Gradient Ultracentrifugation 140
○Yoshiya Kaminosono, Katumi Uchida, Ishii Tadahiro, Yajima Hirofumi
- 3P-11 Effect of water vapor on structure of single-walled carbon nanotubes 141
○Naoki Yoshihara, Hiroki Ago, Masaharu Tsuji
- 3P-12 Dip-pen nanolithography for CNTs patterning 142
○Naoko Kayumi, Tsuyohiko Fujigaya, Naotoshi Nakashima
- 3P-13 TiC formation for metal contact with carbon composite structures consisting of nanotubes and graphene multi-layers 143
○Daiyu Kondo, Shintaro Sato, Mizuhisa Nihei, Eiji Ikenaga, Masaaki Kobata, Jung Jin Kim, Keisuke Kobayashi, Yuji Awano
- 3P-14 Theoretical Study on the Growth of Single Walled Carbon Nanotube (SWNT) 144
Jingshuang Dang, Weiwei Wang, ○Xiang Zhao
- 3P-15 Analysis of Fe Catalyst Behavior on Al/SiO₂/Si Substrate for CNT Growth Using Mössbauer Spectroscopy 145
○Hisayoshi Oshima, Tomohiro Shimazu, Milan Siry, Ko Mibu
- 3P-16 Diameter control of single-walled carbon nanotubes grown by diffusion plasma CVD 146
○Shunsuke Kuroda, Toshiaki Kato, Toshiro Kaneko, Rikizo Hatakeyama
- 3P-17 Comparison of thermal and plasma CVD for the growth of single-walled carbon nanotubes from nonmagnetic nanoparticles 147
○Zohreh Ghorannevis, Toshiaki Kato, Toshiro Kaneko, Rikizo Hatakeyama

Wednesday, March 4th

- 3P-18 Effect of Al Oxide Buffer Layer on SWNT Growth at Low Temperature in Alcohol Gas Source Method in High Vacuum 148
○Yoshihiro Mizutani, Kuninori Sato, Takahiro Maruyama, Shigeoya Naritsuka
- 3P-19 Synthesis of DWNTs using arc discharge by adjusting gas pressure 149
○K. Kato, H. Wang, X. Zhao, S. Inoue and Y. Ando
- 3P-20 Purification of Single-walled Carbon Nanotubes Generated with Arc-burning Apparatus by Utilizing Mono-dispersion Technique 150
○Shinzo Suzuki, Kazuto Hara, Takuya Fujita, Takashi Mizusawa, Toshiya Okazaki, Yohji Achiba
- 3P-21 Measurement of Cohesion Process of Carbon-Clusters by the Mie-Scattering Method in Gravity-free Arc-Synthesis of Nanotubes 151
○Tetsu Mieno, Tan Guodong, Shu Usuba, Kazunori Koga, Masaharu Shiratani

Graphene

- 3P-22 Open and Closed Edges of Graphene Layers 152
○Zheng Liu, Kazu Suenaga, Peter J. F. Harris, Sumio Iijima
- 3P-23 New Carbon Thin Film Growth on YSZ (111) by Very High Temperature Surface Pyrolysis of C₆₀ 153
○Takuya Noguchi, Toshihiro Shimada, Akinori Hanzawa, Tetsuya Hasegawa
- 3P-24 Temperature dependence of Raman spectra in epitaxial few-layer graphene on vicinal 6H-SiC 154
○Ryoji Naito, Susumu Kamoi, Hitoshi Kakehi, Noriyuki Hasuike, Kenji Kisoda, Hiroshi Harima, Kouhei Morita, Satoru Tanaka, Akihiro Hashimoto
- 3P-25 Probing graphene-metal contacts in bilayer graphene nanoconstriction 155
○Y. Ujiie, S. Motooka, T. Morimoto, D. K. Ferry, J. P. Bird, Y. Ochiai
- 3P-26 Edge States of ZigZag Boron Nitride Nanoribbons 156
○Fawei Zheng, Ken-ichi Sasaki, Riichiro Saito, Wenhui Duan and Bing-Lin Gu
- 3P-27 Edge phonon of nano-graphite ribbons 157
○Masaru Furukawa, Zheng Fawei, Riichiro Saito
- 3P-28 Ultra-fast structural change of graphite surface by pulse laser irradiation: A time-dependent first-principles approach 158
○Yoshiyuki Miyamoto

Nanohorns

- 3P-29 Detailed Structure Analysis of Carbon Nanohorns 159
Michiko Irie, Ryota Yuge, Sumio Iijima, ○Masako Yudasaka
- 3P-30 Isolating Individual Single-Wall Carbon Nanohorns From Their Aggregate 160
○Minfang Zhang, Sumio Iijima, Masako Yudasaka
- 3P-31 Plugs Formed by Hydrogen Peroxide Treatment at Holes of Carbon Nanohorns 161
○Jianxun Xu, Minfang Zhang, Sumio Iijima, Masako Yudasaka

Fullerene Solids

- 3P-32 Epitaxial growth and electronic characterization of Mg-doped C₆₀ 162
○Masato Natori, Nobuaki Kojima, Hidetoshi Suzuki, Masafumi Yamaguchi
- 3P-33 Pressure-Induced Structural Phase Transition of Solid C₆₀ 163
○Yuichiro Yamagami, Susumu Saito
- 3P-34 Electronic transport properties of photo-irradiated C₆₀ 164
○Y.Chiba, H.Tsujii, M.Ueno, Shih-Ren Chen, N.Aoki, and Y.Ochiai

Wednesday, March 4th

3P-35	Assembling behaviors of [70]fullerene on addition of aliphatic amines ○ <i>Ken-ichi Matsuoka, Tsuyoshi Akiyama, Sunao Yamada</i>	165
3P-36	Length growth measurement of C ₆₀ fullerene nanowhiskers ○ <i>Kayoko Hotta, Kunichi Miyazawa</i>	166
3P-37	Internalization of Fullerene Nanowhiskers by PMA-treated THP-1 Cells ○ <i>Shin-ichi Nudajima, Kun'ichi Miyazawa, Junko Okuda-Shimazaki and Akiyoshi Taniguchi</i>	167
3P-38	Water-Dispersible Fullerene Whisker ○ <i>Yasuhiko Fujita, Yutaka Takaguchi</i>	168
3P-39	Transmission Electron Microscopy Observation of Cross-Sectional Structure of C ₆₀ Nanofibers ○ <i>Ryoei Kato, Kun'ichi Miyazawa</i>	169
3P-40	Insulating behavior of Cs ₃ C ₆₀ at ambient pressure as probed by optical reflectivity measurements ○ <i>Takumi Takano, Alexey Y. Ganin, Yasuhiro Takabayashi, Matthew J. Rosseinsky, Kosmas Prassides, Yoshihiro Iwasa</i>	170

特別講演
Special Lecture

1S - 1

2S - 2 ~ 2S - 3

3S - 4 ~ 3S - 6

SWCNT Growth on Substrates Studied by a Combinatorial Method

Suguru Noda

Dept. of Chemical System Engineering, The University of Tokyo, Tokyo 113-8656, Japan

Catalytic growth of SWCNTs on substrates by CVD is promising for direct fabrication of SWCNT devices. Catalyst nanoparticles have crucial roles in controlling their diameter, density, and length. We have developed "combinatorial masked deposition (CMD)" method [1] for preparing catalyst layers with controlled gradients in thickness and composition, and applied it to study SWCNT growth from both basic and application viewpoints.

Growth methods of SWCNTs on substrates have been remarkably improved in recent years. People had been able to grow SWCNTs in a sub- μm thickness and obtain them in a "grass" morphology. Murakami, et al. realized micrometer-thick vertically aligned "forests" by alcohol CVD [2]. Soon after, Hata, et al. realized millimeter-thick forests by water-assisted CVD [3]. We applied our CMD method to these CVD methods, realized SWCNT forests [4,5], and found essential roles of Mo co-catalyst [6] and Al-Si-O "catalytic" support [7]. Real-time monitoring of growing SWCNTs on a CMD catalyst library (Fig. 1) now gives us growth curves for a series of catalysts in a single experimental run.

Such remarkable progresses provide us new opportunities for practical application of SWCNTs. SWCNTs growing at $\sim \mu\text{m/s}$ can have a variety of morphologies from individuals, grasses, spikes to forests (Fig. 2). It enables *instant mounting* of a large number of SWCNT device elements with controlled morphologies. Field emitters are a typical example: people have focused on individual tubes such as single-/double-/multi-walled and believed printing to be much easier than CVD. Figure 3 shows emitters of MW-/SW-CNTs at high/low densities grown on a textured substrate [8]. We can systematically study catalyst conditions, CNT structure/morphologies, and emission performance in a single experimental run.

Catalysts with engineered spatial distribution will further bring out SWCNTs' potential.

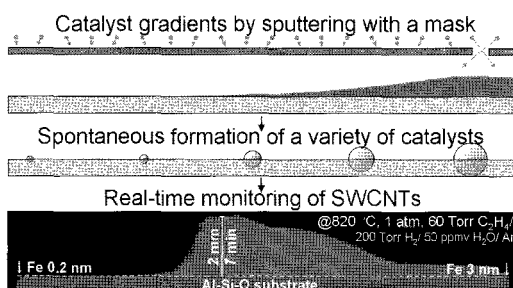


Fig. 1. Real-time monitoring of rapidly growing SWCNTs on a combinatorial catalyst library.

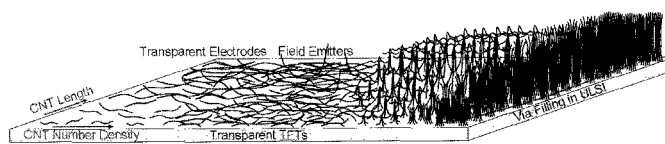


Fig. 2. Schematic of morphological variety in SWCNTs.

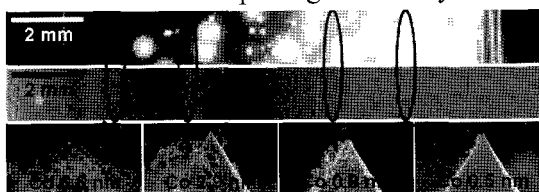


Fig. 3. Combinatorial emitter fabrication and evaluation.

- [1] S. Noda, et al., Appl. Surf. Sci. **225**, 372 (2004). [2] Y. Murakami, et al., Chem. Phys. Lett. **385**, 298 (2004). [3] K. Hata, et al., Science **306**, 1362 (2004). [4] S. Noda, et al., Carbon **44**, 1414 (2006). [5] S. Noda, et al., Jpn. J. Appl. Phys. **46**, L399 (2007). [6] H. Sugime, et al., Carbon, in press. [7] K. Hasegawa, et al., J. Nanosci. Nanotechnol., in press. [8] Y. Shiratori, et al., J. Phys. Chem. C, in press.

Corresponding Author: Suguru Noda

TEL: +81-3-5841-7330, FAX: +81-3-5841-7332, E-mail: noda@chemsys.t.u-tokyo.ac.jp

Synthesis and properties of fullerene nanowhiskers and related fullerene nanomaterials

Kun'ichi Miyazawa

*Fullerene Engineering Group, Advanced Nano Materials Laboratory,
National Institute for Materials Science, Tsukuba 305-0044, Japan*

Fine single crystalline fibers composed of C₆₀, “C₆₀ nanowhiskers (C₆₀NWs)” , were discovered in 2001 in a colloidal solution of lead zirconate titanate (PZT) added with a small amount of C₆₀ [1]. C₆₀ was used as an oxygen scavenger to hinder the formation of pyrochlore phase of PZT. The PZT sol contained both the good solvent of C₆₀ (toluene) and the poor solvent of C₆₀ (isopropyl alcohol). This combination of good fullerene solvents and poor fullerene solvents is the basis of the liquid-liquid interfacial precipitation method (LLIP method) to prepare a variety of fullerene nanomaterials shown below [2].

The C₆₀NWs can be classified into the category of “fullerene nanofibers (FNFs)”. The FNFs are composed of various fullerene molecules including higher fullerenes like C₇₀, endohedral fullerenes and the other fullerene molecules with various functional groups. The FNFs can take single crystalline, polycrystalline, amorphous or polymerized structures. The fullerene nanowhiskers (FNWs) are the crystalline FNFs, and are normally single crystalline. On the other hand, the fullerene nanotubes (FNTs) are the FNFs with tubular structure and exhibit single crystalline, polycrystalline or amorphous structures. Fullerene nanorods and fullerene nanowires are classified into the category of FNFs. The FNWs are sometimes called “fullerene nanorods” or “fullerene nanowires” .

The LLIP method can produce fullerene nano and micro sheets as well [3]. Recently, Cha et al. invented the method to prepare vertically aligned C₆₀ microtubes on AAO membrane substrates by modifying the LLIP method [4], which is expected to open new and wider applications of the nano and micro fibers of fullerenes. Up to now, attempts to apply C₆₀NWs to field-effect transistors and solar cells have been reported. The C₆₀ whiskers exhibit size-dependent unusual properties. For example, the electrical resistivity of C₆₀ whiskers decreases with decreasing the whisker diameter [5,6] and the Young's modulus of C₆₀ whiskers increases with decreasing the whisker diameter [7,8]. In the presentation, the synthesis, property characterization and application of fullerene nanowhiskers and related fullerene nanomaterials are to be reported.

[1] K.Miyazawa, A.Obayashi and M.Kuwabara, *J.Am.Ceram.Soc.*, **84**, 3037 (2001) .

[2] K.Miyazawa, Y.Kuwasaki, A.Obayashi and M.Kuwabara, *J.Mater.Res.*, **17**, 83(2002).

[3] M.Sathish and K.Miyazawa, *J.Am Chem Soc.*, **129**, 13816 (2007) .

[4] S. I. Cha, K. Miyazawa and J.-D. Kim, *Chem.Mater.*, **20**, 1667 (2008).

[5] K. Miyazawa , Y.Kuwasaki, K.Hamamoto, S.Nagata, A.Obayashi and M.Kuwabara, *Surface and Interface Analysis*, **35**, 117 (2003) .

[6] M. P. Larsson, J. Kjelstrup-Hansen and S. Lucyszyn, *ECS Transactions*, **2**, 27 (2007).

[7] K. Asaka, R. Kato, K. Miyazawa, T.Kizuka, *Appl. Phys. Lett.* **89**, 071912 (2006).

[8] M. P. Larsson and S. Lucyszyn, Abstracts of IUMRS-ICA 2008, P.NI-7, Nagoya Congress Center, Dec. 9-13, 2008.

Corresponding Author: Kun'ichi Miyazawa

TEL: +81-29-860-4528, TEL&FAX: +81-29-860-4667, E-mail: miyazawa.kunichi@nims.go.jp

Business Development of Fullerenes in Life Science Applications

Shuichi Yamana

Vitamin C60 BioResearch Corporation

1-3-19 Yaesu Chuo-ku, Tokyo 103-0028, Japan

Fullerene(C₆₀) is an excellent anti-oxidant material[1][2], and that is why we, VitaminC60 BioResearch Corporation(VC60) started development of world-first cosmetic ingredient using Fullerene named “Radical Sponge(RS)”. After its launch in year 2004, RS rapidly captured interest of cosmetic industry as the effective ingredient for skincare topics such as brightening, and today, RS is used in more than 170 cosmetic brands and 300 kinds of cosmetic items.

Here, we will introduce you RS with evidences to show it is useful to prevent skin problems from oxidative stress as well as its safety data.[3] We will also explain that the market of RS is expanding beyond skincare to hair care and laser care applications.

In addition, the sister product of RS, “Lipo Fullerene”, purified oil containing fullerenes, targeting prevention of wrinkle formation is scheduled to be available this April.

Finally, VC60 is committed to serve development of new applications for fullerenes in life science segment, and the cosmetic ingredient is just the first target. We will touch on our middle to long term targets to invite possible partners.

References:

[1]H.Takada et al., Biosci.Biotechnol.Biochem.,70, 3088(2006)

[2]L.Xhao et al., Archives of Dermatological Research, 299, 245(2007)

[3]T.Mori et al., Toxicology, 255, 48(2006)

Corresponding Author :Shuichi Yamana

E-mail: Shuichi.Yamana@vc60.com

Tel: +81-3-3517-3251

Fax:+81-3-3517-3260



Fig: Examples of Fullerene Cosmetic Products

Creation of Fullerene- and Carbon Nanotube-Based Artificial Photosynthetic Systems

Hiroshi Imahori

¹ *Institute for Integrated Cell-Material Sciences (iCeMS), Kyoto University,
Nishikyo-ku, Kyoto 615-8510, Japan*

² *Department of Molecular Engineering, Graduate School of Engineering,
Kyoto University, Nishikyo-ku, Kyoto 615-8510, Japan*

Exhaustion of the fossil fuels and the global energy concerns have never been recognized as seriously as recent days. In this context, research activities to acquire energy from the sun, as clean and inexhaustible resource, are being extensively exploited. Therefore, it is necessary to develop low-cost solar cells with high power conversion efficiency (η). Organic solar cells would be promising candidates if they fulfill the requirements. It should be noted here that they bear unique advantages over inorganic solar cells (*i.e.*, flexibility, lightness, and colorfulness). Since the beginning of the 1990s, substantial advances in power conversion efficiency have been made in organic solar cells including dye-sensitized (up to $\eta=7-11\%$) and bulk heterojunction solar cells (up to $\eta=3-6\%$).

In this context, extensive efforts have been made in recent years to explore the photovoltaic and photoelectrochemical properties of electrodes modified with various donor and acceptor components toward the realization of highly efficient organic solar cells. In the design of organic solar cells we consider the following criteria: i) extensive light-harvesting in the visible region, ii) efficient energy transfer (exciton migration) to an interface of heterojunction and subsequent charge separation, and iii) efficient transport of separated electron and hole to respective electrodes, minimizing undesirable charge recombination. Accordingly, it is of vital importance to develop excellent donor and acceptor and organize the donor and/or acceptor on the electrode surface at nanometer scale for fulfilling the requirements.

In this talk, we will present chemical functionalization and application of a variety of fullerene- and carbon-nanotube-based systems toward the realization of efficient solar energy conversion. In particular, various donors and acceptors including porphyrins, fullerenes, and carbon nanotubes have been successfully deposited electrophoretically onto nanostructured SnO₂ and TiO₂ electrodes which exhibit efficient photocurrent generation (up to IPCE of 60%). Such examples will give a deep insight for the design of organic solar cells with high cell performance.

[1] T. Umeyama and H. Imahori, *Energy Environmental Sci.* (Perspective), **1**, 120 (2008). [2] T. Umeyama, M. Fujita, N. Tezuka, N. Kadota, Y. Matano, and H. Imahori, *J. Phys. Chem. C*, **111**, 11484 (2007). [3] T. Umeyama, N. Tezuka, M. Fujita, S. Hayashi, N. Kadota, Y. Matano, and H. Imahori, *Chem. Eur. J.*, **14**, 4875 (2008). [4] T. Umeyama, N. Tezuka, M. Fujita, Y. Matano, N. Takeda, K. Murakoshi, K. Yoshida, S. Isoda, and H. Imahori, *J. Phys. Chem. C*, **111**, 9734 (2007).

Corresponding Author: Hiroshi Imahori

TEL: +81-75-383-2566, FAX: +81-75-383-2571, E-mail: Imahori@scl.kyoto-u.ac.jp

Biological Reaction of Nanotubes and Nanoparticles : Functions and Risk Assessment

○ Fumio Watari

Graduate School of Dental Medicine, Hokkaido University, Sapporo 060-8586, Japan

Nanosizing causes the conversion of functions different from the properties in macroscopic size, which may work both in merit and demerit for human beings. CNTs show the biological reaction different from macro graphite.

Fig.1 shows the lysosome inside the macrophage in the subcutaneous tissue after 1 week implantation of CNTs, observed by TEM at 75kV. Many CNTs with the length 220nm and the diameter 20-40nm were observed inside the lysosome after phagocytosis. Most of shorter CNTs (220nm) were contained in lysosomes, while for the longer CNTs(825nm) they were in cytoplasm and took more time to be observed in lysomes.

Fig.2 shows the 1.2 MeV HVEM high resolution image of deteriorated fragment of CNF crystallite with about 15 atomic layer thickness in lysosome of macrophage after 1 year implantation. With the implantation period the delamination between stacked graphene sheets occurred and length becomes shorter.

Fig.3 shows the filopodia grown from human osteoblast-like cells (Saos2) cultured on CNT scaffolds observed by SEM. Numerous filopodia were extended far long and combined with CNT meshwork, which reflects the high cell adhesiveness of CNTs. CNTs would work as scaffolds with the biocompatibility and characteristic features.

[1] F.Watari, S Inoue, N Takashi, Y Totsuka, A Yokoyama: Trans.Mat.Res.Soc.Jap. 33, 209-214, 2008

Corresponding Author: Fumio WATARI

TEL: +81-11-706-4253, FAX: +81-11-706-4251, E-mail: watari@den.hokudai.ac.jp



Fig.1 220nm CNTs in lysosome of macrophage (TEM at 75kV)

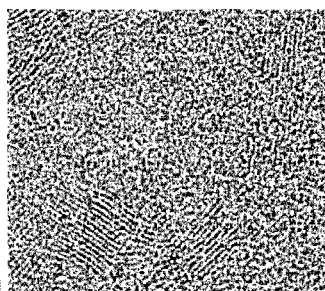


Fig.2 Deteriorated CNF crystal fragment (HVEM)

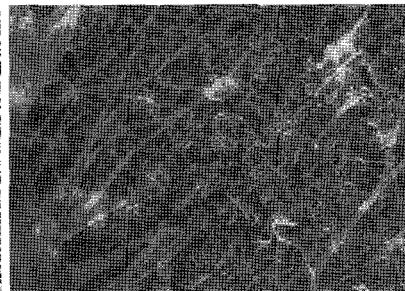


Fig.3 Filopodia extended far from osteoblast-like cell on CNTs

Application of carbon nanohorns to anti-cancer drug carriers.

M. Yudasaka

Nanotube Research Center, Central 5, AIST, Tsukuba, 305-8565, Japan

Potential applications of single-wall carbon nanohorns (SWNH) that have shown little acute toxicity in various tailored animal tests, to the drug delivery system have been studied. We previously reported that the drugs were able to be incorporated inside SWNHs at room temperature through liquid phase, and the drugs were slowly released from SWNHs in the physiological solutions. Chemical modifications of SWNHs with hydrophilic molecules enhanced dispersion of SWNHs in aqueous solutions, and the modifications with the tumor-targeting molecules were also possible. The contrast agent (magnetite nanoparticles) attachments enabled the *in vivo* visualization of SWNHs by magnetic resonance imaging.

The effects of anticancer drugs loaded on SWNHs that were chemically-modified with PEG and proteins were examined *in vivo* by local chemotherapy. It was found that anticancer effects of the drugs were enhanced by using SWNHs. Cancer phototherapy using ZnPc/SWNH also exhibited high therapeutic effects than that without SWNHs. The details are presented in the talk, discussing how the effects of anti-cancer drugs were enhanced by using SWNHs.

Acknowledgment: This work has been done under the CNT project of SORST-JST conducted by Professor S. Iijima. The results described above were obtained in the collaboration with members of SORST/JST Iijima project, Cancer Research Center (Dr. Shiba), and Fujita Health University (Dr. Murakami and Professor Tsuchida).

E-mail m-yudasaka@aist.go.jp

一般講演
General Lecture

1-1 ~ 1-18

2-1 ~ 2-16

3-1 ~ 3-9

Photoluminescence Spectra from SWNTs Encapsulating Water Molecules

○Shohei Chiashi, Tateki Hanashima, Ryota Mitobe and Yoshikazu Homma

*Department of Physics, Tokyo University of Science
1-3 Kagurazaka, Shinjuku, Tokyo 162-8601, Japan*

Photoluminescence (PL) measurement is one of the powerful tools for analysis of SWNTs' chirality, though the PL spectra strongly depend on environmental conditions. SWNTs suspended between micro-structures do not touch any substrates or wrapping materials, and they are suitable for the investigation of the environmental effects of their PL spectra. By using the suspended SWNTs, we found that adsorption and desorption of gas molecules on SWNT surface influenced the optical transition energies [1].

In this study, we focused on the adsorption of the inner surface (so-called "encapsulation") as an additional adsorption site of gas molecules and investigated the PL spectra from opened-SWNTs. The spectra (a, b) in Fig. 1 were measured from as-grown suspended SWNTs in air and in vacuum, respectively. SWNTs in air were adsorbed by water molecules and their PL peaks red-shifted. The same suspended SWNT was heated in air at 300 °C to open the caps, and then the PL measurement was performed. The PL spectra from the oxidized SWNTs measured in air and in vacuum (spectra (c, d)) showed broadening and red-shift as shown in Fig. 1. However, the spectrum (d) gradually blue-shifted and sharpened in vacuum and it agreed with the spectrum (b). After the introduction of water vapor into the vacuum chamber, the spectrum rapidly red-shifted and it coincided with the spectrum (a). After that it gradually red-shifted and broadened in air, and then it agreed with the spectrum (c). The gradual peak shift and the broadening were explained by the insertion of water molecules through the opened-caps. The water molecules inside SWNTs as well as the water molecules adsorbed on the outer surface changed the dielectric constant and the optical transition energies of the SWNTs.

This work was partially supported by Grant-in-Aid for Scientific Research on Priority Area (#19054015) from the MEXT, Japan.

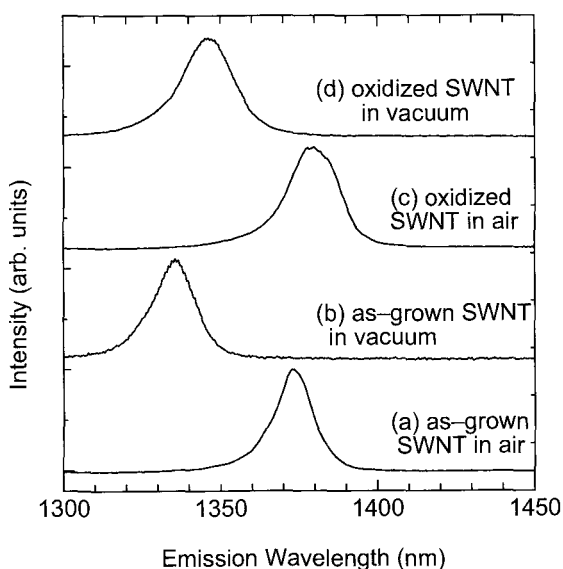


Fig. 1 PL spectra from (a, b) as-grown and (c, d) oxidized SWNTs. The spectra (a, c) and the spectra (b, d) were measured in air and in vacuum, respectively.

[1] S. Chiashi, S. Watanabe, T. Hanashima and Y. Homma, *Nano Letters*, **8**, 3097 (2008).

Corresponding Author: Shohei Chiashi

E-mail: chiashi@rs.kagu.tus.ac.jp

Tel: +81-3-5228-8244, **Fax:** +81-3-5261-1023

Environmental effect on the exciton transition energy of single wall carbon nanotubes

○Riichiro Saito¹, Kentaro Sato¹, Junichiro Shiomi², Shigeo Maruyama²

¹*Department of Physics, Tohoku University, Sendai 980-8578, Japan*

²*Department of Mechanical Engineering, The University of Tokyo, 113-8656, Japan*

The optical transition energy of single wall carbon nanotubes (SWNTs) are frequently used for assigning (n,m) values of SWNTs in the resonance Raman spectroscopy, resonance Rayleigh spectroscopy and photoluminescence spectroscopy. Depending on the surrounding materials of SWNTs, the transition energy is shifted up to 100meV, which is known as the environmental effect. The origin of the environmental effect is the modification of the Coulomb interaction between an electron and a hole of an exciton which is stable even at the room temperature. In the previous work, we discussed the environmental effect of a SWNT by the two dielectric constants of surrounding materials and the SWNT itself [1], which explains well the dependence of the transition energy as a function of the dielectric constant of the surrounding materials. However, the effective dielectric constants which are used for the exciton calculation depend on the diameter of SWNTs, which was difficult for making a reasonable transition energy as a function of diameter (the Kataura plot) which can be applicable for many different surfactant materials [2]. Here, we present three major results of the progress of the environmental effect; (1) a fitting function of the dielectric function for reproducing the experimental Kataura plot, (2) a numerical simulation of the Coulomb interaction of the exciton in the presence of the surrounding the materials and (3) an analytic expression of the exciton Coulomb energy for two different dielectric constants. Now we can give a bright exciton Kataura plot for given dielectric constants of the surrounding materials. We will show the comparison with the experimental results of resonance Raman spectroscopy, too, which will give an accurate results for a wide range of diameter up to 3nm and for an energy up to 3eV.

[1] Y. Miyauchi, R. Saito, K. Sato, Y. Ohno, S. Iwasaki, T. Mizutani, J. Jiang, S. Maruyama, *Chem. Phys. Lett.* 442, 394-399, (2007).

[2] K. Sato, R. Saito, J. Jiang, G. Dresselhaus, M. S. Dresselhaus, *Vibrational Spectroscopy*, 45, 89-94 (2007).

Corresponding Author: Riichiro Saito

TEL: +81-22-795-7754, FAX: +81-22-795-6447, E-mail: rsaito@flex.phys.tohoku.ac.jp

Low-Temperature Magneto-Optical Spectroscopy for *Single* SWNTs

○Ryusuke Matsunaga, Kazunari Matsuda, and Yoshihiko Kanemitsu

Institute for Chemical Research, Kyoto University, Uji, Kyoto 611-0011, Japan

Optical properties of single-walled carbon nanotubes (SWNTs) originated from one-dimensional excitons have attracted much attention. Very recently, the absorption and photoluminescence (PL) spectroscopy under pulsed magnetic fields have been performed to investigate an optically-forbidden (dark) exciton state. The dark exciton state near the lowest optically-allowed (bright) state has great influence on the optical properties of SWNTs. However, the ensemble-averaged optical spectra are inhomogeneously broadened, and the spectral changes in high magnetic fields have not been clearly observed.

In this work, we performed magneto-optical spectroscopy for *single* SWNTs [1]. The samples used in this work were isolated SWNTs, suspended on patterned Si substrates, synthesized by alcohol catalytic CVD methods. The PL spectra of single SWNTs have very narrow linewidths (~ 2 meV) at low temperatures (~ 20 K), which allow us to observe small spectral changes under low magnetic fields. As shown in Fig. 1, a single PL peak from the bright exciton was observed at zero magnetic field. With increasing the magnetic field parallel to the tube axis, we have observed another PL peak a few meV below the bright exciton PL peak at low temperatures. This additional peak arises from the dark exciton due to the symmetry breaking caused by the Aharonov-Bohm effect [2]. We have also investigated temperature dependence of the PL intensity ratio of the dark exciton to the bright exciton, and found that excitons are anomalously distributed between the bright and dark exciton states. Detailed mechanism will be discussed.

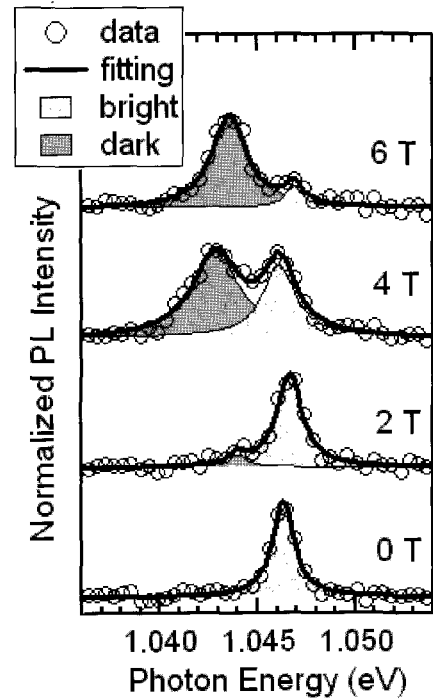


Fig. 1. PL spectra of a single SWNT under the magnetic fields at 9 K.

[1] R. Matsunaga, K. Matsuda, and Y. Kanemitsu, *Phys. Rev. Lett.* **101**, 147404 (2008).

[2] T. Ando, *J. Phys. Soc. Jpn.* **75**, 024707 (2006).

Corresponding Author: Ryusuke Matsunaga

TEL: +81-774-38-4513, FAX: +81-774-38-4511, E-mail: matsunagaryusuke@2059.mbox.media.kyoto-u.ac.jp

Optical Properties of Single-Walled Carbon Nanotube in the UV Region

Yoshiteru Takagi^{1,2} and Susumu Okada^{1,2}

¹Center for Computational Sciences and Graduate School of Pure and Applied Science,
University of Tsukuba, Tsukuba 305-8577, Japan

²CREST, Japan Science and Technology Agency, 4-1-8 Honcho, Kawaguchi, Saitama
332-0012, Japan

Optical absorption spectroscopy is one of powerful tools to characterize the single-walled carbon nanotubes (SWCNTs). The spectra clearly depend not only on the diameter but also on chirality of the SWCNT. These properties are ascribed to the fact that the inter band transition originated from the discrete one-dimensional wave number around the K point of the graphene. In addition to the low-energy absorption spectra, recent experiments show that the significant diameter dependence of the absorption spectra in ultra-violet region [1,2]. However, it is still unclear the origin of the diameter dependence. Thus, in the present work, we investigate the absorption spectra in terms of the inter band transition in the UV region based on a tight-binding approximation to unravel the origin of the dependence. We thoroughly calculate absorption coefficient of SWCNT whose diameter is thinner than 1.4 nm. Calculated spectra of the absorption coefficient are shown in Fig.1. We find that the peaks in the spectra substantially shift by changing the diameter of the nanotubes: The peaks in the UV region shift upward in energy by increasing tube diameter. These results are in good agreement with the recent spectroscopic experiments. In addition, we also find the chiral index parity dependence of the peak shift in spectra.

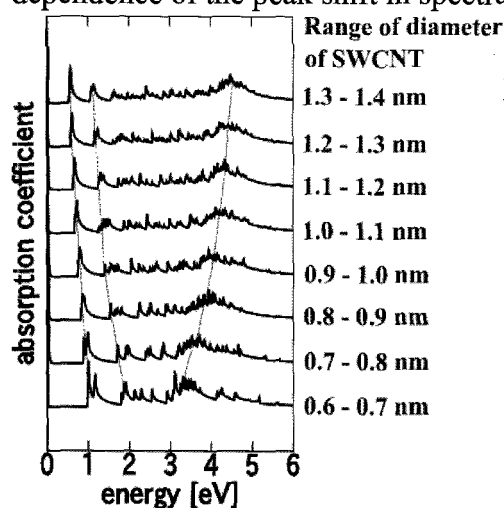


Fig. 1. Absorption coefficient of SWCNT. Each spectrum is obtained by the sum of the spectrum of SWCNT ranging in the diameter shown in right side of spectrum.

[1] T.Saito, S.Ohshima, T.Okazaki, S.Ohmori, M.Yumura, and S. Iijima, *J. Nanosci. Nanotechnol.*, **8**, 6153 (2008)

[2] K.Yanagi, private communication.

Corresponding Author: Yoshiteru Takagi

E-mail: ytakagi@comas.frsc.tsukuba.ac.jp, TEL: +81-29-853-5600(8233), FAX:+81-29-853-5924

Electronic and Optical Properties of SWCNT Thin Films Deposited on Flexible Substrates by Dry-Process

○Takeshi Saito^{1,2}, Bikau Shukla, Motoo Yumura¹ and Sumio Iijima^{1,3}

¹ *Nanotube Research Center, National Institute of Advanced Industrial Science and Technology (AIST), Tsukuba 305-8565, Japan*

² *PRESTO, Japan Science and Technology Agency, Kawaguchi 332-0012, Japan*

³ *Department of Materials Science and Engineering, 21st century COE (Nanofactory), Meijo University, Nagoya 468-8502, Japan*

Single-wall carbon nanotubes (SWCNTs) conduct electricity well, which could make them promising for many electronic applications, such as transistor, chemical sensor, solar cell, and so on. Recently, it was found that the thin film constructed by networks of SWCNTs could perform a variety of basic electronic functions [1]. The thin film of SWCNTs has prepared by the WET process using the liquid dispersion of SWCNTs so far, but that is not generally as easy as it sounds. Once SWCNTs are mixed in solvents, they tend to bundle together, requiring surfactants to keep them isolated. It should be expected that surfactants would give an impediment to the electronic conductivity. Furthermore, SWCNTs can be cut and shorten in the dispersion process that will cause the lowering of the device performance. Therefore development of the DRY process for preparing homogeneous thin films of dispersed SWCNTs is eagerly anticipated. In the 33rd FN symposium, we had reported about the development of the dry-process deposition system for preparing the thin film of SWCNTs synthesized by the enhanced direct injection pyrolytic synthesis (e-DIPS) method.

Here we have prepared thin films of SWCNTs with different diameter ranges deposited on flexible substrates by the abovementioned system. The electronic and optical properties of these films will be discussed in detailed.

[1] G. Gruner, Scientific American, pp. 76-83, May 2007.

Corresponding Author: Takeshi Saito

TEL: +81-29-861-4863, FAX: +81-29-861-3392, E-mail: takeshi-saito@aist.go.jp

Pressure dependence of superconductivity in thin films of boron-doped carbon nanotubes

M. Matsudaira¹, J. Haruyama^{1,2}, J. Nakamura¹, T. Shimizu¹, T. Eguchi², T. Nishio², Y. Hasegawa², H. Sano², Y. Iye², J. Reppert³, A. M. Rao³

¹*School of Science and Engineerings, Material Science course, Aoyama Gakuin University, 5-10-1 Fuchinobe, Sagamihara, Kanagawa 229-8558, Japan*

²*Institute for Solid State Physics, University of Tokyo, Kashiwanoha 5-1-5, Kashiwa, Chiba 277-8581, Japan*

³*Department of Physics and Astronomy, Center for Optical Materials Science and Engineering Technologies, Clemson University, Clemson, SC 29634, USA*

Abstract

It is known that the small mass of carbon can promote high transition temperature (T_c) in Bardeen-Cooper-Schrieffer (BCS) -type superconductivity (SC) and novel behaviors of SC can also be expected [1 - 3]. In this viewpoint, SC in carbon nanotubes (CNTs) is attracting considerable attention and high T_c is expected [4 – 7]. Recently, we have reported successful boron doping into single-walled CNTs (SWNTs) via catalyst and revealed its correlation with Meissner effect (SC) by assembling the boron-doped SWNTs to thin film structures [8].

In the present study, we report pressure dependence of Meissner effect in the thin films of boron-doped SWNTs. We find an increase in T_c of Meissner effect from $T_c = 8\text{K}$ to 20K by applying small pressure, while we also find out that behaviors of magnetization under pressure is highly sensitive to film structures and magnitude of applied pressure. Optimization of these parameters may lead to higher T_c .

References

1. T. E. Weller et al., *Nature Physics* **1**, 39 (2005).
2. N. Emery et al., *Phys. Rev. Lett.* **95**, 87003 (2005).
3. E. A. Ekimov et al., *Nature* **428**, 542 (2004).
4. I. Takesue, J. Haruyama, S. Maruyama, H. Shinohara et al., *Phys. Rev. Lett.* **96**, 057001 (2006).
5. N. Murata, J. Haruyama, S. Maruyama, H. Shinohara et al., *Phys. Rev. B* **76**, 245424 (2007).
6. T. Koretsune, S. Saito, *Phys. Rev. B* **77**, 165417 (2008)
7. M. Kociak et al., *Phys. Rev. Lett.* **86**, 2416 (2001).
8. N. Murata, J. Haruyama, T. Koretsune, S. Saito et al., *Phys. Rev. Lett.* **101**, 027002 (2008)

Corresponding Author: Junji Haruyama

E-mail: J-haru@ee.aoyama.ac.jp

Tel&Fax: 042-759-6256 (Fax: 6524)

Current-voltage Property Analysis of Carbon Nanotube at Room Temperature on Substrate

○Tomohiro TOJO* Tomoko HARA* Yoshitaka MURAMOTO† Takuya YOKOMAE†
Takuya HAYASHI† Yoong-Ahm KIM† Morinobu ENDO†

**Department of Electrical and Electronic Engineering Graduate School of Science and
Technology, Shinshu University*

*†Department of Electrical and Electronic Engineering, Faculty of Engineering, Shinshu
University*

Short Abstract:

Carbon Nanotube (CNT) can be thought that a hexagonal network of carbon atoms has been rolled up cylindrically. Depending on unique structure, CNT has a lot of excellent properties. For example, CNT has high electrical conductivity, mechanical strength, thermal conductivity, and so on. When we focus on the electronic properties, ballistic transport property^[1] is expected to be useful for CNT-based FET because miniaturization of Si-based circuit is reaching its practical limit. If it is possible to substitute CNTs for the devices, electronic mobility and current density will be higher than Si-based ones. Although observations of electronic transport of CNT at room temperature are reported, the effects of the other factors such as substrate, etc. are not sufficiently elucidated^[2].

Therefore, in the present study, to explain the electronic transport of CNTs on the substrate at room temperature, we have measured and simulated the current-voltage (I_{DS} - V_{DS}) property. In the measurements, we found the ohmic relation from the I_{DS} - V_{DS} curve. However, we found the current was anomalously changed at around $V_{DS} = 0.25[V]$. We performed the simulation of I_{DS} - V_{DS} property for several CNT models, and found a similar feature in the perfectly conducting tube models of zigzag type. Although there are other possibilities such as the lattice temperature and contact condition for the unusual feature, electronic property of CNTs might also be playing a role in such features. Full results with in-depth discussion will be presented at the conference.

[1] A. Javey, J. Guo, M. Paulsson, Q. Wang, D. Mann, M. Lundstrom and H. Dai, "High-Field, Quasi-Ballistic Transport in Short Carbon Nanotubes," vol. 92, p. 106804, *Phys. Rev. Lett.* (2004)

[2] H. T. Soh, C. F. Quate, A. F. Morpurgo, C. M. Marcus, J. Kong, and H. J. Dai, "Integrated nanotube circuits: Controlled growth and ohmic contacting of single-walled carbon nanotubes" vol. 75, p. 627, *Appl. Phys. Lett.* (1999)

Corresponding Author: Tomohiro TOJO

E-mail: tojo@endomoribu.shinshu-u.ac.jp

Tel & Fax: +81-26-269-5205 / +81-26-269-5208

Electric characterization of CNTs grown in nanosized via interconnects at low temperatures by remote plasma CVD

○Masatomo Iizuka¹, Kentaro Ishimaru¹, Daisuke Yokoyama¹,
Takayuki Iwasaki¹, Isamu Yuito², Teruaki Takeuchi², Shintaro Sato³,
Mizuhisa Nihei³, Yuji Awano³ and Hiroshi Kawarada¹

¹*School of Science and Engineering, Waseda university, Tokyo 169-8555, Japan*

²*Wadeda Nanotechnology Foundry, Tokyo 162-0041, Japan*

³*MIRAI-Selete, Atsugi 243-0197, Japan*

We have grown multi-walled carbon nanotubes (MWCNTs) in vias (2 μ m) with remote plasma CVD, and measured their electric properties [1]. However the resistance of the CNTs grown in smaller vias are needed to be evaluated because actual via sizes in LSI are smaller than we made. In this study, we fabricated fine vias (< 500 nm) made of MWCNTs, and characterized their properties by 4 probe mesurment.

The via interconnects are designed in damascene process, and Co particles on TiN layer are used as catalysts [2]. Co particles were size classified (3.8nm) and deposited with impactor [3]. CNTs are grown at 390°C, which is under allowable temperature in Si LSI process. Then, CNTs were flattened with chemical mechanical polishing (CMP) to use inner shell conductions[1].

Figure 1 shows SEM images of vias shaved and filled with CNTs before and after CMP. CNT density is $3.5 \times 10^{11} \text{ cm}^{-2}$ and CNT diameter is 7 nm. Figure 2 shows I-V properties of 270 nm and 500 nm diameter vias. Resistivity is $5.0 \times 10^2 \mu\Omega\text{cm}$ at 270 nm via, which is equivalent to the lowest value at 2 μ m via in our previous study [1], in spite of decreasing via size.

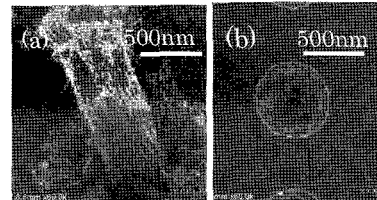


FIG. 1. SEM image of via (a)before CMP (b)after CMP

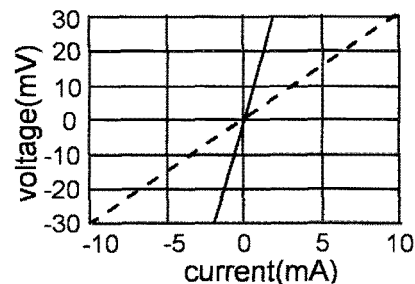


FIG.2 I-V properties of 270 nm(solid line) and 500 nm(dotted line) vias.

Acknowledgements: This work was completed as part of the MIRAI Project supported by NEDO.

[1] D. Yokoyama, H. Kawarada, et al., Appl. Phys. Lett. 91, 263101(2007)

[2] M. Nihei, et al., IEEE Int Interconnect Technol. Conf. 2007, 204 (2007)

[3] S. Sato, et al., Proc. IEEE Int. Interconnect Technol. Conf. 2006, 230 (2006)

Corresponding Author: H. Kawarada

E-mail : kawarada@waseda.ac.jp Tel&Fax : +81-3-5286-3391

Characterizing thermal conductivity of vertically-aligned single-walled carbon nanotube films

○Kei Ishikawa¹, Saburo Tanaka², Koji Miyazaki², Junichiro Shiomi¹, Shigeo Maruyama^{1*}

¹ Department of Mechanical Engineering, The University of Tokyo, Tokyo 113-8656, Japan

² Department of Biological Functions and Engineering, Kyushu Institute of Technology, 2-4 Hibikino, Wakamatsu-ku, Kitakyushu-city, Fukuoka 808-0196

Single-walled carbon nanotubes (SWNTs) are expected to possess high thermal conductivity. Thermal conductivity of individual SWNTs has been measured to be around $3000 \text{ Wm}^{-1}\text{K}^{-1}$ [1,2]. Detailed heat conduction characteristics of SWNTs have been widely investigated numerically [3,4]. On the other hand, there are only a few reported works on the thermal conductivity of vertically-aligned SWNTs (VA-SWNTs); experimental measurements using laser flash method [5,6] and thermoreflectance method [7], and thus the property is far from being fully exploited.

In this work, thermal conductivity of VA-SWNTs has been measured by utilizing the 3-omega method, which is commonly used for thin-films [8,9]. The obtained film thermal resistance $1 \sim 10 \times 10^{-6} \text{ m}^2\text{KW}^{-1}$ is in fairly good agreement with the previous work [7]. Substituting the film thickness and neglecting the thermal resistance at the boundary, the film thermal conductivity is obtained to be around $1 \text{ Wm}^{-1}\text{K}^{-1}$. The thermal conductivity of an individual SWNT estimated based on the filling ratio of the VA-SWNT film is $10^1 \sim 10^2 \text{ Wm}^{-1}\text{K}^{-1}$. This value is quite low compared with that of the experimentally measured values of individual SWNTs [1,2].

The current result suggests that heat conduction through the VA-SWNT film is limited by the thermal resistance at the nanotube-substrate boundary and/or the metal-nanotube boundary. In order to characterize the thermal boundary resistance, we propose and discuss a new measurement method utilizing the temperature dependence of the Raman spectrum of SWNTs.

- [1] Pop, E., Mann, D., Wang Q., Goodson, K. E., and Dai, H., *Nano Lett.*, **6**, 96 (2006).
- [2] Yu, C., Shi, L., Yao, Z., Li, D., and Majumdar, A., *Nano Lett.*, **5**, 1842 (2005).
- [3] Maruyama, S., Igarashi, Y., Taniguchi, Y., and Shiomi, J., *J. Therm. Sci. Tech.*, **1**, 138 (2006).
- [4] Shiomi, J., and Maruyama, S., *Japan J. Appl. Phys.*, **47**, 2005, (2008).
- [5] Akoshima M., Hata, K., Futaba, D., Baba, T., Kato, H., Yumura, M., *26th Japan Symp. Thermophys. Prop.*, 32 (2005).
- [6] Zhao, B., Futaba, D. N., Yasuda, S., Akoshima, M., Yamada, T., and Hata, K., *ACS Nano* (published online).
- [7] Panzer, M. A., Zhang, G., Mann, D., Hu, X., Pop, E., Dai, H., and Goodson, K. E., *J. Heat Transf.*, **130**, 052401-1 (2008).
- [8] Cahill, D. G., *Rev. Sci. Instrum.*, **61**, 802 (1990).
- [9] Borca-Tasciuc, T., Kumar, A. R., and Chen G., *Rev. Sci. Instrum.*, **72**, 2139 (2001).

Corresponding Author: Shigeo Maruyama

Tel&Fax: +81-3-5800-6983, E-mail: maruyama@photon.t.u-tokyo.ac.jp

Molecular-Dynamics Simulations on Thermal Transport in Peapod and Multi-Walled Carbon Nanotube

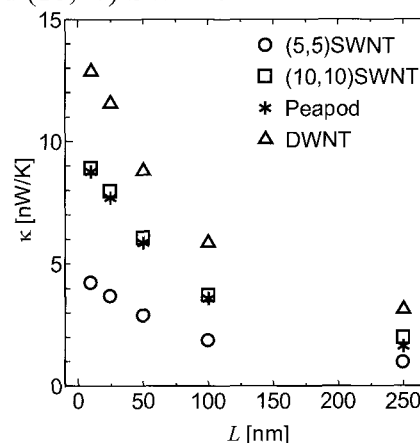
○Fumio Nishimura¹, Kazuyuki Watanabe^{1,2}, Takahiro Yamamoto³

¹ *Department of Physics, Tokyo University of Science,
1-3, Kagurazaka, Shinjuku-ku, Tokyo, 162-8601, Japan*

² *Research Institute for Science and Technology, Tokyo University of Science,
1-3, Kagurazaka, Shinjuku-ku, Tokyo, 162-8601, Japan*

³ *Department of Materials Engineering, The University of Tokyo
7-3-1, Hongo, Shinjuku-ku, Tokyo, 162-8601, Japan*

Carbon nanotubes (CNTs) are expected to have the highest thermal conductivity among all materials. However, most of theoretical researches on the thermal transport in CNTs have focused on individual single-walled CNTs (SWNTs), although there are many experiments on multi-walled CNTs (MWNTs), a SWNT encapsulating fullerenes (peapod), and so on. In this work, we perform the molecular-dynamics (MD) simulations on the thermal transport properties of MWNTs and peapods, focusing on the length dependence of their thermal conductances. In our MD simulations, we adopted Tersoff-Brenner potential for carbon-carbon covalent bonds and Lennard-Jones potential for van der Waals interactions between inter walls of a MWNT and between a wall and fullerenes of the peapod. We use Nosè-Hoover thermostat technique to keep temperatures of the hot and cold heat reservoirs constant with 310K and 290K, respectively. The figure shows the length dependence of thermal conductances of the individual (5,5) and (10,10) SWNTs, a peapod “C₆₀S@(10,10)SWNT”, and double-walled CNT (DWNT) consisting of the (5,5) and (10,10) SWNTs. We found that C₆₀S@(10,10)SWNT has thermal conductance little lower than that of the (10,10) SWNT. In contrast, the thermal conductance of (5,5)-(10,10)DWNT is almost equal to the sum of thermal conductances of the (5,5) and (10,10) SWNTs. In the presentation, we will discuss the physical origin of those phenomena in detail.



Corresponding Author: Kazuyuki Watanabe

TEL: +81-3-3260-4665, FAX: +81-3-5261-1023, E-mail: kazuyuki@rs.kagu.tus.ac.jp

Direct Determined Precise Electronic States of Single-Walled Carbon Nanotubes

○Yasuhiko Tanaka¹, Yasuhiko Hirana¹, and Naotoshi Nakashima^{1,2}

¹*Department of Applied Chemistry, Graduate School of Engineering,
Kyushu University, Fukuoka 819-0395, Japan.*

²*CREST, Japan Science and Technology Agency, 5 Sanbancho, Chiyoda-ku,
Tokyo 102-0075, Japan*

Since the discovery of carbon nanotubes (CNTs), many groups have investigated to understand the fundamental properties of the CNTs and explored their applications in nanomaterials science. Electronic structures of CNTs, one of the most fundamental features of nanotubes, strongly depend on their diameter and chirality[1] and can be tuned by electrochemical or chemical doping[2-6]. For many practical applications of nanotubes including the development of nano-electronic devices, energy cells, supercapacitors, sensors and actuators, redox doping of nanotubes plays a central role.

The work function (WF), or Fermi level, of single-walled carbon nanotubes (SWNTs) is a critical quantity for understanding the fundamental electronic nature of nanotubes[1]. Here we report for the first time a method for determining the redox potentials, Fermi levels and WFs of several (here nine) isolated SWNTs. We detected photoluminescence (PL) signals from the isolated SWNTs, which showed a strong applied-potential dependence. Using the Nernst equation analysis of the PL data, the formal potentials of nine SWNTs could be determined. By using the bandgap values of the SWNTs[7], we calculated the Fermi levels and WFs of the isolated SWNTs, which were compared with values determined from first principles calculations[8,9] and found that both methods show similar SWNT chirality dependencies.

[1] R. Saito, G. Dresselhaus, M. S. Dresselhaus, *Physical Properties of Carbon Nanotubes.*, Imperial College Press: London, **1998**.

[2] L. Kavan, P. Rapt, L. Dunsch, *Chem. Phys. Lett.* **2000**, *328*, 363-368.

[3] S. Kazaoui, N. Minami, N. Matsuda, H. Kataura, Y. Achiba, *Appl. Phys. Lett.* **2001**, *78*, 3433-3435.

[4] S. Kazaoui, N. Minami, H. Kataura, Y. Achiba, *Synth. Met.* **2001**, *121*, 1201-1202.

[5] L. Kavan, P. Rapt, L. Dunsch, M. J. Bronikowski, P. Willis, R. E. Smalley, *J. Phys. Chem. B* **2001**, *105*, 10764-10771.

[6] K.-I. Okazaki, Y. Nakato, K. Murakoshi, *Phys. Rev. B* **2003**, *68*, 035434.

[7] R. B. Weisman, S. M. Bachilo, *Nano Lett.* **2003**, *3*, 1235-1238.

[8] B. Shan, K. Cho, *Phys. Rev. Lett.* **2005**, *94*, 236602.

[9] V. Barone, J. E. Peralta, J. Uddin, G. E. Scuseria, *J. Chem. Phys.* **2006**, *124*, 024709.

Corresponding Author: Naotoshi Nakashima

Tel&FAX: +81-92-802-2840, E-mail: nakashima-tcm@mail.cstm.kyushu-u.ac.jp

Intrinsic Electron Dipoles in Capped Carbon Nanotubes

Minoru Otani^a and Susumu Okada^{b,c}

^a*AIST, Umezono, Tsukuba 305-8568, Japan*

^b*Graduate School of Pure and Applied Sciences & Center for Computational Sciences,
University of Tsukuba, Tennodai, Tsukuba 305-8577, Japan*

^c*CREST, JST, 4-1-8 Honcho, Kawaguchi, Saitama 332-0012, Japan*

Following discoveries of fullerene and carbon nanotube, there have been a lot of experimental and theoretical studies on these nanometer-scale materials. Although, these materials are known to consist of C atoms with three-fold coordination as in the case of the graphite, their global network topologies are vastly different each other: The fullerenes possess hollow-cage structures with zero-dimension due to existence of twelve pentagons; The nanotubes possess one-dimensional structures. These peculiar global network topologies significantly result in interesting variations in their electronic properties. In the fullerenes, it has been clarified that the electronic structure is determined by the size and symmetry of the carbon cage. On the other hand, in the nanotubes, early theoretical studies have revealed that nanotubes are either metals or semiconductors depending on their chiral indexes. Thus, the hybrids consisting of fullerenes and nanotubes exhibit unusual electronic properties depending on those of each constituent. Indeed, our recent calculation show that the charge transfer from nanotubes to C₆₀ are found to take place in the C₆₀-peapods[S. Okada, et al. Phys. Rev. Lett. **86**, 3835 (2001)]. The capped nanotube can be regarded as another prototype for such systems with the dimensional mixing that induces different characteristics from simple sum of each unit.

In the present work, we investigate the electronic structure of capped carbon nanotubes. Here, we consider the (10,10) nanotube one of which ends is capped by a hemispherical piece of a I_h fullerene of C₂₄₀. The other end of the nanotubes are terminated by H atoms to simulate an infinite capped tube. The electronic structure of the nanotube are calculated by using the local density approximation in the density functional theory. Our calculations show that the capped nanotube intrinsically possesses electron-dipole moment around the cap region. Calculated amount of the dipole is 10.2 debye. The dipole causes from the charge transfer from the nanotube to the hemisphere due to the electron affinity difference of these constituent. The results give a key to unravel the self-organized alignment of the nanotubes under the electron field.

Corresponding Author: Minoru Otani, minoru.otani@aist.go.jp

Hydrogen Adsorption on Carbon Nanotubes under Tensile Strains

○Takazumi Kawai¹, Yoshiyuki Miyamoto^{1,2}

¹*Nano Electronics Research Laboratories, NEC Corporation, 34 Miyukigaoka, Tsukuba 305-8501, Japan*

²*CREST, Japan Science and Technology Agency, 4-1-8 Honcho, Kawaguchi, Saitama 332-0012, Japan*

A control of the adsorption of molecules on carbon nanotubes (CNTs) is important for the application for molecular storages and also modification of electronic structure of CNTs since the electronic structure largely depends on the adsorption sites and the quantity of adsorption. Especially, a chemisorption of gas molecule introduces a defect in the network of π -electrons, where the corresponding electronic states appeared near at the Fermi level and drastically change the electronic properties of carbon nanotube.

The properties of molecular adsorption are known to depend on the electronic states of the nanotubes. The electronic states are decided by the chirality of the nanotube, which is difficult to change reversibly. However, the tensile strains can also modify the electronic states of the nanotubes, and they vary by the chirality of the nanotubes. Thus, there is a possibility for control of the molecular adsorption by using a tensile force acting on the CNTs.[1]

Here, we performed first principles calculations for adsorption of hydrogen molecule on the nanotube surface under tensile strains. We found that the change in the electronic structures under tensile strain affects not only the energetics of a hydrogen adsorption but also the reaction barrier heights for the dissociative adsorption of hydrogen molecule. The change in the reaction barrier is explained by the band gap modulation due to the tensile strain. We will also discuss the stability of several adsorption geometries and change in the electronic structures. (Fig.1)

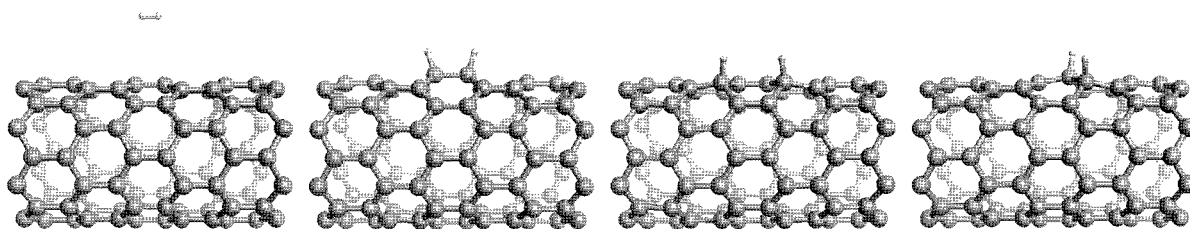


Fig.1 Schematics of adsorption geometries for hydrogen molecule on CNTs.

References

[1] L. Yang and J. Han, *Phys. Rev. Letts.* **85**, 154 (2000).

Corresponding Author: Takazumi Kawai

E-mail: takazumi-kawai@mua.biglobe.ne.jp

Tel&Fax: 029-850-1554 (029-856-6136)

Observation of Photoinduced Current in Azafullerene C₅₉N Encapsulated Single-Walled Carbon Nanotubes at Low Temperatures

○Yongfeng Li, Toshiro Kaneko and Rikizo Hatakeyama

Department of Electronic Engineering, Tohoku University, Sendai 980-8579, Japan

In this work, the photoinduced electrical transport properties of azafullerene C₅₉N encapsulated single-walled carbon nanotubes (C₅₉N@SWNTs) are investigated by fabricating them as the channels of field effect transistors (FETs). The synthesis of C₅₉N fullerenes is realized by a nitrogen plasma irradiation method, and they are confirmed by a laser-desorption time-of-flight mass spectrometer. The encapsulation of C₅₉N azafullerene into SWNTs is prepared by either a vapor reaction method or a plasma ion irradiation method. The transport properties of azafullerene peapod are studied both in dark and upon light illumination. Compared with *p*-type characteristics of pristine SWNTs or C₆₀ fullerenes encapsulated SWNTs, *n*-type semiconducting SWNTs are observed for the C₅₉N fullerene peapod [1]. Our findings demonstrate that azafullerene molecules inside SWNTs make nanotube FET devices extremely sensitive to light, and the prominent response of the device to light is the sharp decrease of source-drain current under incident illumination at room temperature, as shown in Fig. 1(a). The photoswitching effect is found to depend on wavelengths of light and becomes gradually weak when the wavelength is increased to 480 nm. However, at low temperatures, the current shows an increase upon incident illumination, as seen in Fig. 1(b). This photoinduced current depends strictly on the temperature and becomes negligible with increasing temperatures over 100 K, from which the decrease of current appears to occur again with incident illumination. The observed photoinduced current is possibly due to a mobility increase of the carrier at low temperatures.

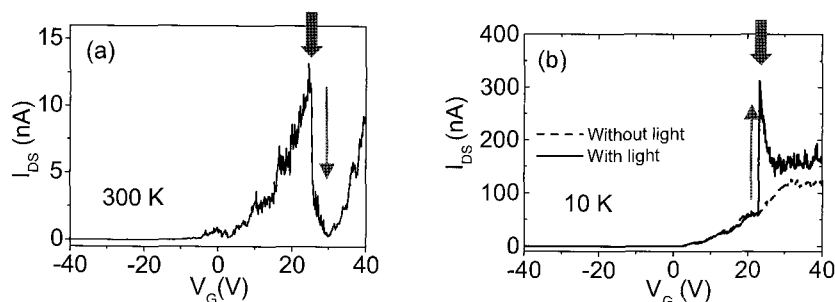


Fig.1 Characteristics of source-drain current (I_{DS}) vs. gate voltage (V_G) upon incident illumination (390 nm, 1s) for a C₅₉N@SWNT at 300 K (a) and 10 K (b)

[1] T. Kaneko, Y.F. Li, and R. Hatakeyama, *J. Am. Chem. Soc.* **130**, 2714 (2008).

Corresponding Author: Yongfeng Li

Tel : 81-22-795-7046, FAX: 81-22-263-9225, E-mail: yfli@plasma.ecei.tohoku.ac.jp

Improvement of the performance of CNT thin-film transistor by using high purity semiconducting SWCNTs

○Shunjiro Fujii¹, Takeshi Tanaka¹, Hehua Jin¹, Yasumitsu Miyata¹, Hiroshi Suga¹, Yasuhisa Naitoh¹, Takeo Minari¹, Tetsuhiko Miyadera¹, Kazuhito Tsukagoshi¹, Hiromichi Kataura^{1,2}

¹Nanotechnology Research Institute, National Institute of Advanced Industrial Science and Technologies (AIST), Tsukuba, Ibaraki 305-8562, Japan

²JST, CREST, Kawaguchi 330-0012, Japan

Semiconducting single-wall carbon nanotubes (SWCNTs) are a candidate material for high-performance thin-film transistors (TFTs) because of their superior transport properties. Recently, we achieved enrichment of semiconducting SWCNTs by a new separation method using agarose gel [1,2]. In this study, we have fabricated a number of SWCNT TFTs using separated semiconducting SWCNTs (S-TFT) and compared the performance with that of pristine SWCNTs (P-TFT) without electrical breakdown treatment.

SWCNT TFTs were fabricated by dropping a SWCNT dispersion in N-methylpyrrolidone onto a SiO₂/Si substrate covered with self-assembled monolayer of 3-aminopropyltriethoxysilane, followed by depositing Au/Cr electrodes on it. The channel length and width were 10 and 200 μm, respectively. SWCNT network structures in the channels of S- and P-TFTs were confirmed to be the same by AFM observation.

Figure 1 shows typical transfer characteristics. Figure 2 shows on-state current (I_{on}) versus on/off ratio for all TFTs fabricated in this work. It can be seen that S-TFTs achieved 100 to 1000 times higher on/off ratios than those of P-TFTs without decreasing I_{on} . These results indicate that the performance of TFTs was highly improved by using high purity semiconducting SWCNTs.

References:

[1] T. Tanaka *et al.*, Appl. Phys. Express **1** (2008)114001

[2] T. Tanaka *et al.*, submitted

Corresponding Author: Hiromichi Kataura

E-mail: h-kataura@aist.go.jp, **Tel:** +81-29-861-2551, **Fax:** +81-29-861-2786

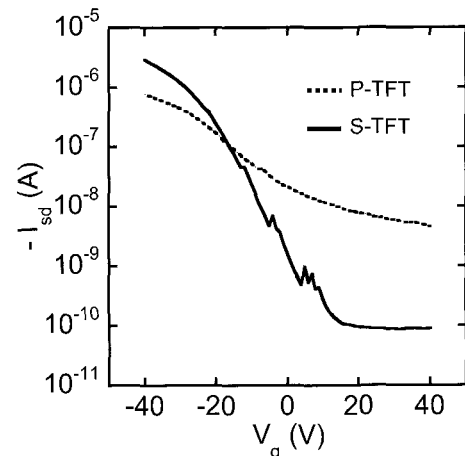


Fig. 1 Source-drain current (I_{sd}) vs gate voltage (V_g) characteristics ($V_{sd} = -1$ V).

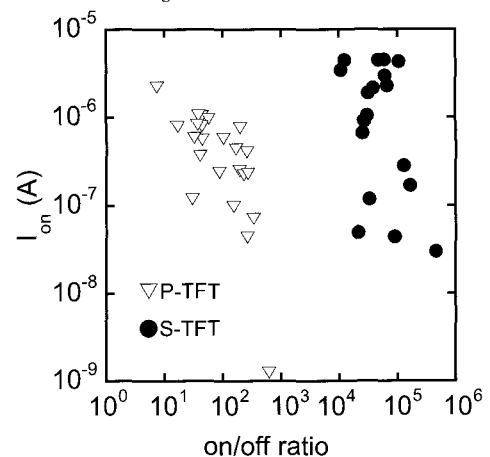


Fig. 2 On-state current plotted against on/off ratio.

**Carbon Nanotube Black Body:
Highly Efficient Light Absorber
by Vertically Aligned Single Walled Carbon Nanotubes**

○Kohei Mizuno¹, Juntaro Ishii², Hideo Kishida³, Yuhei Hayamizu¹, Satoshi Yasuda¹,
Don N. Futaba¹, Motoo Yumura¹, Kenji Hata¹

¹*Reserch Center for Advanced Carbon Materials, National Institute of Advanced Industrial
Science and Technology (AIST), Tsukuba, Ibaraki 305-8565, Japan*

²*National Metrology Institute of Japan, National Institute of Advanced Industrial Science and
Technology (AIST), Tsukuba, Ibaraki 305-8565, Japan*

³*Department of Applied Physics, Nagoya University, Chikusa-ku, Nagoya, 464-8603, Japan*

Among all the known materials, we found that a forest of vertically aligned single walled carbon nanotubes behaves most similarly to a black body; a theoretical material that absorbs all incident light.

The requirement for an object to behave as a black body is to perfectly absorb light of all wavelengths. As a result, it appears perfectly black at room temperature and is the most efficient thermal absorber and emitter, which makes it valuable for many applications. The radiation spectrum of a black body is determined solely by the temperature and not by the material, properties, and structure. These features as an ideal source to emit or absorb thermal radiation make the black body valuable for many applications. However, this important feature has not been observed for real materials because materials intrinsically have specific absorption bands due to their structure and composition.

For the first time, we found a material that can absorb light almost-perfectly across a very wide spectral range. Specifically, from optical studies, we revealed that a SWNT forest possesses a nearly constant and near unity emissivity (absorptivity) of 0.98-0.99 across a wide spectral range from ultraviolet (200 nm) to far infrared (200 μm) [1, 2]. We attribute this black body behaviour to stem from the sparseness and imperfect alignment of the vertical single walled carbon nanotubes.

[1] K. Hata, D. N. Futaba, K. Mizuno, T. Namai, M. Yumura and S. Iijima, *Science* **306**, 1362-1364 (2004).

[2] K. Mizuno, J. Ishii, H. Kishida, Y. Hayamizu, S. Yasuda, D. N. Futaba, M. Yumura and K. Hata, *Proc. Natl. Acad. Sci. USA*, submitted.

Corresponding Author: Kenji Hata

TEL: +81-29-861-4654, FAX: +81-29-861-4851, E-mail: kenji-hata@aist.go.jp

Evaluation of dispersion state of carbon nanotubes/UV-curable resin nanocomposites by resonance Raman spectroscopy

○Takahiro Fukumaru¹, Tsuyohiko Fujigaya¹ and Naotoshi Nakashima^{1,2}

¹Department of Applied Chemistry, Graduate School of Engineering, Kyushu University,
744 Motooka, Fukuoka 819-0395, Japan

²Japan Science and Technology Agency, CREST, 5 Sanbancho, Chiyoda-ku, Tokyo,
102-0075, Japan

The homogeneous dispersion of carbon nanotubes (CNTs) in polymer matrix is essential to maximize the CNTs' properties such as exceptional mechanical strength and electric conductivity of the composites. We reported composites of single-walled carbon nanotubes (SWNTs) and UV-curable monomer (**1** : Fig. 1) by solvent-free photopolymerization and the composite films exhibited extremely low electric percolation threshold at around 0.05 wt% SWNT-loading and excellent processability requirements [1].

In this presentation, we report the evaluation of bundled degrees of SWNTs in the composite films based on the intensity change in the radial breathing mode (RBM) of their Raman spectra at a 785 nm excitation [2]. The RBM in the SWNT Raman spectra at a 785 nm excitation reflects the degree of aggregation of SWNTs based on the fact that the RBM at around 267 nm of (10, 2) SWNTs is absent in the isolated SWNTs but is present in the bundles of the SWNTs. Fig. 2 shows the Raman spectra in the RBM region of SWNT/1 films with 0.05 wt% and 5.0 wt% loading of the SWNTs. This result indicated that the composite films contain bundled SWNTs and degree of debundling varies with the SWNT concentration.

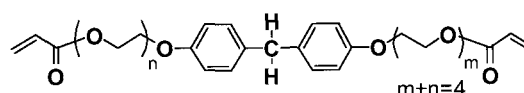


Fig. 1 Chemical structure of monomer 1.

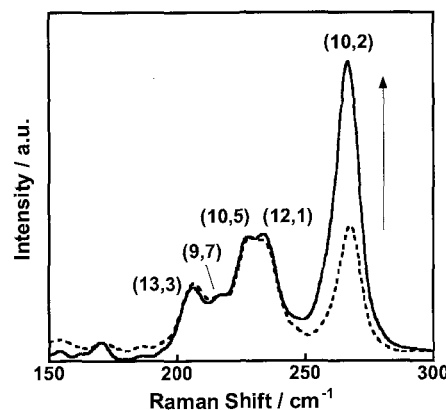


Fig. 2 Raman spectra (excitation at 785 nm) in the RBM region of SWNT/1 films with 0.05 wt% (dotted line) and 5.0 wt% (solid line) loading of the SWNTs.

[1] T. Fujigaya, S. Haraguchi, T. Fukumaru, N. Nakashima, *Adv. Mater.* **2008**, *20*, 2151.

[2] T. Fujigaya, T. Fukumaru, N. Nakashima, *Synthetic Metals*. in press.

Corresponding Author: Naotoshi Nakashima

E-mail: nakashima-tcm@mail.cstm.kyushu-u.ac.jp

Tel&Fax: +81-92-802-284

Near-IR Laser-Driven Reversible Volume Phase Transition of Single-Walled Carbon Nanotubes / Polymer Gel Composites

○Tatsuro Morimoto¹, Tsuyohiko Fujigaya¹, and Naotoshi Nakashima^{1,2}

¹*Department of Applied Chemistry, Graduate School of Engineering, Kyushu University, 744 Motooka, Fukuoka 819-0395, Japan*

²*JST-CREST, 5 Sanbancho, Chiyoda-ku, Tokyo 102-0075, Japan*

Single-walled carbon nanotubes (SWNTs) are nanomaterials possessing remarkable electrical, mechanical and thermal properties and show characteristic absorption bands in the near-infrared (NIR) region [1]. On the other hand, polymer gels, such as poly (*N*-isopropylacryl- amide) gel is of interest in wide area of science and technology from the aspects of both fundamentals and applications, because it shows volume phase transition [2].

The particular properties of SWNTs and polymer gels motivated us to composite them, aiming at novel functions. Therefore, we have developed SWNTs / Polymer gel composites. Illuminating the NIR laser light caused volume phase transitions of the composite gels thorough the photothermal effects of SWNTs [3], and desired responses of the composite gels were achieved easily by varying some parameters like the concentration of SWNTs and the laser output. Then we focused on the way to prepare composite gel, particularly the means to dissolve SWNTs as another parameter. The previous technique was to treat SWNTs with strong acid for dissolving them in water. It was however, treating SWNTs with acid resulted in much lower absorption around NIR region than the pristine ones as well as transformation into very short debris, which may disturb the distinctive properties of SWNTs.

In this study, we used surfactants, sodium dodecylbenzenesulfonate, to dissolve SWNTs. That realized SWNTs / Polymer composite gel which SWNTs of it were intact, and the gel showed some interesting behavior. For example, it showed very rapid response time derived from large absorption than the case of acid-treated SWNTs. We expect it to have large elastic modulus because SWNTs and polymer gel are considered to form the inter penetrating network by their long silhouette. We also anticipate the gel to work as a drug delivery carrier utilizing the surface of the SWNTs as hydrophobic scaffolds.

[1] M. J. O'Connell et al., *Science* **2002**, 297, 593-596.

[2] T. Tanaka et al., *Phys. Rev. Lett.* **1985**, 55, 2455-2458.

[3] T. Fujigaya et al., *Adv. Mater.* **2008**, 20, 3610-3614.

Corresponding Author: Naotoshi Nakashima

TEL & FAX: +81-92-802-284, E-mail: nakashima-tcm@mail.cstm.kyushu-u.ac.jp

Examination of the factors affecting *in vitro* evaluation of cellular responses induced by fullerene C60

○Masanori Horie¹, Keiko Nishio¹, Naohide Shinohara², Haruhisa Kato³,
Ayako Nakamura³, Katsuhide Fujita¹, Shinichi Kinugasa³, Shigehisa Endoh⁴,
Hitoshi Iwahashi¹, Yasukazu Yoshida¹ and Junko Nakanishi²

¹ *Health Technology Research Center, National Institute of Advanced Industrial Science and Technology (AIST) Kansai, Ikeda 563-8577, Japan*

² *Research Institute of Science for Safety and Sustainability, AIST Tsukuba, Tsukuba 305-8569, Japan*

³ *National Metrology Institute of Japan, AIST Tsukuba*

⁴ *Research Institute for Environmental Management Technology, AIST Tsukuba*

Fullerene is gaining attention as a material with new functionalities; it has been used not only for industrial purposes but also for life-science-related applications such as cosmetics. On the other hand, the influence of fullerene on human health has not been elucidated. *In vitro* experiments are useful in understanding the potential risk and underlying mechanisms and also risk assessment. The determination of fullerene concentration, secondary particle size, and dispersion stability is important in understanding the cellular responses to fullerene. In this study, we prepared a cell-culture medium in which C60 is dispersed without dispersant. The secondary particle size was determined by using the dynamic light scattering (DLS) method. The C60 dispersed in the medium was stable during the experimental procedure. The dispersion was applied to culture cells and its influence on cell viability was examined. The C60-dispersion exhibited very little influence on cell viability; however, apoptosis was induced. Furthermore, we examined the protein-adsorbing ability of C60 and found that C60 adsorbed proteins in the culture medium. Protein adsorption is an important property in evaluating the cellular influence of C60, because protein adsorption induces medium depletion and changes the biological activity of C60. The cellular responses induced by C60 may include the effect of protein adsorption. We aim to conduct future studies to assess the role of protein adsorption in the cellular responses to C60.

This work was funded by NEDO Grant “Evaluating risks associated with manufactured nanomaterials (P06041)”.

Corresponding Author: Masanori Horie

TEL: +81-72-751-9693, FAX: +81-72-751-9964, E-mail: masa-horie@aist.go.jp

Detailed characterization of cellular responses induced by fullerene C60

○Keiko Nishio¹, Masanori Horie¹, Naohide Shinohara², Haruhisa Kato³,
Ayako Nakamura³, Katsuhide Fujita¹, Shinichi Kinugasa³, Shigehisa Endoh⁴,
Hitoshi Iwahashi¹, Yasukazu Yoshida¹ and Junko Nakanishi²

¹ *Health Technology Research Center, National Institute of Advanced Industrial Science and Technology (AIST) Kansai, Ikeda 563-8577, Japan*

² *Research Institute of Science for Safety and Sustainability, AIST Tsukuba, Tsukuba 305-8569, Japan*

³ *National Metrology Institute of Japan, AIST Tsukuba*

⁴ *Research Institute for Environmental Management Technology, AIST Tsukuba*

In vitro experiments are useful in understanding the potential risk and underlying mechanisms and also risk assessment. In order to understand the cellular responses induced by exposure to fullerene C60, we examined and characterized the cellular responses induced by dispersion of C60 in cultures of human keratinocyte HaCaT cells and human lung carcinoma A549 cells. C60 was dispersed in cell-culture media (10% fetal bovine serum -supplemented DMEM). The cellular analyses and dynamic light scattering (DLS) measurements for secondary particle size and stability were performed simultaneously. The C60-medium dispersion was almost stable during the experimental period. Flow cytometric measurements revealed that there was a slight increase in the number of apoptotic cells, but we did not observe the activation of caspase-3. Furthermore, we assessed the oxidative stress in C60-exposed cells. The intracellular reactive oxygen species (ROS) level showed a tendency to increase, but there was no significant increase in the intracellular lipid peroxidation level. We observed an increase in the gene expression of heme oxygenase-1 (HO-1), which is an antioxidative marker. These results indicate that C60 induces oxidative stress and subsequent apoptosis. However, the influence of C60 on culture cells is weaker than that of toxic nanoparticles such as nickel oxide. In this study, C60 adsorbed proteins in the culture medium. Further investigation on the effect of protein adsorption on cellular responses is needed to clarify this observation.

This work was funded by NEDO Grant “Evaluating risks associated with manufactured nanomaterials (P06041)”.

Corresponding Author: Masanori Horie

TEL: +81-72-751-9693, FAX: +81-72-751-9964, E-mail: masa-horie@aist.go.jp

Structure determination and chemical functionalization of metallofullerene Sc₂C₈₂

○ Hiroki Kurihara¹, Yuko Yamazaki¹, Naomi Mizorogi¹, Midori O. Ishitsuka¹, Takahiro Tsuchiya¹, Shigeru Nagase² and Takeshi Akasaka¹

¹*Center for Tsukuba Advanced Research Alliance, University of Tsukuba, Tsukuba, Ibaraki 305-8577, Japan*

²*Department of Theoretical and Computational Molecular Science, Institute for Molecular Science, Okazaki, Aichi 444-8585, Japan*

Endohedral metallofullerenes have attracted special attention as new spherical molecules with unique properties that are unexpected for empty fullerenes [1]. Scandium metallofullerenes are of special interest because of the high variety of fullerene sizes and of encapsulated structures inside a hollow fullerene cage. Recently, it was corrected that the structure of several Scandium metallofullerenes were not metal but metal carbide encaged inside fullerenes (Sc₂C₂@C₈₄ [2], Sc₂C₂@C₈₂ [3], Sc₃C₂@C₈₀ [4] etc) by both ¹³C NMR and X-ray structural analyses.

For the metallofullerene Sc₂C₈₂ was only characterized by UV/Vis/NIR absorption spectrometric measurements and theoretical calculation. While experimental evidence of structure has not yet been reported because of ¹³C NMR measurements was precluded by the very low solubility [5].

Recently, we have found that the addition of adamantylidene (Ad:) to La@C₈₂ regioselectively proceeds to afford the mono-adducts [6]. The selectivity of the addition reaction is very important for further applications of endohedral metallofullerenes.

In this context, we report here the preparation and its characterization of both Sc₂C₈₂ and Sc₂C₈₂(Ad) by means of spectroscopic analysis, and redox property, theoretical calculation and X-ray single-crystal structure analysis.

[1] Endofullerenes: A New Family of Carbon Clusters; Akasaka, T., Nagase, S.; Eds.; Kluwer: Dordrecht, 2002.

[2] Wang, C. R. et al. *Angew. Chem. Int. Ed.* **2001**, *40*, 397.

[3] Iiduka, Y. et al. *Chem. Commun.* **2006**, 2057.

[4] Iiduka, Y. et al. *J. Am. Chem. Soc.* **2005**, *127*, 12500.

[5] Wang, C. R. et al. *Chem. Phys. Lett.* **1999**, *300*, 379.

[6] Maeda, Y. et al. *J. Am. Chem. Soc.* **2004**, *126*, 6858.

Corresponding Author: Takeshi akasaka

Tel & Fax : +81-298-53-6409, E-mail : akasaka@tara.tsukuba.ac.jp

Ultraviolet Photoelectron Spectroscopy of $\text{Sc}_2\text{C}_2@C_{82}(\text{II})$

○Takafumi Miyazaki¹, Yuusuke Aoki¹, Youji Tokumoto¹, Ryohei Sumii², Haruya Okimoto³,
Hisashi Umemoto³, Yasuhiro Ito³, Hisanori Shinohara³, Shojun Hino¹

¹ Graduate School of Science & Technology, Ehime University

² Institute for Molecular Science

³ Graduate School of Science, Nagoya University

Photoelectron spectroscopy and theoretical calculation have determined the electronic structure of metallofullerenes. As the results it has been found that oxidation state of $\text{Sc}@C_{82}$ was determined to be $\text{Sc}^{2+}@C_{82}^{2-}$ and that $\text{C}_{3v}\text{-Sc}_2\text{C}_2@C_{82}$ and $\text{Y}_2\text{C}_2@C_{82}$ (III) as well as $\text{Y}_2@C_{82}$ (III) have analogous electronic structure. In this study ultraviolet photoelectron spectra (UPS) of $\text{Sc}_2\text{C}_2@C_{82}$ (II) were measured and compared with other endohedral C_{82} cage fullerenes.

Figure 1 shows the $h\nu$ dependence of the UPS of $\text{Sc}_2\text{C}_2@C_{82}$ (II). The UPS show the intensity oscillation as were observed in the other fullerenes. The spectral onset of $\text{Sc}_2\text{C}_2@C_{82}$ (II) (E_{onset}) is 0.52 eV at 40eV irradiation, which is smaller than that of empty C_{82} ($E_{\text{onset}}=1.2\text{eV}$). The spectra deeper than 5 eV resemble the ones of other C_{82} endohedral fullerenes having the same cage symmetry. As for upper valence band region (0-5 eV), the UPS of $\text{Sc}_2\text{C}_2@C_{82}$ (II) are different from $\text{C}_{2v}\text{-Sc}@C_{82}$. This could be interpreted in the difference of the amounts of transferred electrons from the entrapped species. However, the UPS are quite analogous to those of $\text{M}_2@C_{82}$ ($\text{M}=\text{Y}, \text{C}, \text{Lu}, \text{Er}$) having the same C_{2v} cage structure. These findings could be helpful information to deduce the electronic structure of endohedral fullerenes.

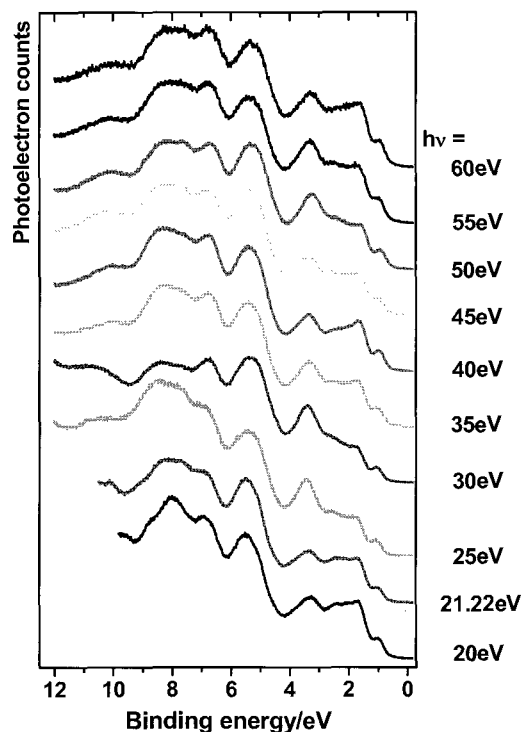


Figure 1 The $h\nu$ dependence of UPS of $\text{Sc}_2\text{C}_2@C_{82}(\text{II})$.

Corresponding Author : S. Hino, E-mail: hino@eng.ehime-u.ac.jp, phone: 089-927-9924

Energy Level Alignment of Interfaces Related to PCBM: PCBM/Ag Substrate, PCBM/Phthalocyanines

○Kouki Akaike¹, Kaname Kanai², Yukio Ouchi¹ and Kazuhiko Seki¹

¹*Department of Chemistry, Graduate School of Science, Nagoya University, Nagoya
464-8602, Japan*

²*Research Center for Materials Science, Nagoya University, Nagoya 464-8602, Japan*

Recently, the soluble C₆₀-derivatives have been synthesized for the fabrication of organic photovoltaics (OPVs) using solution-processes. [6,6]-phenyl-C₆₁-butyric acid methyl ester (PCBM) is one of them and often used as the *n*-type semiconductor for OPVs. Since the charge extraction and separation in OPVs occur at PCBM/metal and PCBM/organic interfaces, respectively, understanding the interfacial electronic structure of PCBM is desired. However, it has not been studied yet. In this study, we investigated the energy level alignment of PCBM/Ag substrate, PCBM/copper phthalocyanine (CuPc) and zinc phthalocyanine (ZnPc) interfaces by ultraviolet/X-ray photoelectron spectroscopy (UPS/XPS) and inverse photoemission spectroscopy (IPES).

The UPS and IPES spectra showed the formation of the interfacial states at PCBM/Ag substrate, which can be derived from the hybridization between the lowest unoccupied molecular orbital of PCBM and *d*-bands of Ag. The vacuum level (VL) is lowered by PCBM molecules charged positively at PCBM/Ag, while the VL is raised at C₆₀/Ag interfaces. The XPS spectra showed the charge transfer from the oxygen of the side chain of PCBM to Ag, which leads the positive charge on PCBM. These findings indicate that the side chain of PCBM strongly influences the interfacial electronic structure of PCBM/Ag.

At PCBM/CuPc and PCBM/ZnPc interfaces, the valence and core levels of CuPc shift toward low binding energy (BE), while those of PCBM shift toward high BE. The VL is raised with increasing the thickness of PCBM. This suggests that the energy level alignment at these interfaces is clearly different from that at typical *pn*-junctions in inorganic semiconductors, which means that the depletion layer is not formed at these interfaces. We also found that the ionization energies of PCBM, CuPc and ZnPc change at the interfaces, compared to the bulk region. This is due to the different polarization energy between interface and bulk region. Therefore, we consider that the energy level alignment at organic *pn*-junctions is achieved by the following two phenomena; (1) the charge transfer from CuPc or ZnPc to PCBM, (2) the changes of the ionization energies of PCBM, CuPc and ZnPc.

Corresponding Author: Kouki Akaike

TEL: +81-52-789-2945, FAX: +81-52-789-2944, E-mail: kakaike@mat.chem.nagoya-u.ac.jp

Geometric curvature effects on Tomonaga-Luttinger states of one-dimensional peanut-shaped C₆₀ polymers

○Hiroyuki Shima¹, Hideo Yoshioka², and Jun Onoe³

¹*Department of Applied Physics, Graduate School of Engineering,
Hokkaido University, Sapporo 060-8628, Japan*

²*Department of Physics, Nara Women's University, Nara 630-8506, Japan*

³*Research Laboratory for Nuclear Reactors and Department of Nuclear Engineering,
Tokyo Institute of Technology, 2-12-1 Ookayama, Meguro, Tokyo 152-8550, Japan*

We present a theoretical framework that describes the Tomonaga-Luttinger liquids (TLL) behavior of one-dimensional (1D) peanut-shaped C₆₀ polymers. It has been observed that electron-beam irradiation of a C₆₀ film produces C₆₀-based polymers via a sequence of the general Stone-Wales rearrangements [1,2]. Due to the 1D properties, the C₆₀ polymers exhibit the TLL behavior characterized by the exponent α in the density of states (DOS) $\rho(E) \propto |E - E_F|^\alpha$ at low temperatures, as well as the temperature-dependent DOS $\rho(T, E = E_F) \propto T^\alpha$ at the Fermi energy E_F [3]. Our main goal is to formulate the correlation between the value of α and the degree of surface curvature appearing in the peanut-shaped C₆₀ polymer. To this aim, we reduce the problem to a correlated electron system embedded on a continuum cylindrical surface, in which the diameter r of the hollow cylinder is periodically modulated in the axial direction as given by $r(z) = r_0 + A \cos(\lambda z)$. We demonstrate that the exponent α realized in the cylindrical surface shows a monotonic increase with the modulation amplitude A . The increase in α is attributed to the growth of a curvature-driven potential [4] that acts on conducting electrons in the curved surface. These results give a clue to understand the experimentally obtained value of $\alpha \approx 0.6$ in the actual C₆₀ polymers [3], and further suggest that the change in electron-beam irradiation time causes a quantitative alteration in α that will be obtained from the resultant C₆₀ polymer. Comparison with the TLL behavior of carbon nanotubes [5] is also discussed.

[1] Y. Toda, S. Ryuzaki, and J. Onoe, Appl. Phys. Lett. **92**, 094102 (2008)

[2] J. Onoe, T. Ito and S. Kimura, J. Appl. Phys. **104**, 103706 (2008)

[3] T. Ito, J. Onoe, S. Ryuzaki and S. Kimura, presented in the JPS Autumn meeting 2008 (22aWF-7).

[4] H. Taira and H. Shima, Surf. Sci. **601**, 5270 (2007)

[5] H. Yoshioka, Physica E **18**, 212 (2003)

Corresponding Author: Hiroyuki Shima

TEL: +81-11-706-6624, FAX: +81-11-706-6859, E-mail: shima@eng.hokudai.ac.jp

Physical Properties of Hydrogen-molecule Endohedral C₆₀

○ Ryotaro Kumashiro¹, Takeshi Rachi¹, Yasujiro Murata², Koichi Komatsu², Hiroshi Sawa³, Yoshimitsu Kohama⁴, Satoru Izumisawa⁴, Hitoshi Kawaji⁴, Tooru Atake⁴ and Katsumi Tanigaki^{1,5}

¹ *Department of Physics, Graduate School of Science, Tohoku University, Sendai 980-8578, Japan*

² *Institute of Chemical Research, Kyoto University, Kyoto 611-0011, Japan*

³ *Department of Applied Physics, Nagoya University, Nagoya 464-8602, Japan*

⁴ *Materials and Structures Laboratory, Tokyo Institute of Technology, Yokohama 226-8503, Japan*

⁵ *World Premier International Research Center, Tohoku University, Sendai 980-8577, Japan*

The physical properties of atoms or molecules encapsulated inside nona-size cages have been one of the very intriguing scientific issues. For performing experiments in order to have reasonable insight to this issue, a large scale synthesis of such materials is needed. Recently, hydrogen-molecule endohedral C₆₀, H₂@C₆₀, was synthesized by organic chemical reaction in macroscopic scale [1]. The success in macroscopic scale production of H₂@C₆₀ has opened a door to a scientifically realistic research stage. In the present study, we have measured the heat capacity of H₂@C₆₀ and related materials in the low temperature region, and discussed the state of encapsulated hydrogen molecule in C₆₀ fullerene cage.

The heat capacity of H₂@C₆₀ was measured in the temperature region from 0.085 K to 300 K. In the lowest temperature region, heat capacity anomaly was found around 0.6 K with the excess entropy of about $0.75R\ln 3$, which indicated that the rotational ground state ($J = 1$) of the ortho-hydrogen should be split due to lower symmetry of C₆₀ cage than that in the higher temperature phase above the rotational phase transition at 260 K. This interpretation was also supported by the heat capacity of deuterium-molecule endohedral C₆₀ which have opposite state in nuclear spin isomer.

This work was performed by a Grant-in-Aid from the Ministry of Education, Science, Sports and Culture of Japan, No.15201019, 1771088, 18204030, 18651075 and 19014001.

References: [1] K. Komatsu, M. Murata, Y. Murata, *Science* **307**, 238 (2005).

Corresponding Author: Ryotaro Kumashiro

E-mail: rkuma@sspns.phys.tohoku.ac.jp

Tel&Fax: +81-22-795-6468(tel), +81-22-795-6470(fax)

A Simple Formation Mechanism of a Fullerene from a Carbon Onion

○Teruhiko Ogata and Yoshio Tatamitani

Department of Chemistry, Shizuoka University, Shizuoka 422-8529, Japan

We have proved the fullerene growth from C_{60} to C_{70} by atomic carbon addition using ring-opening reaction (ACAROR) [1]. On the other hand, inner-hollow onions, reminiscing of the origin of fullerenes, have been found in many carbon soots [2a]. These facts, together with the Huang and co-workers' *in situ* observing of the shrinkage of a single-layer giant fullerene (GF) to form a small fullerene [3], persuade us to propose a simple formation mechanism of a fullerene from a carbon onion as shown in Figure 1.

Carbon onions form during the annealing of graphitic nanoparticles in carbon soot [2b]. Continuous insertion of carbon atoms into the outer-most layer of the carbon onion by the ACAROR induces the expansion of the surface layer and the following insertions of carbon atoms into the nested inner-layers balloon them and leave behind an inner-hollow onion [1]. Repeating these processes finally form a small or a giant fullerene (insert-wrap). Then the giant fullerene thermally dissociates linear or cyclic-ring clusters (shrink-wrap) [3].

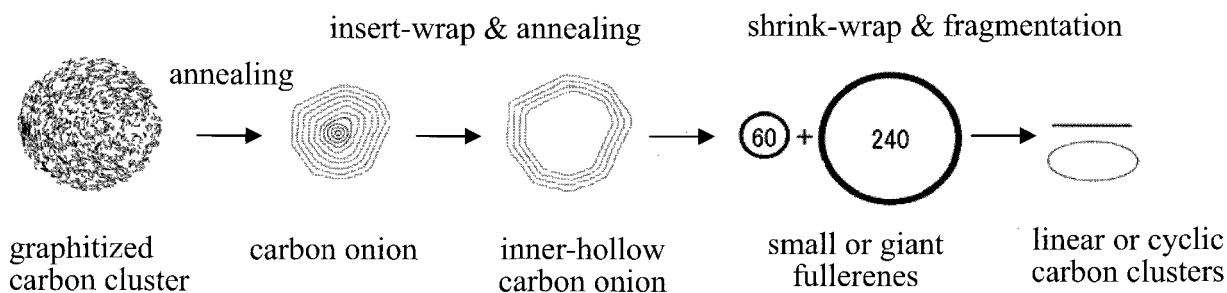


Figure 1. A formation mechanism of a fullerene from a carbon onion.

Cox [4a] Achiba [4b] and Pellarin [4c] and their co-workers reported that carbon clusters were produced from two spatially separated sources; the first source produced mostly smaller ($n < 32$) carbon clusters when the laser fluence was higher, the preferential evaporation of C_{10} , C_{14} , and C_{18} reminiscent of the Hückel rule $4n+2$ for aromaticity, and the second source mostly larger ($n > 32$) carbon clusters were produced when the laser fluence was lower. The first and second sources above correspond to the linear or cyclic carbon clusters and the small or giant fullerenes, respectively, in the proposed growth mechanism of a fullerene from a carbon onion.

References:

- [1] T. Ogata, Y. Tatamitani, T. Mieno, *Carbon*, doi:10.1016/j.carbon.2008.10.048 (2008).
- [2] (a) P.J.F. Harris, *Chemistry and Physics of Carbon*, 28, 1-39 (2003); (b) F. Banhart, T. Füller, Ph. Redlich and P.M. Ajayan, *Chem. Phys. Lett.* 269, 349-355 (1997).
- [3] J.Y. Huang, D. Ding, K. Jiao, and B.I. Yakobson, *Phys. Rev. Lett.*, 99, 175503 (2007).
- [4] (a) D.M. Cox, K.C. Reichmann, A. Kaldor, *J. Chem. Phys.*, 88, 1588 (1988); (b) Y. Achiba & co-workers, *JCP*, 106, 9954 (1997) and *JCP*, 107, 8927 (1997); (c) M. Pellarin, et al., *JCP*, 117, 3088 (2002).

Corresponding Author: Teruhiko Ogata, **Tel&Fax:** +81-54-238-5105, **E-mail:** sctogat@ipc.shizuoka.ac.jp

Formation Mechanism of Polyynes Molecules upon Laser Ablation of Carbon Particles in Organic Solvents

○Tomonari Wakabayashi, Mao Saikawa, and Yoriko Wada

Department of Chemistry, Kinki University, Higashi-Osaka 577-8502, Japan

The small carbon cluster with a linear configuration can be stabilized by capping its reactive end with a hydrogen atom or a group of atoms containing other elements than hydrogen. Among such derivatives, polyynes, $\text{H}(\text{C}\equiv\text{C})_n\text{H}$, and cyanpolyynes, $\text{H}(\text{C}\equiv\text{C})_n\text{C}\equiv\text{N}$, are stable enough to be isolated in organic solvents. In recent years, these molecules have been formed by laser ablation of carbon particles in organic solvents and successfully isolated according to the size n . So far, the relative abundance has been merely controllable by changing the elements that the solvent molecule carries. Why are the products independent on the molecular structure of the solvent used? How can one control the abundance among the polyynes family? A key to the mechanism is to clarify from which, the powder or the solvent, atoms in the product molecule are coming.

In order to distinguish atoms in the carbon powder from those in the solvent, we used isotope-enriched carbon powder (10% ^{13}C or 96% ^{13}C) for laser ablation in the solvent with natural isotopic abundance (1.1% ^{13}C). After the separation of chemical species by using HPLC, ^1H and ^{13}C NMR spectra were measured. For ^{13}C NMR, the spectra for off-resonance conditions as well as those for proton-decoupled conditions were recorded, by which the coupling for the ^{13}C spin with the terminal ^1H could be determined. From the experimental data for the chemical shift δ and the spin-spin coupling constant, J_{CH} , the assignments for the NMR lines were given first, then the intensity for these lines were analyzed to deduce relative abundance of isotopomers. As a result, it turned out that the hydrogen in the product polyynes molecules were donated in the form of atomic hydrogen or proton rather than in the form of fragment of hydrocarbons.

Corresponding Author: Tomonari Wakabayashi

E-mail: wakaba@chem.kindai.ac.jp

Tel. 06-6730-5880 (ex. 4101) / FAX 06-6723-2721

Synthesis and Characterization of Crystalline Gold Nanowires encapsulated within Single-Wall Carbon Nanotubes

○Keita Kobayashi¹, Ryo Kitaura^{1,2}, Hisanori Shinohara^{1,2,*}

¹Department of Chemistry, Nagoya University, Nagoya 464-8602, Japan

²Institute for Advanced Research, Nagoya University, Nagoya 464-8602, Japan

Gold nanostructures, such as nanowires and nanoclusters, have been extensively investigated due to their novel structural and electronic properties that are not observed in bulk Au crystals. These studies include structural instability [1], surface Plasmon scattering [2], electronic conductivity [3], catalytic activity [4] and magnetic properties [5]. The gold nano-materials have been not only of fundamental interests in chemistry, physics and materials science but also held promise as versatile materials for development of novel nanotechnologies. Here, we report a bulk synthesis of crystalline gold nanowires using nano-sized one dimensional space of single-wall carbon nanotubes (SWCNTs)

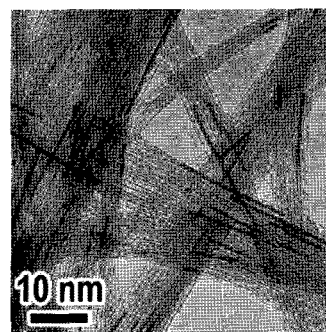


Figure 1: Typical TEM image of gold nanowires encapsulated within SWCNT

Au nanowires with 1-2 nm diameters have been synthesized by nano-template reaction of AuCl₃ within SWCNTs [6]. In the reaction, AuCl₃ was thermally decomposed to form Au nanowires in SWCNTs by high-temperature heating of AuCl₃@SWCNTs at 573 K under vacuum condition. Figure 1 shows a low-magnification TEM image of Au-nanowire@SWCNTs so-synthesized. Dark linear contrasts observed in SWCNTs correspond to the crystalline Au nanowires encapsulated. In the presentation, further structural analyses and optical properties of Au nanowires are discussed.

References: [1] S. Iijima and T. Ichihashi, *Phys. Rev. Lett.*, **56**, 616 (1986). [2] D. J. Smith *et al.*, *Science*, **233**, 872 (1986). [3] T. Nagao *et al.*, *Phys. Rev. Lett.*, **97**, 116802 (2006). [4] M. Haruta *et al.*, *J.Catal.*, **144**, 175 (1993). [5] T. Kizuka, S. Umehara and S. Fujisawa, *Jpn. J. Appl. Phys.* **40**, L71 (2001). [6] R. Kitaura *et al.*, *Nano Res.*, **1**, 152 (2008).

Corresponding Author: Hisanori Shinohara

E-mail: noris@nagoya-u.jp

Tel&Fax: +81-52-789-3660 / +81-52-789-6442

Semimetallic Molecular Nanowire: Oxygen Molecules Encapsulated into Carbon Nanotubes

○Michiko Tanaka¹, Takazumi Kawai², and Susumu Okada^{3,4}

¹*Physics Laboratory, College of Science and Technology, Nihon University,
Narashinodai, Funabashi, Chiba 274-8501, Japan*

²*Nano Electronics Research Laboratories, NEC Corporation,
Miyukigoka, Tsukuba, Ibaraki 305-8501, Japan*

³*Graduate School of Pure & Applied Sciences Center for Computational Sciences, University
of Tsukuba, Tennodai, Tsukuba, Ibaraki 305-8577, Japan*

⁴*CREST, JST, 4-1-8 Honcho, Kawaguchi, Saitama 332-0012, Japan*

One-dimensional space with the nanometer scale in carbon nanotubes is capable of encapsulating foreign molecules and atoms inside. Indeed, in this decade, fullerenes, organic molecules, water molecules, and metal atoms have been encapsulated and found to exhibit different characteristics to those are in their bulk three-dimensional phases. For instance, complexes comprising of fullerenes and nanotubes (carbon nano-peapods) exhibit interesting multiplicity of their electronic properties depending not only on encapsulated fullerene species but also on the space between fullerenes and nanotubes. In the case of water molecules, they form cylindrical crystalline phases under the unusual transition temperature depending on the diameter of the outer nanotubes. Thus, the foreign materials encapsulated inside the nanotubes are a novel class of their crystalline phases due to confinement and dimensionality effects inside the nanotubes.

In the present work, we examine the possibility of one-dimensional crystalline phases of the oxygen molecules inside the nanotubes based on the first-principle total-energy calculation within the framework of the density functional theory. In the calculations, we take zigzag (n,0) carbon nanotubes as container for the oxygen molecules and consider the polygonal tubes of the oxygen molecules along the wall of the nanotubes. Our calculations clearly show that the encapsulation of the oxygen molecules is exothermic. The calculated energy gain on the oxygen molecule encapsulation is found to be about 100 meV/molecules. The complexes are semimetals in which the electrons are distributed on majority spin bands of oxygen molecules while the holes are distributed on the nanotubes. Owing to the semimetallic characters, the non-integer spin polarization takes place on the polygonal chain of the oxygen molecules inside the nanotubes.

Corresponding Author: Michiko Tanaka

E-mail: rin@phys.ge.cst.nihon-u.ac.jp

Long Continuous Copper Nanowires Encapsulated in Carbon Nanotubes

○Akira Koshio^{1,2}, Hironobu Kito¹, Hiroyuki Nakano¹, Yuji Fujiwara^{2,3}, Hideki Sato^{2,4}
and Fumio Kokai^{1,2}

¹*Division of Chemistry for Materials, Graduate School of Engineering,*

²*The Center of Ultimate Technology on nano-Electronics, MIE-CUTE,*

³*Division of Physics Engineering, Graduate School of Engineering,*

⁴*Division of Electrical and Electronic Engineering, Graduate School of Engineering,
Mie University, 1577 Kurimamachiya-cho, Tsu, Mie 514-8507, Japan*

Metal nanowires have been extensively studied as one-dimensional nanomaterials with nanocable structures suitable for nanoelectronic and sensor applications. However, some problems related to quality, such as stability, crystallinity, and long one-dimensional growth, still remain. The hybridization of metal nanowires and carbon nanotubes has been tried as one of the ideas for improving the quality of metal nanowires. Some metal encapsulated carbon nanotubes have been generated by arc vaporization of carbon electrodes containing metal or metal oxide. We have succeeded in the effective production of copper nanowires encapsulated in carbon nanotubes (CuNW@CNTs). The CuNW@CNTs can be produced at more than 90% of the filling rate by using the hydrogen arc discharge method. Here we report the simple synthesis of high density and high purity CuNW@CNTs with micrometers in length and their useful properties for applications.

CuNW@CNTs were produced by the conventional DC arc discharge. A hole (3 mm diameter) was drilled in the center of a graphite anode (5 mm diameter) and filled with copper powder. 20 mm in diameter graphite rod was used for the cathode. The two electrodes were set vertically in a vacuum chamber. Hydrogen gas was filled up the chamber at a pressure of 0.1 MPa and was flowed at 500 ml/min during arc vaporization. Arc discharge was maintained at 50-90 A for 1 min.

CuNW@CNTs deposited on surfaces of the inner chamber wall (chamber soot) and the cathode (cathode soot). The yield and filling rate of CuNW@CNTs in the chamber soot were extremely high. Many TEM observations clarified that more than 90% of the as-prepared CNTs were filled perfectly with CuNWs. Their diameters and lengths were about 40 nm and more than 1 μm , respectively. The CuNW@CNT consists of less than 10-nanotube layers and fcc copper crystals inside the CNT in a long-range order. On the other hand CuNW@CNTs included in the cathode soot were very long and thick. Their diameters and lengths were about 120 nm and more than 10 μm , respectively. However the filling rate was about 30%. The structure and yield depend on the arc discharge condition such as arc current and content of copper powder in the graphite anode.

We have also found that CuNW melted and came out from the tip of CNT by heat treatment at the temperature of more than about 500 °C in vacuum. This simple technique would be useful for “nano-welding” between CNT and metallic materials. Moreover we are now studying to utilize CuNW@CNTs as applications such as transparent conductive films and conduction enhancement for batteries.

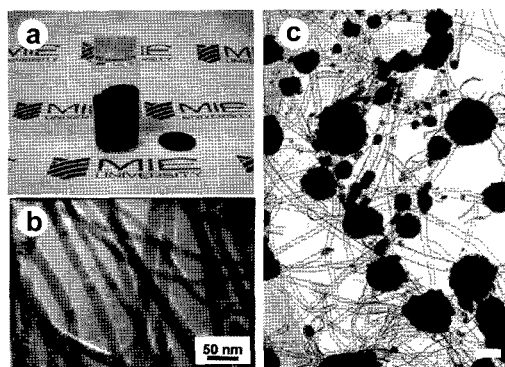


Fig. 1 (a) as-prepared sample of about 5 g , (b) as-prepared and (c) 700 °C heat treated-CuNW@CNTs.

Corresponding Author: Akira Koshio, **E-mail:** koshio@chem.mie-u.ac.jp, **Tel & Fax:** +81-59-231-5370

Fabrication and Chemical modification of Nanographene

○K.Takai*, Y. Nishimura, T. Enoki

Department of Chemistry, Tokyo Institute of Technology, 2-12-1-W4-1, Ookayama, Meguro, Tokyo, JAPAN

Like other materials, nano-size effect is interesting on graphene. Indeed, nano-sized graphene (nanographene) has been known to have enhanced magnetism in spite of its non-magnetic nature in its bulk form [1, 2, 3]. When a graphene sheet is cut along the zigzag direction, strongly spin-polarized non-bonding π -state (edge state) appears along the created edges, in spite that cutting along the armchair direction produces no such state. Meantime, the presence of edges gives graphene the potential to control its electronic properties through the chemical modification. According to the ab initio calculation [4], The fluorine-termination of the zigzag edge vanishes magnetism, while the combination of the mono-hydrogenated and di-hydrogenated zigzag edges gives rise to strong ferromagnetism, where ferromagnetic spin polarization is distributed homogeneously in the entire area of the nanographene. Here, I present the novel magnetic and transport properties of nanographene and its assembly systems, and tuning its electronic properties through chemical modification. For fabricating single nanographene sample, the nano-patterned gold mask was fabricated on graphene sample prepared by cleaving method, where oxygen plasma was used for etching process. Through this process, nanographene sample (ribbons, grids, dots) with the size down to 50 nm was successfully fabricated. On the other hand, magnetism of graphene and its chemical modification effect was examined by using nanographene network material (activate carbon fibers; ACFs). Magnetic susceptibility of nanographene with 2-3 nm shows localized spin magnetism feature with Curie-Weiss type temperature dependence, which is attributed to the edge-state spin [2, 3]. On the other hand, the orbital diamagnetism is much suppressed by the reduction in size of systems, which is major feature of the magnetism of bulk graphene. The chemical modification features the peculiar character of the edge-state spin magnetism well. In the lower fluorine concentration of F/C~0.4, the reaction with fluorine atoms takes place mainly around the edges of nanographene due to its chemical activity, resulting in the decreasing in the concentration of edge state spins. The spin polarization of the edge state is suppressed by fluorine termination of the edge sites as mentioned above. After the fluorination is completed at the edges, fluorine attacks the interior carbon sites of nanographene, where a vacancy of π -electron network is generated with creation of a σ -dangling bond spin. Dangling bond spins are soon terminated by other fluorine, which causes a maximum in the spin concentration at F/C~0.8, and complete vanishment of spin magnetism at F/C~1.2 [5]. Such the radical reactivity of fluorine with carbon enables the modification of the topology of π -electron network of nanographene. The chemical modification of the nanographene edge by bromine gives other interesting aspect of the edge-state spin magnetism. By terminating the edge of nanographene with bromine, the edge-state slightly hybridizes with the bromine orbital as suggested by the hyper fine broadening in the ESR line width, followed by the gradual reduction in the g-value as bromine content increases [6]. This suggests the tunable nature of the spin-orbit coupling in nanographene by the chemical modification. The present study is partially supported by MEXT Nanotechnology Network Project in the Tokyo Institute of Technology.

References

- [1] M. Fujita, K. Wakabayashi, K. Nakada, and K. Kusakabe, *J. Phys. Soc. Jpn.* **65**, 1920 (1996).
- [2] T. Enoki, K. Takai, "Unconventional magnetic properties of nanographite" (*Carbon-based magnetism*, p. 397, ed. F. Palacio and T. Makarova, Elsevier, Amsterdam, 2006).
- [3] T. Enoki, K. Takai, *Dalton Trans.*, 3773 (2008)
- [4] K. Kusakabe and M. Maruyama, *Phys. Rev. B* **67**, 092406 (2003).
- [5] K. Takai, H. Sato, T. Enoki, N. Yoshida, F. Okino, H. Touhara, and M. Endo, *J. Phys. Soc. Jpn.*, **70**, 175 (2001).
- [6] K. Takai, H. Kumagai, H. Sato, and T. Enoki, *Phys. Rev. B* **73**, 035435 (2006).

Corresponding: Kazuyuki Takai

E-mail: ktakai@chem.titech.ac.jp, **Tel:** +81-3-5734-2610, **Fax:** +81-3-5734-2242

Half-metallic Armchair Graphene Nanoribbon

○Keisuke Sawada¹, Fumiyuki Ishii^{1,2}, Mineo Saito¹

¹ Division of Mathematical and Physical Science, Graduate School of Natural Science and Technology, Kanazawa University, Kakuma, Kanazawa 920-1192, Japan

² Reserach Institute for Computational Sciences, National Institute of Advanced Industrial Science and Technology (RICS-AIST), 1-1-1 Umezono, Tsukuba, Ibaraki 305-8568, Japan

Success of fabrication of graphenes allows experimental studies of this system and then unique electronic properties are revealed[1]. Among a variety of applications of graphenes, nano-scale spintronics applications are considered to be hopeful. For an example, spin transport has been experimentally observed by using graphene layers[2]. There are two type of shaped edge in graphene nanoribbon (GNR), one of them is armchair GNR (AGNR) and another is zigzag GNR (ZGNR). Armchair edges are often observed compared with the zigzag[3]. Previous first-principles calculation predicted that the armchair edge is more stable than the zigzag edge in the edge of graphene[4]. However, the AGNR is believed to have the nonmagnetic structure whereas the magnetic properties due to the flat-band ferromagnetism in ZGNR attracted much attention.

In this paper, we perform first-principles density functional calculation on dehydrogenated AGNR (See Fig. 1). Surprisingly, we find that dehydrogenated AGNR has a magnetic state in the case of carrier doping. Magnetic state of the carrier-induced AGNR has ferromagnetic chains at the two edges having the same directions of the magnetic moments. We conclude that the carrier-doped AGNR is *half-metallic* as shown in Fig. 2.

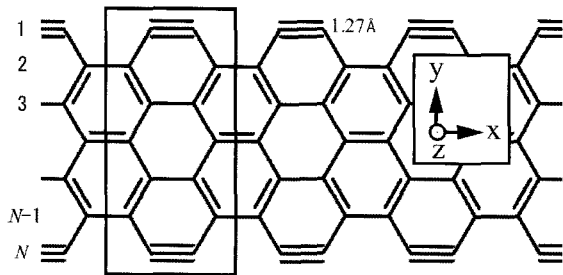


Figure 1. The lattice structure of AGNR.

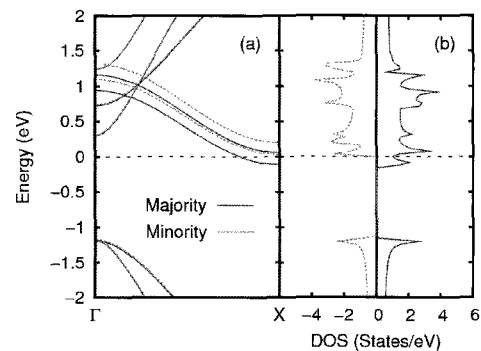


Figure 2. The band structure and density of states of FM state in AGNR.

[1] K. S. Novoselov *et al.*, *Science* **306**, 666 (2004).

[2] M. Ohishi *et al.*, *Jpn. J. Appl. Phys.* **46**, L605 (2007).

[3] Y. Kobayashi *et al.*, *Phys. Rev. B* **71**, 193406 (2005).

[4] S. Okada, *Phys. Rev. B* **77**, 041408(R) (2008).

Corresponding Author: Keisuke Sawada

E-mail: sawada@cphys.s.kanazawa-u.ac.jp

Selective synthesis of carbon nanotubes and graphene multi-layers by controlling catalyst thickness

○Daiyu Kondo^{1,2,3}, Shintaro Sato^{1,2,3}, Mizuhisa Nihei^{1,2,3}, and Yuji Awano¹

¹*Nanotechnology Research Center, Fujitsu Laboratories Ltd., 10-1 Morinosato-Wakamiya, Atsugi 243-0197, Japan*

²*Fujitsu Limited, 10-1 Morinosato-Wakamiya, Atsugi 243-0197, Japan*

³*CREST-JST, 4-1-8 Hon-machi, Kawaguchi, Saitama 332-0012, Japan*

Carbon nanotubes (CNTs) and graphene are two of carbon allotropes. CNTs and graphene are usually synthesized using different CVD methods and/or conditions [1-2]. In this study, we demonstrate selective synthesis of CNTs and graphene multi-layers just by changing catalyst thickness and discuss the synthesis mechanism of such carbon allotropes.

CNTs and graphene multi-layers were obtained by hot-filament chemical vapor deposition (CVD). The CVD process was performed in a low-pressure vacuum chamber. As the carbon source, a mixture of acetylene and argon gases was introduced into the CVD chamber. The substrate temperature and total pressure were 620 °C and 1kPa, respectively. As a catalyst, an iron film sputtered on a silicon substrate with 350-nm thick silicon dioxide was used. The iron (Fe) films with thicknesses between 2.5-100 nm were prepared. CNTs and graphene thus synthesized were analyzed by using scanning electron microscopy (SEM), transmission electron microscopy (TEM) and Raman measurements.

Figure 1 shows SEM images of the samples observed after CVD growth with different Fe thicknesses of (a) 2.5 and (b) 100 nm. At a thickness of 2.5 nm, vertically aligned CNTs were obtained. On the other hand, a film-like structure with multiple domains was observed on the substrate with a 100-nm thick Fe film. The product was found to be 13-nm thick graphene multi-layers by TEM analyses. In fact, we have found that only CNTs were obtained with Fe films thinner than 7.5 nm, while graphene multi-layers was formed with the catalyst films thicker than 20 nm. These results show that one can obtain CNTs or graphene just by controlling the catalyst thickness under the same growth condition. The authors thank Dr. N. Yokoyama, Fellow of Fujitsu Laboratories Ltd. for his support and useful suggestions.

[1] M. Yudasaka *et al.*, *JVST A* 13(1995)2142.

[2] D. Kondo *et al.*, *Nanotechnology* 19(2008) 435601.

Corresponding Author: Daiyu Kondo

E-mail: kondo.daiyu@jp.fujitsu.com

Tel&Fax: +81-46-250-8234&+81-46-250-8844

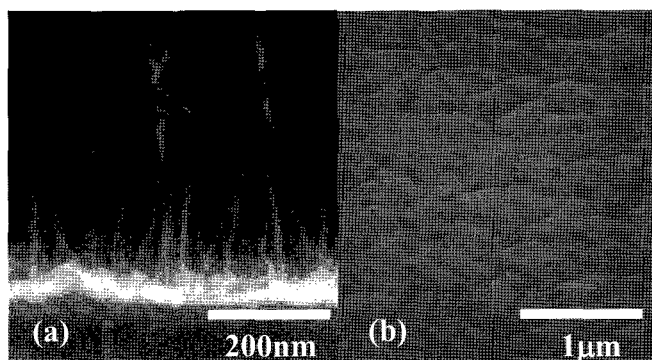


Figure 1 SEM images of (a) CNTs and (b) graphene multi-layers.

**Consequences of multi-pole electrostatic potential fields on the surface of
single-nano buckydiamond (SNBD) particles**

Eiji Ōsawa¹, Dean Ho^{2,3}, Houjin Huang², Michail V. Korobov⁴,
and Natalia N. Rozhkova⁵

¹ NanoCarbon Research Institute, AREC, Faculty of Textile Science and Technology, Shinshu University, 3-15-1 Tokita, Ueda, Nagano 386-8567, Japan

² Departments of Biomedical and Mechanical Engineering, Robert R. McCormick School of Engineering and Applied Science, Northwestern University, Evanston, Illinois 60208, USA

³ Robert H. Lurie Comprehensive Cancer Center of Northwestern University, Chicago, Illinois 60611, USA

⁴ Department of Chemistry, Moscow State University, Moscow 19899, Russia

⁵ Institute of Geology, Karelian Research Centre RAS, Petrozavodsk 185610, Russia

Abstract

Discovery of strong electrostatic fields on the surface of primary particles of detonation nanodiamond or SNBD[1] by Barnard and Sternberg[2,3] not only provided a likely explanation on the origin of agglutination in the crude detonation product in terms of ‘*coherent Coulombic interfacial interaction*.’ The event also marked the first recognition in nanoscience of a novel interparticle interaction type that can be as strong as C-C covalent bonding. The sign and potential distribution of the electrostatic field are characteristic to the crystallographic indices of facets and size of particles, thus the electrostatic feature could well be unique to lower-nano crystalline particles, and of internal origin. A mechanism of self polarization in the energy-minimized nanodiamond crystals by means of orbital interactions through space and bond is presented [4].

The facet-to-facet binding interactions among SNBD particles manifest themselves when the dispersed particles aggregate to form gel and dry flakes. However, aggregation usually takes place so fast that there is no time for the interacting particles to reach coherent configurations in the binding of facet. Here we deal with *incoherent Coulombic interactions*, still much stronger than the usual *van der Waals* interactions. Interestingly, the aggregates produce a certain network structure having nanopores with 10 nm in diameter in both gel and dried flake [5]. These incoherent aggregates can be re-dispersed into primary particles, especially readily in gel. The gel is particularly interesting in that its complex with ionic drugs like Adriamycin hydrochloride offers highly promising platform for novel drug carrier system, wherein drug molecules are firmly bound to the facet of SNBD by charge-charge interaction, but can be slowly released by adjusting pH of medium [6].

[1] Ōsawa, E. *Pure & Appl. Chem.*, **2008**, *80*, 1365-1379.

[2] Barnard, A.; Sternberg, M. *J. Mater. Chem.* **2007**, *17*, 4811-4819.

[3] Barnard, A. *J. Mater. Chem.* **2008**, *18*, 4038-4041.

[4] Ōsawa, E.; Ho, D.; Huang, H.; Korobov, M. V.; Rozhkova, N. N. submitted for publication in *Diam. Rel. Mater.*

[5] Korobov, M. V.; Efremova, M. M.; Avramenko, N. V.; Ivanova, N. I.; Rozhkova, N. N.; Ōsawa, E. submitted for publication in *J. Am. Chem. Soc.*

[6] Huang, H.; Pierstorff, E.; Ōsawa, E.; Ho, D. *Nano Lett.* **2007**, *7*, 3305-3314.

Corresponding Author: Eiji Ōsawa

E-mail: osawaeiji@aol.com

Tel&Fax: 0268-75-8381, 0268-75-8551

Chirality Sorting of Single-Walled Carbon Nanotubes Using Density Gradients Centrifugation

○Yuichi Kato¹, Yasuro Niidome¹ and Naotoshi Nakashima^{1,2}

¹*Department of Applied Chemistry, Graduate School of Engineering, Kyushu University, 744 Motoooka, Fukuoka, 819-0395, Japan*

²*Japan Science and Technology Agency, CREST, 5 Sanbancho, Chiyoda-ku, Tokyo, 102-0075, Japan*

Single-walled carbon nanotubes (SWNTs) are consist of a single graphite sheet seamlessly wrapped into a cylindrical tube. SWNT chirality sorting has been an anticipated technique for realizing practical applications of SWNTs especially in the field of nanoelectronic devices since the properties of the SWNTs depend on their size and electronic structures. Density gradients centrifugation allows SWNTs to be sorted by their buoyant density which depend on their diameter^[1].

We solubilized SWNTs HiPco in water using sodium cholate. We tried to realize chirality sorting using density gradients centrifugation. The SWNT solution was layered on the top of the density gradient, and centrifuged for 8 h at 174000 ×g. The centrifuged SWNT solution was collected, and their absorption and luminescence spectra in near infrared regions were measured using a microcell.

[1] M. S. Arnold, A. A. Green, J. F. Hulvat, S. I. Stupp, M. C. Hersam, *Nature Nanotech.*, **1**, 60 (2006).

Corresponding Author: Naotoshi Nakashima

TEL: 092-8022-2841, FAX: 092-8022-2843, E-mail: nakashima-tcm@mail.cstm.kyushu-u.ac.jp

Diameter and Chirality Distribution of SWNTs Grown from Zeolite Surfaces

○Yoichi Murakami¹, Takahiko Moteki¹, Suguru Noda¹,
Tatsuya Okubo¹, Shigeo Maruyama²

¹*Dept. of Chemical System Engineering, The University of Tokyo, Tokyo 113-8656*

²*Dept. of Mechanical Engineering, The University of Tokyo, Tokyo 113-8656*

Zeolites are microporous, crystalline aluminosilicates constructed from tetrahedral base units. We have been using the *b*-surfaces of silicalite-1 zeolite (framework: MFI) as catalyst support for catalytic CVD growth of single-walled carbon nanotubes (SWNTs). Figure 1a shows an FE-SEM image of the zeolite crystals directly synthesized on a Ti-deposited quartz substrate. We sputtered Co and grew SWNTs by alcohol CVD method. SWNTs were grown only from the top surfaces (i.e., *b*-surfaces) of the crystals since the underneath Ti layer suppressed the catalyst activity of Co. Figure 1b shows an example of suspended SWNTs between top surfaces of the adjacent crystals. In addition, we develop crystalline silicate layers, prepared such as by delaminating ITQ-2 layered material [1], for catalyst support in the SWNT growth.

The diameter/chirality distribution of obtained SWNTs is directly determined by characterizing suspended individual SWNTs one by one with micro-photoluminescence spectroscopy (Fig. 2). We discuss the effect of catalytic CVD conditions as well as the support material on the resultant diameter/chirality distribution.

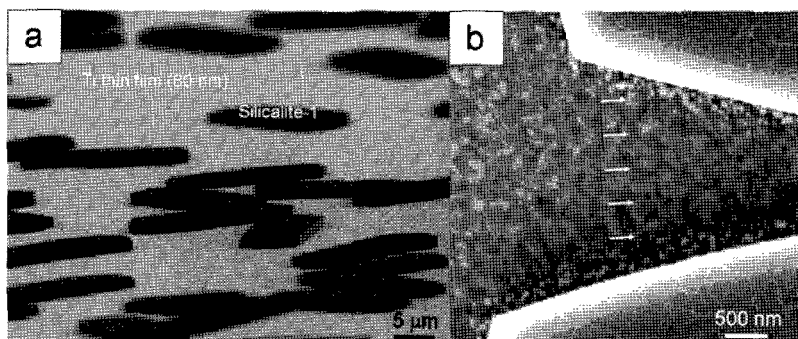


Fig. 1: FE-SEM images of the sample. (a) Silicalite-1 crystals directly grown on a Ti-deposited quartz substrate. (b) Suspended SWNT between top surfaces of two adjacent silicalite-1 crystals (indicated by arrows).

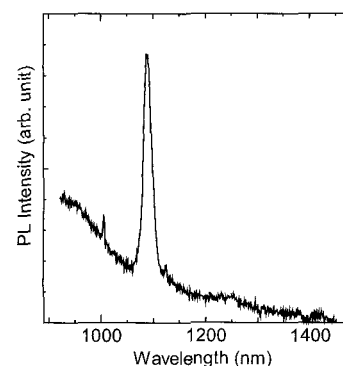


Fig.2: Typical photoluminescence emission measured from a suspended individual SWNT.

[1] A. Corma et al., *Microporous Mesoporous Mater.* **38** (2000) 201

Corresponding Author: Shigeo Maruyama

TEL: +81-3-5841-6421, FAX: +81-3-5841-6408, E-mail: maruyama@photon.t.u-tokyo.ac.jp

Highly Selective Production of Single-Wall Carbon Nanotubes by Laser Vaporization method

- Yohji Achiba¹⁾, Takashi Nakaya¹⁾, Akihito Inoue¹⁾, Yuki Onishi¹⁾, Takeshi Kodama¹⁾ and Toshiya Okazaki²⁾

¹*Department of Chemistry, Tokyo Metropolitan University, Tokyo 192-0364, Japan*

²*AIST, Tsukuba, Ibaraki 305-8568, Japan*

1. Introduction

Chirality control and selective production of single wall carbon nanotubes with a specific chiral index is undoubtedly one of the essential issues in the science and technology of carbon nanotubes, particularly in the application field such as electronic devices. However, so far no direct evidence showing the production of SWNT with a single chirality has been reported, even though the several reports have pointed out that the formation of near armchair structure would possibly be much more favorable in comparison with other (n,m) species. In the present paper, we will demonstrate highly selective production of SWNTs with very specific (n,m) induces by means of laser vaporization-furnace method which could be notified as the first step for the future development of the SWNT's with a single (n,m) chiral distribution.

2. Experimental Method

Single-wall carbon nanotubes were prepared by a laser vaporization method with use of NiCo and RhPd catalyst under variety of conditions such as gas temperature, gas pressure and laser power etc.. As-grown sample was characterized by laser Raman scattering method, and optical absorption and fluorescence measurements were taken place in toluene solution with use of PFO polymer after conventional dispersion treatments such as homogenization, sonication as well as centrifugation .

3. Results and Discussion

The size and chirality distribution of SWNTs prepared at the different laser vaporization condition were investigated mainly by optical absorption measurements as well as fluorescence measurements. More than hundred different samples prepared at different conditions were studied and characterized. Major aspects revealed in the present paper are: 1) The (7,6) chiral species is the most abundant in the RhPd system. 2) The (8,7) tube is the one for the NiCo system. 3) Broad chirality distribution is found for the tubes with the size larger than (9,7). The detailed discussion will be presented in the symposium.

Corresponding Author: Yohji Achiba

TEL: +81-42-677-2534, FAX: +81-42-677-2525, E-mail: achiba-yohji@tmu.ac.jp

Impact of Molecular Structure of Carbon Source in CVD Growth of SWCNTs

○Bikau Shukla¹, Takeshi Saito^{1,2}, Motoo Yumura¹ and Sumio Iijima¹,

¹ AIST, Higashi-1-1, Tsukuba, Ibaraki, Japan

²PRESTO, Japan Science and Technology Agency, Kawaguchi 332-0012,

Although chemical vapor deposition (CVD) growth of single walled carbon nanotubes (SWCNTs) is a promising process, its growth mechanism hasn't been understood yet. Physical mechanism¹⁻³ reported earlier is not enough to understand this complex process which shows the need of reaction mechanism of growth. Considering this necessity SWCNTs were grown from intentionally selected nine aromatic hydrocarbons differ in functional groups of sp , sp^2 and sp^3 under very dilute condition i.e 5 μ L/min feedstock in \sim 7 L/min H_2 carrier gas. Particularly they are toluene, ethylbenzene, p-xylene, propylbenzene, styrene, allylbenzene, p-divinylbenzene, phenylacetylene and 3-phenyl-1-propyne. Analysis of these results suggested an obvious fact about the efficient precursor accountable for the growth. Production of different

quantities of CNTs differ in diameters only from propylbenzene, styrene, allylbenzene and p-divinylbenzene is remarkable (fig.1).

Resonance Raman (fig.2), SEM and TEM analysis confirm that produced CNTs are SWCNTs. To understand these differences in yields and properties of SWCNTs, thermal decomposition patterns of those hydrocarbons have been analyzed which suggested the molecular structure of hydrocarbons as key factor. More particularly hydrocarbons that can supply directly or indirectly sp^2 species, C_2H_3/C_2H_4 can grow SWCNTs effectively. Since C_2H_3/C_2H_4 directly affects quantity and diameter of SWCNTs, it deserves to be the most efficient precursor.

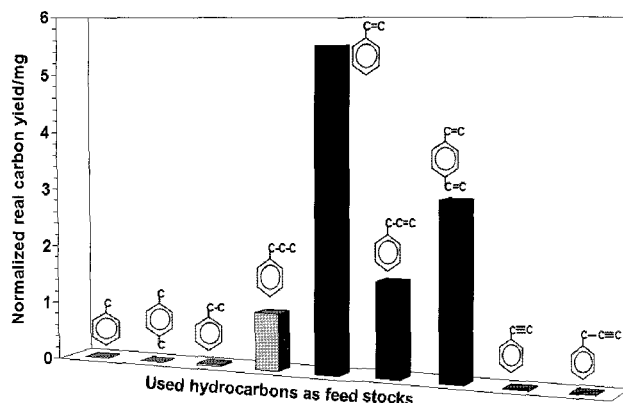


Fig.1. Carbon contents in as grown products

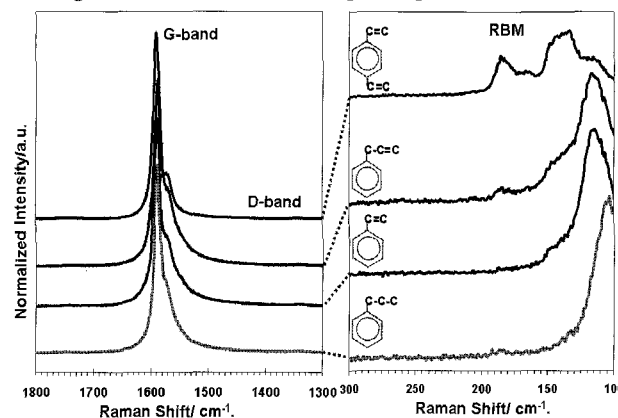


Fig.2. Resonance Raman spectra of as grown products

References

1. S. Huang, M. Woodson, R. Smalley, J. Liu, Nano Lett., 2004, 4, 6, 1025.
2. W.H.Wang, Y.R.Peng, P.K. Chuang, C.T.Kuo, Diamond and Related Materials, 2006, 15, 1047
3. S. Inoue, Y. Kikuchi, Chem. Phys. Lett., 2005, 410, 209.

Corresponding Author: Takeshi Saito, TEL: 029-861-5080, FAX: +81-29-861-4413, E-mail: takeshi-saito@aist.go.jp

Geometry Control of Vertically Aligned SWNTs through Liquid-based Catalyst Manipulation

Rong Xiang, Erik Einarsson, Junichiro Shiomi, Shigeo Maruyama*

Department of Mechanical Engineering, the University of Tokyo

We present a versatile wet chemistry method to localize the growth of SWNTs to desired regions via surface modification. By functionalizing the silicon surface using a classic self-assembled monolayer (SAM) and then selectively removing the SAM by ultraviolet (UV) light, the catalyst can be dip-coated onto only the hydrophilic areas of the substrate. This technique was successful in producing both random and aligned SWNTs with various patterns. (Schematic and examples in Figure) The precise control of the morphology of SWNTs, achieved by simple and scalable liquid-based surface chemistry, could facilitate the application of SWNTs as the building blocks of future nano-devices.

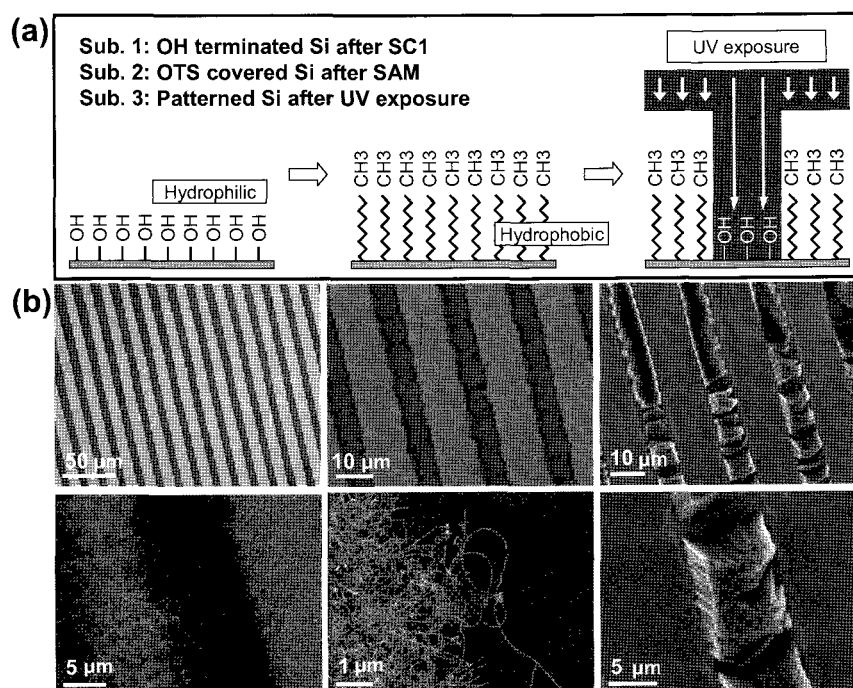


Figure. (a) Schematics describing the fabrication procedure of hydrophilic/hydrophobic patterns using a selective removal of OTS SAM by UV exposure; (b) SEM images of random and vertically aligned SWNT line-shape patterns.

*Email address: maruyama@photon.t.u-tokyo.ac.jp

Top-Down Approach to Align Single-Walled Carbon Nanotubes on Silicon Substrate

○Carlo M. Orofeo,¹ Hiroki Ago,^{*1,2,3} Naoki Yoshihara,¹ and Masaharu Tsuji^{1,2}

¹ Graduate School of Engineering Sciences, Kyushu University, Fukuoka 816-8580, Japan

² Institute for Materials Chemistry and Engineering, Kyushu University

³ PRESTO, Japan Science and Technology Agency

In order to fully exploit the superior electronic properties of single-walled carbon nanotubes (SWNTs), the growth of horizontally aligned SWNTs on suitable substrates is a critical step for large-scale nanotube-based electronics. Such alignment has been demonstrated on single-crystal substrates such as sapphire (α -Al₂O₃) [1] and quartz (SiO₂) [2]. The proposed mechanism is that SWNTs align on a particular atomic arrangement or along the ordered atomic steps after substrate treatment. These results are important for future nanoelectronics applications because the nanotubes' alignment on a substrate improves the efficiency of device fabrication and enables nanotube integration on circuits. SWNT alignment on a SiO₂/Si substrate is expected since the current FET configuration is fabricated on a Si wafer with an oxide SiO₂ layer. The most obvious path for the realization of this device configuration is the transfer of the nanotubes aligned on single crystals. However, this approach is often tedious and possesses an intrinsic possibility for carbon nanotube contamination and deterioration. Here, we present a new, top-down based approach to align SWNTs directly on SiO₂/Si substrate after substrate modification [3].

We modify the silicon substrate by creating trenches via electron beam (EB) lithography followed by reactive ion etching (RIE). After CVD, it was observed that nanotubes align in the direction along the created trenches regardless of the gas flow. Furthermore,

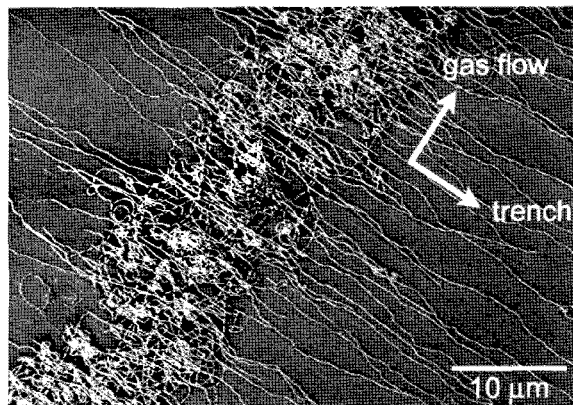


Fig. 1. SEM image of the as-grown SWNTs aligned along the created trenches on SiO₂/Si wafer.

devices created on the aligned SWNTs showed acceptable on/off ratio and mobilities comparable to transferred nanotubes on SiO₂/Si substrate [4]. This is the first observation of the aligned nanotubes along the artificially-made trench structure as far as we know. Our method opens up the possibility of large-scale integrated nanotube electronics for mass production.

References: [1] H. Ago *et al.*, *Chem. Phys. Lett.*, **408**, 433 (2005). [2] C. Kocabas *et al.*, *Small*, **1**, 1110 (2005).
[3] C. M. Orofeo *et al.*, *Appl. Phys. Lett.*, submitted. [4] L. Qu *et al.*, *NanoLett.* **8**, 2682 (2008).

Corresponding Author: Hiroki Ago (Tel&Fax: +81-92-583-7817, E-mail: ago@cm.kyushu-u.ac.jp)

Fluidized Bed Synthesis of Sub-Millimeter-Long Single-Walled Carbon Nanotubes

○Dong Young Kim, Hirofumi Fukai, Hisashi Sugime, Kei Hasegawa,
Toshio Osawa, Suguru Noda

*Department of Chemical System Engineering, School of Engineering,
The University of Tokyo, 7-3-1 Hongo, Bunkyo-ku, Tokyo 113-8656, Japan*

Single-walled carbon nanotubes (SWCNTs), possessing unusual one-dimensional structures and peculiar properties, have great potential for their applications in frontier nanotechnological fields. However, applications for SWCNT-based nanotechnologies such as electronic devices and flexible displays are still limited by difficulty of mass production of SWCNTs with high quality.

In this study, we applied the rapid growth method of vertically aligned SWCNTs on substrates [1] to fluidized bed using spherical ceramic spheres as catalyst supports [2]. Fe/Al₂O₃ catalyst was prepared on commercially available Al₂O₃ or ZrO₂ spheres (0.5 mm in average diameter) either by sputtering using Al and Fe targets or impregnation using aqueous solution of Al(NO₃)₃ and Fe(NO₃)₃, as shown in Figure 1(a). These spheres were treated under H₂/Ar and chemical vapor deposition (CVD) was carried out for 10 min with C₂H₄ or C₂H₂ feedstocks at 1093 K. Figure 2 shows the fluidized bed reactor (quartz tube with inner diameter of 22 mm) after CVD and 0.5-mm-tall, vertically aligned SWCNTs on Al₂O₃ spheres. These SWCNT forests have a catalyst impurity level below 0.1 wt% and can be synthesized at about 230 mg/ batch by using fluidized bed reactor of about 50 cm³ in volume. This SWCNT yield is 20 times larger than by SWCNTs growth on flat substrates in the preceding study [1]. Fluidized bed synthesis, which utilizes 3D space of the reactor volume and is practically used in hydrocarbon reforming at a large scale, is promising in realizing mass production of high-purity, sub-millimeter long SWCNTs.

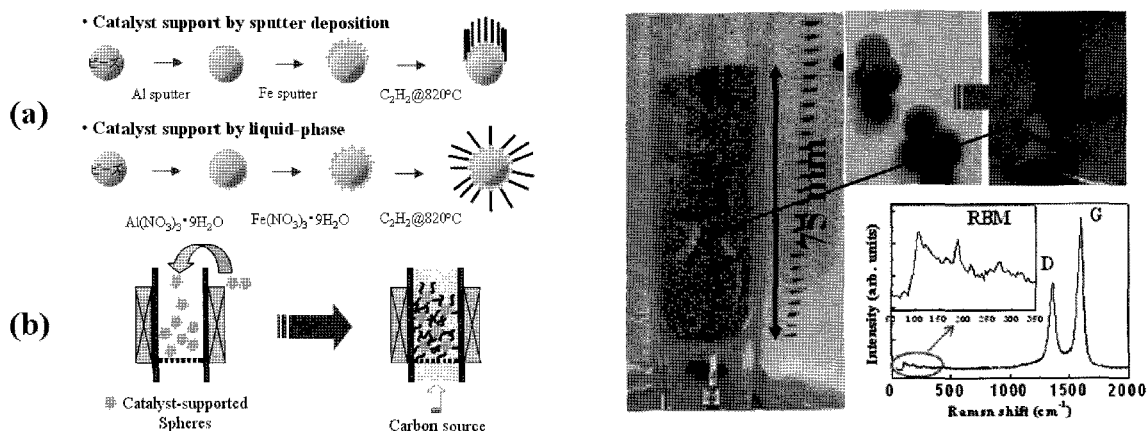


Fig. 1. Catalyst preparation & fluidized bed CVD. **Fig. 2.** Synthesized SWCNTs & Raman spectrum

[1] S. Noda, K. Hasegawa, H. Sugime, K. Kakehi, Z. Zhang, S. Maruyama, and Y. Yamaguchi, *Jpn. J. Appl. Phys.* **46**, L399 (2007).

[2] R. Xiang, G. Luo, W. Qian, Y. Wang, F. Wei, and Q. Li, *Chem. Vap. Deposit.* **13**, 533 (2007).

Corresponding Author: Suguru Noda, Tel&Fax: +81-3-5841-7332, E-mail: noda@chemsys.t.u-tokyo.ac.jp

Purity Evaluation of Single Wall Carbon Nanotubes based on Raman Spectroscopy

○D. Nishide^{1,2}, Y. Miyata¹, K. Yanagi^{1,2}, T. Tanaka¹, H. Kataura^{1,2}

¹*Nanotechnology Research Institute, AIST, Tsukuba, Ibaraki 305-8562, Japan*

²*JST, CREST, Kawaguchi, Saitama, 332-0012, Japan*

Purity evaluation is an important problem awaiting solution in the fundamental research field and the consumer market of single wall carbon nanotubes (SWCNTs). For the quantitative purity evaluation, we need probe signals which are proportional to the abundance of SWCNTs in the sample and a 100% purity SWCNT sample as a standard. Intrinsic optical absorption intensity of SWCNTs can be used as a probe signal for the purity evaluation [1,2]. However, a baseline correction is required to obtain the accurate absorption intensity of SWCNTs from the spectrum because a tail of the broad UV absorption is overlapping. On the other hand, Raman intensity is also related to the intrinsic optical absorption of SWCNT by way of the resonance effect.

In this paper, we prepared various purity samples by mixing high-purity SWCNTs and amorphous carbon, and measured Raman spectra. Here, an extremely high-purity SWCNT sample was obtained by an ultracentrifugation without changing chirality distribution. It was found that the Raman signal from the isolated SWCNTs in a water solution is proportional to the abundance of SWCNTs. Figure 1 shows G-band Raman intensity as a function of the purity of SWCNTs with some SEM images. Linear correlation between the purity and the Raman intensity was clearly observed. Finally we propose a new method for quantitative purity evaluation of SWCNTs based on Raman spectroscopy. We will introduce the detailed protocol and will demonstrate the purity of various SWCNTs evaluated by this method.

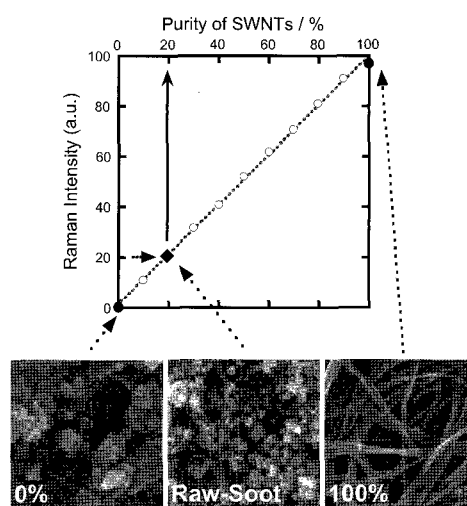


Fig.1: Raman intensity plot as a function of the purity of SWCNTs

[1] M. E. Itkis *et al.*, *J. Am. Chem. Soc.* **127** (2005) 3439. / [2] M. S. Jeong *et al.*, *Nano* **3** (2008) 101.

Corresponding Author: Hiromichi Kataura

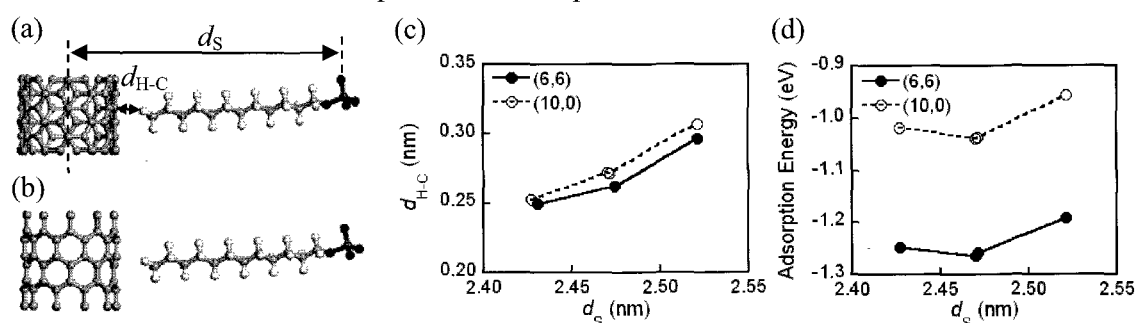
E-mail: h-kataura@aist.go.jp / **Tel:** +81-29-861-2551 / **Fax:** +81-29-861-2786

***Ab Initio* Energetics of Sodium Dodecyl Sulfate on Metallic and Semiconducting Single-Wall Carbon Nanotubes**

Mari Ohfuchi

*Nanotechnology Research Center, Fujitsu Laboratories Ltd.,
10-1 Morinosato-Wakamiya, Atsugi 243-0197, Japan*

Recently several experiments on separation of metallic and semiconducting single-wall carbon nanotubes (SWCNTs) have been reported [1-3]. Sodium dodecyl sulfate (SDS) seems to play an important role individually [1] and in combination with another surfactant [2] or agarose gel [3] by interacting more strongly with metallic SWCNTs than with semiconducting ones. In this study, we examine the adsorption energies E_a of a SDS anion on metallic (6, 6) and semiconducting (10, 0) SWCNTs (Figs. (a), (b)) having similar diameters of 0.82 and 0.79 nm. We adopt *ab initio* method using localized basis functions optimized for biological molecules [4, 5]. The real and reciprocal space grids are set to ensure accuracy within 0.01eV of E_a per SDS molecule. When the SDS anion is moved toward the SWCNTs and the atomic structure is optimized, mainly the end of the hydrophobic tail of SDS deforms (Fig. (c)) and E_a dose not change much (Fig. (d)). The lowest E_a for the (6, 6) tube is -1.26 eV, which is stronger than -1.04 eV for the (10, 0) tube. This can be attributed to the larger charge transfer Q from SDS to the metallic SWCNT: Q are 0.31 and 0.28 e for the (6, 6) and (10, 0) tubes. The result is consistent with the recent experiments of separation.



Figs. Optimized structures of SDS on (a) (6, 6) and (b) (10, 0) carbon nanotubes (CNTs). The symbols d_S and d_{H-C} denote the distance of the sulfur atom in SDS from the axis of the CNT and the distance between the nearest atoms of SDS and the CNT, respectively. (c) The distance d_{H-C} and (d) the adsorption energies per SDS molecule for both CNTs are shown as functions of d_S .

References:

- [1] R. Krupke *et al.*, Science 301, 344 (2003). [2] M. S. Arnold *et al.*, Nature Nanotech. 1, 60 (2006).
 [3] T. Tanaka *et al.*, Appl. Phys. Express 1, 114001 (2008). [4] T. Ozaki, Phys. Rev. B 67, 155108 (2003).
 [5] T. Ozaki and H. Kino, J. Chem. Phys. 121, 10879 (2004).

Corresponding Author: Mari Ohfuchi

Tel: +81-46-250-8234, Fax: +81-46-250-8844, E-mail: mari.ohfuti@jp.fujitsu.com

ポスター発表
Poster Presentation

1P-1 ~ 1P-40

2P-1 ~ 2P-40

3P-1 ~ 3P-40

Molecular Geometry and Electronic Structure of Single Wall Carbon Nanotube in Non-equilibrium States

Somphob Thompho, Oraphan Saengsawang, Uthumporn Arsawang and Supot Hannongbua^{1,}*

Department of Chemistry, Faculty of Science, Chulalongkorn University, Bangkok, Thailand

Abstract

The computational models of single-wall carbon nanotube (CNT) were created and studied using quantum chemical calculations at HF/6-31G(d) and density functional theory at PBE/6-31G(d). In order to model the CNT under high pressure, diameter (L) of the CNT in certain direction was systematically decreased. To seek for the optimal geometry of the distorted CNT, the L distance was fixed at certain value. Then, other parameters representing molecular geometry of CNT were fully optimized. The structural properties, *i.e.*, the C-C bond length and C-C-C angle, were examined. Moreover, the electronic properties such as HOMO, LUMO and charge were monitored. Interestingly, the distortion of CNT does significantly effect to the geometry and electronic properties, especially the HOMO-LUMO gap.

Keywords: Single Wall Carbon Nanotube, Electronic Properties, Non-equilibrium States, Quantum Chemical Calculations

Defect creation and annihilation of Single-Walled Carbon Nanotubes with Scanning Tunneling Microscopy

Yuta Ebine¹, Maxime Berthe¹, Shoji Yoshida¹, Atsushi Taninaka¹, Satoru Suzuki²,
Koji Sumitomo², Osamu Takeuchi¹ and Hidemi Shigekawa¹

¹ *Institute of Applied Physics, University of Tsukuba, Tsukuba, Ibaraki 305-8573, Japan.*

² *NTT Basic Research Laboratories, Atsugi, Kanagawa 243-0198, Japan*

Single-Walled Carbon Nanotube (SWNT) is one of most promising candidates for the material of future electronic devices because of its excellent one-dimensional electronic property. Electronic transport property of SWNT depends not only on their atomic structure, but also on the presence of defects. Therefore, several experimental approaches (electron beam or plasma irradiation) have been demonstrated to introduce defects in SWNT [1].

In this paper, we present a new method to create and annihilate defects on SWNT by local carrier injection to the SWNT with a STM tip. The experiments were conducted with an Omicron LT-STM operated at 77K and 4K. The sample was prepared by spin-coating 1-2-dichloroethane dissolved HiPCO SWNTs solvent on the freshly cleaned Au(111) surface.

Figure 1 shows the process of defect creation on a SWNT. Carrier injection to a SWNT was performed by tunnel bias voltage ramp from -1V to -8V with tunneling current kept constant (1nA). After the STM imaging of clean SWNT (fig.1(a)), carrier injection was applied above the triangle mark in fig.1(b). STM image obtained after applied voltage ramp shows the defect on the SWNT (a bright part in fig.1(b)). During carrier injection process, sudden height change was observed due to change of the electrical current by the defect creation (fig.1(c)). Surprisingly, applying voltage ramp in the same way led to annihilation of this defect. This reversible reaction suggests that number of carbon atoms in a SWNT were preserved during the manipulation. In addition, STS measurement on the defect confirmed the formation of pentagon/heptagon derived electronic state inside the band gap of SWNT. From these results, we conclude that the point defect corresponds to a Stone-Wales defect (fig.2).

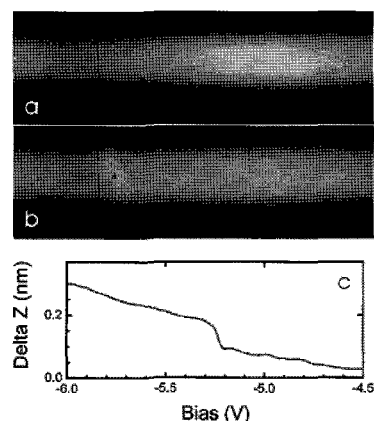


Fig. 1. STM image of a SWNT before (a) and after (b) bias voltage ramp. (c) Z-V curve measured during bias voltage ramp.

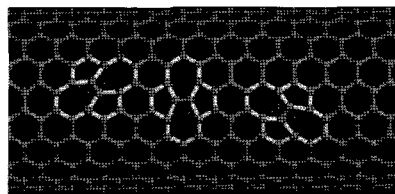


Fig. 2. Structural model of a Stone-Wales defect on a SWNT.

Reference

<http://dora.bk.tsukuba.ac.jp/>

[1] A. Vijayaraghavan et al., *Nano Lett.*, 5, 1575 (2005)

[2] M. Berthe et al., *Nano Lett.*, 7, 3623 (2007)

First principles study of substitutional impurities in carbon nanotubes

○Takashi Koretsune and Susumu Saito

*Department of Physics, Tokyo Institute of Technology
2-12-1 Oh-okayama, Meguro-ku, Tokyo 152-8551, Japan*

For the electronic transport properties of semiconductors, impurities play a significant role. In carbon nanotubes, there are several experimental studies about the boron or nitrogen doped carbon nanotubes. However, the basic properties of the impurities such as the depth of the impurity level have not been well understood. To clarify the effect of the impurities in carbon nanotubes theoretically, we study the electronic structures of boron or nitrogen doped carbon nanotubes using the density functional theory.

We first calculate doping rate dependence of the gap of the doped nanotubes. From the extrapolation of the gap[1], we estimate the depth of the impurity level and the spatial extent of the impurity state. It is found that the gap of doped tube is always smaller than that of pristine tube and this reduction of the gap is considered to give the depth of the impurity level in the low impurity concentration limit. In fact, the derived depth of the impurity level agrees well with the spatial extent of the impurity state. The depth of the impurity level depends on the diameter, and in the narrow nanotubes there is an influence of nearly free electron states for nitrogen impurity state (donor state). In the thick nanotubes, nitrogen makes a deeper impurity state than boron, which is similar to the case of diamond. We also calculate the shift of the work function in the doped tube, which is important in discussing the charge transfer effect in the multiwalled or bundled carbon nanotubes.

[1] T. Koretsune and S. Saito, Phys. Rev. B **77** (2008) 165417.

Corresponding Author: Takashi Koretsune

E-mail: koretune@stat.phys.titech.ac.jp

Constant-Pressure Molecular Dynamics Study of Single-Walled Carbon Nanotubes with a Small Diameter

○Masahiro Sakurai and Susumu Saito

*Department of Physics, Tokyo Institute of Technology
2-12-1 Oh-okayama, Meguro-ku, Tokyo 152-8551, Japan*

So far various experimental compression studies of fullerene solid have been carried out and novel carbon phases are synthesized. For example, fullerene polymers, which are composed of both sp^2 and sp^3 carbon atoms, have attracted attention as a novel semiconducting material in science and engineering. In addition, new carbon form called amorphous diamond is produced using shock compression. These reports indicate that nano structured carbon materials are good precursors to interesting new carbon phases. Recent studies of the diameter-controlled synthesis of the single-walled carbon nanotube and the metal-semiconductor separation techniques show that it would be possible to obtain the nanotube solid with mostly uniform geometries. Then, by using the pressure and temperature treatment of the single-walled nanotube solid, synthesis of new carbon phases will be made in the foreseeable future.

In this study, we perform the constant-pressure molecular dynamics (MD) simulations for single-walled carbon nanotubes with a small diameter using the Parrinello-Rahman method [1,2] and transferable tight-binding (TB) model [3]. Omata TB model we used is based on LDA energetics and reproduces well not only sp^2 and sp^3 covalent bonds but also sp^2 interlayer interaction. First, we study the nanotube bundle composed of (n,n) and (n+1,n+1) tubes. At about 10 GPa, the system turns into an interesting sp^2 - sp^3 structure which include the zigzag nanoribbons in the sp^2 part. It is also found that some of the sp^3 -rich phases obtained at the higher external pressure possess anisotropy in the direction of the initial tube-axis. Secondly, the bundle composed of (n,n) and (n,m) tubes is studied. In this case, near-armchair tube is chosen as (n,m) tube. Structural properties of transformed materials are discussed. We also discuss the electronic structures of new phases obtained in MD study, using the realistic TB model proposed by N. Hamada and S. Sawada [4], which shows a good agreement with the electronic structure calculated by local-density approximation (LDA) in the density-functional theory (DFT).

References:

- [1] M. Parrinello and A. Rahman, *Phys. Rev. Lett.* **45**, 1196 (1980).
- [2] M. Parrinello and A. Rahman, *J. Appl. Phys.* **52**, 7182 (1981).
- [3] Y. Omata, Y. Yamagami, K. Tadano, T. Miyake and S. Saito, *Physica E* **29**, 454 (2005).
- [4] N. Hamada and S. Sawada, private communication; S. Okada and S. Saito, *J. Phys. Soc. Jpn.* **64**, 2100 (1995).

Corresponding Author: Masahiro Sakurai

E-mail: sakurai@stat.phys.titech.ac.jp

Microwave plasma CVD synthesis and characterization of boron-doped carbon nanotubes

○ T. Watanabe^{A,B}, Y. Mizuguchi^A, S. Tsuda^{A,C}, T. Yamaguchi^A, Y. Takano^{A,B}

National Institute for Materials Science^A, University of Tsukuba^B, WPI-MANA^C

Carbon nanotube (CNT), which has low resistivity, is hoped for to various applications, for example, transparent electrodes, nanowiring for future LSIs, probes for scanning probe microscopes and so on. Then, we try to dope boron, as a career, to CNT, referring to boron-doped diamond⁽¹⁾. Boron-doped CNTs were synthesized by Microwave plasma CVD method. As a source material, methane gas and trimethyl borate were used. Last year, we tried to synthesize of boron-doped CNT by methanol/boric acid method⁽²⁾. However, to synthesize better quality CNT, we tried this method. Boron-doped CNTs were characterized by raman scattering and its electrical properties were measured.

⁽¹⁾ Y. Takano, APL. 85, 2851

⁽²⁾ S. Ishii, et.al. APL.92,202116

WATANABE Tohru

E-mail WATANABE.Tohru@nims.go.jp

TEL 029-851-3354

FAX 029-851-2601

Phase Breaking in Low Temperature Magneto-resistance of Thin Multi-Walled Carbon Nanotubes

M. Kida,¹ T. Hatori,¹ Y. Nakamura,¹ Y. Togashi,¹ N. Aoki,¹ J. P. Bird,² and Y. Ochiai¹

¹Graduate School of Advanced Integration Science, Chiba University, 1-33 Yayoi, Inage, Chiba 263-8522, Japan.

²Department of Electrical Engineering, University at Buffalo, The State University of New York, New York 14260-1900, USA.

ochiai@faculty.chiba-u.jp

The low temperature magneto-resistance (MR) has been studied in thin multi-walled carbon nanotube (MWNT) FETs. From prior work on the magneto-transport properties of MWNTs, metallic conduction and a weak localization (WL) peak near zero magnetic field are expected to arise from conduction via the outermost surface layer (1). Nanoscale confinement of electrons in such curved spaces should strongly and coherently influence the WL-MR behavior. In our study, AB type oscillations are observed in the low-temperature MR of MWNTs, in spite of their multi layer structure. In our MR measurements, two kinds of metallic leads (Au/Ti or Pd) , have been employed for four-terminal resistance measurements. The contact resistance of the Pd leads is found to be much lower than that of the Au/Ti ones. In an analysis of the phase coherence of carriers in these nanotubes, several phase breaking behaviors have been observed and show a dependence on both the magnitude and angular orientation of the applied field (2). In this study, we have discussed on the WL peak and flux cancellation in parallel field direction on the axis of the MWNT (3, 4).

Among these phase breaking processes, one is found to be temperature dependent while the other is almost independent of temperature. These processes can be ascribed to different origins of phase breaking, for example, due to the intrinsic nature of the tube, to local effects at the lead contacts, or to thermal contact processes. It is clear that the phase coherence of the electron spreads over the whole region of the MWNT between the voltage leads. A large (almost hundred percent) MR is observed for the nanotubes contacted with Pd, and we discuss the different phase breaking processes for the Pd- and Au-contacted CNTs. It is very important to determine a phase breaking effect based on the impurity scattering in the MWNT in order to clarify electron transport in the metallic wires (5).

References

- 1) T. Mihara et al., *Superlattices & Microstructures*, 34, 383 (2003)
- 2) *Phys. Rev. B*77, 113408 (2008)
- 3) A. Fujiwara et al., *Phys. Rev. B*60, 13492 (1999)
- 4) T. Ando, *J. Phys. Soc. Jpn.*, 74, 777 (2005)
- 5) T. Nakanishi et al., *J. Phys. Soc. Jpn.*, 74, 3027 (2005)

Temperature dependence of radial breathing modes in double walled carbon nanotubes

○Hitoshi Kakehi¹, Ryoji Naito¹, Noriyuki Hasuike¹, Kenji Kisoda², Koji Nishio¹,
Toshiyuki Isshiki¹ and Hiroshi Harima¹

¹Department of Electronics, Kyoto Institute of Technology, Kyoto 606-8585, Japan
²Physics Department, Wakayama University, Wakayama 640-8510, Japan

Double-walled carbon nanotubes (DWCNT) have gathered much attention because they have unique physical and chemical properties to be a key material for future electronic devices. However, many basic properties of DWCNT have not been clarified due to uncertainty in interactions between the inner and outer tubes. Difficulties in preparing pure DWCNT also hinders solving the issue. Here we observed DWCNT by Raman scattering to study the interwall interaction between the inner and outer tubes.

DWCNT samples were grown by chemical vapor deposition using MgO powder as a supporting material of Fe and Mo catalysts. Carbon nanotubes were grown at 850°C and subsequently annealed at 700°C in air for purification of DWCNT. The purified samples were measured by Raman scattering in the temperature range from room temperature to 600°C. Figure 1 shows temperature dependence of phonon frequency in the radial breathing modes (RBM). Circles (●, ○), triangles (▲, △) and squares (■, □) correspond to different DWCNTs, and filled and open marks derive from the outer and inner tubes, respectively. Roughly speaking, the temperature dependence $d\omega/dT$ of inner tube clearly increases with decreasing the phonon frequency, or increasing the tube diameter d , while the outer tubes show saturating behavior against d . Single wall nanotubes showed the opposite behavior [1]: $d\omega/dT$ decreased with increasing d . This result suggests a unique phonon dynamics of RBM in DWCNT. It may reflect interwall interaction between the inner and outer tubes.

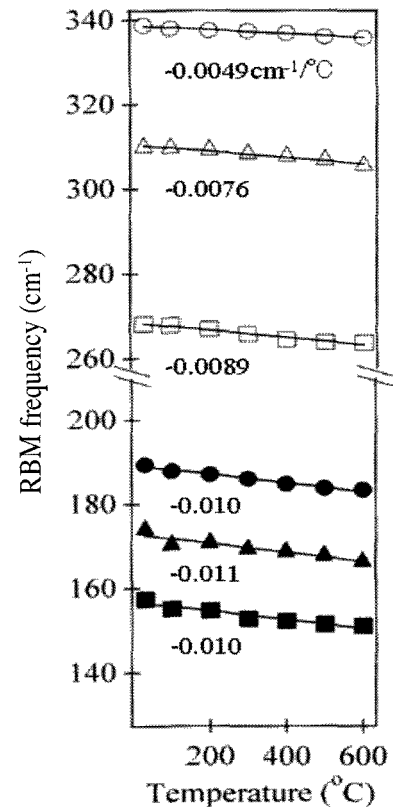


Fig.1 Temperature dependence of RBM frequency in DWCNT

[1] N. R. Raravikar, P. Keblinski, A. M. Rao, M. S. Dresselhaus, L. S. Schadler, and P. M. Ajayan, *Phys. Rev. B* **66**, 235424 (2002)

○Corresponding Author: Hitoshi Kakehi, TEL: +81-75-724-7421, E-mail: m8621009@edu.kit.ac.jp

Work Function of Single-Walled Carbon Nanotube

○Koichiro Kato and Susumu Saito

*Department of Physics, Tokyo Institute of Technology,
2-12-1 Oh-okayama, Meguro-ku, Tokyo 152-8551, Japan*

Ever since the discovery of carbon nanotubes (CNTs), many experimental and theoretical works have been devoted to them. According to the study using the tight-binding approximation, their electronic structures sensitively depend on their diameter and chirality and they are classified into three types [1]. As for the thick nanotubes, these classifications agree with the results of the density functional calculations. On the other hand, it has been pointed out from the first-principle electronic-structure calculations with structural relaxation for zigzag nanotubes that above classifications may not apply to the small-diameter nanotubes [2-4]. While several thin zigzag CNTs are predicted to be semiconductors in the tight-binding study, they are metallic in the density functional theory. The origin of this difference is explained by the following two reasons. First, large π - σ hybridization effects can occur in small nanotubes which drastically change the energy of the lowest lying conduction band states [2]. This effect can be taken into account even in the tight-binding method if not only π but also σ states are incorporated. Secondly, the effect of nearly free electron (NFE) state is found to be sizable due to a relative large interspace of carbon nanotube [3]. The NFE states can not be represented in the tight-binding approximation. In addition, structural optimization using the density functional theory play an important role in predicting their electronic and optical properties [3-4]. Importantly, there are serious differences between the first-principles results and the tight-binding results for thin nanotubes.

We study the work function of isolated single-walled carbon nanotubes in the framework of the density functional theory. The work function is one of the crucial quantities in understanding the field emission properties and applying CNTs to electronic devices. We carry out the complete geometrical optimizations of various CNTs which include several chiral CNTs, and we determine the work function from the difference between the Fermi level and the vacuum level. In the semiconducting CNTs, the Fermi level is chosen at the midgap. Consequently, it is found that the work functions of CNTs are not depending on their chiralities and diameters when their diameters are larger than about 7 Å. Their values are very close to those of graphene. On the other hand, there are significant chirality dependences of the work functions for thin nanotubes. We also find that the considerable effects of the structural optimizations.

[1] N. Hamada, S. Sawada and A. Oshiyama, *Phys. Rev. Lett.*, **68**, 1579 (1992).

[2] X. Blasé, L. X. Benedict, E. L. Shirley and S. G. Louie, *Phys. Rev. Lett.*, **72**, 1878 (1994)

[3] K. Kanamitsu and S. Saito, *J. Phys. Soc. Jpn.*, **71**, 483 (2002)

[4] O. Gülseren, T. Yildirim and S. Ciraci, *Phys. Rev. B*, **63**, 153405 (2002)

E-mail : kato@stat.phys.titech.ac.jp (K. Kato)

Electrical features of FETs using boron-doped single-walled carbon nanotubes

○T. Shimizu¹, J. Haruyama^{1,2}, H. Sano², Y. Iye², T. Eguchi², T. Nishio², Y. Hasegawa²,
J. Reppert³, A. M. Rao³

¹*School of Science and Engineerings, Material Science course, Aoyama Gakuin University, 5-10-1
Fuchinobe, Sagamihara, Kanagawa 229-8558, Japan*

²*Institute for Solid State Physics, University of Tokyo, Kashiwanoha 5-1-5, Kashiwa, Chiba 277-8581,
Japan*

³*Department of Physics and Astronomy, Center for Optical Materials Science and Engineering
Technologies, Clemson University, Clemson, SC 29634, USA*

The small mass of carbon atom can realize high transition temperature (T_c) due to its high phonon frequency in Bardeen-Cooper-Schrieffer (BCS) -type superconductivity (SC) [1 - 3]. In this viewpoint, SC in carbon nanotubes (CNTs) is attracting considerable attention and high T_c is expected, because CNTs have other advantages for high T_c (e.g., strong electron-phonon coupling between radial breathing mode and σ - π band electrons, which originates from sp^3 hybrid orbitals in very thin CNTs) [4 - 7]. Recently, we have reported successful boron doping into single-walled CNTs (SWNTs) via catalyst. We showed evidence of substitutional boron doping and revealed correlation of boron concentration with Meissner effect in thin films consisting of the boron-doped SWNTs (B-SWNTs) [8].

In the present study, we report electrical features of B-SWNTs. We have fabricated the following two-type FETs using B-SWNTs; 1. FETs using one rope of B-SWNTs as a current channel and 2. FETs fabricated on thin films consisting of B-SWNTs. To date, latter FETs have shown an abrupt resistance drop with the highest T_c of $\sim 10K$, which could be attributed to a superconducting transition of the B-SWNTs. In contrast, the former FETs have exhibited only either semiconducting or metallic behaviors. We discuss origins of these electrical behaviors of B-SWNT FETs.

References

1. T. E. Weller et al., *Nature Physics* **1**, 39 (2005).
2. N. Emery et al., *Phys. Rev. Lett.* **95**, 87003 (2005).
3. E. A. Ekimov et al., *Nature* **428**, 542 (2004).
4. I. Takesue, J. Haruyama, S. Maruyama, H. Shinohara et al., *Phys. Rev. Lett.* **96**, 057001 (2006).
5. N. Murata, J. Haruyama, S. Maruyama, H. Shinohara et al., *Phys. Rev. B* **76**, 245424 (2007).
6. T. Koretsune, S. Saito, *Phys. Rev. B* **77**, 165417 (2008)
7. M. Kociak et al., *Phys. Rev. Lett.* **86**, 2416 (2001).
8. N. Murata, J. Haruyama, T. Koretsune, S. Saito et al., *Phys. Rev. Lett.* **101**, 027002 (2008)

Corresponding Author: Junji Haruyama E-mail: J-haru@ee.aoyama.ac.jp

Tel&Fax: 042-759-6256 (Fax: 6524)

Effects of laser irradiation and thermal oxidation on CoMoCAT nanotubes probed by Raman spectroscopy

○Mari Hakamatsuka, Dongchul Kang, Kenichi Kojima, Masaru Tachibana
*International Graduate School of Arts and Sciences, Yokohama City University,
22-2 Seto Kanazawa-ku, Yokohama 236-0027, Japan*

In real single-wall carbon nanotubes (SWCNTs), various types of defects such as vacancies, Stone-Wales defects, ad-atoms, or H-C complex are contained. Understanding the properties of defects is important for improving nanotube growth methods, tailoring their physical properties, and controlling the irradiation-induced damages. Resonant Raman spectroscopy is one of the most powerful methods for characterizing defects in SWCNTs. It has been reported that D band at around 1350 cm^{-1} are influenced by defects produced by laser irradiation. From the analysis in the D band intensity with the thermal annealing, two relaxation processes for the defects were revealed; one is the fast process with an activation energy of 0.4 eV and the other is the slow process with an activation energy of 0.7 eV [1]. These energies can correspond to those of vacancy-interstitial recombination and vacancy migration along the tube axis, respectively. Moreover, it was more recently reported that the laser-induced defects also affect G^- peak at around 1540 cm^{-1} associated with metallic SWCNTs, which is attributed to the electron-phonon coupling with Kohn anomaly [2]. The G^- peak can recover to the original one due to the thermal annealing. The electron-phonon coupling for metallic SWCNTs can be reversibly controlled by the generation and annihilation of specific defects due to the laser irradiation and thermal annealing. However, these studies have been carried out for only SWCNTs with the mean diameter of 1.4 nm . For the comprehensive understanding of defects in SWCNTs, the studies on SWCNTs with smaller diameters are required. It is expected that the energies of generation and annihilation of defects in SWCNTs with smaller diameters are different from those in larger ones. In this paper, we report the effects of laser irradiation and thermal oxidation on CoMoCAT nanotubes with the mean diameter of 0.8 nm .

[1] T. Uchida *et al.*, *J. Appl. Phys.* **101**, 084313 (2007)

[2] D.Kang *et al.*, *Appl. Phys. Lett.* **93**, 133102 (2008)

Corresponding Author: Masaru Tachibana,

TEL/FAX: 045-787-2307, E-mail: tachiban@yokohama-cu.ac.jp

$C_{60}(OH)_n$ Assisted Dispersion of Single-walled Carbon Nanotubes

○Yutaka Maeda^{1,2}, Takaaki Kato¹, Junki Higo¹, Tadashi Hasegawa¹, Takahiro Tsuchiya³, Takeshi Akasaka³, Jing Lu⁴, Shigeru Nagase⁴

¹Department of Chemistry, Tokyo Gakugei University, Koganei 184-8501, Japan

²PRESTO, Japan Science and Technology Agency, Chiyoda, Tokyo 102-0075, Japan

⁴Center for Tsukuba Advanced Research Alliance, University of Tsukuba, Tsukuba, Ibaraki 305-8577, Japan

⁵Department of Theoretical and Computational Molecular Science, Institute for Molecular Science, Okazaki, Aichi 444-8585, Japan

Peapods (SWNTs encapsulating fullerenes) have currently attracted great interest as a new form of SWNTs-based materials that may find application in nanometer-sized devices. On the other hand, exohedral interaction between SWNTs and fullerene has also been reported. Liu *et al.* directly observed C_{60} derivatives stabilizing the surface of SWNTs with the help of a high-resolution transmission electron microscope.¹ Takaguchi *et al.* reported that fullerodendron having dendritic poly(amidoamine) substituents assisted dispersion of SWNTs into D_2O and tetrahydrofuran via non-covalent functionalization.² In this presentation, we report the dispersion of SWNTs in an aqueous and nonaqueous solution by using amphiphilic C_{60} derivatives.³

SWNTs were dispersed in D_2O containing 1 wt% NaOH and 0.1 mg/ml $C_{60}(OH)_n$ and in IPA containing 0.1 mg/ml $C_{60}(OH)_n$. The characteristic absorption bands of SWNTs were observed around the 600-1600 nm region. These bands are attributed to electronic transitions of the first (S11) and second (S22) pairs of van Hove singularities in semiconducting SWNTs. The effect of $C_{60}(OH)_n$ on the dispersibility of the SWNTs in a solution containing 1 wt% Triton-X was also studied. The absorption intensity of SWNTs dispersed in D_2O containing 1 wt% NaOH, 1 wt% Triton-X, and 0.1 mg/ml $C_{60}(OH)_n$ increased compared to that dispersed in D_2O containing NaOH and Triton-X. This result suggests that $C_{60}(OH)_n$ effectively increases the dispersibility of SWNTs even in the presence of Triton-X. Photoluminescence spectra of dispersion and Raman spectra of SWNTs films prepared from dispersion by filtration were also performed for analysis of the dispersion.

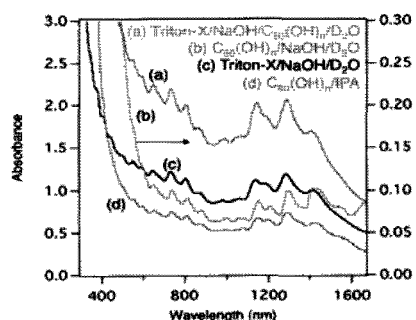


Fig. 1. Vis-NIR spectra of SWNTs dispersion. Conditions: 0.1 mg/ml $C_{60}(OH)_n$, 1 wt% Triton-X, 1 wt% NaOH, D_2O . (b) 0.1 mg/ml $C_{60}(OH)_n$, 1 wt% NaOH, D_2O . (c) 1 wt% Triton-X, 1 wt% NaOH, D_2O . (d) 0.1 mg/ml $C_{60}(OH)_n$, IPA.

[1] Z. Liu, K. Suenaga and S. Iijima, *J. Am. Chem. Soc.* **129**, 6666 (2007). [2] Y. Takaguchi, M. Tamura, Y. Sako, Y. Yanagimoto, S. Tsuboi, T. Uchida, K. Shimamura, S. Kimura, T. Wakahara, Y. Maeda and T. Akasaka, *Chem. Lett.* **34**, 1608 (2005). [3] Y. Maeda, T. Kato, J. Higo, T. Hasegawa, T. Kitano, T. Tsuchiya, T. Akasaka, T. Okazaki, J. Lu, S. Nagase, *Nano. In press.*

Corresponding Author: Y. Maeda

TEL: +81-42-329-7512, FAX: +81-42-329-7512, E-mail: ymaeda@u-gakugei.ac.jp

Molecular-Dynamics Simulations on Phonon-Assisted Mass Transport in Carbon Nanotubes

○T.Shiga¹, T.Takahashi¹, R.Rurali², E.R.Hernández² and K.Watanabe^{1,3}

¹*Department of Physics, Tokyo University of Science, 1-3 Kagurazaka,
Shinjyuku-ku, Tokyo 162-8601, Japan*

²*Institut de Ciència de Materials de Barcelona(ICMAB-CSIC), Campus de
Ballaterra, 08193, Barcelona, Spain*

³*Research Institute for Science and Technology, Tokyo University of Science, 1-3
Kagurazaka, Shinjyuku-ku, Tokyo 162-8601, Japan*

Experiments and numerical simulations on fascinating phenomena of mass transport along carbon nanotubes (CNTs) have been reported very recently. [1-4] In particular, propagation of nano-scale objects driven by temperature gradient along CNTs [2,4] attracts our interest, because thermomigration at nano-scale is not only a new phenomenon but also a challenging issue to understand from a microscopic level.

Motivated by the previous studies, we performed the molecular dynamics (MD) simulations of C₆₀ encapsulated in a single wall carbon nanotube (SWNT) and carbon nano-ring (CNR) sliding along a SWNT with temperature gradient. The Brenner potential and the Lennard-Jones potential have been used for carbon-carbon covalent bonds and van der Waals interactions between C atoms in the different objects. We first observed through a conventional nonequilibrium MD simulations that both of C₆₀ and CNR are accelerated toward the cold region. Second, we performed the phonon-wave MD simulation to reveal the microscopic origin for the motion observed under temperature gradient. The most important finding in the present simulations is that C₆₀ and CNR are pushed toward the cold region by scattering with particular phonon modes with certain wave numbers. We discuss the details of the mechanism of phonon-assisted mass transport in CNTs in our presentation.

References:

- [1] B.C. Regan, S. Aloni, R.O. Ritchie, U. Dahmen and A. Zettl, *Nature* **428**, 924 (2004).
- [2] A.Barrieiro, R.Rurali, E.R.Hernández, J.Moser, T.Pichler, L.Forró, A.Bachtold, *Science* **320**, 775 (2008).
- [3] H. Somada, K. Hirahara, S. Akita and Y. Nakayama, *Nano Lett.*, inpress.
- [4] J. Shiomi and S. Maruyama, *Nanotechnology*, in press.

Corresponding Author: Kazuyuki Watanabe

E-mail: kazuyuki@rs.kagu.tus.ac.jp , **Tel:**+81-3-3260-4665 , **Fax:**+81-3-5261-1023

Energy level of defect-induced state in semiconducting single wall carbon nanotube

K. Sasaki¹, K. Wakabayashi^{1,2} and R. Saito³

¹*Graduate School of Advanced Sciences of Matter, Hiroshima University,
Higashi-Hiroshima 739-8530, Japan*

²*PRESTO, Japan Science and Technology Agency, Kawaguchi 332-0012, Japan*

³*Department of Physics, Tohoku University, Sendai 980-8576, Japan*

A defect of lattice in a single wall carbon nanotube (SWNT) is a matter of particular importance in the electronic property. A lattice vacancy is a defect on an atomic scale. It works as a short-range impurity and gives rise to an inter-valley scattering. In the studies of electronic transport, a lattice vacancy has attracted much attention since an inter-valley scattering can decrease the conductance. A lattice vacancy works not just as a source of a resistivity but produces a zero energy state that localizes near a vacancy. The wave function of a vacancy-induced state has amplitude only on one of the two sub-lattices in the hexagonal unit cell and the energy appears close to the Fermi level. These properties are the same as the edge state [1]. Since there are various subjects relating to a vacancy, it is valuable to examine a vacancy-induced state. In this presentation, we report on the energy level of a vacancy-induced state in a semiconducting SWNT and the relationship between the edge state and vacancy-induced state.

Using a tight-binding model with nearest-neighbor and next nearest-neighbor hopping integrals, we found that the localization of a vacancy-induced state enhances near a vacancy in semiconducting SWNTs. The accumulation of density of a vacancy-induced state is robust against a possible perturbation because of the energy gap of a semiconducting SWNT. In addition to the accumulation of density, the phase of the wave function is important in lowering the energy position of a vacancy-induced state. A relationship between the localization and the energy gap of a semiconducting SWNT is discussed.

[1] M. Fujita *et al.*, *J. Phys. Soc. Jpn.* **65**, 1920 (1996); Y. Niimi *et al.*, *Appl. Surf. Sci.* **241**, 43 (2005); Y. Kobayashi *et al.*, *Phys. Rev.* **B71**, 193406 (2005).

Corresponding Author: Kenichi Sasaki

TEL: +81-82-424-4418, FAX: +81-82-424-4418, E-mail: sasaki@hiroshima-u.ac.jp

Mechanism of Radial Corrugation in Many-Walled Carbon Nanotubes

○Motohiro Sato¹ and Hiroyuki Shima²

¹*Department of Socio-Environmental Engineering, Graduate School of Engineering,
Hokkaido University, Sapporo 060-8628, Japan*

²*Department of Applied Physics, Graduate School of Engineering, Hokkaido University,
Sapporo 060-8628, Japan*

In this presentation, we demonstrate theoretically a novel radial deformation, called the radial corrugation, of MWNTs under hydrostatic pressure [1]. Theoretical analyses based on the continuum elastic theory have revealed that multiwalled carbon nanotubes (MWNTs) consisting of a large number of concentric walls undergo elastic deformations at critical pressure $p_c \approx 1$ GPa, above which the cross-sectional circular shape becomes radially corrugated. We found various corrugation modes can be obtained by tuning the innermost tube diameter D and the number of constituent walls N , which is a direct consequence of the core-shell structure of MWNTs. A phase diagram has been established to obtain the requisite values of D and N for observing a desired corrugation mode. It is remarkable that in all corrugation modes, the cylindrical symmetry of the innermost tube is maintained even under high external pressures. This persistence of the cylindrical symmetry of the innermost tube of MWNTs is completely in contrast to the pressure-induced collapse of singlewalled nanotubes. We hope that the present results provide useful information for developing nanofluidic or nanoelectrochemical devices whose performance depends on the geometry of the inner hollow cavity of nanotubes.

[1] H. Shima and M. Sato “Multiple radial corrugations in multiwalled carbon nanotubes under pressure”, *Nanotechnology* **19**, 495705 (2008)

Corresponding Author: Hiroyuki Shima

TEL: +81-11-706-6624, FAX: +81-11-706-6859, E-mail: shima@eng.hokudai.ac.jp

Electrical Characteristics of Single-Walled Carbon Nanotubes Irradiated with Ionic Liquids in Electrolyte Plasmas

○Yu Hirotsu, Toshiro Kaneko and Rikizo Hatakeyama

Department of Electronic Engineering, Tohoku University, Sendai 980-8579, Japan

Ionic liquids have attracted much interest in various fields because of their unique properties, such as existence of only positive and negative ions, nonvolatility, and so on. Especially, since they are highly polar molecules, the ionic liquids are considered to be a candidate for the significant materials to modify the electrical characteristics of single-walled carbon nanotubes (SWNTs). In this study, we have demonstrated the encapsulation of the ionic liquids into the SWNTs using a substrate bias method in electrolyte plasmas [1], and investigated the electrical characteristics of them under a field-effect transistor (FET) configuration.

An experimental apparatus consists of two aluminum electrodes (anode and cathode). Open-ended SWNTs are coated onto the electrodes which are submerged in the ionic liquid ($[\text{C}_8\text{H}_{15}\text{N}_2]^+ [\text{BF}_4]^-$). A DC bias voltage V_{DC} is 5 V and the irradiation time is 3 min. When V_{DC} is applied to the anode electrode, the ionic liquid is considered to be irradiated to each electrode because the ionic liquid consists of positive and negative ions.

Figure 1 presents electrical characteristics of the pristine and ionic-liquid irradiated SWNTs (V_{G} : gate voltage, I_{DS} : source-drain current). The electrical characteristic of the pristine SWNT is the p-type and the threshold gate voltage is -20 V as shown in Fig. 1(a) (dotted line). The solid line in Fig. 1(a) shows the electrical characteristic of the negative ion irradiated SWNT, and it is found that the threshold gate voltage for the p-type characteristic tends to shift positively compared with that of the pristine SWNT. On the contrary, the positive ion irradiated SWNT exhibits the n-type characteristic [Fig. 1(b)]. These results are caused by the negative and positive ions of the ionic liquid exerting the electron acceptor and donor effects, respectively. Therefore, it is expected that the electrical characteristics of the SWNTs are controlled by the ionic liquids which are irradiated toward the SWNTs.

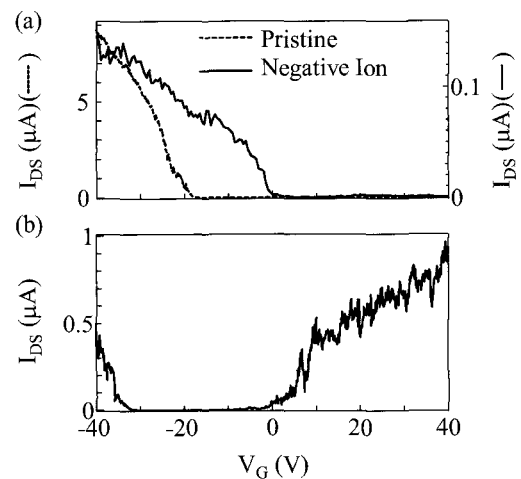


Fig. 1: Electrical characteristics of (a) pristine and negative ion irradiated SWNTs, (b) positive ion irradiated SWNT.

[1] T. Kaneko, T. Okada and R. Hatakeyama, *Contrib. Plasma Phys.*, **47**, 57 (2007).

Corresponding Author: Yu Hirotsu

TEL: +81-22-795-7046, FAX: +81-22-263-9225, E-mail: hirotsu@plasma.ecei.tohoku.ac.jp

Individually dispersed single-walled carbon nanotubes in both liquid and dried solid states using a new dispersant

○Tatsuhiko Yamamoto¹, and Masaru Kato^{1,2}

¹Center for NanoBio Integration, The University of Tokyo, 7-3-1 Hongo,
Bunkyo-ku, Tokyo 113-8656, Japan

²Graduate School of Pharmaceutical Sciences, The University of Tokyo, 7-3-1 Hongo,
Bunkyo-ku, Tokyo 113-8656, Japan

We have developed a novel dispersant for single-walled carbon nanotubes (SWNTs) that remains isolated in both liquid and dried solid states.

We developed a novel triphenylene-based surfactant, which is amphiphilic compound with a triphenylene skeleton having six alkyl carboxylic acids. The SWNTs complexed with triphenylene derivative were easily dispersed into water using a common bath sonicator with mild conditions.¹

In this work, we examined the properties of the SWNTs dispersed solution using triphenylene derivative. Optical absorption spectra revealed that the SWNTs complexed with triphenylene derivative remained isolated following perturbations: 1) freeze-drying, 2) redispersion, 3) condensation, and 4) addition of methanol (up to 70%). These unique features of the triphenylene derivatives promised to be highly useful for practical applications of SWNTs.

[1] T. Yamamoto, Y. Miyauchi, J. Motoyanagi, T. Fukushima, T. Aida, M. Kato, S. Maruyama, *Jpn. J. Appl. Phys.*, 47, 2000-2004 (2008)

Corresponding Author: Masaru Kato

Tel: +81-3-5841-1840, FAX: +81-3-5841-1841, E-mail: kato@cni.t.u-tokyo.ac.jp

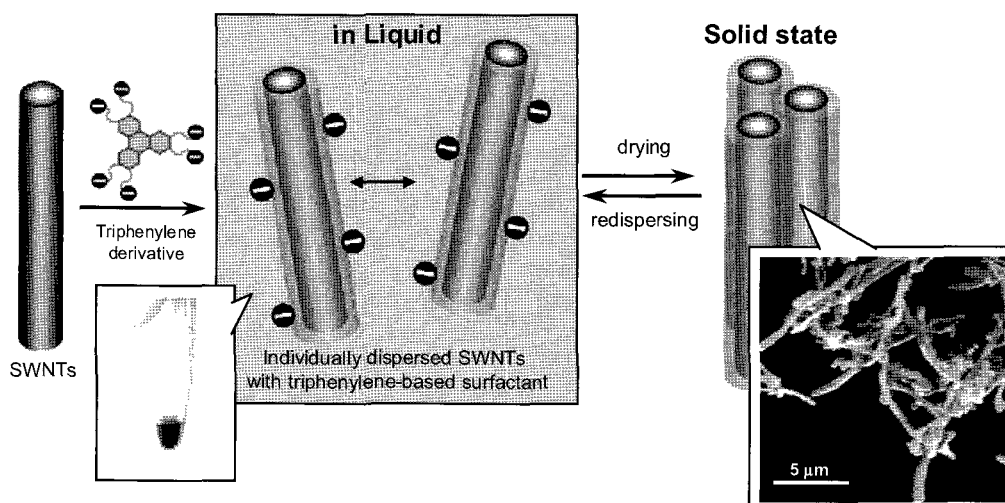


Fig.1 The model of Individually dispersion of single-walled carbon nanotubes using triphenylene derivative in both liquid and dried solid states, and photographs of each state.

G band resonance Raman spectra of single-wall carbon nanotubes

* Jin Sung Park¹⁾, Kenich Sasaki²⁾, Riichiro Saito¹⁾, Gene Dresselhaus³⁾, Mildred S. Dresselhaus^{4), 5)}

¹⁾Department of Physics, Tohoku University, Sendai 980-8578, Japan

²⁾Graduate School of Advanced Science of Matter, Hiroshima University, Higashi-Hiroshima 739-8530, Japan

³⁾Francis Bitter Magnet Laboratory, ⁴⁾Department of Electrical Engineering and Computer Science, ⁵⁾Department of Physics, Massachusetts Institute of Technology, Cambridge, MA 02139-4307, USA

The G band Raman peak of single-wall carbon nanotubes (SWNTs) is the first-order Raman scattering process which gives Raman spectra involving one-phonon emission. The G band consists of high frequency peak (G+) around 1580~1590 cm^{-1} and low frequency peak (G-) around 1550~1570 cm^{-1} , in which the two peaks correspond to the longitudinal-optical (LO) and transverse-optical (TO) phonon modes at the Γ point in the two-dimensional Brillouin zone (2D BZ) of a graphene sheet. While the two line shape in a semiconducting (S-) SWNT are given by a Lorentzian, the G- peak in a metallic (M-) SWNT has a asymmetric-broad Breit-Wigner-Fano (BWF) line shape which is known as the interaction between a phonon state and a free electron continuum state. The metallic G- peak appears at a lower frequency than that for the semiconducting one. The frequency shift of the G band is produced by electron-phonon interaction for the optical phonon mode, so called Kohn anomaly effect [1]. The both peaks of G band depend on chirality and diameter [2]. While the G+ peak is dominant near the zigzag chiral angle, the G- peak is dominant near the armchair chiral angle. It has been known that the electron-phonon interaction gives rise to the chirality dependence of the G band Raman intensity [3]. Although the G band Raman intensity have been calculated by the electron-phonon and electron-photon interactions, the G band Raman spectra have not been calculated yet. In this poster, the G band Raman spectra will be shown by including the Kohn anomaly effect and the resonance window values [4]. As a result, the chiral angle dependence of the G band Raman spectra can be directly compared to the experiment. The gate voltage dependence of the G band Raman spectra for metallic nanotubes is also directly compared to the experiment in which the Kohn anomaly effect appears by change of the Fermi energy.

Reference:

- 1) K. Sasaki, R. Saito, G. Dresselhaus, M. S. Dresselhaus, H. Farhat, J. Kong, Phys. Rev. B, 77, 245441, (2008)
- 2) R. Saito, A. Jorio, J. H. Hafner, C. M. Lieber, M. Hunter, T. McClure, G. Dresselhaus, M. S. Dresselhaus, Phys. Rev. B, 64, 085312 (2001)
- 3) J. Jiang, R. Saito, Ge. G. Samsonidze, S. G. Chou, A. Jorio, G. Dresselhaus, and M. S. Dresselhaus, Phys. Rev. B, 72, 235408 (2005)
- 4) J. S. Park, Y. Oyama, R. Saito, W. Izumida, J. Jiang, K. Sato, C. Fantini, A. Jorio, G. Dresselhaus, M. S. Dresselhaus, Phys. Rev. B, 74, 165414, (2006)

*Email address: park@flex.phys.tohoku.ac.jp

Magnetic attractive multiwalled carbon nanotubes formed by high temperature treatment of multiwalled carbon nanotube/boric-oxide composite in hydrogen environment

○ Hiroki Endo, Shunji Bandow, Sumio Iijima

*Department of Materials Science and Engineering, Meijo University,
1-501 Shiogamaguchi, Tenpaku, Nagoya 468-8502, Japan*

High purity closely filled multiwalled carbon nanotubes (c-MWNTs) can be prepared by RF plasma vaporization of pure carbon rod [1]. Boron doping to c-MWNTs was examined by using the same method but replacing pure carbon rod to boron including composite carbon rod [2], and the enhancement of $N(E_F)$ was confirmed [3]. Magnetic response of such boron doped MWNTs indicated interesting phenomenon like superconductivity or spin-glass. In the present study, we try to dope boron atoms to carbon network via high temperature reaction between c-MWNTs and boric oxide in various conditions of hydrogen environment, and study the magnetic features of the sample thus prepared.

RF plasma method was used to prepare c-MWNTs, and a powdered B_2O_3 (3N) was purchased from a Rare Metallic. First, we prepared a composite of c-MWNTs and B_2O_3 simply by mixing both materials with a ratio of 1:10 by weight, and then the mixture was loaded onto tungsten boat. Heat-treatments were carried out in the tube furnace at 1200 °C in H_2 flux of 200 sccm at various pressures of 0.01, 0.05, 0.1, 0.2, 0.3 and 1 atm for 1 hour. After such treatments, products remained in W-boats were collected and a part of each product was dispersed in ethanol liquid. A pair of Sm-Co magnets (10 mm in dia., columnar) was attached on the vial (12 mm in dia.), and then we examined magnetic responses of these dispersed products. Results are in Fig. 1. After waiting for 5 min when the magnets were attached, dispersed MWNTs were well attracted to the magnet for the MWNTs prepared under the conditions of 0.05, 0.1 and 0.2 atm (see blackened region near the center of vials in Figs. 1b, c and d), but not for others. Similar magnetic response was examined by using a product from nanohorn/ B_2O_3 composite prepared at the pressure of 0.1 atm. However, the movement toward the magnet was not so much clear like as the case for MWNTs. Another wrapping of c-MWNTs from ethanol solution of B_2O_3 was also examined, and the same high temperature treatment was conducted at 0.1 atm. Resulting product was indicated much stronger magnetic response than that prepared from just mixed composite. According to TEM observations, remarkable structural damage of c-MWNTs could not be recognized after high temperature reactions. Quantitative analyses of magnetic properties will be presented in the meeting.

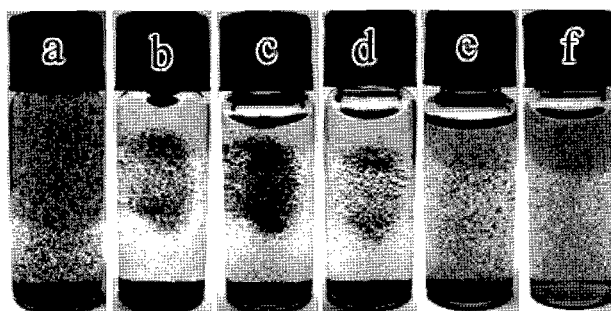


Fig. 1. Movements of MWNTs in ethanol toward the magnet after 5 minutes left when the magnets were attached on the sidewall of vials. MWNTs in (a) was prepared in 0.01 atm of H_2 flux at 1200 °C, (b) was 0.05 atm, (c) 0.1, (d) 0.2, (e) 0.3 and (f) 1 atm.

- [1] A. Koshio *et al.*, *Chem. Phys. Lett.* **356**, 595 (2002).
[2] S. Numao *et al.*, *J. Phys. Chem. C* **111**, 4543 (2007).
[3] S. Bandow *et al.*, *J. Phys. Chem. C* **111**, 11763 (2007).

Corresponding Author: Shunji Bandow, **E-mail:** bandow@ccmfs.meijo-u.ac.jp, **Tel&Fax:** +81-52-834-4001.

Characterization of CNT-FET by Scanning Gate Microscopy

O Yuki Okigawa¹⁾, Shigeru Kishimoto^{1,2)}, Yutaka Ohno¹⁾, Takashi Mizutani¹⁾

¹⁾*Department of Quantum Engineering, Nagoya University, Nagoya 464-8603, Japan*

²⁾*Venture Business Laboratory, Nagoya University, Nagoya 464-8603, Japan*

Scanning probe microscopy is a powerful technique to characterize the CNT-FETs because of its advantage of high special resolution. In the previous work, we measured the potential profile along the CNTs by electrostatic force microscopy (EFM) and obtained the nonuniform potential profile which reflected the existence of the defects in CNTs or SiO₂ [1]. In this study we have evaluated the CNT-FETs by scanning gate microscopy (SGM) [2].

The CNTs used for the fabrication of CNT-FETs with back gate was grown by grid-inserted plasma-enhanced chemical vapor deposition [3]. In the SGM, the tip acts as a local gate and the modulation of the current through the CNT is detected. Fig.1 (a) shows the AFM image and Fig.1 (b) and (c) show the SGM images with positive and negative tip biases, respectively. The current modulation was observed at large area of CNT for positive tip bias (Fig.1 (b)). In the case of negative tip bias, on the other hand, it was obtained only near the source electrode (Fig.1 (c)). These results are consistent with Schottky barrier transistor model, in which the channel current is dominated by the Schottky barrier formed at the source contact. The SGM image which reflects the existence of defects has also been obtained for different CNT-FET.

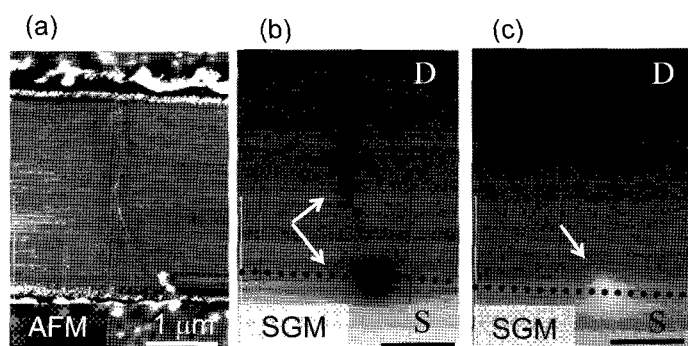


Fig. 1. (a) AFM image of the device. CNT bridges between the source (bottom) and drain (top) electrode. (b) and (c) SGM images with positive and negative tip biases, respectively.

[1] Y. Okigawa *et al Nano* **3** 51 (2008) [2] M. Freitag *et al APL* **89** 216801 (2002)

[3] Y. Kojima *et al Jpn. J. Appl. Phys.* **44** 2600 (2005)

Corresponding Author: Takashi Mizutani

Tel: +81-52-789-5230 **Fax:** +81-52-789-5232 **E-mail:** tmizu@nuce.nagoya-u.ac.jp

Pressure dependence of Meissner effect in thin films of boron-doped single-walled carbon nanotubes

○J.Nakamura¹, M. Matsudaira¹, J. Haruyama^{1,2}, T. Shimizu¹, T. Eguchi², T. Nishio², Y. Hasegawa², H. Sano², Y. Iye², J. Reppert³, A. M. Rao³

¹*School of Science and Engineerings, Material Science course, Aoyama Gakuin University, 5-10-1 Fuchinobe, Sagamihara, Kanagawa 229-8558, Japan*

²*Institute for Solid State Physics, University of Tokyo, Kashiwanoha 5-1-5, Kashiwa, Chiba 277-8581, Japan*

³*Department of Physics and Astronomy, Center for Optical Materials Science and Engineering Technologies, Clemson University, Clemson, SC 29634, USA*

The small mass of carbon atom can realize high transition temperature (T_c) due to its high phonon frequency in Bardeen-Cooper-Schrieffer (BCS) -type superconductivity (SC) [1 - 3]. In this viewpoint, SC in carbon nanotubes (CNTs) is attracting considerable attention and high T_c is expected, because CNTs have other advantages for high T_c (e.g., strong electron-phonon coupling between radial breathing mode and $\sigma - \pi$ band electrons, which originates from sp^3 hybrid orbitals in very thin CNTs) [4 - 7]. Recently, we have reported successful boron doping into single-walled CNTs (SWNTs) via catalyst. We showed evidence of substitutional boron doping and revealed correlation of boron doping with Meissner effect in thin films consisting of the boron-doped SWNTs [8].

In the present study, we report pressure dependence of Meissner effect in the thin films of boron-doped SWNTs. We find an increase in T_c of Meissner effect from $T_c = 8\text{K}$ to 20K by applying pressure as small as 20 M Pascal in highly homogeneous thin films. In contrast, we also find that T_c is mostly independent of applied pressure in inhomogeneous films. These results imply a possibility that condensation of the SWNTs by applied pressure is one of the origins for the increased T_c . Optimization of uniformity of the films may lead to higher T_c .

References

1. T. E. Weller et al., *Nature Physics* **1**, 39 (2005).
2. N. Emery et al., *Phys. Rev. Lett.* **95**, 87003 (2005).
3. E. A. Ekimov et al., *Nature* **428**, 542 (2004).
4. I. Takesue, J. Haruyama, S. Maruyama, H. Shinohara et al., *Phys. Rev. Lett.* **96**, 057001 (2006).
5. N. Murata, J. Haruyama, S. Maruyama, H. Shinohara et al., *Phys. Rev. B* **76**, 245424 (2007).
6. T. Koretsune, S. Saito, *Phys. Rev. B* **77**, 165417 (2008)
7. M. Kociak et al., *Phys. Rev. Lett.* **86**, 2416 (2001).
8. N. Murata, J. Haruyama, T. Koretsune, S. Saito et al., *Phys. Rev. Lett.* **101**, 027002 (2008)

Corresponding Author: Junji Haruyama E-mail: J-haru@ee.aoyama.ac.jp

Tel&Fax: 042-759-6256 (Fax: 6524)

Molecular-Dynamics Simulations on Carbon-Nanotube Phonon Fiber

○Takahiro Yamamoto¹, Fumio Nishimura², Toru Takahashi² and Kazuyuki Watanabe^{2,3}

¹ Department of Materials Engineering, The University of Tokyo 7-3-1, Hongo, Shinjuku-ku, Tokyo, 162-8601, Japan

² Department of Physics, Tokyo University of Science, 1-3, Kagurazaka, Shinjuku-ku, Tokyo, 162-8601, Japan

³ Research Institute for Science and Technology, Tokyo University of Science, 1-3, Kagurazaka, Shinjuku-ku, Tokyo, 162-8601, Japan

Nanoscale thermal transport is a new and challenging topic in condensed matter physics involving many veiled phenomena, and shows novel features that are not observed in bulk systems. Recent progress has made it possible to develop novel nanotube-based *phononic devices* using phonons as information carriers, such as a thermal rectifier [1], tunable thermal links [2], etc.

In this work, we found by molecular-dynamics simulations that the carbon nanotubes act as *phonon fiber* retaining their excellent thermal conductances even if they are severely bent (See the figure) [3]. In contrast, the thermal conductance is dramatically reduced when the outer shells of a multi-walled nanotube are disconnected although the inner shells maintain their tube structure [3]. These MD results are in good agreement with a recent experiment [4].

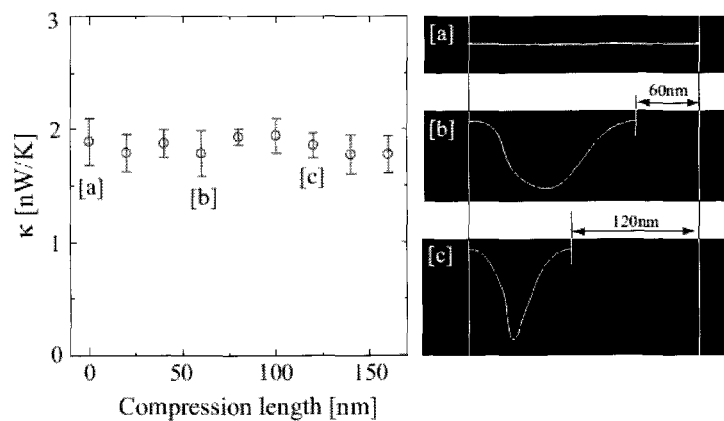


Figure: The thermal conductance of (5,5) CNT with 200nm length as a function of the compression length.

[1] C.W. Chang, et al., Science **314**, 1121 (2006).

[2] C.W. Chang, et al., Appl. Phys. Lett. **90**, 193114 (2007).

[3] F. Nishimura, T. Takahashi, K. Watanabe and T. Yamamoto (submitted)

[4] C.W. Chang, et al., Phys. Rev. Lett. **99**, 045901 (2007).

Corresponding Author: Takahiro Yamamoto

TEL: +81-03-5841-7136, FAX: +81-03-5841-1286, E-mail: takahiro@cello.t.u-tokyo.ac.jp

Energetics and Electronic Structures of Carbon Nanowires

Susumu Okada

*Graduate School of Pure and Applied Sciences & Center for Computational Sciences,
University of Tsukuba, Tennodai, Tsukuba 305-8577, Japan
CREST, JST, 4-1-8 Honcho, Kawaguchi, Saitama 332-0012, Japan*

The dimensionality and the boundary condition in nanometer scale materials are crucial to determine their electronic properties those are drastically modulated from the starting materials. Indeed, for the sp^2 carbon system, the carbon nanotubes are either metals or semiconductors depending on their atomic arrangement along the circumference corresponding to the boundary condition imposed on the graphite monolayer. In sharp contrast, a little is known for the electronic and geometric structures of the low-dimensional structures consisting of sp^3 carbon atoms. Thus, in the present work, we explore the energetics of the nanowires consisting of sp^3 carbon atoms and unravel their electronic structures based on the first-principle total-energy calculation in the framework of the density functional theory.

Here, we consider the diamond nanowire with clean surfaces of which nanowire axis is parallel to the (111) direction of hexagonal diamond. Our calculations show that the total energy of nanowires monotonically decreases with increasing the nanowire diameter. The total energy of the nanowire of which diameter is 4 nm is almost the same as that of the single walled carbon nanotubes with 1 nm diameter. Detailed structural analyses indicate that the outermost atomic shell of the nanowire is flattened compared with the ideal (100) surfaces of the diamond to reduce the dangling bond nature of the surface atoms. As a result of this surface reconstructions, the outermost shell of the nanowire possesses both sp^2 and sp^3 characters. Indeed, we find the dimensional crossover in their electronic structure around the energy gap: Edge localized electrons emerge for the electron injection into the lowest branch of the conduction band. Further injection results in the two dimensional electron systems similar to the graphitic pi network. On the other hand, holes are distributed whole cross sections of the nanowire indicating its three-dimensional character.

Corresponding Author: Susumu Okada, sokada@comas.frsc.tsukuba.ac.jp

A high-resolution laboratory x-ray diffractometer for the bulk structure analysis of nanotubes and peapods

○Shinobu Aoyagi¹, Eiji Nishibori¹, Ryo Kitaura², Hiroshi Sawa¹, Makoto Sakata³ and Hisanori Shinohara^{2,4}

¹*Department of Applied Physics, Nagoya University, Nagoya 464-8603, Japan*

²*Department of Chemistry, Nagoya University, Nagoya 464-8602, Japan*

³*SPRING-8/JASRI, Kouto, Sayo, Hyogo 679-5198, Japan*

⁴*Institute for Advanced Research, Nagoya University, Nagoya 464-8602, Japan*

Bulk structure analysis by x-ray diffraction can provide essential information of nanotubes and peapods such as the mean diameter of nanotubes and the filling ratio of the peapods, which is complementary to the local micro-structure observation by transmission electron microscopy (TEM). X-ray structure analysis of nanotubes and peapods is usually difficult owing to their weak diffraction intensities. X-ray diffraction experiments of nanotubes have been often carried out using synchrotron-radiation with high brilliance. We developed a high-resolution laboratory x-ray diffractometer to enable the accurate structure analysis of nanotubes and peapods in laboratory.

The diffractometer consists of an 18 kW rotating anode generator with a Mo target, a curved graded multilayer mirror, two Ge channel-cut monochromators, and a two-axis goniometer equipped with a cylindrical imaging plate detector. This setup enables rapid collection of a powder diffraction pattern with high counting statistics and high angular resolution over a wide d -spacing range from a few milligrams of powder sample.

Diffraction patterns of C₁₀H₂@SWNTs[1] and C₇₀@DWNTs[2] were measured and they were structurally characterized by using our diffractometer. In-situ powder diffraction experiment for fullerene peapods was also carried out by the diffractometer.

[1] D. Nishide, H. Dohi, T. Wakabayashi, E. Nishibori, S. Aoyagi, M. Ishida, S. Kikuchi, R. Kitaura, T. Sugai, M. Sakata and H. Shinohara, *Chem. Phys. Lett.*, **428**, 356 (2006).

[2] G. Ning, N. Kishi, H. Okimoto, M. Shiraishi, Y. Kato, R. Kitaura, T. Sugai, S. Aoyagi, E. Nishibori, M. Sakata and H. Shinohara, *Chem. Phys. Lett.*, **441**, 94 (2007).

Corresponding Author: Shinobu Aoyagi

TEL: +81-52-789-4455, FAX: +81-52-789-3724, E-mail: aoyagi@mcr.nuap.nagoya-u.ac.jp

Nucleation of an SWNT inside a carbon nanotube

○Yoshifumi Izu, Junichiro Shiomi and Shigeo Maruyama

*Department of Mechanical Engineering, The University of Tokyo
7-3-1 Hongo, Bunkyo-ku, Tokyo 113-8656, Japan*

Molecular encapsulation in the hollow space of a carbon nanotube has attracted interests with various applications. Experiments have been reported on formation of DWNT from C₆₀ fullerenes peapods [1] and ferrocene filled SWNT [2, 3]. The reports demonstrate that the growth mechanism of the inner tube depends on filler precursor.

In this work, we have performed MD simulations of the SWNT nucleation inside an SWNT template based on the potential model as in the previous work [4] to gain understanding in the growth mechanism. The MD simulations were carried out for two cases with different initial conditions and precursor models. In the first case, a Ni cluster with dissolved carbon atoms was initially placed inside the nanotube template, and then the SWNT nucleation was simulated by supplying only carbon atoms (Fig. 1). On the other hand, in the second case, instead of a cluster, Ni and carbon were initially placed inside an SWNT template as individual atoms, and simulations were run by feeding both Ni and carbon atoms with the carbon/metal number ratio of 10, corresponding to that of ferrocene (Fig. 2). As seen in the figures, both cases resulted in the sufficient growth of inner SWNTs. Differences and similarities in growth scenarios, resulting SWNT structures, and growth speeds will be discussed.

[1] S. Bandow *et al.*, *Chem. Phys. Lett.* **337** (2001) 48. [2] L. Guan *et al.*, *Carbon* **43** (2005) 2780. [3] H. Shiozawa *et al.*, *Adv. Mater.* **20** (2008) 1443. [4] Y. Shibuta and S. Maruyama, *Chem. Phys. Lett.*, **382** (2003) 381.

Corresponding author: Shigeo Maruyama E-mail: maruyama@photon.t.u-tokyo.ac.jp, Tel/Fax: +81-3-5800-6983

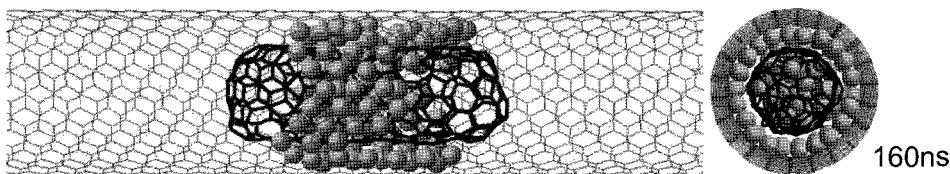


Fig. 1 Nucleation of the inner SWNT from a catalytic metal cluster.

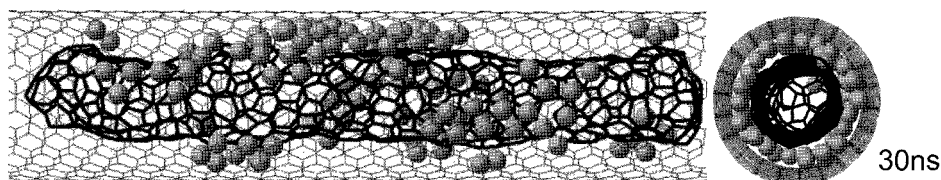


Fig. 2 Nucleation of the inner SWNT from catalytic metal atoms.

First principles calculations of electronic states in SWCNTs encapsulating oxygen molecules

○Keitaro Harada¹, Kazuyuki Matsuda¹, Yutaka Maniwa^{1,3}, Syogo Tejima²,
and Hisashi Nakamura²

¹Tokyo Metropolitan University, Minami-osawa, Hachi-oji, Tokyo, 192-0397, Japan

²Research Organization for Information Science & Technology,
2-2-54, Nakameguro, Meguro-ku, Tokyo, 153-0061, Japan

³JST, CREST, Kawaguchi, Japan

Materials in very small cavities in crystals are expected to show unusual and novel properties which cannot be observed in bulk states [1, 2]. Here, we investigated oxygen molecules encapsulated inside SWCNTs, O₂@SWCNT. Because oxygen is a functional molecule with spin S=1, it would be a candidate of new magnetic systems. The first principles calculations within the generalized gradient approximation to the density functional theory were performed on rather small diameter SWCNTs with one-dimensional array of oxygen molecules, as shown in Fig. 1.

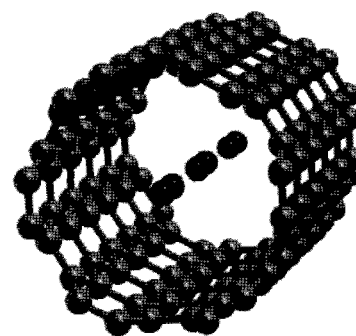


Fig. 1. O₂@SWCNT

Figure 2 shows the band structures of O₂@(n, n) SWCNTs. The O-derived minority spin states can be found around the Fermi level E_F (E=0). With decreasing SWCNT diameter, this band becomes lower, leading to a reduction of spin polarization due to occupation of the O_{ppπ}* band with electrons.

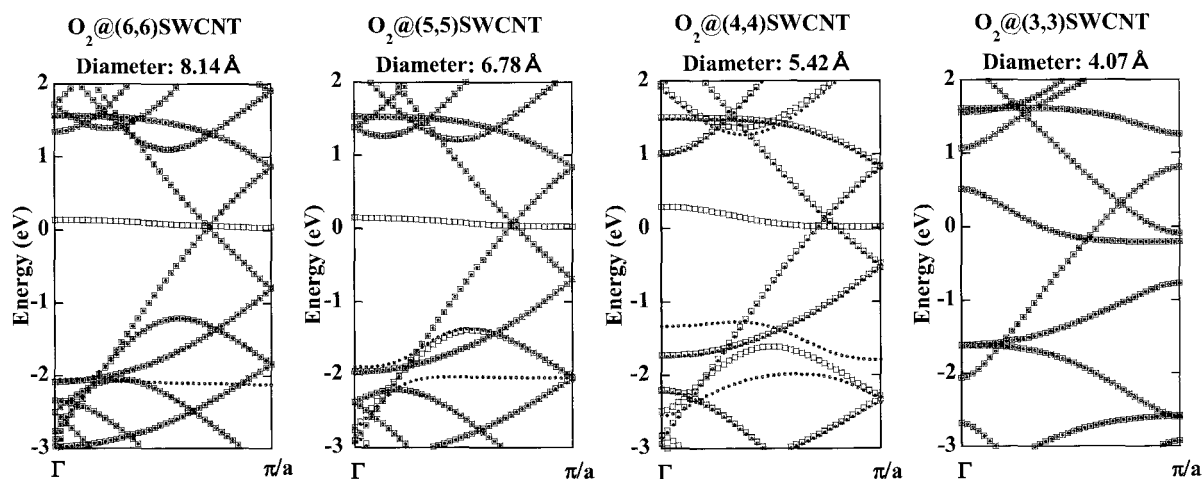


Fig.1. Band structures of O₂@SWCNT.

[1] Y. Maniwa, et al., Chem. Phys. Lett. **401**, 534-538 (2005), and J. Phys. Soc. Jpn. **71**, 2863-2866 (2002).

[2] R. Kitaura, et al. : Science **298**, 2358 (2002)

Corresponding Author: Keitaro Harada, Yutaka Maniwa (maniwa@phys.metro-u.ac.jp)

Dielectric properties of water clusters inside SWCNTs

○FUMINORI MIKAMI¹, KAZUYUKI MATUDA¹, YUTAKA MANIWA^{1,2}

¹ *Department of physics ,Faculty of science, Tokyo Metropolitan University
1-1 Minami-osawa , Hachioji, Tokyo 192-0397*

² *JST, CREST, Kawaguchi, Japan*

Water forms ice nanotubes (ice NTs) inside SWCNTs below the freezing temperatures T_m depending on the SWCNT diameter [1]. T_m becomes higher with decreasing SWCNT diameter. The ice NTs have ordered structures of both oxygen and hydrogen atoms of water molecules, so that interesting dielectric properties are expected. Here, we present our recent results of classical molecular dynamics simulations on water inside SWCNTs. It was found that n-gonal ice NTs with odd number, n, are ferroelectric water although n-gonal ice NTs with even n are anti-ferroelectric. Novel polarization properties were also observed, as shown in Fig. 1.

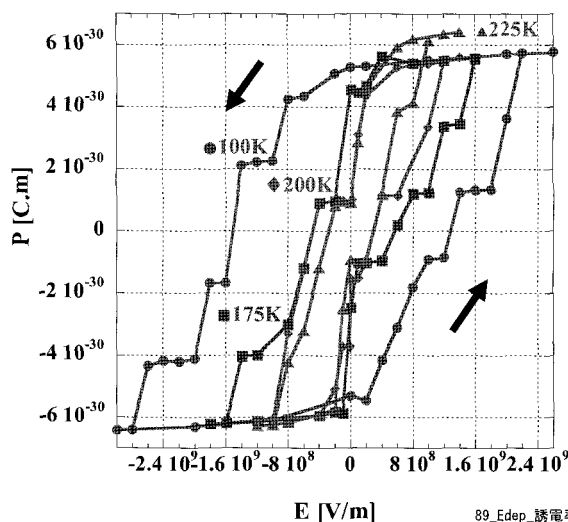


Fig. 1 Polarization properties of pentagonal ice NT at 100, 175, 200, 225 K. The electric field is applied to the tube axis. Clearly shown the ferroelectric behaviors with unusual novel step-wise variation

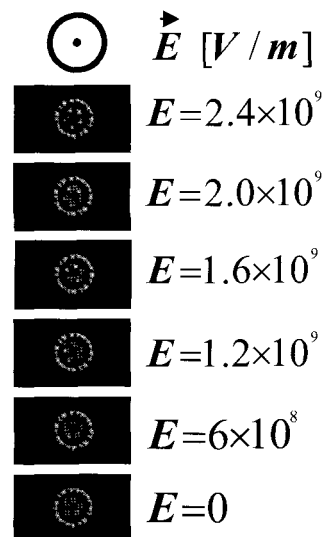


Fig. 2 Views of pentagonal ice NT from the SWCNT axis at 100 K. White spheres: hydrogen atoms. Red spheres: oxygen atoms.

References: 1. Y. Maniwa, et al., Chem. Phys. Lett. **401**, 534-538 (2005), and J. Phys. Soc. Jpn. **71**, 2863-2866 (2002).

E-mail: mikami@kke.biglobe.ne.jp, maniwa@phys.metro-u.ac.jp

Scanning Tunneling Microscopy/Spectroscopy on the Electronic Structure of Metallofullerene Peapods (Gd@C_{82})_n@SWCNTs

○Kazunori Ohashi, Yuki Iijima, Naoki Imazu, Ryo Kitaura and Hisanori Shinohara

*Department of Chemistry & Institute for Advanced Research,
Nagoya University, Nagoya 464-8602, Japan*

Previous studies of low temperature scanning tunneling spectroscopy have shown that Gd@C_{82} metallofullerenes encapsulated in single-walled carbon nanotubes (SWCNTs) significantly modify the local electronic structure of SWCNTs¹. The origin of the localized electronic modification has been explained by elastic strain and charge transfer at metallofullerene sites. One of our main goals is to understand the origin of encapsulation-induced electronic structure modification of SWCNTs. For this purpose, a systematic study on various nanopeapods using low-temperature STM/STS measurements is indispensable. Here, we report STM/STS observation on gadolinium metallofullerene peapod ($(\text{Gd@C}_{82})_n$ @SWCNTs) at 110 K.

SWCNTs synthesized by arc-discharge method (Meijo Carbon, SWCNT SO type, diameter: 1.3-1.5 nm) were used to prepare the peapod. Encapsulation of Gd@C_{82} into SWCNTs was performed via the gas-phase reaction method. $(\text{Gd@C}_{82})_n$ @SWCNTs synthesized were dispersed in 1,2-dichloroethane, and the dispersed solution was dropped onto gold coated mica substrates. STM/STS measurements were performed by using an Omicron VT-STM.

Figure1 shows an STM image of $(\text{Gd@C}_{82})_n$ @SWCNTs corresponding to unoccupied states (taken at $V_s=+0.5$ V, $I_t=0.5$ nA) at 110 K in UHV. The image shows both lattice image of the SWCNT and protrusions at a interval of ca. 1 nm, which is almost equal to the intermolecular distance of neighboring Gd@C_{82} molecules as determined by HRTEM observations (ca. 1.1 nm). These results suggest that the observed modulation on the local electronic structure here can be associated with the position where Gd@C_{82} molecules are encapsulated.

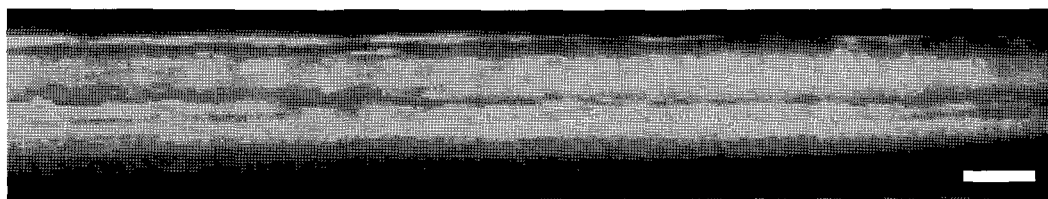


Figure 1: STM image of $(\text{Gd@C}_{82})_n$ @SWCNTs taken at $V_s=+0.5$ V, $I_t=0.5$ nA at 110 K. Scale bar is 1 nm.

1) J. Lee et al., Nature, **415**, 1005 (2002).

Corresponding Author: Hisanori Shinohara

TEL: +81-52-789-2482, FAX: +81-52-747-6442, E-mail: noris@nagoya-u.jp

Fabrication of the air stable n-type single-walled carbon nanotube transistor based on calcium atoms encapsulation

○T. Shimizu, T. Kato, W. Oohara*, and R. Hatakeyama

Department of Electronic Engineering, Tohoku University, Sendai 980-8579, Japan

** Graduate School of Science and Engineering, Yamaguchi University,
Yamaguchi 755-8611, Japan*

Carbon nanotubes (CNTs) with nanometer-order diameter and millimeter-order length attract a great deal of attentions aiming for their novel applications such as next-generation nanoelectronic devices. Accommodation of various dopant atoms, molecules, and compounds is available for modifying the intrinsic electronic and optical properties of single-walled carbon nanotubes (SWNTs). According to our past research, alkali-metal- and halogen-encapsulated SWNTs have been known to exhibit n-type and p-type transport properties under the field effect transistor (FET) configuration [1-2]. This fact promotes us to focus on an alkaline-earth metal atom which can be a doubly-charged positive ion and strongly enhance the n-type transport properties of SWNTs. Based on these backgrounds, it is attempted to encapsulate Ca atoms in the hollow space of SWNTs with an alkaline-earth plasma consisting of Ca positive ions. Electrical transport characterization of Ca encapsulated SWNTs under the FET configuration is also precisely investigated.

Figure 1 represents the drain current (I_{DS}) -gate voltage (V_G) characteristics of Ca irradiated SWNTs measured with drain-source voltage (V_{DS}) = 1 V in vacuum and air. The Ca ion irradiation time is about 4 h. The I_{DS} dependence on V_G in vacuum is shown by the solid line in Fig. 1. The result of this experiment indicates that Ca atoms are encapsulated in SWNTs and operate as an electron donor. Therefore, the conduction band of SWNTs is considered to be approached the work function of the electrodes (Au), and electrons easily come to be conducted. Surprisingly, the n-type I_{DS} - V_G characteristic still remains even after exposure to the air as represented by the dot-line in Fig. 1. It can be concluded that the SWNTs based air stable n-type transistor can be realized by encapsulating Ca atoms inside SWNTs.

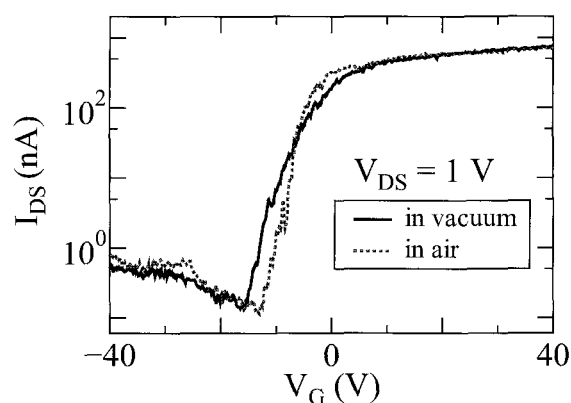


Fig. 1. I_{DS} - V_G characteristics of Ca@SWNTs measured at V_{DS} = 1 V in vacuum (a) and air (b) condition.

[1] T. Izumida, R. Hatakeyama, Y. Neo, H. Miura, K. Omote, and Y. kasama, *Appl. Phys. Lett.* **89**, 093121 (2006).

[2] J. Shishido, T. Kato, W. Oohara, R. Hatakeyama, and K. Tohji, *Jpn. J. Appl. Phys.* **47**, 2044 (2008).

Corresponding Author: T. Shimizu

TEL:+81-22-795-7046, FAX:+81-22-263-9225, E-mail: shimizu@plasma.ecei.tohoku.ac.jp

Encapsulation of Room Temperature Ionic Liquid inside Single-Wall Carbon Nanotubes

Shimou Chen, Ryo Kitaura, and Hisanori Shinohara

Department of Chemistry and Institute for Advanced Research, Nagoya University, Nagoya, 464-8602, Japan

We demonstrated for the first time the different morphologies of ionic liquids inside single-walled carbon nanotubes (SWNTs). A zinc contained quaternary ammonium based ionic liquid $[\text{Me}_3\text{NC}_2\text{H}_4\text{OH}]^+[\text{ZnCl}_3]^-$ (named as ChZnCl_3 for simplicity) was chosen to achieve better imaging contrast and resolution for high-resolution TEM observation. The arrangement of encapsulated ChZnCl_3 shows clear dependence on the diameter of SWNTs. As shown in Figure 1, with successively increasing the diameter of SWNTs ranging from 1.4 to 2.3 nm, the ChZnCl_3 patterns appear to be single molecular chains, double helix, zigzag tube and finally random tube. The resulting ChZnCl_3 patterns generally display structural characteristics unknown in bulk or film forms of ChZnCl_3 . This phenomenon is an observable manifestation of the confinement effect on ionic liquids.

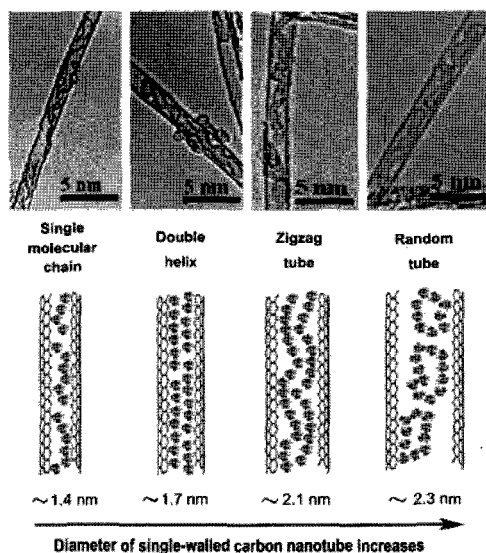


Figure 1. Dependence of the packing arrangement of ChZnCl_3 inside SWNTs on nanotubes diameters. (The labeled numbers are the representative value of the nanotubes diameters, it should be a range for each configuration.)

Corresponding Author: Hisanori Shinohara

TEL: +81-52-789-2482, FAX: +81-52-747-6442, E-mail: noris@nagoya-u.jp

Electronic Spectra and Fragmentation of Polyynes in the Gas Phase

○ Takeshi Yamada¹, Yoriko Wada¹, Tomonari Wakabayashi^{1*}
Koji Okuda², and Masa-aki Ubukata²

¹Department of Chemistry, Kinki University, Higashi-Osaka 577-8502, Japan

²Application & Research Group, Analytical Instrument Division, JEOL Ltd.,

Akishima, Tokyo 196-8558, Japan

The electronic state of polyynes, $\text{H}(\text{C}\equiv\text{C})_5\text{H}$, was studied by resonant two-photon ionization (R2PI) spectroscopy in the gas phase. We used a time-of-flight mass spectrometer (TOFMS) with a tunable laser system for ionization. Solutions of C_{10}H_2 were introduced into vacuum and irradiated with UV laser pulses at a selected wavelength. The ion intensity was plotted as a function of the excitation wavelength to obtain R2PI spectra (closed circle in bottom panel in Fig. 1). In the region of 225–230 nm, we observed enhancement in the peak intensity for $\text{C}_{10}\text{H}_2^+$ (m/z 122) relative to that for hexane (m/z 86), showing a peak maximum at 228.0 nm. The position of the resonance is compatible with the extrapolation of those reported in the previous work for the origin band of the ${}^1\Sigma_u^+ \leftarrow X{}^1\Sigma_g^+$ electronic transition of longer polyynes, C_{2n}H_2 of $n = 8\text{--}13$ [1]. Concerning the absorption band for hexane solutions (solid line in top panel in Fig. 1), the red shift by $\sim 4250\text{ cm}^{-1}$ ($228.0 \rightarrow 252.5\text{ nm}$) as well as the broadening is related to the interaction with solvent molecules. Similarly to the second peak at 240.1 nm in hexane, which is due to the excitation of a stretching vibrational mode of $\sim 2050\text{ cm}^{-1}$, another peak is expected at $\sim 218\text{ nm}$ for R2PI spectra in the gas phase.

Fragmentation of size-selected polyynes, C_8H_2 , was investigated by using a GC-TOFMS system (JEOL JMS-T100GCV) with electron ionization (EI). We observed that, next to the parent peak for C_8H_2^+ (m/z 98.017), the fragment peak for C_5H^+ (m/z 61.006) was intense, indicating preferential loss of neutral C_3H upon the electron impact of C_8H_2 .

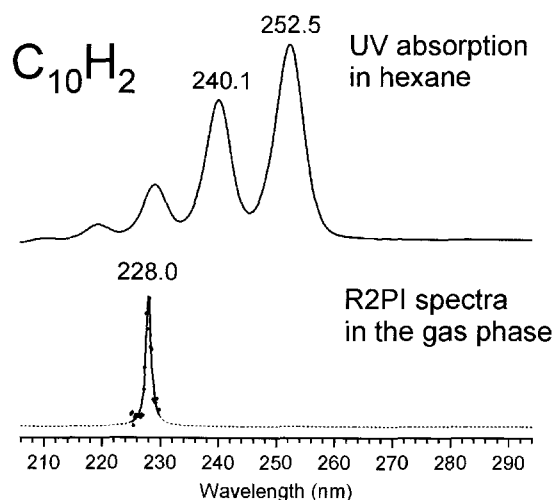


Figure 1. R2PI spectra of polyynes, C_{10}H_2 , in the gas phase (bottom). The signal peaking at 228.0 nm corresponds to the origin band of the ${}^1\Sigma_u^+ \leftarrow X{}^1\Sigma_g^+$ electronic transition of the linear molecule. Absorption spectrum for C_{10}H_2 in hexane is shown for comparison (top). Note that the band at 228.0 nm in the gas phase red-shifts to 252.5 nm in hexane.

[1] T. Pino, H. B. Ding, F. Guthe, and J. P. Maier, *J. Phys. Chem.* **114**, 2208-12 (2001).

Corresponding Author: Tomonari Wakabayashi

E-mail: wakaba@chem.kindai.ac.jp

Tel. 06-6730-5880 (ex. 4101) / FAX 06-6723-2721

Formation of Polyne-Iodine Complexes in Solutions

○Yoriko Wada¹, Tomonari Wakabayashi^{1*}, Ryoichi Osada², and Tatsuhisa Kato^{2*}

¹Department of Chemistry, Kinki University, Higashi-Osaka 577-8502, Japan

²Department of Chemistry, Josai University, Sakado, Saitama 350-0295, Japan

Polyne molecules, $H(C\equiv C)_nH$ of $n=5-7$, were prepared in a size-selective manner by using HPLC and contacted with I_2 molecules in solutions of hexane at room temperature. The reaction was then followed by measuring the electronic absorption spectra. We found that, as the concentration of I_2 increased, absorption bands for the dipole-allowed transition of polyynes in the UV diminished, while those for the forbidden transition of polyynes in the near UV increased. We have analyzed the spectral change in absorption to deduce stoichiometry for a polyne-iodine complex presumably formed upon mixing in solutions.

Figure 1 shows the spectral change for the $C_{12}H_2/I_2$ system in hexane for relatively low concentrations of iodine. The series of bands for $C_{12}H_2$ at 276 nm and shorter wavelengths decreased upon increasing iodine concentration. By assuming the equilibrium, $C_{12}H_2 + n I_2 \leftrightarrow C_{12}H_2(I_2)_n$, we solved the mass-balance equation and compared with the observation (open circle in Fig. 2). The fitting curve (solid line in Fig. 2) suggests the number being $n \sim 3$.

As the concentration of iodine increased, a new absorption feature appeared in-between the allowed and forbidden bands, including a few peaks having a characteristic spectral shape, namely “W-bands”. Further increase of iodine results in the growth in intensity for one of the new peaks at 328 nm (see dotted line spectrum in Fig. 1). This observation implies that the formation of a primary complex, $C_{12}H_2(I_2)_3$, is followed by the growth of another complex having a well-defined structure.

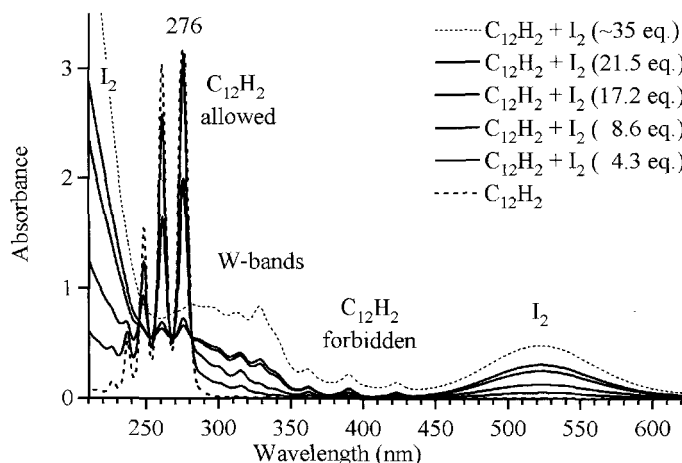


Figure 1. Absorption spectra of $C_{12}H_2/I_2$ in hexane for different iodine concentrations.

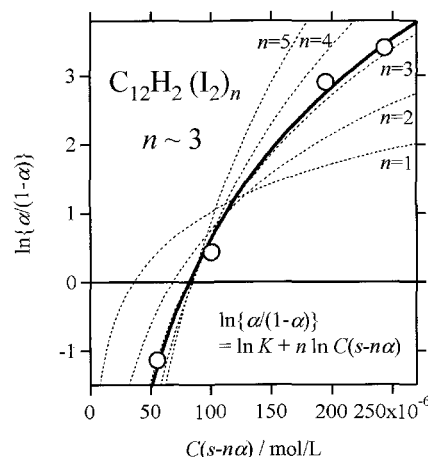


Figure 2. Equilibrium analysis for the decrease in $C_{12}H_2$ as estimated from the intensity of 261 nm band upon increase in the concentration of I_2 .

Corresponding Author: Tomonari Wakabayashi

E-mail: wakaba@chem.kindai.ac.jp

Tel. 06-6730-5880 (ex. 4101) / FAX 06-6723-2721

Characterization of La fullerene soot and formation of LaC₂ containing multi-shell carbon nanocapsules by heat treatment

○Kazunori Yamamoto^a, Takeshi Akasaka^b

^a*Nanomaterials Research Group, Quantum Beam Science Directorate,*

Japan Atomic Energy Agency, Tokai-mura, Naka-gun, Ibaraki 319-1195, Japan

^b*Center for Tsukuba Advanced Research Alliance, University of Tsukuba, Ibaraki 305-8577, Japan*

Abstract:

The technology of carbon-encapsulated metal nanocrystals was developed fairly recently [1, 2], and at present it encompasses several different synthesis methods[3]. Fullerenes encapsulating one La atom (called endofullerenes) were discovered in the fullerene soot formed by laser vaporization of La with carbon under Ar flow [4]. On the other hand, carbon nanocapsules containing La element were not found in the fullerene soot, which were discovered in carbonaceous cathode deposits formed by arc-discharge evaporation and following deposition of La with carbon on the cathode surface [1, 2]. Electron diffraction (ED) revealed that the capsules were filled with LaC₂ single crystals, not La metals [2]. Transmission electron microscopy (TEM) characterization showed that the endohedral graphitic nanoparticles were usually seen in the deposit, not in the soot.

La fullerene soot prepared by a conventional DC arc discharge method at low He pressure (15, 20, 35, 45 Torr) have been characterized, then used as precursors of LaC₂ containing multi-shell carbon nanocapsules by our heat treatment method [3]. The soot materials have been treated at temperatures between 1000 and 2200°C in vacuum. The soot materials have been characterized by TEM and Thermo gravimetric (TG) method. Multi-shell single-digit nanoparticles filled with La have been found in La fullerene arc soot synthesized at 35 and 45 Torr He, which is lower than the ordinal pressure for the fullerene and nanotube condition. On the other hand the nanoparticles have not been found in La fullerene arc soot synthesized at 15 Torr He. Detailed results of characterization will be presented in the presentation.

1. R. S. Ruoff, et al., *Science*, **259**, 336(1993).
2. M. Tomita, et al., *Jpn. J. Appl. Phys.*, **32**, L280(1993).
3. K. Yamamoto, et. al., The 34th Fullerene Nanotube General Symposium Abstract 2-14.
4. Y. Chai, et al., *J Phys Chem.*, **95**, 7564(1991).

Corresponding Author: Kazunori Yamamoto

E-mail: yamamoto.kazunori@jaea.go.jp

Tel&Fax: +81-29-282-6474&+81-29-284-3813.

Formation of Polyhedral Graphite Particles by High-density Carbon Arc Discharge with Alcohol Vapor

○Yoji Katagiri, Akira Koshio and Fumio Kokai

Division of Chemistry for Materials, Graduate School of Engineering, Mie University, 1577 Kurimamachiya-cho, Tsu, Mie 514-8507, Japan

It is known that polyhedral graphite (PG) particles having a structure composed of many polyhedra with 100 nm - 1 μm diameters are formed by the laser vaporization of graphite in a high-pressure Ar atmosphere [1]. These PG particles can be used as a lubricant because of their unique structures and properties, such as chemical and mechanical stability during high-pressure compression. We have reported that PG particles can be formed efficiently by using cellulose char as an additional carbon source in the arc discharge (high-density carbon arc discharge) [2]. Recently we found another high-density carbon arc discharge method using alcohol vapor. In this study, we investigated more effective formation condition of PG particles in carbon arc plasma with alcohol vapor.

The PG particles were produced by conventional carbon arc discharge with ethanol vapor introduced into the arc plasma in an Ar atmosphere. The ethanol vapor was introduced into the chamber by bubbling argon through ethanol heated at 50 °C. The high-density carbon arc discharge was maintained by pyrolysis of ethanol during sublimation of the graphite anode.

Figure 1 shows TEM images of carbon nanoparticles (PG particles, balloon-like particles and platelet graphite) formed by high-density carbon arc discharge with alcohol vapor. The PG particles have facets and highly graphitized concentric structures that are the same as those formed by laser vaporization. The interlayer spacing was approximately 0.34 nm. The diameters of the PG particles ranged from 120 to 700 nm and the average diameter was 314 nm. These results are similar to those for laser vaporization. It is usually necessary to have a high-pressure of 0.9 MPa to form PG particles by laser vaporization. However, PG particles can be formed efficiently at a low-pressure of 0.1 MPa by using our arc technique. We assume that the additional carbon source from the ethanol vapor lead to the high density carbon species equivalent to that of laser vaporization in high-pressure Ar.

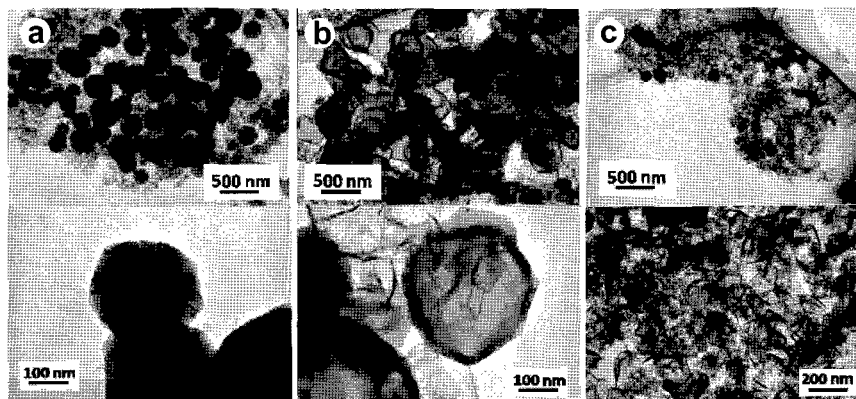


Fig. 1 TEM images of carbon nanoparticles produced by high-density carbon arc discharge with alcohol vapor. (a) PG particles, (b) balloon-like particles, (c) platelet graphite.

References: [1] F. Kokai *et al.*, *Appl. Phys. A*, 77, 69 (2003).

[2] Y. Katagiri *et al.*, *The 33rd Fullerene-Nanotubes General Symposium*, 2P-22.

Corresponding Author: Akira Koshio, E-mail: koshio@chem.mie-u.ac.jp, Tel & Fax: +81-59-231-5370

Formation Peculiarities, Structure and Morphology of C₆₀-PANI and C₆₀-PTFE Thin Composite Films

Victor Kazachenko^{1,2}, Tetsu Mieno³, Ihar Razanau^{1,3}

¹*Francisk Skorina Gomel State University, Gomel 246019, Belarus*

²*Belarusian State University of Transport, Gomel 246653, Belarus*

³*Department of Physics, Faculty of Science, Shizuoka University, Shizuoka 422-8529, Japan*

Vacuum electron beam dispersion (EBD) method allows forming multilayer, nanocomposite coatings on the basis of insoluble and thermostable polymers, lowmolecular organic substances and nanoparticles [1]. On the other hand we have previously showed that it is possible to deposit polymerized C₆₀ coatings using the EBD method and polymerization degree of the coating in that case can be controlled through the EBD process parameters [2, 3]. At the same time as far as we know thin composite films on the basis of organic polymers and polymerized C₆₀ hadn't been studied before and thus are new research objects.

In this report we discuss the EBD deposition of two types of thin composite fullerene based films: C₆₀-polytetrafluoroethylene (PTFE) and C₆₀-polyaniline (PANI). Deposition kinetics such as target surface temperature, coating growth rate and pressure in the vacuum chamber are analyzed. The structure of deposited coatings studied by FTIR and Raman spectroscopy and morphology of coatings surface studied using AFM measurement in dynamic force mode are discussed.

It is showed that thin composite C₆₀-PTFE coatings deposited by the vacuum EBD method contain both initial components, however some changes in their structure were observed. In particular, at certain process parameters formation of linear orthorhombic polymerized C₆₀ in the composite was revealed. Thus this kind of coatings contain organic polymer PTFE, fullerene C₆₀ and C₆₀ polymer. The possible interaction between PTFE and C₆₀ in the coating is discussed. For C₆₀-PANI composite thin films deposited using the vacuum EBD method it is showed that both initial components present in the composite. However certain changes in their structure were revealed as well. The formation of conductive areas in the such composite films is discussed on the basis of FTIR and Raman spectroscopy data.

[1] K. Gritsenko, A. Krasovsky, *Chemical Reviews*, **103** (9), 3607 (2003).

[2] V.P. Kazachenko, I.V. Ryazanov, *Technical Physics Letters*, **34** (11), 930 (2008).

[3] V.P. Kazachenko, I.V. Ryazanov, T. Mieno, *Abstracts of IUMRS-ICA 2008*, **NP-1** (2008).

Corresponding Author: Ihar Razanau

TEL: 08069271152, E-mail: ir23.by@gmail.com

New Method of Sidewall Functionalization of SWNT with Fuming Nitric Acid

○Hiroshi Kitamura¹, Masaru Sekido², Hisato Takeuchi³, Masatomi Ohno¹

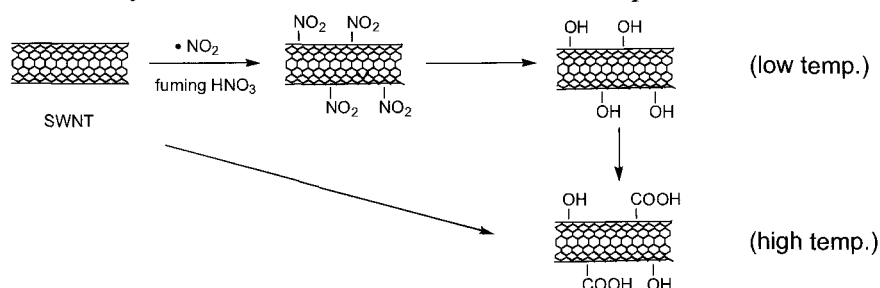
¹*Department of Advanced Science and Technology, Toyota Technological Institute, Nagoya 468-8511, Japan*

²*Department of Materials Science and Engineering, Miyagi National College of Technology, Miyagi 981-1239, Japan*

³*Materials Fundamental Research Department, Toyota Central R & D Labs. Inc, Nagakute, Aichi 480-1192, Japan*

Functionalization of CNT has been attracted in view of the solubilization of CNT leading to mechanical and electrochemical applications. Smalley et al. disclosed carboxylic acid functionalization on the open-edge with HNO₃/H₂SO₄ for the first time [1], which was utilized for the solubilization of SWNT in the water or organic solvents by its esterification or formation of ammonium salts. Alternatively sidewall functionalization has been achieved by using organic radical, which substantiated higher solubility in various solvents, because of destruction of the bundle structure.

Here we wish to report the new method of sidewall functionalization of SWNT by using fuming nitric acid as a NO₂ radical source [2]. The reaction of the SWNT with fuming nitric acid at 10-90 °C under sonication followed by NaOH treatment gave the material having the high affinity with polar solvents such as DMF. The measurement of IR spectrum showed the product to have OH group (3400, 1200cm⁻¹), which was expected to arise by the addition of NO₂ radical to surface double bonds and subsequent substitution with OH group. Furthermore it was found that the intensity of the COOH peak increased with raising the reaction temperature, probably due to progressive oxidation. Product analysis was also investigated in detail by other measurements such as Raman spectrum, XPS and TGA.



[1] J. Liu, A. G. Rinzler, H. Dai, J. H. Hafner, R. K. Bradley, P. J. Boul, A. Lu, T. Inverson, K. Shelimov, C. B. Huffman, F. R.-Macias, Y.-S. Shon, T. R. Lee, D. T. Colbert, R. E. Smalley, *Science*, **280**, 1253 (1998).

[2] H. Moriyama, Y. Yamamoto, Y. Ito, The 25th symposium abstract p.119 (in organic medium).

Corresponding Author: Masatomi Ohno

TEL: +81-52-809-1889, FAX: +81-52-809-1721, E-mail: ohno@toyota-ti.ac.jp

Theoretical Study of Spin Injection from Fe into Oligoacene

○Yoshitaka Kato, Hiroyuki Fueno and Kazuyoshi Tanaka

*Department of Molecular Engineering, Graduate School of Engineering,
Kyoto University, Kyoto 615-8510, Japan*

It is known that the relaxation of injected spin in molecular materials occurs slowly, because spin-orbit interaction of molecular materials composed of light element like hydrogen, carbon, oxygen and nitrogen is small. Especially, in the case of carbon materials (carbon nanotube, graphene, oligoacene and so forth), electron scattering is less apt to occur and spin scattering also occurs slowly. So, carbon materials can be good molecular materials for spin injection.

In this study, we chose hexacene for molecular materials and Fe for ferromagnetic electrodes as shown in Fig. 1. The nonequilibrium Green's function method based on the density functional theory (DFT) is used to compute the spin transport properties by the ATK (Atomistix ToolKit) program package.

We obtain I-V (current-voltage) characteristics and transmission spectra for each spin types (Up-Spin (majority) / Down-Spin (minority)) when Fe electrodes are parallel magnetization. From a series of calculations, it is found that one type of spin polarized current flows more easily.

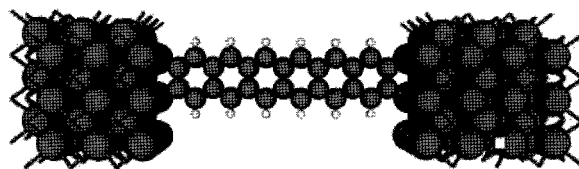


Fig. 1 Hexacene between Fe ferromagnetic electrodes.

Corresponding author: Yoshitaka Kato

TEL: 075-383-2549, FAX : 075-383-2555, E-mail: kato-yoshitaka@mail.goo.ne.jp

**Density-functional tight-binding molecular dynamics
simulations of the self-capping process in open-ended (n,n)
SWCNTs (n=3 to 10)**

Hironori Hara¹, Stephan Irle^{1*}

¹*Institute for Advanced Research and Department of Chemistry, Nagoya University,*

Nagoya 464-8602, Japan ²*Fukui Institute, Kyoto University, Kyoto*

E-mail: sirle@iar.nagoya-u.ac.jp

Using canonical molecular dynamics (MD) simulations based on the density-functional tight-binding (DFTB) quantum chemical method, we studied the self-capping processes of 35 Å-long, open-ended armchair (n,n) single-walled carbon nanotubes (SWCNTs) (n=3 to 10, the diameter ranges from 4 Å for n=3 to 13.5 Å for n=10) at 3000 K and 3500 K. We find that, with the exception of the (3,3) tube, all of these open-ended SWCNTs can self-cap during simulation times on the order of 10 to 1000 ps, but the time for self-capping increases steeply with the tube diameter. The very small (3,3) tube is highly strained and typically falls apart at such high temperatures. Ring statistics and an estimate for carbon loss will be discussed in dependence on tube type and temperature.

Synthesis and Search for Superconductivity of Alkaline Earth Graphite Intercalation Compounds

○Satoshi Heguri, Nozomu Kimata, Mototada Kobayashi

*Department of Material Science, Graduate School of Material Science
University of Hyogo, Ako, Hyogo 678-1297, Japan*

Recently, graphite intercalation compounds (GICs) have attracted great attention due to the discovery of superconductivity in CaC_6 and YbC_6 with fairly high transition temperatures T_c of 11.5 and 6.5K, respectively [1,2]. Mazin explained the difference in T_c by the “isotope effect” due to the difference in Yb and Ca atomic masses on the basis of first-principles calculations and suggested that the codoping with Mg might be a route to even higher T_c [3].

Calandra et al., predicted superconductivity for SrC_6 at 3.1K and BaC_6 at 0.2K using density functional theory [4]. Kim et al. confirmed the superconductivity in SrC_6 at $T_c = 1.65\text{K}$ and the absence of superconductivity in BaC_6 down to $\sim 0.3\text{K}$ [5]. Thus, the superconductivity in BaC_6 and MgC_6 is an interesting subject from experimental and theoretical points. However, no superconductivity has been found in BaC_6 and there has been no report on the synthesis of MgC_6 .

In this work, we report synthesis and search for superconductivity of BaC_6 and MgC_6 . We adopted conventional vapor phase reaction in order to prepare high quality GICs. BaC_6 and MgC_6 were synthesized from highly oriented pyrolytic graphite (grade ZYA), and excess Sr metal (99.95%) or Mg metal (99.98%). They were sealed into quartz tube after evacuating. Thermal treatment was performed in a furnace at 623~743K for several weeks. After the reaction, the graphite surface changed from black to metallic luster. It is expected that metals are intercalated into graphite and electronic charge transfer may occur from alkaline earth metal to graphite.

The x-ray diffraction profiles and the magnetic susceptibility for the alkaline earth GICs will be discussed at the meeting.

- References:** [1] T. E. Weller et al., Nature Physics 1 (2005) 39.
[2] N. Emery et al., Phys. Rev. Lett. 95 (2005) 087003.
[3] I. I. Mazin Phys. Rev. Lett. 95 (2005) 227001.
[4] M. Calandra et al., Phys. Rev. B 74 (2006) 094507.
[5] J. S. Kim et al., Phys. Rev. Lett. 99 (2007) 027001.

Corresponding Author: Satoshi Heguri

E-mail: rk07d004@stkt.u-hyogo.ac.jp

Tel&Fax: +81-791-58-0156/+81-791-58-0131

Studies on Ion RF Devices for Ion Mobility Measurement

○Toshiki Sugai

Department of Chemistry, Toho University, Miyama 2-2-1 Funabashi, 274-8510, Japan

Ion mobility/mass spectroscopy measurements have been utilized for nano carbon materials, such as carbon clusters and metallofullerenes[1,2] by utilizing potential high sensitivity and high throughput for mixed and unstable materials to clarify new structures. However, the measurement requires high pressure buffer gas for high-resolution mobility or structure separation which prevent the high sensitivity because the ions are diluted with the buffer gas. To overcome these difficulties we are developing an ion RF devices[3,4] to separate the target ions from the neutral buffer gas. Figure 1 shows these devices utilizing RF fields with a frequency of 0.1 to 10 MHz and a voltage of 10 to 1000 V. These RF have multi-pole or ring-stack structures, where the RF voltages are applied to the adjacent electrodes alternatively. The ions with buffer gas are passing through the devices feel averaged field which keep the ion positions at the center of the devices even if there is the buffer gas and the diffusion. The buffer gas, on the other hand, diffuses and escapes from the devices. We will discuss the device properties to separate ions and buffer gas for the mobility/mass measurements.

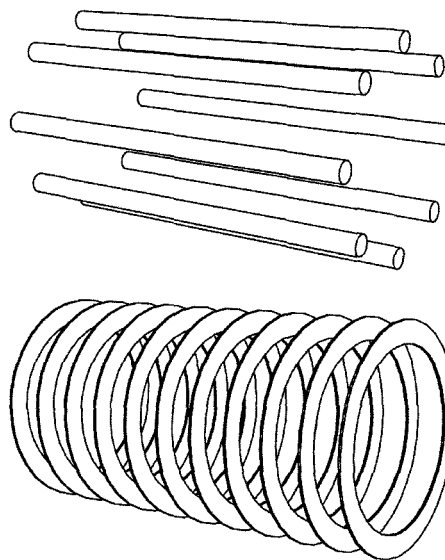


Fig.1 Ion RF Devices

- [1] T. Sugai *et al.*, *J. Am. Chem. Soc.* **123**, 6427 (2001).
- [2] von Helden *et al.*, *J. Chem. Phys.* **95**, 3835 (1991).
- [3] W. Paul, *Rev. Mod. Phys.* **62**, 531 (1990).
- [4] A. V. Tolmachev *et al.*, *Int. J. Mass Spec.* **203**, 31 (2000).

TEL: +81-47-472-4406, FAX: +81-47-472-4406, E-mail: sugai@chem.sci.toho-u.ac.jp

Growth of One-dimensional Array of Graphitic Cones in Vertically Aligned Carbon Nanofibers

○Takayuki Yamasaki, Akira Koshio, Yuta Tango, Tomohito Imai and Fumio Kokai

*Division of Chemistry for Materials, Graduate School of Engineering, Mie University,
1577 Kurimamachiya-cho, Tsu, Mie 514-8507, Japan*

Catalytic chemical vapor deposition (CVD) has been extensively investigated as a promising method for growing of carbon nanofibers (CNFs). It is well known that various periodic structures of CNFs are formed by controlling growth conditions, such as metal catalysts and reactant gases. We previously reported that CNFs containing a conical cavity array were formed by alcohol CVD using indium tin oxide (ITO) and Fe as the metal catalysts. We named these CNFs “conical-cavity CNFs (CC-CNFs)” because they have a unique structure containing conical cavities in a one-dimensional array at uniform intervals. We succeeded in growing the vertically aligned CC-CNFs on a substrate by using precisely temperature-controlled CVD. Recently we have also developed precisely flow-controlled system for introducing ethanol and CS₂ vapor independently. In this study, we discuss what influence the growth temperature and ratios of ethanol and CS₂ had upon the degree of vertical alignment and their inner structures.

A substrate was prepared by using the electrically controlled spray method. Ethanol solutions of InCl₃, SnCl₂, and FeCl₃ were used as catalysts and were sprayed on a Si plate maintained at 400°C followed by heating at 640°C for 30 min. in an Ar atmosphere. The CVD growth of the CNFs was carried out at 890-1030°C for 30 min. at a vapor pressure of ethanol containing a small amount of CS₂ in a vacuum.

A typical CC-CNF formed after the CVD growth had a diameter of about 300 nm and an array of periodic conical cavities on the inside. The CC-CNFs cannot grow at 890°C or less. We confirmed that vertically quasi-aligned CC-CNFs were formed at more than 900°C, and that vertically well-aligned CC-CNFs grew on the substrate at about 1000°C (Fig. 1(a)). Tangled CNFs (not vertically aligned) were formed at 1030°C. The SEM observation and precisely temperature-controlled CVD revealed the existence of two important critical temperatures and the narrow temperature range for the vertically well-aligned growth of the CC-CNFs. Figure 1(b) shows the well-aligned CC-CNF film with a thickness of about 1 mm. In addition, we investigated the relationship between the growth temperature and the inner structure by using TEM observations. Cone angle of the conical cavities decreases gradually with an increase in growth temperatures (Fig. 1(c)). The cone angles would depend on viscosity of metal particles as catalysts.

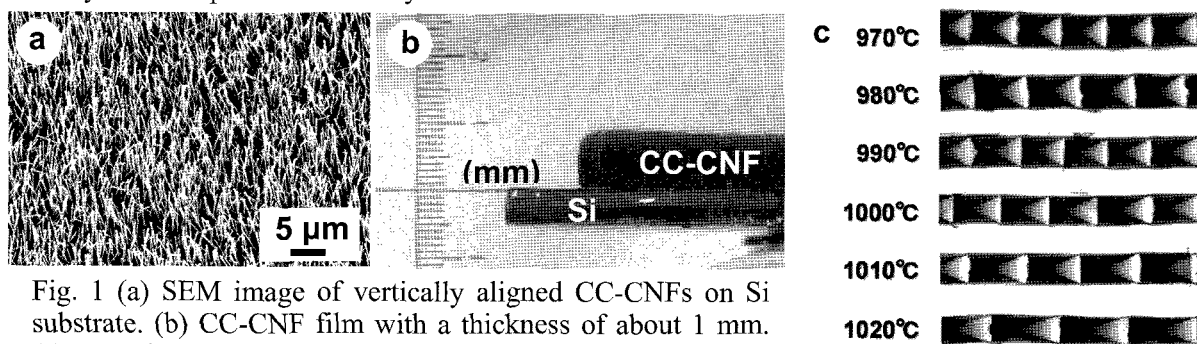


Fig. 1 (a) SEM image of vertically aligned CC-CNFs on Si substrate. (b) CC-CNF film with a thickness of about 1 mm. (c) Conical-cavity array formed at various growth temperatures.

References: [1] Y. Tango *et al.*, *The 33rd Fullerene-Nanotube General Symposium*, 3P-40.

Corresponding Author: Akira Koshio, **E-mail:** koshio@chem.mie-u.ac.jp, **Tel & Fax:** +81-59-231-5370

Applications of vertically well-aligned CNT films to capacitors

○Haruo Kato, Michiko Kusunoki*, Shigeyuki Sugimoto**, Kunihiro Sugihara**,
Nobuyuki Yamamoto**, Hideki Fujita, Noriyoshi Shibata

2-4-1 Mutsuno, Atsuta-ku, Nagoya 456-8587, Japan Japan Fine Ceramics Center

*Furo-cho, Chikusa-ku, Nagoya 464-8603, Japan

Eco Topia Science Institute, Nagoya University

**20-1 Kitasekiyama, Odaka-cho, Midori-ku, Nagoya 459-8522, Japan

Chubu Electric Power Co., Inc.

Abstract: We achieved high levels of performance in electric double-layer capacitors¹⁾ applied well-aligned and high-density CNT films formed by SiC surface decomposition²⁾. We deposited Pt nano-particles on CNT surface by introducing an electrochemical activation and they were oxidized by an anode oxidation treatment.

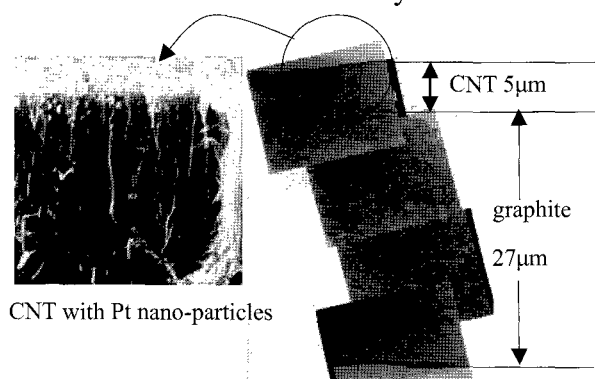


Fig.1 Cross-section TEM & SEM image of CNT film electrode

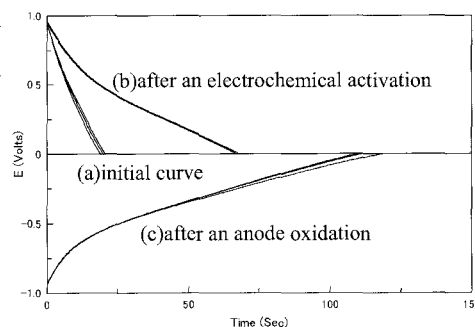


Fig.2 Discharge curves of electric double-layer capacitor developed

We obtained the result that the pseudocapacitance of the CNT film electrode was achieved 4 times higher capacitance (100F/g) than initial (25F/g) and no decrease in degree of capacitance under conditions of higher current density was confirmed in comparison with commercial activated carbon electrode.

References

- 1) H.Kato et al., *The 34th Fullerene-Nanotubes general Symposium*, **1P-13**(2008).
- 2) M.Kusunoki, M.Rokkaku, and T.Suzuki : *Appl.Phys.Lett.* **71**,2620(1997).

Corresponding Author Haruo Kato (E-mail: hakato@jfcc.or.jp)

Tel +81-52-871-3500 & Fax +81+52-871-3599)

Electrochemical Behaviors of Cytochrome c at Carbon Nanotube Surfaces

Masato Tominaga, Hiroiyuki Yamaguchi, Shingo Sakamoto, Toshifumi Nishimura, Shiori Kaneko and Isao Taniguchi

*Graduate School of Science and Technology, Kumamoto University,
Kumamoto 860-8555, Japan*

The increasing interest in direct electron transfer (DET) reaction type bioelectrocatalysis is driven by its important applications as biosensors, biofuel cells and bioreactors. The carbon nanotubes (CNTs) are used for DET reaction with the biomolecules because of their unique structures and conductivities. However, it would be expected that the DET reaction of biomolecules at the CNT surface is strongly influenced by the surface condition of CNTs. In this study, we investigated that the electrochemical behaviors of cytochrome c at CNT surfaces.

CNTs were synthesized onto a gold electrode surface by using chemical vapor deposition method using Co-Mo alloy nanoparticles as a catalyst. The average diameter size of the synthesized CNTs was evaluated to be 1-1.5 nm.

Fig. 1 shows the cyclic voltammograms at the CNT/Au electrode in 0.1 mM cytochrome c solution. At UV-ozone treated CNT/Au electrode, well-defined redox wave of cytochrome c was observed. On the other hand, the redox reaction could not be observed at the untreated CNT/Au electrode. The surface defects of CNT surface would play an important role for DET reactions of cytochrome c. The redox potential evaluated from the middle point of the oxidation and reduction potentials was to be 35-60 mV (vs. Ag/AgCl/saturated KCl), which was similar to the evaluated value using a promoter-modified gold electrode [1].

[1] I. Taniguchi et al., *J. Chem. Soc., Chem. Commun.*, 1032 (1982).

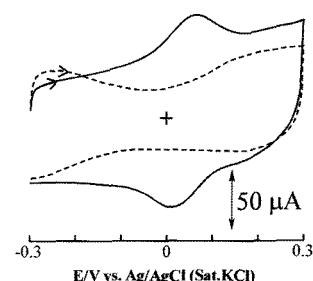


Fig. 1 Cyclic voltammograms at UV-ozone treated (solid line) and untreated (broken line) CNT/Au electrode in a phosphate buffer (pH 7) solution with 0.1 mM cytochrome c. Potential sweep rate was 80 mV/s. Electrode area: 0.25 cm².

Corresponding Author: Masato Tominaga

E-mail: masato@gpo.kumamoto-u.ac.jp

Tel&Fax: +81-096-342-3656

Analysis of interfacial behaviors of carbon nanotubes using *in-situ* Raman spectroelectrochemistry

Masato Tominaga, Shingo Sakamoto, Toshifumi Nishimura and Isao Taniguchi

*Graduate School of Science and Technology, Kumamoto University,
Kumamoto 860-8555, Japan*

Carbon nanotubes (CNTs) are remarkable nanostructures with promising perspectives for application as charge storage devices and various electronic devices. In this study, electrochemical interfacial behaviors of CNTs in an aqueous solution were investigated using *in situ* Raman spectroelectrochemistry.

CNTs synthesized onto Pt electrode by using CVD method. The average diameter size of the CNTs was evaluated to be *ca.* 1.3 (\pm 0.5 nm). Carbon nanofibers (CF) with 20 ~ 50 nm in diameter were also synthesized onto Pt electrode surface. Cyclic voltammetric and *in-situ* Raman spectroelectrochemical measurements were performed to investigate the electrochemical interfacial behaviors of CNTs. An Ag/AgCl (saturated KCl) electrode and a platinum electrode were used as the reference and counter electrodes, respectively.

In the negative direction at CNTs/Pt electrode, the cathodic current corresponding to hydrogen adsorption increased from *ca.* -0.8 V (Fig. 1c). After the direction of polarization was changed, the hydrogen desorption peaks were observed around -0.6 V. On the other hand, the peaks corresponding to hydrogen adsorption and desorption could not be observed at CF/Pt electrode (Fig. 1b). The results indicate that hydrogen adsorption and desorption in the potential region at -0.5 ~ -1.0 V were based on CNTs. In the positive direction, large oxidation peak was observed around 0.9 V at CNTs/Pt electrode. This peak would be due to the partial oxidation of CNTs, because the peak could not be observed at CF/Pt electrode.

In-situ Raman spectroelectrochemical measurements in 0.1 M NaClO₄ solution were performed to investigate the CNT interface behaviors. The G/D ratio was *ca.* 16, when the electrode was applied at 0 V. After the potential was applied at 1.0 V, the G/D ratio decreased to 13. The some peaks in the region of RBM decreased after the potential was applied at 1.0 V. These results also support that CNTs were partially oxidized at 1.0 V.

Corresponding Author: Masato Tominaga

E-mail: masato@gpo.kumamoto-u.a.jp, TEL&FAX: 096-342-3656,

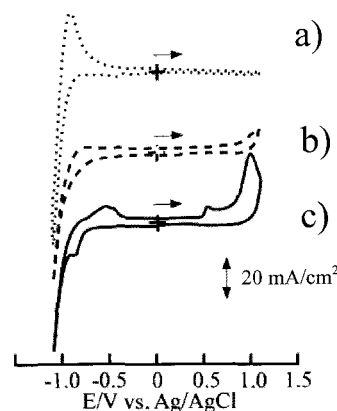


Fig. 1 Cyclic voltammograms at Pt (a), CF/Pt (b) and CNTs/Pt (c) electrodes in 0.1 M NaClO₄. Scan rate: 20 mV/s.

Diameter-Independent Thermal Oxidation of Single-Walled Carbon Nanotubes with NaCl under Microwave Heating

Yuki Kobayashi and ◯Masahito Sano

*Department of Polymer Science and Engineering, Yamagata University,
Yonezawa, Yamagata 992-8510, Japan*

Studying thermal oxidation of carbon nanotubes (CNTs) is important for the applications as well as the CNT growth. Higher oxidation temperatures are wanted for applications requiring thermal stability, whereas lower temperatures are attractive for incineration after use. Controlled oxidation of defect tubes and amorphous carbons improves quality of the resulting CNTs. The exact oxidation temperature depends on various factors such as the defect density, the aggregation structure, the presence of impurities, and the tube diameter. It has been reported [1] that NaCl lowers the oxidation temperature of multi-walled CNTs by introducing disorder at the early stage of oxidation. Here, we report the effects of NaCl on thermal oxidation of single-walled CNTs (SWCNTs) under microwave heating.

SWCNTs were sonicated lightly in strong acids to make them temporarily dispersible in water. After through rinsing with water, the acid-treated SWCNTs were divided into two fractions; one dispersed in pure water and another in aqueous NaCl solution. All SWCNTs were collected by mild centrifugation and casted on glass plates. The dried SWCNTs on glass were heated by microwave radiation at 100 W. Longer irradiation times imply higher temperatures. The addition of NaCl was found to cause faster oxidation. Raman spectroscopy on the acid-treated SWCNTs revealed increasing D-band and WBF shoulder, as well as decreasing RBM peaks at larger wavenumbers as the irradiation time increased. This indicates that smaller diameter SWCNTs are oxidized faster and that individual tube burns faster, resulting in the increased fraction of bundled tubes. On the other hand, SWCNTs with NaCl show only a small change on relative peak intensities around D and G-bands and no regular changes on RBM peaks, despite the fact that the tubes burned faster. NaCl causes diameter- and aggregation structure-independent oxidation. We propose NaCl under microwave radiation acts like a catalyst, lowering oxidation temperature of any SWCNTs and burning instantaneously even before defects have a time to spread.

[1] M. Endo, K. Takeuchi, T. Tajiri, K. C. Park, F. Wang, Y-A. Kim, T. Hayashi, M. Terrones, M. S. Dresselhaus, *J. Phys. Chem. B*, **110**, 12017 (2006).

Corresponding Author: Masahito Sano

TEL/FAX: +81-238-26-3072, E-mail:mass@yz.yamagata-u.ac.jp

Growth of Carbon Nanotubes on Flexible Carbon Fiber Sheet for Field Emitter

^oBongyong Jang¹, Y. Ito¹, Y. Hayashi¹, N. Kishi¹, T. Tokunaga², H. Matsumoto³,
K. Fukuzono⁴, M. Tanemura¹, A. Tanioka³, Gehan A. J. Amaratunga⁵

¹*Department of Frontier Materials, Nagoya Institute of Technology, Gokiso, Showa, Nagoya
466-8555, Japan*

²*Department of Quantum Engineering, Nagoya University, Furo, Chikusa, Nagoya 464-8601,
Japan*

³*Department of Organic and Polymeric Materials, Tokyo Institute of
Technology, 2-12-1-S8-27 Ookayama, Meguro-ku, Tokyo 152-8552, Japan*

⁴*Seiwa Electric Mfg. Co., Ltd., 36 Terada-Shinike, Joyo, Kyoto 610-0192, Japan*

⁵*Department of Engineering, University of Cambridge, 9 JJ Thomson Avenue, Cambridge
CB3 0FA, United Kingdom*

Flexible carbon fiber (CF) sheet prepared by electrospray deposition was used for the substrate of carbon nanotubes (CNTs) field emitter (FE) arrays[1]. CNTs was grown on the CF sheet by a microwave plasma CVD system (MPCVD). For the growth of the CNTs, a 1-nm-thick Pd layer was initially coated onto the CF sheet. After annealing the CF sheets, the CNTs were grown by the MPCVD using CH₄/H₂ mixture gases at 800°C using a microwave power of 600 W. The H₂ gas flow rate was adjusted to achieve a CH₄:H₂ ratio of 1:9 at a total pressure of 20 Torr. The dense CNTs were grown on the CF sheet, as shown in Fig 1. The CNT FE arrays on CF sheet produced a higher current density at a lower turn-on voltage compared to ones on a Si substrate.

References: [1]Suzuki et al., Polymer Journal, Vol. 39, No. 11,
pp. 1128–1134 (2007)

Corresponding Author: Yasuhiko Hayashi

E-mail: hayashi.yasuhiko@nitech.ac.jp

Tel&Fax: 052-735-5104

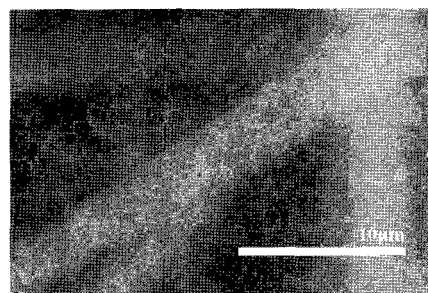


**Figure 1 SEM image of CNTs on Carbon
Fiber sheet**

Direct Growth of Single-walled Carbon Nanotubes Films and Their Opto-electric Properties

○Huafeng Wang¹, Kaushik Ghosh¹, Zhenhua Li², Takahiro Maruyama¹, Sakae Inoue¹,
Yoshinori Ando¹

¹21st COE Program “Nano Factory”, Department of Materials Science & Engineering,
Meijo University, Shiogamaguchi 1-501, Tenpaku-ku, Nagoya 468-8502, Japan

² Department of Mechanics, Zhejiang University, Hangzhou 310027, China

In this study, we introduce a new method to synthesize semi-transparent continuous single-walled carbon nanotubes (SWNTs) films by arc discharge process. We employ an effective technique to purify as-grown samples and check their field emission performance. The SWNTs films are sparse SWNTs bundles network structure containing metal particles

with thin layers of amorphous carbon coating. The two-step purification processes almost remove all impurities without disturbing the continuous network structure of films. In addition, we have observed the transmittance as well as electric conductivity improved to a considerable extent after purification. The unique continuous network structure results in a sheet resistance of a 150 nm film with transmittance higher than 77 % is measured to be $117 \Omega/\square$ (Fig. 1 a). In view of field emission measurement, the easily transferable films are pasted on quartz substrates used as cathodes and show an excellent field emission property with a low turn-on ($E_{to} = 0.4 \text{ V}/\mu\text{m}$) and threshold ($E_{th} = 1.4 \text{ V}/\mu\text{m}$) corresponding to the emission current density of $0.1 \mu\text{A}/\text{cm}^2$ and $1 \text{ mA}/\text{cm}^2$, respectively (Fig. 1 b).

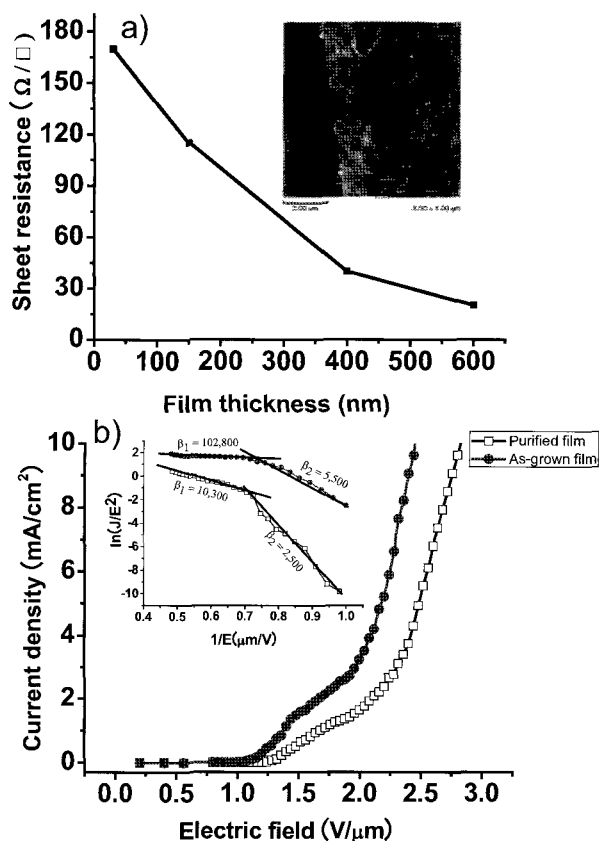


Fig. 1 a) The correlation between the film thickness and the sheet resistance. Inset: SPM image of film with thickness of 30 nm. b) Field emission from purified and as-grown SWNTs

Corresponding Author: Huafeng Wang

Tel:+81-52-838-2409, Fax:+81-52-832-1170

E-mail: wanghf@ccmfs.meijo-u.ac.jp

Optical properties of single-wall carbon nanotube-P3HT composites

○Ye Feng^{1,2}, Yasumitsu Miyata², Kiyoto Matsuishi¹, Hiromichi Kataura^{2,3}

¹Graduate school of Pure and applied Physics, Tsukuba University, 1-1-1 Tenodai, Tsukuba, Ibaraki 305-8573, Japan

²Nanotechnology Research Institute, AIST, 1-1-1 Higashi, Tsukuba 305-8562, Japan

³JST-CREST, Kawaguchi 330-0012, Japan

Recently, single-wall carbon nanotubes (SWCNTs) in conjugated polymer composites have attracted much attention because of their great potential in optical and electronic device applications such as sensors, p-n diodes, and photovoltaic cells. To design advanced materials for these applications, it is necessary to understand their foundational physical properties. To date, many researchers have investigated various polymer-SWCNT composites.[1-3] However, no detailed study about the pure polymer-SWCNT composites has been reported because the excess polymers are remained in the samples. These excess polymers hinder the observation of intrinsic interaction between polymers and SWCNTs. To solve this problem, in this study, pure SWCNT-poly(3-hexylthiophene) (P3HT) composites were separated from the excess polymers using ultracentrifugation and then their optical absorption and photoluminescence (PL) spectra were measured.

Figure 1 shows the absorption spectra of pristine P3HT and SWCNT-P3HT composites in toluene solution. The absorption peak at 600 nm in the composites is attributed to the absorption of P3HT attached to the SWCNTs. It shows a large red shift from the original peak position at 460 nm of the pristine one. No absorption peak around 460nm for the composites indicates that most of the free P3HT was removed from the sample. In the case of composites, PL of SWCNTs was observed, while that of P3HT was quenched. Interestingly, strong PL of SWCNTs was observed for high energy excitation (550 -600 nm) which was not seen in the surfactant-encapsulated individual SWCNTs. This suggests the high-efficiency energy transfer from the excited P3HT to SWCNTs.

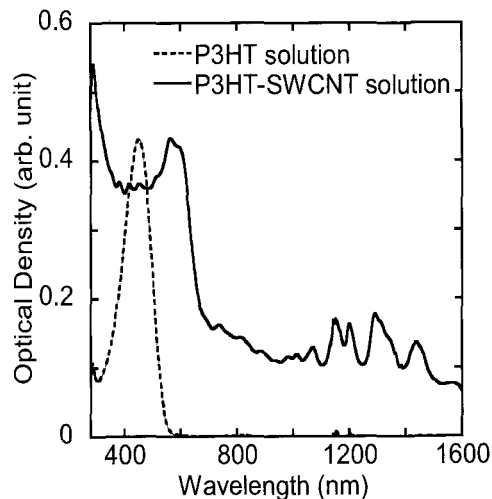


Fig. 1 Optical absorption spectra of pristine P3HT (dash line) and SWCNT-P3HT composites (Solid line).

References:

[1] E. Kymakis, G.A.J. Amaratunga, Rev. Adv. Mater. Sci. 10, 300-305 (2005), [2] A. Nish *et al.*, Nature Nanotechnology 2, 640-646 (2007), [3] S. Kazaoui *et al.*, Appl. Phys. Lett. 87, 211914 (2005)

Corresponding Author: Hiromichi Kataura

E-mail: h-kataura@aist.go.jp

Tel: +81-29-861-2551, **Fax:** +81-29-861-2786

Ionization Vacuum Gauge with a Carbon Nanotube Field Electron Emitter Combined with a Shield Electrode

○ Huarong Liu^{1,2}, Hitoshi Nakahara¹, Sashiro Uemura³ and Yahachi Saito¹

Dept. of Quantum Eng., Nagoya University¹, Nagoya University VBL², Noritake Co. Ltd.³

Thermal electron sources are widely used in commercial vacuum gauges. However, the thermal radiation induced by a hot cathode disturbs both the pressure measurement and the vacuum condition, especially in ultrahigh or extreme high vacuum (UHV/XHV). Carbon nanotubes (CNTs) are a promising cold cathode material owing to their remarkable physical and chemical properties [1]. Here, the applicability of carbon nanotubes to an electron source for a vacuum gauge has been investigated so as to effectively overcome the thermal effects.

A multi-walled CNT film, covered by a gate cathode, was selected as a cathode in this experiment [2]. This emitter was used to replace the hot filament of a commercial Bayard-Alpert (B-A) gauge. The modified gauge was installed in a vacuum chamber with a base pressure of 10^{-9} Torr, and it is tested for various ambient gas conditions. Several gauge configurations were tested in this experiment. An optimized one is shown in Fig 1. The introduction of the shield electrode can remarkably increase the electron transmission efficiency even with a reduced grid potential of ~ 200 V.

This gauge exhibits excellent measurement linearity between the ion current and the system pressure from 10^{-9} to 10^{-4} Torr, as shown in Fig. 1. Since the low pressure limit in this experiment is determined by the pumping system employed, this limit is expected to be extended to lower pressures. It is found that the cathode position plays an important role in the gauge sensitivity. So far, a gauge sensitivity of 6.4 Torr^{-1} has been achieved under $100 \mu\text{A}$ emission current for nitrogen, and it is comparable with the sensitivity of commercial B-A gauges ($\sim 10 \text{ Torr}^{-1}$). This gauge shows a low power consumption of ~ 0.14 W, and is therefore free from ill effects due to thermal radiation such as outgassing. This type of gauge is expected to find applications in UHV/XHV systems.

Reference

[1] Y. Saito, et al., *Jpn. J. Appl. Phys.*, **37**, L346 (1998).

[2] S. Uemura et al., *Proc. 10th Int. Conf. on the Science & Technology of Light Source* (July 18-22, 2004, Toulouse, France), pp.125-134.

Corresponding authors: Huarong Liu
and Yahachi Saito

E-mail: liu@surf.nuqe.nagoya-u.ac.jp

and ysaito@nagoya-u.jp

TEL: +81-52-789-3714

FAX: +81-52-789-3703

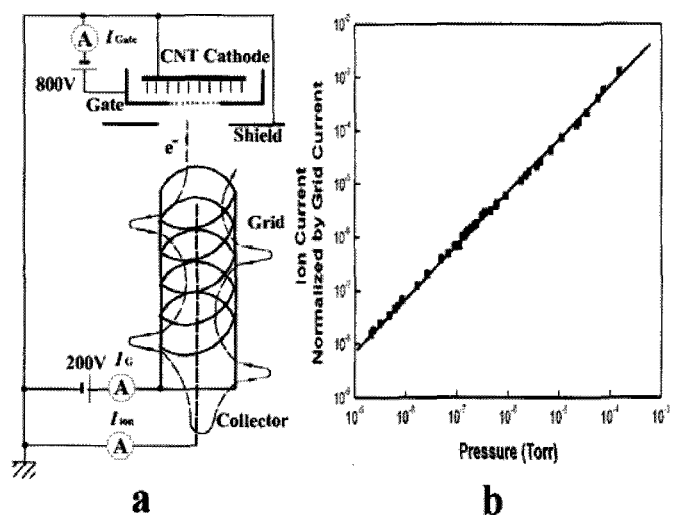


Fig. 1 a) CNT ionization gauge with a shield electrode. b) Ion current vs. pressure.

Dispersion of Single-Walled Carbon Nanotubes Using Poly(amidoamine) Dendrimer Having Alkyl Chain at the Core

○Ryouta Ikeuchi¹, Tetsuya Uchida², Tatsuo Fujii², Jun Takada² and Yutaka Takaguchi¹

¹Graduate School of Environmental Science, Okayama University, Okayama 700-8530, Japan

²Graduate School of Natural Science and Technology, Okayama University, Okayama 700-8530, Japan

Noncovalent functionalization of single-walled carbon nanotubes (SWNTs) have attracted considerable attention, because the study would lead to the chemical and biochemical design to create functional carbon nanotubes in solution systems without alteration of their inherent properties. During our studies on the synthesis, characterization, and property of fullerodendrion, we found that a solution of fullerodendrons disperses SWNTs via formation of supramolecular nanocomposite.[1] Although there are many reports described π - π interaction between dispersant and SWNTs[2,3], literature of surface modification of SWNTs employing CH- π interaction are quite limited.

Here we report that SWNTs are well dispersed in water by the use of poly(amidoamine) dendrimer having alkyl chain at the core (Figure 1). Surface modification of SWNTs using CH- π interaction between the alkyl chain and SWNTs was confirmed by VIS/NIR spectroscopy (Figure 2), Raman spectroscopy, AFM, and TEM observation.

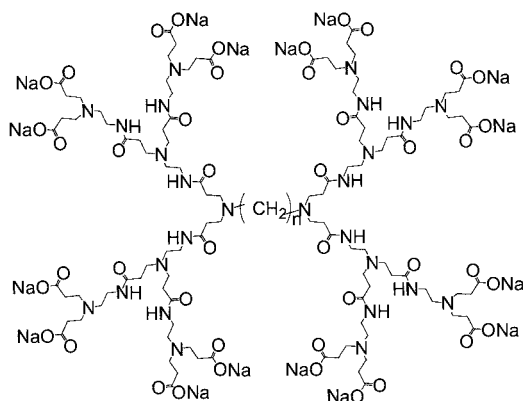


Figure 1. Structure of $C_nG_{1.5}(COONa)_{16}$.

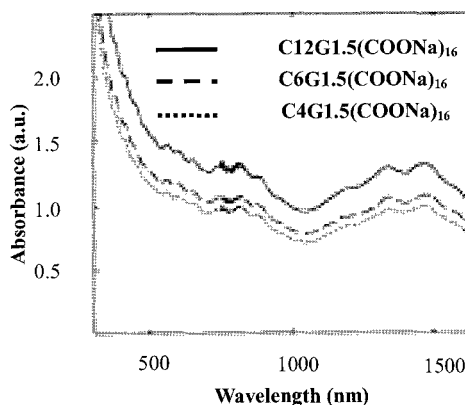


Figure 2. Vis-NIR spectra of SWNTs in D_2O in the presence of $C_nG_{1.5}(COONa)_{16}$.

[1] Y. Takaguchi, M. Tamura, Y. Sako, Y. Yanagimoto, S. Tsuboi, T. Uchida, K. Shimamura, S. Kimura, T. Wakahara, Y. Maeda, T. Akasaka, *Chem. Lett.*, **34**, 1608 (2005).

[2] N. Nakashima, Y. Tomonari, H. Murakami, *Chem. Lett.*, **31**, 638 (2002).

[3] J. Chen, C. P. Collier, *J. Phys. Chem. B*, **109**, 7605 (2005).

Corresponding Author: Yutaka Takaguchi

TEL: +81-86-251-8903, FAX: +81-86-251-8903, E-mail: yutaka@cc.okayama-u.ac.jp

Field Emission Characteristics of Carbon Nanotubes for Electron Microscopes

○Y.Kusano, K.Asaka, H. Nakahara, and Y. Saito

Dept. of Quantum Eng., Nagoya University, Furo-cho, Nagoya 464-8603

Carbon nanotubes (CNTs) possess promising properties such as small tip radius, high aspect ratio and robustness for field emission (FE) electron sources. We have developed a test system of the FE electron gun to evaluate the performance of CNT emitters and compare it with that of a conventional tungsten (W) cold emitter.

CNTs used in this experiment are multiwalled nanotubes (MWNTs) produced by catalyst free arc discharge method. Average diameter of MWNTs is about 15 nm. CNT emitters were mounted to a W needle by the following two methods. One is the electrophoresis method by which a thin bundle of MWNT was attached to the tip of a chemically etched W needle (Fig. 1(a)). The other is the manipulation method by which a MWNT was fixed to the tip of a W needle under SEM by manipulators and electron beam induced deposition (EBID) (Fig. 1(b)). A commercially available single crystalline W (310) emitter for a SEM (S-800; Hitachi) was used for comparative experiments. The emitter, the extractor and the anode are designed to be compatible with the SEM described above. Base pressure of the apparatus is about 10^{-8} Pa. Total emission current I was measured as a function of voltage V applied between the emitter and the extractor. The cathode-extractor distance was 3 mm.

Fig. 2 shows Fowler-Nordheim (F-N) plots of the three emitters. The slope and the intercept of the F-N plots depend on a voltage-to-field conversion factor β , an emission area A , and a work function ϕ of an electron emitter. Using reported values of ϕ for CNT (4.6 eV) and W (4.35 eV), β and A values for each emitter are obtained, as listed in Table 1.

The large β and small A of CNT emitters prepared by the two methods show that even a thick MWNT of ~ 15 nm diameter has much higher performance than the conventional single crystalline W emitter.

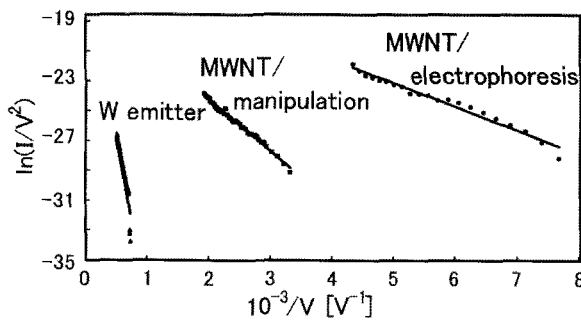


Fig. 2 F-N plots.

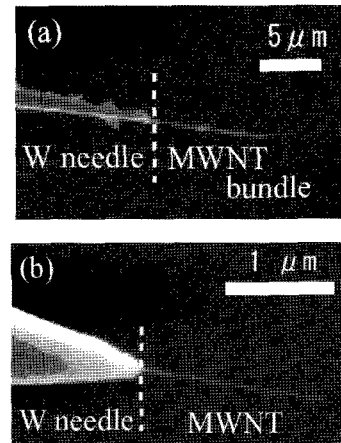


Fig.1

CNT emitters prepared by
(a) electrophoresis and (b)
manipulation methods.

Table 1 β and A values for
CNTs and W emitters.

	β [cm^{-1}]	A [nm^2]
MWNT/ electrophoresis	4.4×10^5	3.8×10^2
MWNT/ manipulation	2.0×10^5	2.0×10^2
W emitter	2.7×10^4	3.7×10^5

Corresponding Author: Yoshikazu Kusano

E-mail: yoshikazu@surf.nuqe.nagoya-u.ac.jp Tel:+81-52-789-3714 , Fax:+81-52-789-3703

Fabrication of CaCO₃/SWNT Nanocomposite Using Fullerodendron-Assisted Approach

○Akira Tsutsui, Yutaka Takaguchi

Graduate School of Environmental Science, Okayama University, Okayama 700-8530, Japan

One promising application of single-walled carbon nanotubes (SWNTs)[1] is the fabrication of a new hybrid materials containing SWNTs as a scaffold. However, these composite materials have been limited, due to the chemical inertness and poor solubility of carbon nanotubes. During our studies on the synthesis, characterization, and property of fullerodendron, we found that a solution of fullerodendrons disperses SWNTs via formation of supramolecular nanocomposite (Figure 1).[2] Furthermore, we have demonstrated the controlled fabrication of spherical vaterite CaCO₃ crystals using the fullerodendron with carboxylate groups at the terminals.[3]

Here we report the synthesis of a new composite material consisting of SWNTs and CaCO₃ via the supramolecular nanocomposite, of which surface was covered with carboxylate groups as shown in Figure 1. The composite materials were characterized by SEM observation, FT-IR, and XRD analysis. Interestingly, SEM observation showed uniform spherical CaCO₃ composites with a size of ca. 12 μm, of which surface was composed of rhombohedral subunits with size of 1 μm, and the existence of SWNTs (Figure 2).

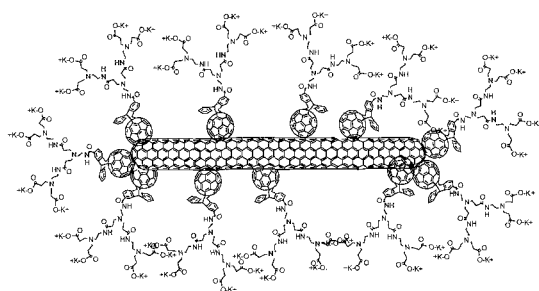


Figure 1. The structure of SWNT/fullerodendron supramolecular nanocomposite.

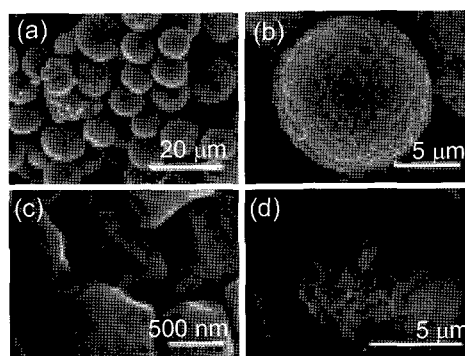


Figure 2. SEM images of (a) SWNT/CaCO₃ composite, (b) magnified image of (a), (c) magnified image of (b), (d) a cross section of the composite.

[1] S. Iijima, *Nature*, **1991**, 354, 56.

[2] Y. Takaguchi, M. Tamura, Y. Sako, Y. Yanagimoto, S. Tsuboi, T. Uchida, K. Shimamura, S. Kimura, T. Wakahara, Y. Maeda, T. Akasaka, *Chem. Lett.* **2005**, 34, 1608.

[3] B. Talukdar, Y. Takaguchi, Y. Yanagimoto, S. Tsuboi, M. Ichihara, K. Ohta, *Bull. Chem. Soc. Jpn.* **2006**, 79, 1983.

Corresponding Author: Yutaka Takaguchi

TEL: +81-86-251-8903, FAX: +81-86-251-8903, E-mail: yutaka@cc.okayama-u.ac.jp

Measurement of Thermal Conductivity of CNT-nanofluids by Transient Short-Wire Method

○ Takeshi Morimatsu¹, Shogo Moroe¹, Yasuyuki Takata¹,
Motoo Fujii², Shinzo Suzuki³, Masamichi Kohno¹

¹ *Department of Mechanical Engineering, KYUSHU University*

² *AIST, Research Center for Hydrogen Industrial Use and Storage*

³ *Department of Physics, Kyoto Sangyo University,*

Nanofluids are liquid suspensions where nano-sized particles are contained. Since the first report on the enhancement of effective thermal conductivity of water in the presence of Au nano-sized particles, many studies on effective thermal conductivity of nanofluids have been reported [1]. However, there are large differences among the values of effective thermal conductivity measured by different researchers, because it is very difficult to measure the accurate effective thermal conductivity of nanofluids.

Recently, Zhang and Fujii succeeded to measure the accurate effective thermal conductivity of CNT-nanofluids by transient short-wire method [2]. The uncertainty of their measurements is estimated to be within 1% for the thermal conductivity and 5% for the thermal diffusivity. The transient short-wire method developed in the late 90s by Fujii et al., is a variant of the conventional transient hot-wire method with the novelty that only one short conductivity cell is used and end-effects are accounted for by numerical simulation of unsteady heat conduction in the cell. This method has been successfully used to measure the thermal conductivity and thermal diffusivity of various fluids, molten polymer, and carbon nanofluids.

In this study, we measured thermal conductivity and thermal diffusivity of CNT-nanofluids and Al₂O₃-nanofluids by transient short-wire method. The influence of the shape and kinds of containing nano-sized materials on thermal properties will be presented and discussed.

References

[1] X. Wang et al., *J. Thermophys. Heat Transfer*, **13** (1999) 474-480.

[2] X. Zhang et al., *Experimental Thermal and Fluid Science*, **31** (2007) 593-599.

Corresponding Author: Masamichi Kohno

E-mail: kohno@mech.kyushu-u.ac.jp

TEL & FAX+81-92-802-3099

Gate voltage dependence of electroluminescence from single-walled carbon nanotubes

Norihito Hibino^{1,3}, Hideyuki Maki², Tetsuya Sato², Satoru Suzuki³ and Yoshihiro Kobayashi³

¹Department of Integrated Design Engineering, Faculty of Science and Technology Keio University, Hiyoshi, Yokohama 223-8522, Japan

²Department of Applied Physics and Physico-Informatics, Faculty of Science and Technology Keio University, Hiyoshi, Yokohama 223-8522, Japan

³NTT Basic Research Laboratories, Nippon Telegraph and Telephone Corporation, Morinosato-Wakamiya, Atsugi 243-0198, Japan

Single-walled carbon nanotubes (SWNTs) are attractive materials for the electronic and optoelectronic nanodevices because of their unique properties. Recently, some studies about the electroluminescence (EL) from an individual SWNT and SWNT network were reported^[1-4]. However, correlation of the EL emission with the transport behavior of FET is not clear. In this paper, we fabricate a SWNT-FETs and SWNT film-FETs, in which SWNTs are grown by chemical vapor deposition (CVD) method, and measure the electrical and optical properties. We observe the EL from these devices and investigate the emission mechanisms. In order to investigate the correlation of the EL emission with the transport behavior of FET, we simultaneously measured the EL and electric properties of SWNT-FET. A p++ Si wafer with thermally oxidized SiO₂ layer of 500 nm thickness was used as the substrate. SWNTs were grown on a Si/SiO₂ substrate by CVD using ethanol and Co catalyst at 850°C. Source and drain contacts were fabricated by means of electron beam lithography and lift-off process.

The gate voltage (V_g) dependences of the drain-source current (I_{ds}) and EL intensity for ambipolar FET are shown in Fig.1. In Fig.1 (a) and (b), V_g is swept to the positive and negative side respectively. Note that a strong hysteresis is observed during a gate voltage sweep. The EL emission is dominated by electron because the EL emission intensity increases in positive V_g region. In addition, in this device, the Schottky barrier height for holes is low due to the high work function of Pd electrode metal. These suggest that electron is minority carriers in whole V_g region, and the EL is dominated by minority carries. Therefore, the EL emission might be caused by the recombination of electrons and holes injected from the source and drain electrodes^[1]. On the other hand, in p-type FET (Fig.2) the EL emission is dominated by majority carriers, i.e. hole because the EL emission intensity increases in negative V_g region. The EL emission might be caused by the impact exciton or thermal heating^{[2][3]}. These V_g dependence of drain current and EL intensity indicated that the mechanism of EL correlates with the transport behavior of FET, i.e. p-type or ambipolar. EL is also observed for the SWNT film-FETs. Since a large number of SWNT exists in SWNT film-FET, the broad EL spectrum due to the superposition of the many SWNT peaks is observed as compared with that of SWNT-FET.

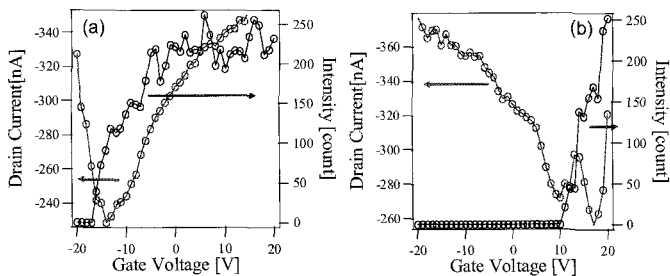


Fig.1 V_g dependences of the I_{ds} and EL intensity for ambipolar FET (a) from -20 V to 20 V and (b) from 20 V to -20 V

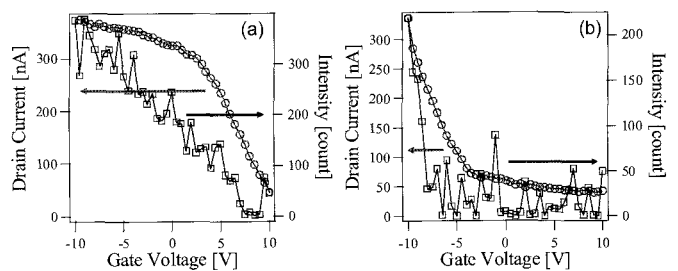


Fig.2 V_g dependences of the I_{ds} and EL intensity for p-type FET (a) from -10 V to 10 V and (b) from 10 V to -10 V

[1] J.A.Misewich et al., Science, **300**, 785(2003). [2] J.Chen et al, Science,**310**,1171(2005). [3] D.Mann et al, Nature technology, **2**,33(2007). [4] E.Adam et al., Nano Letter , **8**, 2351 (2008).
E-mail:maki@appi.keio.ac.jp TEL:045-566-1643

Study on Hydrocarbon Adsorption on MWNTs Using Field Emission Microscopy (FEM)

○T. Yamashita, K. Asaka, H. Nakahara, and Y. Saito

Dept. of Quantum Eng., Nagoya University, Furo-cho, Nagoya 464-8603

Carbon nanotube (CNT) is an ideal cold cathode material, but there are some difficulties to be overcome in order to apply as a nano-field emitter. The subjects to be solved include reduction of the turn-on voltage and improvement of emission current. Adsorption and/or coating of CNT surfaces by foreign material are possible methods to solve these subjects. Here, we investigated the effect of methane and ethane gas exposure to multiwalled carbon nanotubes (MWNTs) on their field emission characteristics by using field emission microscopy (FEM).

MWNTs produced by arc discharge were attached to a tungsten hairpin by graphi-bond. The base pressure of the FEM chamber was 8.0×10^{-8} [Pa]. Methane and ethane were exposed to MWNTs under the pressure of $\sim 10^{-6}$ [Pa] for 10 minutes. The distance between the screen and the emitter was about 30 mm.

We discovered that the exposure of hydrocarbon gases usually increased emission current. However, no enhancement was observed under following circumstances; (1) when emitters were exposed with no field emission, (2) when the emitter was heated, and (3) when FEM patterns did not show pentagon patterns. The rate of emission current increase brought about by the gas adsorption was nearly the same between methane and ethane, though adsorption energy of a methane molecule on graphene was weaker than ethane [1]. Figure 1 and 2 show I - V curves measured before the gas exposure (\circ), right after the exposure (\triangle), and after 3 hours emission (\times). For both gases, emission current increased when I - V curves were measured promptly after the exposure. In subsequent I - V measurements (\times) after 3 hours emission experiment, the current decreased for both gases, though the rate of current decrease was different between gases. For the emitter exposed to methane, the current dropped to almost the same level of the emitter before exposure, while the ethane-exposed emitter retained high level of field emission. Since ethane has larger adsorption energy than methane, ethane molecules are bound stronger and thus retain longer time to the surface than methane. This may be a cause of the observed the prolonged high emission for ethane.

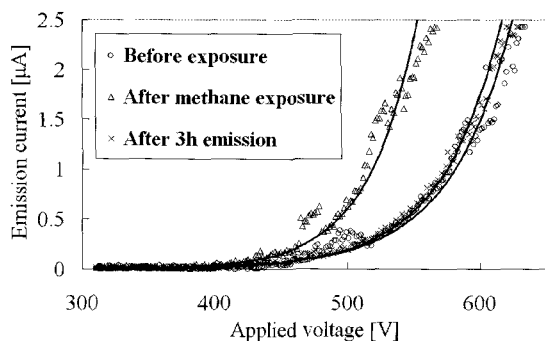


Fig.1 I - V curves for methane exposure

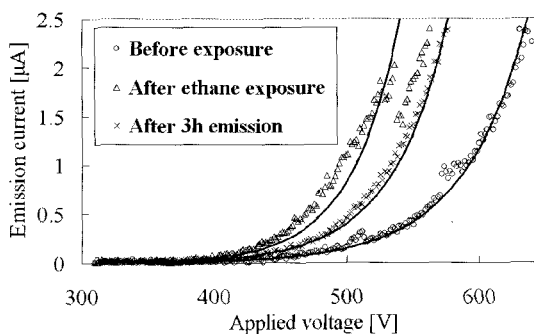


Fig.2 I - V curves for ethane exposure

[1] T. R. Rybolt *et al.*, *J. of Colloid and Interface Sci.*, **296**, (2006) 41-50

Corresponding author: Tetsuya Yamashita E-mail: yamashita@surf.nuqe.nagoya-u.ac.jp

TEL: +81-52-789-3714, FAX: +81-52-789-3703

Application of Vertically-Aligned SWNT Films to the Counter Electrode of Dye-Sensitized Solar Cells

○Jun Okawa, Erik Einarsson, Junichiro Shiomi and Shigeo Maruyama

*Department of Mechanical Engineering, The University of Tokyo
7-3-1 Hongo, Bunkyo-ku, Tokyo 113-8656, Japan*

We aim to apply vertically aligned single-walled carbon nanotube (VA-SWNT) films [1] synthesized by ACCVD method [2] to counter electrodes (CEs) of dye-sensitized solar cells (DSCs). Previously [3], we developed a DSC with VA-SWNT films installed as a CE, in place of conventional sputtered Pt on fluorine-doped tin oxide (FTO) layers, by transferring a VA-SWNT film on a FTO-coated glass substrate using our hot-water detachment technique [4]. However, I-V curves of the fabricated DSCs showed smaller *fill factor* than our reference DSC with sputtered-Pt CE. Based on fitting analyses of these I-V characteristics using the one-diode equivalent circuit model [5], we attributed the small *fill factor* to the contact resistance at the interface between the VA-SWNT film and the FTO layer.

In the present study, in order to reduce the contact resistance, we adopted Si substrates deposited with Au/Cr metallic bilayer (Fig. 1) instead of the FTO-coated glass substrates. Figure 2 shows an improvement of the *fill factor* achieved by this change. We will discuss the reason of this improvement as well as the possibility of replacing conventional Pt/FTO CEs with VA-SWNT films in DSCs.

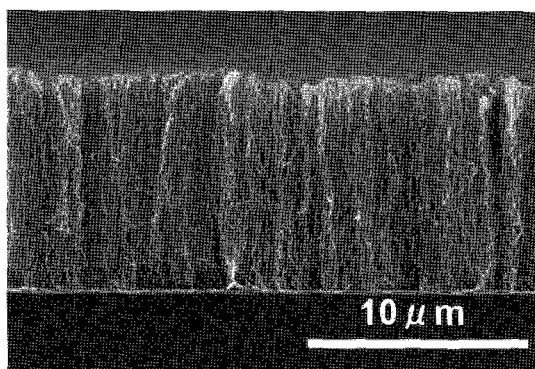


Fig. 1 An SEM image of the transferred SWNT film on Au/Cr bilayer deposited onto a Si substrate.

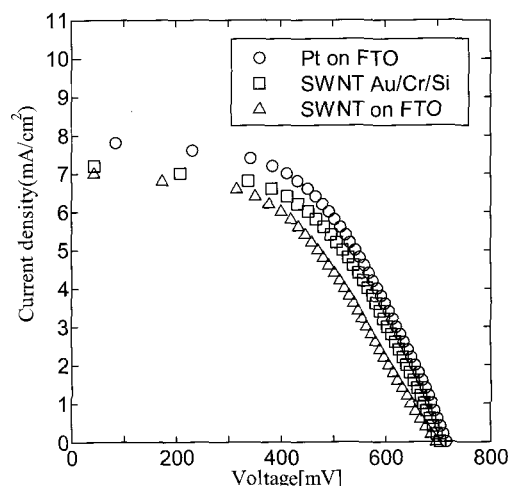


Fig. 2 I-V characteristics of DSCs with Pt and SWNT CEs.

- [1] Y. Murakami *et al.*, *Chem. Phys. Lett.* **385** (2004) 298.
- [2] S. Maruyama *et al.*, *Chem. Phys. Lett.* **360** (2002) 229.
- [3] J. Okawa *et al.*, *The 35th Fullerene-Nanotube General Symposium*, 3P-28 (2008).
- [4] Y. Murakami and S. Maruyama, *Chem. Phys. Lett.* **422** (2006) 575.
- [5] Z. Ouennoughi and M. Chegaar, *Solid-State Electron.* **43** (1999) 1985.

Corresponding Author: Shigeo Maruyama Tel/Fax: +81-3-5800-6983 E-mail: maruyama@photon.t.u-tokyo.ac.jp

Carbon nanotube growth on atomic force microscope cantilever by using liquid Co catalyst

Chien-Chao Chiu[○], Masamichi Yoshimura, Kazuyuki Ueda

Nano High-Tech Research Center, Toyota Technological Institute, 2-12-1 Hisakata, Tempaku, Nagoya 468-8511, Japan

Abstract:

Carbon nanotubes (CNTs)[1] have been growth on the tip of atomic force microscope (AFM) cantilever by Microwave plasma enhanced chemical vapor deposition (MPECVD). Because of the excellent properties which include high aspect ratio, strength, and conductivity, CNT has been used for the nanomaterial on tip of the scanning probe. The catalyst of CNT growth was prepared by liquid Co acetate[2] at the concentration of 5-30 wt% with ethanol as a solvent. The cantilever was coated on by dip coating method in the prepared Co solution. The cantilevers were put up side down to centralize the catalyst on the apex of tips until the evaporation of solvent. The CNTs were grown in the MPECVD growth system at the temperature of 630 °C for 3-15 min under H₂ and CH₄ mixture. Figure 1 shows the SEM images of the tips before and after CNTs growth. After growth, the only one independent CNT with the diameter of 30 nm and height of 300 nm was found on the apex of the tip for the further measurement.

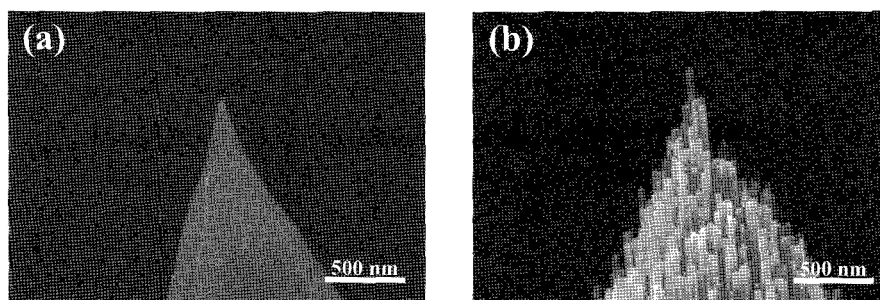


Figure 1. SEM images of the tips (a) before and (b) after CNTs growth.

Reference: 1. C.-C. Chiu, T.-Y. Tsai, and N.-H. Tai, *Nanotechnology* 17 (2006) 2840.

2. Y. Murakami et al., *Chemical Physics Letters* 385 (2004) 298.

Corresponding Author: Chien-Chao Chiu

E-mail: kcttjip@gmail.com

Tel: (052)809-1852, Fax: (052)809-1853

A molecular dynamics study of metal coating on SWNT

○Teppei Matsuo, Junichiro Shiomi and Shigeo Maruyama

*Department of Mechanical Engineering, The University of Tokyo
7-3-1 Hongo, Bunkyo-ku, Tokyo 113-8656, Japan*

Metal coating on an SWNT is an important element technology in CNT-based electric and thermal device integrations. With the strong motivation, vacuum-evaporation experiments of various metals onto SWNT have been reported [1,2], and the observed metal morphologies have been explained based on the static energetics. However, in order to grasp the full picture of the coating mechanism, one would also need to consider the contribution of dynamics, and thus, molecular dynamics approach is useful [3]. In the current simulations, we take a similar MD model to the previous report [3] with Brenner bond order potential [4] for carbon covalent bonds, but use different metal models; the GEAM potential [5] for metal-metal, and Lennard-Jones fitted potential for the carbon-metal interactions. The coating processes were simulated for various metal kinds, temperatures, and deposition conditions such as initial cluster sizes and deposition rates.

The morphology of the deposited metal strongly depends on the metal kind as seen in Figure 1. For these cases, the metal morphologies are confirmed to be insensitive to temperature in a realistic range. While Ti atoms cover the entire SWNT, Au and Fe atoms locally cling onto SWNT and forms clusters, where Au clusters are more spherical than Fe ones. The results of Ti and Au are consistent with the metal coating experiments [1,2], though that of Fe is not. The deposition processes will be presented for various parameters and conditions, and the mechanism will be discussed, also for the cases with bundled SWNTs.

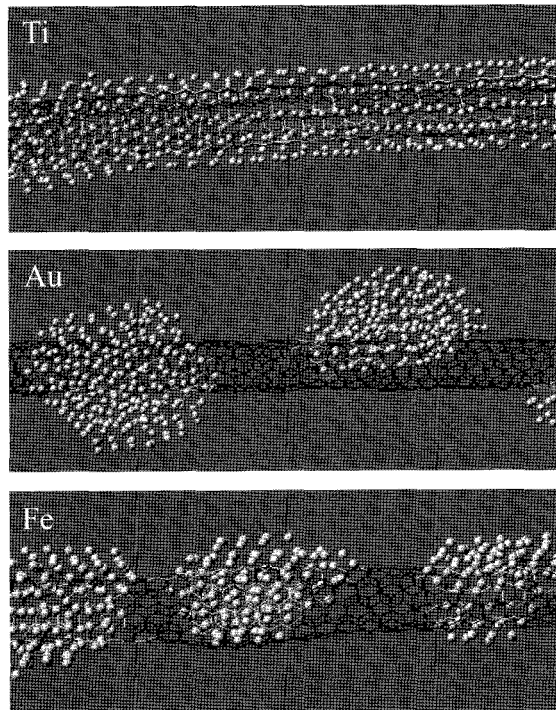


Fig. 1 Various metals deposited on SWNT

- [1] Y. Zhang et al., Chem. Phys. Lett., **331** (2000) 35. [2] K. Ishikawa et al., Proceedings of ASME-JSME Thermal Engineering Summer Heat Transfer Conference (2007) 32783. [3] S. Inoue et al., Chem. Phys. Lett., **464** (2008) 160. [4] D. W. Brenner, Phys. Rev. B, **42** (1990) 9458. [5] X. W. Zhou et al., Phys. Rev. B, **69** (2004) 144113.

Line-Patterned Carbon Nanotube Cold Cathodes

○Yosuke Shiratori¹, Koji Furuichi², Suguru Noda¹

¹Dept. of Chemical System Engineering, The University of Tokyo, Tokyo 113-8656, Japan

²DAINIPPON SCREEN MFG. CO., LTD., Kyoto 602-8585, Japan

Carbon nanotubes (CNTs) are expected as electron emitters to be applied for light emitting devices such as field emission displays and backlight units for LCDs. Improvements of driving voltage, emission uniformity and lifetime are still open subjects. Thinner CNTs such as single-walled and double-walled CNTs (SWCNTs and DWCNTs) can be potentially used as emitters to lower the driving voltage. Here high density implementation is necessary to ensure emission uniformity and lifetime. We proposed the 1D-Array of SWCNT emitters prepared through a quick CVD process for 5 – 15 seconds [1]. A low driving voltage and rather good emission uniformity were demonstrated, however optimized cathode configurations have not yet been obtained.

An assembly of line-patterned micro-cathodes (spacing: 10 – 100 μm) and top-gates (slit width, w : 0.5 – 2 μm) were fabricated through electron-beam or photo-lithography. Al_2O_3 underlayer and Co catalyst layer were then sputter-deposited through the gate slits (Fig. 1a). These two layers on a resist/gate layer were removed by a subsequent lift-off process. Catalyst (Co) and supporting (Al_2O_3) layers were selectively formed on the line patterned cathodes. It should be noted that the gate slits dilute the deposition flux of Co [2], and therefore a gradient thickness profile of the Co catalytic layer is formed on the bottom of cathodes (Fig. 1a). Prepared substrates were annealed under H_2/Ar gas atmosphere for 10 min, and thermal CVD was carried out for 5-90 sec at 800 $^\circ\text{C}$. Here C_2H_2 was used as a source gas. As the illustration in Fig. 1b, CNTs grew on the bottom of trench. A variety of bundle morphologies were obtained for the samples prepared under different CVD conditions and trench structures. An example of FE properties is shown in Fig. 1c. Optimized configurations (emitter morphologies and trench structures) in the line-patterned CNT emitter arrays, which realize both high emitter density and effective electric field enhancement, are discussed.

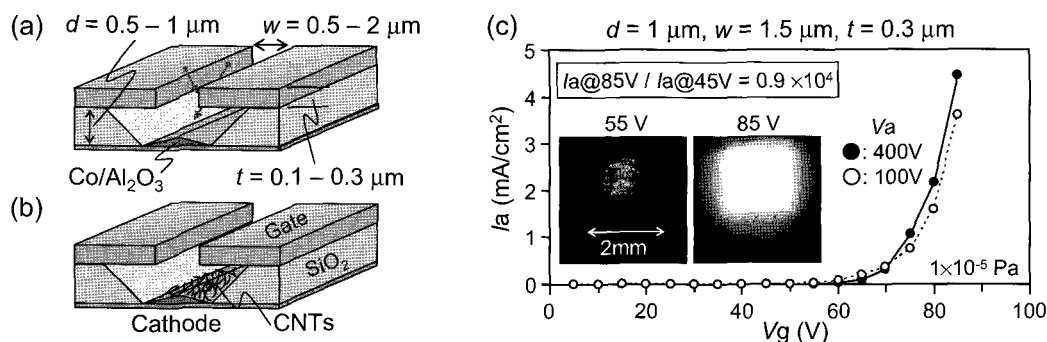


Fig. 1. Illustrations of line patterned cathodes prepared on Si substrates, (a) after catalyst sputtering and (b) after CVD. (c) An example of field emission properties obtained for a representative trench configuration, I_a : anode current, V_g : gate voltage.

[1] K. Furuichi, Y. Shiratori, S. Noda, Y. Tsuji, H. Sugime, and Y. Yamaguchi, "1D-Array of Self-Organized SWCNT Micro-Emitters", presentation C-59 in NT08, Montpellier, France, June 2008.

[2] S. Noda, H. Sugime, T. Osawa, Y. Tsuji, S. Chiashi, Y. Murakami, and S. Maruyama: Carbon **44** (2006) 1414.

Corresponding Author: Suguru Noda, TEL: +81-3-5841-7332, FAX: +81-3-5841-7332, E-mail: noda@chemsys.t.u-tokyo.ac.jp

New electrocatalyst for PEFC based on carbon nanotubes wrapped by polybenzimidazole

Minoru Okamoto¹, ○Tsuyohiko Fujigaya¹, Naotoshi Nakashima^{1,2}

¹*Department of Applied Chemistry, Graduate School of Engineering
Kyushu University, Fukuoka, Japan*

²*JST-CREST, 5 Sanbancho, Chiyoda-ku, Tokyo 102-0075, Japan*

Abstract: Polybenzimidazole (**PBI**; Fig. 1) is widely known as a promising candidate for electrolyte membrane of polymer electrolyte fuel cell (PEFC) operating under dry condition. On the other hand, carbon nanotubes

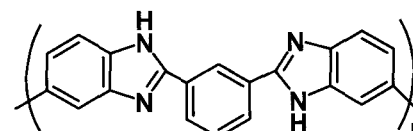


Fig. 1 Polybenzimidazole (**PBI**).

(CNTs) have been emerged as a better carbon support material than conventional material such as carbon black. We have reported the **PBI** is adsorbed onto the surface of CNTs and acts as the good solubilizer [1]. By taking advantage of stable wrapping of **PBI** on CNTs, we utilized this composite as a novel carbon supporting materials for loading the metal catalyst such as platinum (Pt). As the result, the **PBI**-wrapped CNTs show better efficiency of Pt loading than that of pristine CNTs due to the coordination between Pt ion and **PBI**. Furthermore, the obtained electrocatalyst (CNT/**PBI**/Pt) shows excellent Pt utilization

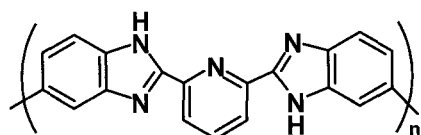


Fig. 2 Chemical structure of **PyPBI**

operations caused by the aggregation of the Pt.

efficiency mainly due to the formation of ideal interfacial structure constructed by the CNTs, **PBI** and Pt [2]. However, we also noticed the electrochemically active area (ECSA) was gradually decreased during long time operations caused by the aggregation of the Pt.

In this study, we chose pyridine-containing **PBI** (**PyPBI**) in order to obtain better topological stability via chelate formation between **PyPBI** and Pt and found new electrocatalyst composed of CNTs, **PyPBI** and Pt (denote as CNT/**PyPBI**/Pt) exhibit, as expected, negligible deterioration under long time operations as presented in Table 1. The detail mechanism of the electrochemical stability of the **PyPBI**-based electrocatalyst will be discussed in the presentation.

Table 1. ECSA values of the catalysts

ECSA [m ² /g]	After 20 cycles	After 250 cycles
CNT/ PBI /Pt	46.1	33.8
CNT/ PyPBI /Pt	38.0	38.2

References: [1] M. Okamoto, T. Fujigaya, N. Nakashima, *Adv. Funct. Mater.* **2008**, 18, 1776-1782

[2] M. Okamoto, T. Fujigaya, N. Nakashima, *Small* inpress. .

Corresponding Author: Naotoshi Nakashima

E-mail: nakashima-tcm@mail.cstm.kyushu-u.ac.jp

Tel&Fax: +81-92-802-2840

Transparent conducting properties of SWCNT films at a range of thickness

○Eisuke Haba¹, Suguru Noda²

¹HITACHI CHEMICAL. CO., LTD, Tokyo 163-0449, Japan

²Dept. of Chemical System Engineering, The University of Tokyo, Tokyo 113-8656, Japan

SWCNTs are an attractive candidate material for transparent electrodes [1] owing to their unique structural and physical characteristics such as high aspect ratio, high electrical conductivity, and flexibility. Extensive research has been made, however, systematic data for the structure and film properties are still important. In this work, we prepared films of both SWCNTs and MWCNTs at a range of thickness and studied their transparent conducting properties.

SWCNT were synthesized by chemical vapor deposition (CVD) using ethylene as a carbon source and Fe/Al-Si-O as a catalyst [2]. SWCNTs formed vertically aligned forests with thicknesses of 160 and 900 μm in 1.5 and 10 min, respectively. Commercially available MWCNTs of 10 nm in diameter were also used as comparative sample. Their aqueous suspensions were prepared by tip sonicator (400 W, 1 h) using sodium dodecyl benzen sulfate (SDBS) as surfactant, and their uniform films were prepared by vacuum filtration (VF) method[3].

Figures below shows SEM images of CNT films and their transparent conducting properties. Three tubes showed different resistance-transparency curves and the sheet resistance was SWCNTs (160 μm) < SWCNTs (900 μm) < MWCNTs. SWCNTs have much smaller resistivity than MWCNTs owing to the better contacts among themselves. On the other hand, these CNT films showed the same curve for transparency vs. CNT loads. These results mean that the transparency of CNT films is solely determined by the CNT loads but the sheet resistance is affected by the structure of individual CNTs and their networks. Therefore, the guideline for developing transparent conducting films is using SWCNTs at a fixed load (ex. 1 $\mu\text{g}/\text{cm}^2$ for 90 % transparency) and improving the conductivity of SWCNT networks by controlling structures and properties of individual SWCNTs and their networks.

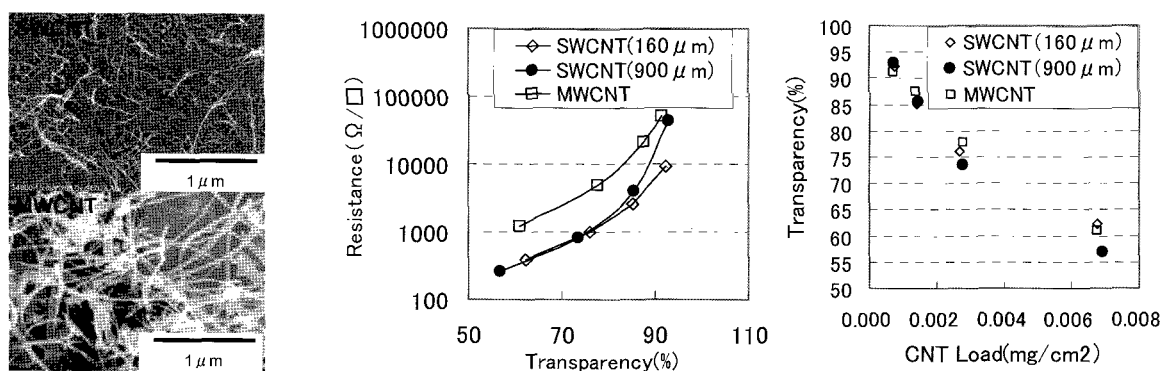


Figure. SEM Images of CNT films and their transparent conducting properties.

[1] D. Zhang, et al., Nano Lett., **6**, 1880 (2006).

[2] S. Noda, et al., Jpn. J. Appl. Phys. **46** (17), L399-L401 (2007).

[3] Z. Wu, et al., Science. **305**, L1273 (2004).

Corresponding Author: Eisuke Haba, Tel&Fax: +81-2-9864-4408, E-mail: e-haba@hitachi-chem.co.jp

Suguru Noda, Tel&Fax: +81-3-5841-7332, E-mail: noda@chemsys.t.u-tokyo.ac.jp

Defects on Multi-walled Carbon Nanotubes by Cobalt Oxide

○Do-Hyun Kim and Keiko Waki

*Dept. of Energy Sciences, Interdisciplinary Graduate school of Sci. & Eng.
Tokyo Institute of Technology,
Mailbox G3-4, Bldg. G3, 4259, Nagatsuta-cho, Midori-ku,
Yokohama-shi, Kanagawa, 226-8502, Japan*

To make defects or modify the superficial properties of CNTs, three kinds of treatments (liquid, gas and solid state reaction) are generally used: acid, O₃, and CO₂ treatment. However, creating defects by solid state reaction has not been studied well till now.

In this study, a new method was studied to create crystal defects on the surface of multi-walled carbon nanotubes (MWCNTs) by using cobalt oxide. Defects on MWCNTs were created at low temperature through the air oxidation of cobalt oxide. Firstly, CoO was deposited on MWCNTs by impregnation method and it was oxidized at 250°C under air atmosphere. XRD analysis revealed that the structure of cobalt oxide changed from CoO to Co₃O₄ after air oxidation. TEM images clearly showed that various shapes of defects were observed on the surface of MWCNTs. After removing cobalt oxide existing on MWCNTs, pure defective MWCNTs were obtained. Only defective sites lost crystallinity and other part showed clear crystal lines.

Corresponding Author: Keiko Waki

TEL: +81- 45-924-5614, FAX: +81- 45-924-5614, E-mail: waki.k.aa@m.titech.ac.jp

Third Isomer of La@C₈₂

○Hidenori Kuga,¹ Hidefumi Nikawa,¹ Naomi Mizorogi,¹ Takahiro Tsuchiya,¹ Midori O. Ishitsuka,¹
Zdenek Slanina,¹ Takeshi Akasaka,¹ Kenji Yoza,² Shigeru Nagase.³

¹Center for Tsukuba Advanced Research Alliance,
University of Tsukuba, Tsukuba, Ibaraki 305-8577, Japan,

²Bruker AXS K.K., Yokohama 221-0022, Japan,

³Department of Theoretical and Computational Molecular Science,
Institute for Molecular Science, Okazaki, Aichi 444-8585, Japan

Endohedral metallofullerenes have attracted special interest because of the unique structure and properties that are unexpected for empty fullerenes.^{1,2} Since Smalley and co-workers reported in 1991 that lanthanum metallofullerenes were produced abundantly in the soot, but only La@C₈₂ was extracted with toluene,³ the chemistry of soluble endohedral metallofullerenes has started, and up to now, many soluble endohedral metallofullerenes have been isolated and characterized.^{1,2,4-8} On the contrary, insoluble endohedral metallofullerenes such as La@C₆₀, La@C₇₀, La@C₇₂, La@C₇₄ and so forth have not yet been isolated, although they are regularly observed in the raw soot by mass spectrometry. Recently, we succeeded in the extraction, isolation, and characterization of a missing metallofullerene La@C_n (n = 72 and 74)^{9,10} as a derivative. This extraction derivatization method is a powerful tool for the extraction, isolation, and conclusive identification of missing metallofullerenes.

We herein report the first structural determination of a mono-metallofullerene derivative, La@C₈₂(C₆H₃Cl₂), that has a novel structure C_{3v}-C₈₂ (82:7) cage by spectroscopic and X-ray crystallographic analysis. Interestingly, theoretical investigation indicates that La@C₈₂ with C_{3v}-C₈₂ (82:7) is not stable, but its derivatization makes it more stable.

References:

- [1] *Endofullerenes: A New Family of Carbon Clusters*; Akasaka, T., Nagase, S., Eds.; Kluwer Academic Publisher: Dordrecht, The Netherlands, **2002**; pp 1. [2] Wilson, S.; Schuster, D.; Nuber, B.; Meier, M. S.; Maggini, M.; Prato, M.; Taylor, R. In *Fullerenes: Chemistry, Physics, and Technology*; Kadish, K. M., Ruoff, R. S., Eds.; Wiley: New York, **2000**; Chapter 3, pp 91. [3] Smalley, R. E. et al. *J. Phys. Chem.* **1991**, *95*, 7564. [4] Bethune, D. S. et al. *Nature* **1993**, *366*, 123. [5] Nagase, S.; Kobayashi, K.; Akasaka, T. *Bull. Chem. Soc. Jpn.* **1996**, *69*, 2131. [6] Nagase, S.; Kobayashi, K.; Akasaka, T. *J. Comput. Chem.* **1998**, *19*, 232. [7] Nagase, S.; Kobayashi, K.; Akasaka, T.; Wakahara, T. In *Fullerenes: Chemistry, Physics and Technology*; Kadish, K., Ruoff, R. S., Eds.; Wiley: New York, **2000**; Chapter 9, pp 395. [8] Akasaka, T. et al. *J. Am. Chem. Soc.* **2000**, *122*, 9316. [9] Wakahara, T. et al. *J. Am. Chem. Soc.* **2006**, *128*, 14228. [10] Nikawa, H. et al. *J. Am. Chem. Soc.* **2005**, *127*, 9684.

Corresponding Author: Takeshi Akasaka

Tel & Fax: +81-29-853-6409

E-mail: akasaka@tara.tsukuba.ac.jp

**Molecular and Electronic Structures of Di-erbium and
Di-erbium-carbide Metallofullerenes $\text{Er}_2(\text{C}_2)\text{@C}_{82}$: Density**

Functional Theory Calculations

Jian Wang¹, Stephan Irle^{1*}, and Keiji Morokuma²

¹*Institute for Advanced Research and Department of Chemistry, Nagoya University,
Nagoya 464-8602, Japan* ²*Fukui Institute for Fundamental Chemistry, Kyoto
University, Kyoto 606-8103*

E-mail: sirle@iar.nagoya-u.ac.jp

Density functional theory geometry calculations have been performed to elucidate the molecular and electronic structures of di-erbium and di-erbium-carbide endohedral metallofullerenes $\text{Er}_2\text{@C}_{82}$ and $\text{Er}_2\text{C}_2\text{@C}_{82}$. $C_s(6)$ (I), $C_{2v}(9)$ (II), and $C_{3v}(8)$ (III) IPR isomers of C_{82} were considered. We have employed B3LYP using Ahlrich's SVP and TZVPP basis sets for carbon, and the Stuttgart-Dresden SRSC97-ECP effective core potential and basis sets both with explicit consideration of f electrons and without, assuming in the latter case a $6s^25d^1$ valence configuration to emulate the effects of strong electron correlation. We find that in each compound the erbium atoms assume a trivalent state, where two electrons from each Er are transferred to the C_{82} cage (LUMO and LUMO+1 become doubly occupied, corresponding to the C_{82}^{4-} electronic state), and one electron is promoted from the Er 4f shell to the 5d shell, which subsequently becomes involved in covalent bonding to the nearest surrounding atoms by utilizing sd hybrid orbitals. Such chemical bonding situation is comparable to that encountered in $\text{Er}_3\text{N@fullerene}$ compounds, where the cages are found to be 6-fold negatively charged, and three covalent Er-N bonds exist. In particular, the C_2 unit engages in strong covalent binding to the Er sd hybrid, which gives rise to the notion of only weak charge uptake as detected by MEM-Rietveld X-ray measurements. Since the Er 4f shell is occupied by only about eleven electrons according to Mulliken population analysis, Er^{3+} -like emission from $^4\text{I}_{13/2}$ to $^4\text{I}_{15/2}$ is consistent with the notion of only 2 electrons per Er fully transferred to the cage. The higher photoluminescent activity of isomer III compared to other isomers I and II stems from a sizable (LUMO+2)-(LUMO+1) gap in the $\text{C}_{3v}(8)$ cage. Our prediction for photoluminescence intensity for all three isomers is consistent with the experimental results by Shinohara and coworkers.

Selective Irradiation of Ionic Heterogeneous Fullerenes Generated by Electron Beam Impact Ionization

○Y. Hanabusa¹, T. Kaneko¹, H. Ishida¹, R. Hatakeyama¹, K. Omote², and Y. Kasama²

¹Department of Electronic Engineering, Tohoku University, Sendai 980-8579, Japan

²Ideal Star Inc., Sendai 989-3204, Japan

Alkali metal endohedral fullerenes have attracted much attention because they are expected to be a candidate for the novel material to modify the electrical and optical properties of single-walled carbon nanotubes (SWNTs). We have developed the plasma ion irradiation method to create the new-functional fullerene encapsulated SWNTs, where the negative and positive ions in the plasma can selectively be irradiated depending on the polarity of substrate biases. Here, we generate a plasma consisting of ionic heterogeneous fullerenes such as C₆₀ and lithium endohedral fullerene Li@C₆₀ by means of an electron beam impact to the sublimated Li@C₆₀/C₆₀ composite which is mass-produced by Ideal Star Inc. in collaboration with Tohoku University.

Figure 1 shows mass spectra of the deposits on the substrates which are (a) positively ($V_{\text{sub}} = +20$ V) and (b) negatively ($V_{\text{sub}} = -20$ V) biased, where a laser desorption time-of-flight mass spectrometer is operated in the positive ion mode. The deposits on the positively biased substrate give the high-intensity mass peak of C₆₀ (720) with the low-intensity mass peak of Li@C₆₀ (727). In contrast, the high-intensity peak of Li@C₆₀ is observed from the deposits on the negatively biased substrate. Figure 2 presents the intensity ratios of mass peaks of Li@C₆₀ to C₆₀ (I_{727}/I_{720}) deposited on the (a) positively and (b) negatively biased substrates as a function of the electron beam impact energy E_e . It is found that the Li@C₆₀ tends to form not negative but positive ions around $E_e=200$ eV and the Li@C₆₀ positive ions are selectively irradiated to the negatively biased substrate. These results imply that the Li@C₆₀ plays a role of electron donor in SWNT-based electronic devices.

Corresponding Author: Yohei Hanabusa

TEL: +81-22-795-7046, FAX: +81-22-263-9225,

E-mail: hanabusa@plasma.ecei.tohoku.ac.jp

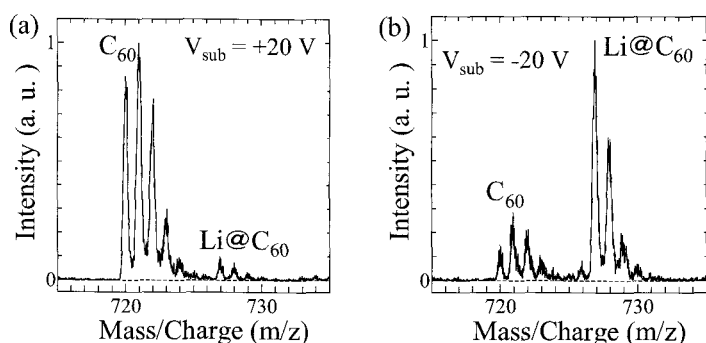


Fig. 1. Mass spectra of the deposits on (a) positively and (b) negatively biased substrates.

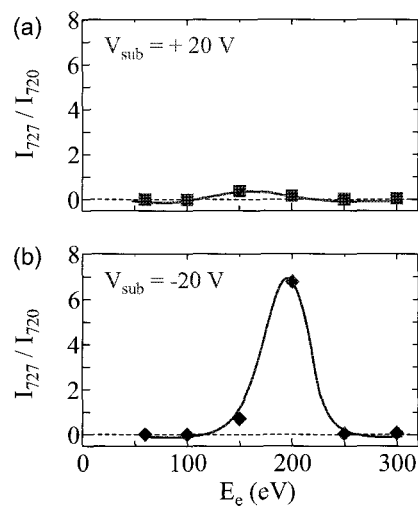


Fig. 2. Intensity ratios of mass peaks of Li@C₆₀ to C₆₀ (I_{727}/I_{720}) as a function of electron impact energy E_e for (a) positive and (b) negative substrate biases.

Change in Molecular Orientation of Individual Lu@C₈₂ on Octanethiol Self Assembled Monolayer Observed by Scanning Tunneling Microscopy

○Masachika Iwamoto¹, Yuhsuke Yasutake¹, Hisashi Umemoto², Yasuhiro Ito²,
Haruya Okimoto², Noriko Izumi², Hisanori Shinohara^{2,3}, and Yutaka Majima¹

¹*Department of Physical Electronics, Tokyo Institute of Technology, Tokyo 152-8552, Japan*

²*Department of Chemistry, Nagoya University, Nagoya 464-8602, Japan*

³*Institute for Advanced Research, Nagoya University, Nagoya 464-8602, Japan*

Abstract:

Endohedral metallofullerenes are one of the candidate materials for nanoelectronics applications due to their unique electronic and magnetic properties which associated with the charge transfer interaction between the encapsulated metal atom and a fullerene cage [1, 2]. We have demonstrated that single endohedral metallofullerene orientation switching phenomena by introducing alkanethiol self-assembled monolayer (SAM) as interlayer to control the interaction between endohedral metallofullerene and metal substrate [3]. To realize molecular orientation switching device by using endohedral metallofullerene, it needs to clarify the switching mechanism. We reported the local electrical properties of Lu@C₈₂ on heptanethiol SAM by scanning tunneling microscopy (STM) and current imaging tunneling spectroscopy (CITS) [4]. Here, we report change in the molecular orientation of individual Lu@C₈₂ on octanethiol SAM under the application of the sample bias voltage.

From molecular resolution STM images of Lu@C₈₂ at 65 K, we observed the stripe structure which indicates intermolecular features of Lu@C₈₂ molecule on octanethiol SAM. Then we measured CITS at different 64 points on individual Lu@C₈₂ molecule on octanethiol SAM at 65 K. From differential conductance (dI/dV) spectra, we observed two peaks centered at -0.5 V and 1.0 V which correspond to HOMO and LUMO energy levels, respectively. We visualized HOMO peak intensity on 64 points. Comparing these molecular resolution STM images and CITS of individual Lu@C₈₂ on octanethiol SAM by density functional theory (DFT) calculations of Lu@C₈₂ in a vacuum, we demonstrate change in the molecular orientation of Lu@C₈₂ under the application of -3.5 V sample bias voltage.

References:

- [1] H. Shinohara, *Rep. Prog. Phys.* **63**, 843 (2000).
- [2] K. Wang, J. Zhao, S. Yang, L. Chen, Q. Li, B. Wang, S. Yang, J. Yang, J. G. Hou, and Q. Zhu, *Phys. Rev. Lett.*, **91**, 185504 (2003).
- [3] Y. Yasutake, Z. Shi, T. Okazaki, H. Shinohara, and Y. Majima, *Nano Lett.*, **5**, 1057 (2005).
- [4] Y. Yasutake, K. Kono, N. Kobayashi, M. Iwamoto, H. Umemoto, Y. Ito, H. Okimoto, H. Shinohara, and Y. Majima, *The 34th Fullerene - Nanotubes General Symposium*, **2-1**, 27 (2008).

Corresponding Author: Yutaka Majima

TEL: +81-3-5734-2673, FAX: +81-3-5734-2673, E-mail: majima@pe.titech.ac.jp

Storage Conditions of Metallofullerenes

○Yosuke Kikuchi^{1,2}, Takuma Ooba^{1,2}, Fuyuko Yamashita¹, Yasuhiro Takabayashi¹, Yoshihiro Ono¹, Kazuhiko Kawachi¹, Kenji Omote¹, Yasuhiko Kasama¹ and Yoshihiro Kubozono³

¹*Ideal Star, Inc., Sendai 989-3204, Japan*

²*Takamori Farm, Ltd., Kurihara, Miyagi 987-2246, Japan*

³*Department of Chemistry, Okayama University, Okayama 700-8530, Japan*

Many studies of endohedral metallofullerenes have been carried out. It is very important to know the best way to store the endohedral metallofullerene samples to perform various experiments. The researchers who have prepared the metallofullerene samples know that the solubility of metallofullerene is decreased after extended storage. In this presentation, we discuss about storage conditions of metallofullerene samples.

Soot containing Ce@C₈₂ was prepared by an arc discharge method. Ce@C₈₂ was extracted by Soxhlet extraction using dimethylformamide and purified by using HPLC [1]. The purified samples were stored under some storage conditions; (1) powder stored

under air, (2) powder sealed in glass tube under vacuum, (3) powder sealed in glass tube under vacuum stored at 100 °C, (5) toluene solution stored in a refrigerator, (6) toluene solution stored in freezer, (7) toluene solution exposed to sunlight.

Fig. 1 shows the HPLC profiles of the Ce@C₈₂, (a) as prepared (b) stored in refrigerator for 10 days and (c) 34 days. The peak of the Ce@C₈₂ was almost gone after 34 days. This result suggests that the form of the Ce@C₈₂ was changed to something after extended storage. The results of the other storage conditions will show at the conference.

[1] S. Iida *et al.*, *Chem. Phys. Lett.* **338**, 21 (2001).

Corresponding Author: Yasuhiko Kasama

yasuhiko.kasama@idealstar-net.com,

Tel: +81-22-303-7336, Fax: +81-22-303-7339

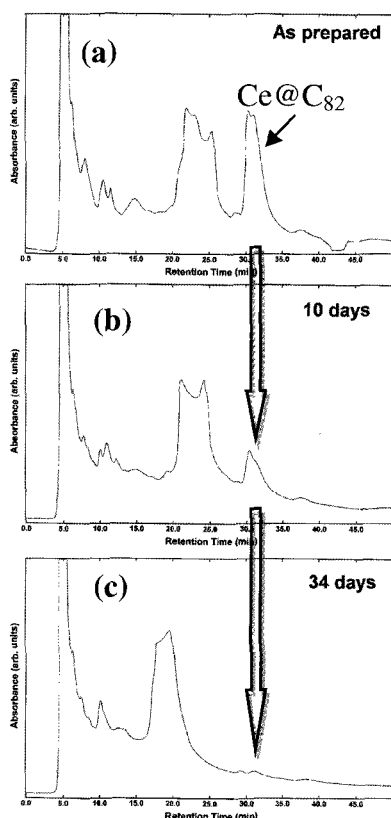


Fig. 1.

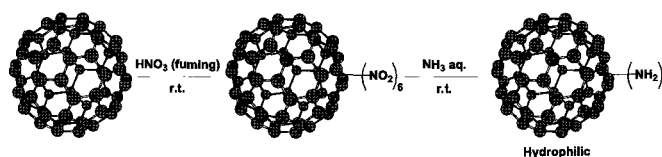
Synthesis of Amino Fullerene Derivative and its Application for PA-6 Nanocomposites

○Masaru Sekido¹, Katsuma Ohno¹, Yasuyuki Ohyama¹, Daisuke Saitou¹, Susumu Kumagai¹,
Mitsuhiro Takeda¹, Hiroshi Kitamura², Masatomi Ohno²

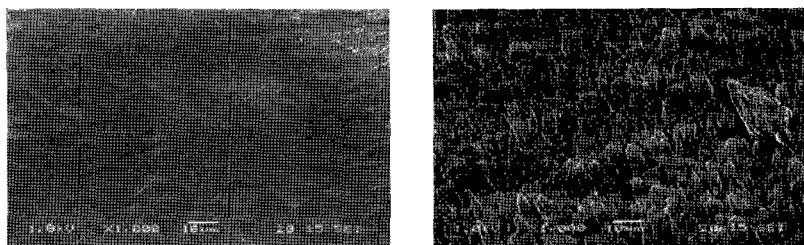
¹Department of Materials Science and Engineering, Miyagi National College of Technology,
Natori 981-1239, Japan

² Department of Advanced Science and Technology, Toyota Technological Institute,
Nagoya 468-8511, Japan

We have developed the effective methods to prepare the nitrofullerene intermediate¹⁾ and its application to synthesize hydrophilic fullerene derivatives, such as hydroxyfullerene derivatives. Aiming at the further application of the nitrofullerene intermediate, amino functional groups were introduced to give aminofullerene derivative.



PA6 (Polyamide 6)/amino-fullerene nanocomposites were prepared by melt-mixing in a conical twin-screw extruder at 260 °C and vacuum dried over night at 80 °C. Since amino groups of amino-fullerene derivatives form hydrogen bonding with PA6 interaction between amino fullerene derivative and PA6 should be quite strong. Mechanical property measurements indicate that the tensile strength of PA6/amino-fullerene composites is improved by 8-10% with addition of only 0.1wt% amino fullerene derivative. Transmission Electron Microscopy (TEM) of PA6/amino-fullerene nanocomposites showed that amino-fullerene derivatives were well-dispersed in PA6 matrix by simple melt-mixing.



TEM of PA6/amino fullerene nanocomposites (left) and PA6 (right).

References: V. Anantharaj, J. Bhonsle, T. Canteenwala, and L. Y. Chiang, *J. Chem. Soc., Perkin Trans. 1*, 1999, 31-36.

Corresponding Author: Masaru Sekido,

Tel:022-381-0329, Fax:022-381-0318, E-mail: sekido@miyagi-ct.ac.jp

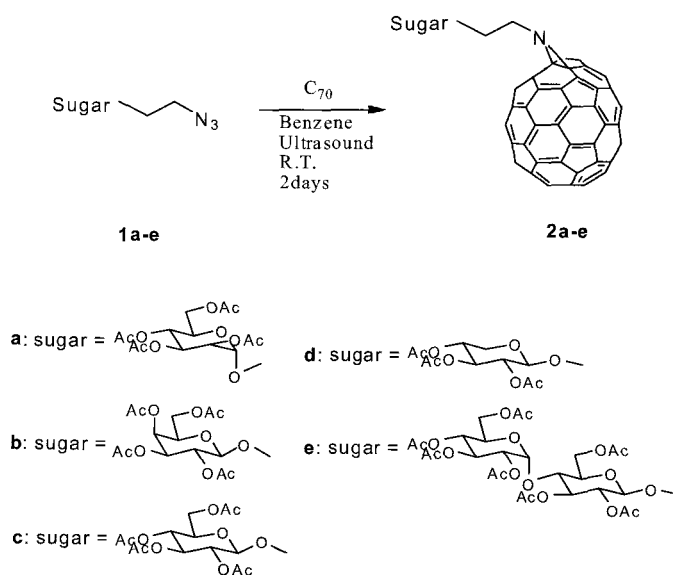
Ultrasound-Assisted Cycloadditions of [70]Fullerene with Various 2-Azidoethyl per-*O*-Acetyl Glycosides

Shinsook Yoon¹, Sung Ho Hwang², Sung Kyu Hong², Jeong Ho Lee² and Weon Bae Ko^{2*}

¹*Faculty of Liberal Arts, Kangnam University, Yongin 449-702, South Korea*

²*Department of Chemistry, Sahmyook University, Seoul 139-742, South Korea*

Under ultrasonication, cycloaddition of [70]fullerene with various 2-azidoethyl per-*O*-acetyl glycopyranoside of D-mannose(1a), D-galactose(1b), D-glucose(1c), D-xylose (1d) and D-maltose(1e) yielded glycosyl [70]fullerene derivatives 2a-2e. Based upon ¹H- and ¹³C-NMR, FT-IR, UV-vis, and FAB-MS analyses, 2a-2c and 2e were a mixture of the major closed [5,6]-bridged isomer product and two isomers as the minor, monoaddition products. However, in the case of D-xylose, 2d was an unusual mixture of four mono-adducts in the ratio of ca. 9:11:10:4.



Scheme

[1] S. Yoon, S. H. Hwang and W. B. Ko, *J. Nanosci. Nanotech.*, **8**, 3136 (2008).

[2] B. Nuber and A. Hirsch, *Full. Sci. Tech.*, **4**, 715 (1996).

[3] H. Kato, A. Yashiro, A. Mizuno, Y. Nishida, K. Kobayashi and H. Shinohara, *Bioorg. Med. Chem. Lett.*, **11**, 2935 (2001).

Corresponding Author : Weon Bae Ko

Tel: +82-2-3399-1700, Fax: +82-2-979-5318, E-mail address: kowb@syu.ac.kr

Enantiomeric Separation of Fullerodendron Formed by Diastereoselective Diels-Alder Reaction

○Naoki Tsugawa, Nobuhiro Takahashi, Yutaka Takaguchi

Graduate School of Environmental Science, Okayama University, Okayama 700-8530, Japan

Chiral fullerene derivatives are likely to play an important role in the areas of pharmaceuticals and optics. In particular, optically active fullerodendrimers are expected to be used for versatile applications. However, there is no report on the synthesis and properties of fullerodendrimer having chiral moiety. During our studies on the synthesis and properties of fullerodendrimer having chiral moiety, we have found that the enantiomeric fullerodendrimer could be obtained by the reaction of C_{60} with anthryl dendron having chiral sugar moiety at the terminals. This paper describes that the enantiomeric separation of fullerodendrimer formed by diastereoselective Diels-Alder reaction of C_{60} with anthryl dendron having D- or L-gluconamides at the terminals. To our knowledge, this is the first example of the diastereoselective [4+2]addition reaction of C_{60} and the enantiomeric separation of fullerene derivatives having dendritic architecture.

Optically active fullerodendrimer (Fig. 1) was obtained by Diels-Alder reaction of fullerene with anthryl dendrons having D-gluconamides at the terminals. Interestingly, diastereoselective addition, of which diastereomer ratio was estimated to be 3:2, was observed by 1H NMR as shown in Fig. 2. Furthermore, the enantiomeric separation of the fullerodendrimer was succeeded by column chromatography. The structure of enantiomeric fullerodendrimer was confirmed by 1H , ^{13}C NMR, MALDI TOF-MS, and CD spectra.

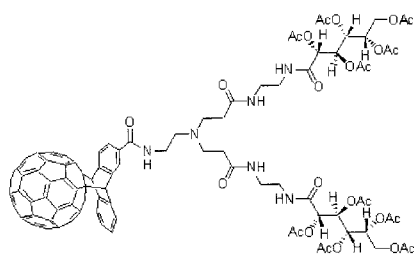


Fig. 1. Enantiomeric fullerodendrimer.

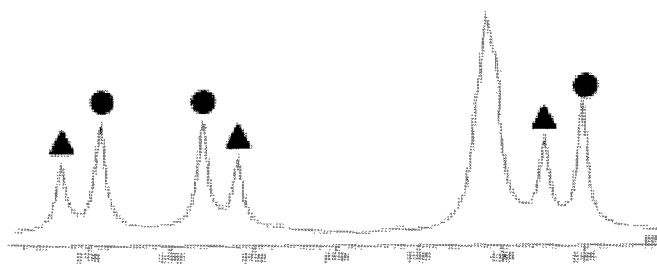


Fig. 2. 1H NMR spectra of the mixture of diastereomer obtained by the Diels-Alder reaction.

[1] Y. Takaguchi, Y. Sako, Y. Yanagimoto, S. Tsuboi, J. Motoyoshiya, H. Aoyama, T. Wakahara, T. Akasaka, *Tetrahedron Letters*, **44**, 5777 (2003).

[2] H. Kusai, T. Nagano, K. Imai, Y. Kubozono, Y. Sako, Y. Takaguchi, A. Fujiwara, N. Akima, Y. Iwasa, S. Hino, *Appl. Phys. Lett.*, **88**, 173509 (2006).

Corresponding Author: Yutaka Takaguchi

TEL: +81-86-251-8903, FAX: +81-86-251-8903, E-mail: yutaka@cc.okayama-u.ac.jp

Syntheses, Electrochemical and Photocurrent-Generating Properties of Penta(carbazolyl)[60]fullerene Derivatives

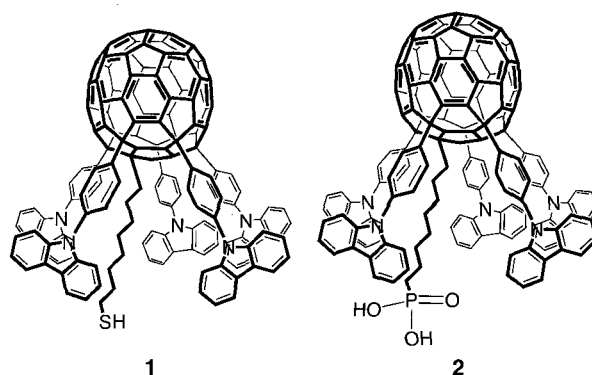
○ Katsumasa Nakahara¹, Yutaka Matsuo² and Eiichi Nakamura^{1,2}

¹*Department of Chemistry, The University of Tokyo, Hongo, Bunkyo-ku, Tokyo 113-0033, Japan*

²*Japan Science and Technology Agency, ERATO, Nakamura Functional Carbon Cluster Project, Hongo, Bunkyo-ku, Tokyo 113-0033, Japan*

The study of deca(carbazolylphenyl)[60]fullerene derivatives revealed that the carbazolyl group acts as an electron-withdrawing group and that efficient energy transfer occurs from the carbazolyl group to the center fullerene part [1]. We anticipated that this carbazolyl group can be used as a light-absorbing part in the new photocurrent generating fullerene derivatives [2].

Herein we report the syntheses and electrochemical properties of penta(carbazolylphenyl)[60]fullerene thiols (**1**) and phosphonic acids (**2**) as well as photocurrent generating properties of self-assembled monolayers (SAMs) of these molecules on gold and indium tin oxide (ITO) electrodes. The thiol **1** on the gold electrode generated cathodic photocurrent in the presence of methyl viologen and oxygen. As for the phosphonic acid **2** on the ITO electrode, anodic current was larger than cathodic one.



Reference: [1] X. Zhang, Y. Matsuo, E. Nakamura, *Org Lett.*, **2008**, *10*, 4146. [2] Y. Matsuo, K. Kanaizuka, K. Matsuo, Y.-W. Zhong, T. Nakae, E. Nakamura, *J. Am. Chem. Soc.* **2008**, *130*, 5016.

Corresponding Authors: Yutaka Matsuo and Eiichi Nakamura

TEL/FAX: +81-3-5841-1476

E-mail: matsuo@chem.s.u-tokyo.ac.jp; nakamura@chem.s.u-tokyo.ac.jp

Luminescent and Liquid Crystalline Deca(organo)[60]Fullerenes

○ Chang-Zhi Li¹, Yutaka Matsuo¹, Eiichi Nakamura^{1,2}

¹Nakamura Functional Carbon Cluster Project, ERATO, Japan Science and Technology Agency (JST), Hongo, Bunkyo-ku, Tokyo 113-0033, Japan

²Department of Chemistry, The University of Tokyo, Hongo, Bunkyo-ku, Tokyo 113-0033, Japan

Supramolecular organic nanostructures created by self-assembling molecules have long attracted attention due to potential applications as functional materials. Fullerene liquid crystals [1] are one of such elegant creatures, which become important with the expectation of enhanced physical properties derivation from anisotropic order of fullerene array. Accordingly, well understanding the organization of fullerene in mesophase will be important for further design of fullerene scaffolds. Luminescent fullerene LC would be ideal for this attempt. By using probe of luminosity, structure-properties relationship of fullerene mesophase can be studied, for instance, stimuli-responsive action and thin film properties.

Recently, a facile deca addition [2] allowed yielding pseudo-D5 **1a** (C18) and pseudo-C2 **1b** (C18) in one-pot reaction (Figure 1). Upon excitation at 366 nm of light, blue emission at maximum of 465 nm derived from pseudo-C2 adduct. And pseudo-D5 adduct yielded yellow emission at maximum of 568 nm (Figure 1). Accordingly, Quantum efficiencies of FL in cyclohexane have been determined.

Furthermore, with annealing sample **1a**, LC behaviors were characterized by x-ray diffraction (XRD), polarized optical microscopy (POM) and differential scanning calorimetry (DSC). Therefore, by combination of anisotropic molecular alignment and luminescence properties, studies towards polarized photophysical properties of luminescent LC have been conducted.

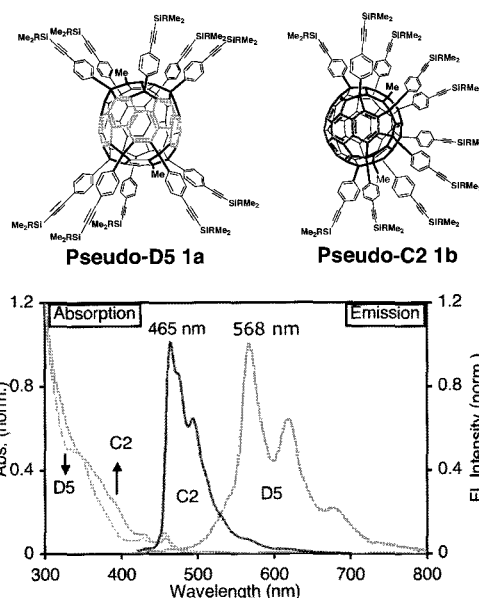


Figure 1. Pseudo-D5 **1a** and C2 **1b** with related absorption and emission spectrums in cyclohexane (excitation at 366 nm).

[1] Y-W. Zhong, Y. Matsuo, E. Nakamura, *J. Am. Chem. Soc.*, *129*, 3052 (2007). [2] Y. Matsuo, K. Tahara, K. Morita, K. Matsuo, E. Nakamura, *Angew. Chem. Int. Ed.*, *46*, 2844 (2007).

Corresponding Author: Yutaka Matsuo and Eiichi Nakamura

TEL/FAX: +81-3-5841-1476 E-mail: matsuo@chem.s.u-tokyo.ac.jp; nakamura@chem.s.u-tokyo.ac.jp

Fullerene Self-Assembled Monolayer as a Nano Capacitor Switchable by Light

○ Sebastian Lacher¹, Aiko Sakamoto², Keiko Matsuo², Yutaka Matsuo² and Eiichi Nakamura^{1,2}

¹*Department of Chemistry, The University of Tokyo, Hongo, Bunkyo-ku, Tokyo 113-0033, Japan*

²*Japan Science and Technology Agency, ERATO, Nakamura Functional Carbon Cluster Project, Hongo, Bunkyo-ku, Tokyo 113-0033, Japan*

Self-assembled monolayers (SAMs) of organic molecules on metal or semiconductor surfaces caused much attention in the past due to their ability in increasing device performance or building functional surfaces with new properties. Fullerene penta-adducts are excellent candidates for self-assembly on gold or indium tin oxide (ITO) substrates due to their compact and rigid Apollo lunar landing module structure (Figure 1). Moreover, fullerenes have unique electrochemical and photophysical properties showing high electron affinity and efficient singlet-to-triplet intersystem crossing.

We report here an unusual photocurrent behavior of fullerene penta-adduct thiols self assembled on gold surface. Unlike in earlier studies [1] the penta-adducts are not connected by direct π conjugation with their five legs to the surface, but by an aliphatic thiol linker causing a higher barrier for electron transfer from gold to fullerene or vice versa. Our system of a fullerene penta-adduct SAM in aqueous ascorbic acid solution shows a charge storage behavior which is switchable by light and depends on the substrate, the fullerene – surface distance as well as electron sacrificial in solution. As shown in the photocurrent profile in Figure 2, an excess charge flow can be observed under light irradiation, which declines with time. In the dark state, a recharging behavior with electron flow in the opposite direction can be observed.

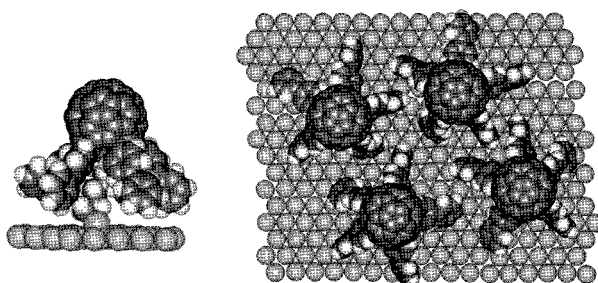


Figure 1: Fullerene penta-adducts self assembled on gold surface via thiol linker.

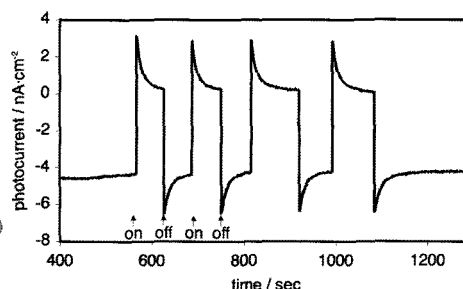


Figure 2: Photocurrent profile of fullerene penta adduct SAM on gold in ascorbic acid solution.

Reference: [1] Y. Matsuo, K. Kanaizuka, K. Matsuo, Y.-W. Zhong, T. Nakae, E. Nakamura, *J. Am. Chem. Soc.* **2008**, *130*, 5016.

Corresponding Authors: Yutaka Matsuo and Eiichi Nakamura

TEL/FAX: +81-3-5841-1476, **E-mail:** matsuo@chem.s.u-tokyo.ac.jp; slacher@chem.s.u-tokyo.ac.jp

Fullerene Functionalization through Palladium Catalysis

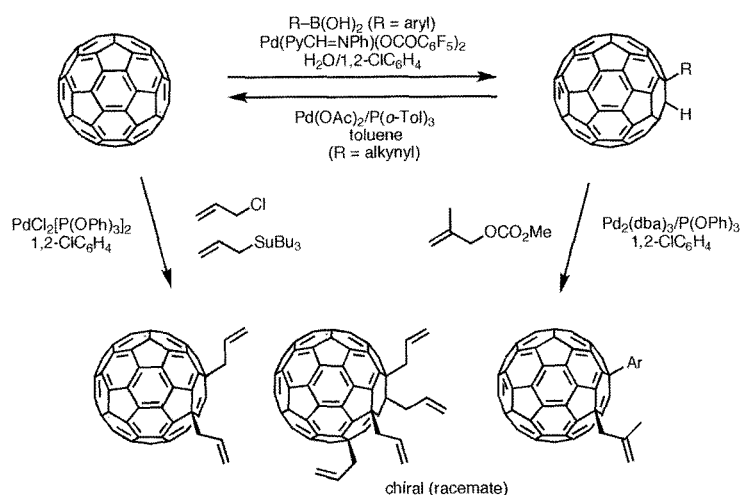
○Masakazu Nambo, Susumu Mori, and Kenichiro Itami

*Department of Chemistry, Graduate School of Science, Nagoya University,
and PRESTO, JST, Nagoya 464-8602, Japan*

The chemical modification of fullerenes has proven to be a promising approach for the preparation of new nanocarbon-based materials, providing the opportunity to tune the properties of these interesting materials. In order to explore new directions in metal-catalysis and nanocarbon chemistry, we recently initiated a program aimed at developing new functionalization chemistry of nanocarbons using transition metal catalysts.¹

As our initial foray into the area of nanocarbon chemistry, we developed a new organoboron-based functionalization of C₆₀ catalyzed by Pd(II) complexes.^{1b} This reaction enables the introduction of various organic fragments and a hydrogen atom on the fullerene surface in a highly regioselective and mono-addition selective manner.

A notable feature of the resultant organo(hydro)fullerenes (R-C₆₀-H) is that they possess an acidic C-H bond reflecting the highly conjugated fullerene backbone. We have recently established that Pd catalysts enable a number of C-H bond transformations of organo(hydro)fullerenes by taking advantage of these highly acidic C-H bonds.² The C-H bond allylation reaction can be a versatile and general method to functionalize fullerenes. Although the C-H bond arylation reaction is still in its infancy, the two new reactions found while investigating the arylation reaction are intriguing. The C-H bond dimerization reaction might contribute in the generation of new fullerene-assembled materials that are otherwise difficult to make. The C-C bond-cleaving reaction may find use in the “deprotection” of fullerenes, assuming an alkynyl(hydro)fullerene as a “masked” soluble fullerene. In addition, we discovered the multiple allylation of fullerene in the presence of Pd(II) catalyst using allyl chloride and allylstannane. The present finding of multidexterous palladium catalysis in transforming fullerenes not only highlights the potential of transition metal catalysis for fullerene functionalization, but also unlocks opportunities for markedly different strategies in nanocarbon synthesis.



References: (1) (a) M. Nambo, R. Noyori, K. Itami, *J. Am. Chem. Soc.* **2007**, *129*, 8080. (b) S. Mori, M. Nambo, L.-C. Chi, J. Bouffard, K. Itami, *Org. Lett.* **2008**, *10*, 4609. (c) M. Nambo, K. Itami, *McGraw-Hill Yearbook of Science & Technology*, in press. (2) M. Nambo, K. Itami, submitted.

Corresponding Author: Kenichiro Itami

E-mail: itami@chem.nagoya-u.ac.jp

Tel&Fax: 052-788-6098

Electron-Transport Property of Fullerene Derivatives $C_{60}X_2$ ($X=H, C_3H_6COOH, C_4H_8SH$)

Ken Tokunaga

Research and Development Center for Higher Education, Kyushu University
Fukuoka 810-8560, Japan

Fullerene C_{60} has been paid attention as carrier-transport material of organic field-effect transistors [1, 2]. Especially, C_{60} is expected as good electron-transport material (n-channel semiconductor) because thin films produced by vacuum processes have electron mobility as much as about $1 \text{ cm}^2\text{V}^{-1}\text{s}^{-1}$. However, in order to realize low-cost production and large-area device, it is necessary for C_{60} to have solution-processable form such as the [6,6]-phenyl C_{61} -butyric acid methyl ester (PCBM). Therefore, electron-transport property of C_{60} derivatives rather than the original C_{60} is of much interest and importance.

In this work, electron-transport property of C_{60} and $C_{60}X_2$ isomers ($X=H, C_3H_6COOH, C_4H_8SH$) is discussed. $C_{60}H_2$ is the simplest C_{60} derivative, and $-COOH$ and $-SH$ groups are often introduced for the purposes of solubility and film-making. Based on the Marcus theory, electron-transport property of the material is closely related to the reorganization energy (λ). λ of C_{60} and $C_{60}X_2$ (Fig. 1) is calculated by the density functional theory (DFT) method.

Figure 2 shows λ of C_{60} and $C_{60}X_2$. X -addition to C_{60} always results in an increase in λ from C_{60} (ca. 130 meV) because of segmentation of π -conjugation of C_{60} . Additionally, there is the large difference in λ between structural isomers. For all three derivatives, 0a and 1a isomers have the smallest and the largest λ , respectively, so that the values of λ mainly depend on the position of X and not on the kind of X . This is because that difference in the electronic and geometric structures of C_{60} part between structural isomers leads to the difference in λ . Other results and detailed analysis will be presented in the symposium.

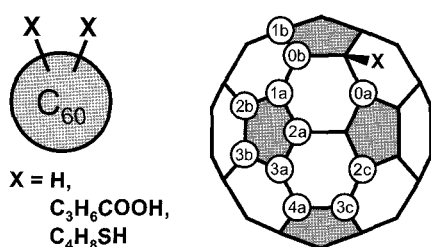


Fig. 1. Isomers of $C_{60}X_2$. The second X is added to one of carbon atoms 0a-4a.

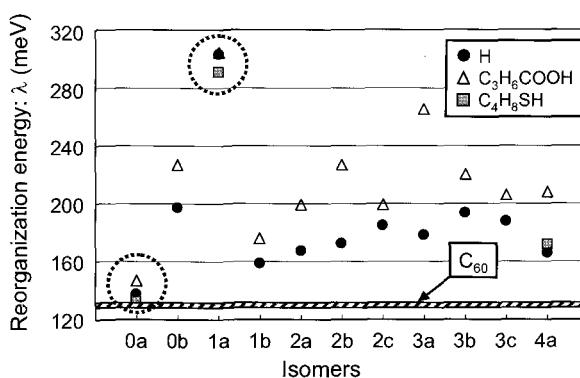


Fig. 2. Reorganization energies of C_{60} and $C_{60}X_2$.

[1] **K. Tokunaga** *et al.*, *Jpn. J. Appl. Phys.*, **47**, 1089 (2008); *ibid.*, **47**, 3638 (2008).

[2] **K. Tokunaga** *et al.*, The 33rd (2P-14) and 34th (3P-45) Fullerene-Nanotubes General Symposiums.

TEL: +81-92-726-4742, FAX: +81-92-726-4842, E-mail: tokunaga@rche.kyushu-u.ac.jp

Preparation of Self-Assembled of α -D-Mannosyl Fullerene[C₆₀] - Gold Nanoparticle Films

Shinsook Yoon¹, Sung Ho Hwang², \circ Sung Kyu Hong², Jeong Ho Lee²,
Jung Mi Kim² and Weon Bae Ko^{2*}

¹Faculty of Liberal Arts, Kangnam University, Yongin 449-702, South Korea

²Department of Chemistry, Sahmyook University, Seoul 139-742, South Korea

α -D-mannosyl fullerene[C₆₀]-functionalized gold nanoparticle films were self-assembled using the layer-by-layer method on the reactive of glass slides functionlized with 3-aminopropyltrimethoxysilane. The functionalized glass slides were alternately soaked in the solutions containing α -D-mannosyl fullerene[C₆₀] and 4-aminothiophenoxide/hexane thiolate-protected gold nanoparticles. α -D-mannosyl fullerene[C₆₀]-functionalized gold nanoparticle films have grown up to 5 layers depending on the immersion time. The self-assembled nanoparticle films were characterized using UV-vis spectroscopy showed that the surface plasmon band of gold at 530 nm gradually became more evident as successive layers were added to the films.

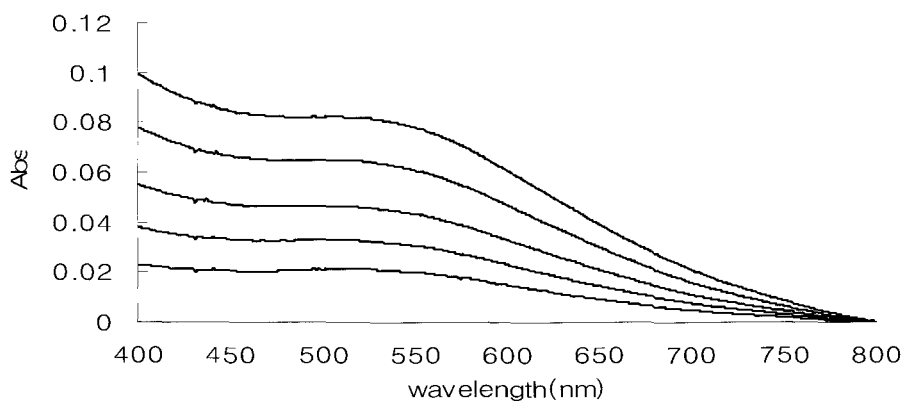


Figure. UV-vis absorption spectrum of the layer-by-layer assemblies of α -D-mannosyl fullerene[C₆₀]-gold nanoparticle multilayer films for the indicated time; +24h, +24h, +24h, +24h, +24h (from bottom to top).

[1] W. B. Ko, J. M. Yun, S. W. Jo and Y. S. Shon, *Ultrasonics*, **44**, e363 (2006).

[2] S. R. Isaacs, H. S. Choo, W. B. Ko and Y. S. Shon, *Chem. Mater.* **18**, 107 (2006).

Corresponding Author : Weon Bae Ko

Tel: +82-2-3399-1700, Fax: +82-2-979-5318, E-mail address: kowb@syu.ac.kr

Synthesis and Structural Characterization of Nano-Peapods Encapsulating Higher Fullerenes by High-Resolution TEM

○Teguh Endah Saraswati¹, Naoki Imazu¹, Kazunori Ohashi¹, Yasuhiro Ito¹,
Ryo Kitaura¹ and Hisanori Shinohara^{1,2}

¹Department of Chemistry, Nagoya University, Nagoya 464-8602, Japan

³Institute for Advanced Research, Nagoya University, Nagoya 464-8602, Japan

The higher fullerenes are not as abundant as C₆₀ and C₇₀. Due to their less amounts in arc-processed soot, one of the most suitable instruments for structural characterization can be done by using high-resolution transmission electron microscopy (HRTEM). Generally, fullerenes condense to form bulk crystals in three-dimension (3D). This becomes one of the constraints in fullerene observation by TEM because the observation of individual fullerene has been extremely difficult. However, the fullerene can be observed nicely when they are encapsulated in the interior space of carbon nanotubes. Hirahara et al. presented a HRTEM study on the structural characterization of fullerene-encapsulating SWNTs filled with various kinds of fullerenes including higher fullerenes up to C₈₄ [1]. However, the suitable conditions especially related to the suitable diameter of CNT and the sublimation temperature of higher fullerenes in the peapod synthesis still need to be carefully studied for successful fabrication of the peapods encapsulating higher fullerenes.

Here, we perform the successful encapsulation of higher fullerenes up to C₁₀₄ into carbon nanotubes with their structural characterization by HRTEM. The higher fullerene samples were isolated by the multistage high performance liquid chromatography (HPLC) using 5PYE and 5PBB column. Laser-desorption mass spectra and UV/Vis/NIR absorption spectra were taken to confirm their sample purity (99 %). The peapod synthesis has been successfully done by the vapor phase reaction method already reported [2]. The TEM images of peapods were observed by using JEM-2010F electron microscopy at acceleration voltages of 80-120 kV. Based on these studies and also compared to the simulation images, the most probable molecular structures of the higher fullerenes and their dynamical behavior entrapped in CNTs will be discussed in detail.

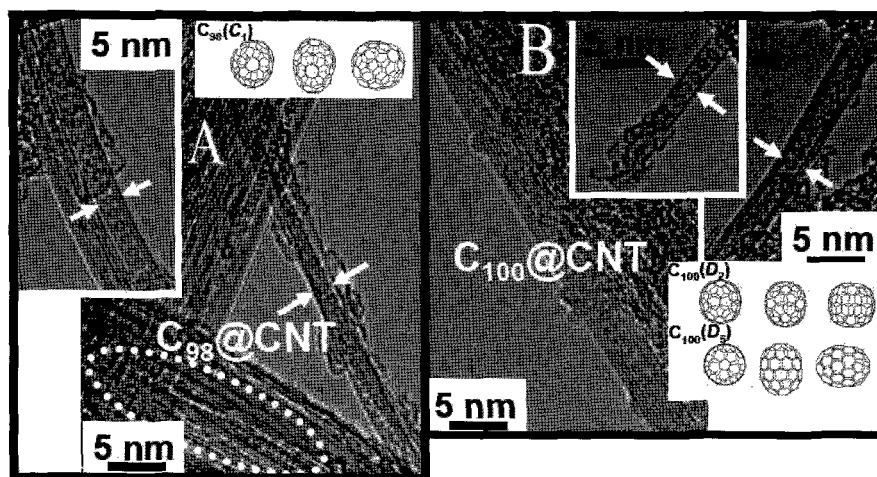


Figure 1. HRTEM images of some nano-peapods with the most probable fullerenes proposed structure. A: C₉₈ fullerene ; B: C₁₀₀ fullerene encapsulated inside single- and double wall carbon nanotubes.

References :

- [1] K. Hirahara, S. Bandow, K. Suenaga, H. Kato, T. Okazaki, H. Shinohara, and S. Iijima, Phys. Rev. B 64, 115420-115424 (2001).

[2] Ning, G.; Kishi, N.; Okimoto, H.; Shiraishi, M.; Kato, Y.; Kitaura, R.; Sugai, T.; Aoyagi, S.; Nishibori, E.; Sakata, M.; Shinohara, H. Chem. Phys. Lett., 441, 94, (2007)

Corresponding Author: Hisanori Shinohara

TEL: +81-52-789-2482, FAX: +81-52-747-6442, E-mail: noris@nagoya-u.jp

NMR Characterization of Cyanopolyynes HC₇N and HC₉N

○Mao Saikawa, Toshie Minematsu, and Tomonari Wakabayashi*

Department of Chemistry, Kinki University, Higashi-Osaka 577-8502, Japan

Carbon powder was irradiated with laser pulses in acetonitrile to produce carbon chain molecules. From the dark, brownish solution after laser ablation, we successfully isolated a submilligram- or a milligram-order of cyanopolyynes (HC₇N and HC₉N) and polyynes (C₈H₂ and C₁₀H₂), through repetitive operation of concentration and separation using HPLC. For the NMR characterization, we took advantage of 10% enrichment in ¹³C isotope for the precursory carbon powder. The proton-decoupled ¹³C NMR spectra for HC₇N clearly showed six peaks in-between 48-71 ppm for alkyne carbon and a single peak at 105.2 ppm for carbon in a cyano group. Figure 1 compares ¹H NMR spectra for the four polyynes in solutions of 1,1,2,2-tetrachloroethane-*d*₂. We observed peaks at the chemical shift of 2.37, 2.16, 2.34, and 2.24 ppm for protons in HC₇N, C₈H₂, HC₉N, and C₁₀H₂, respectively. In the poster, detailed assignments for the NMR peaks are presented and growth mechanism of carbon chains upon laser ablation in acetonitrile will be discussed.

We are indebted to Professor Wolfgang Krätschmer (Max-Planck-Institut für Kernphysik, Heidelberg) for his kind donation of isotope enriched carbon powder.

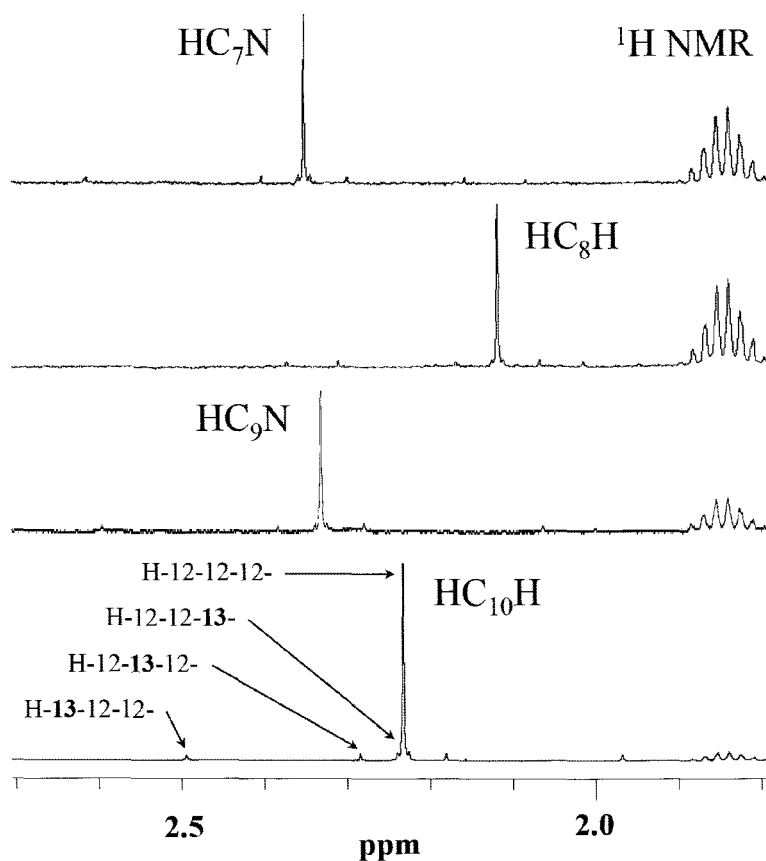


Figure 1. ¹H NMR spectra for HC₇N, C₈H₂, HC₉N, and C₁₀H₂. A single peak is characteristic for each spectrum. Cyanopolyynes, HC₇N and HC₉N, have less shielded proton compared to polyynes, C₈H₂ and C₁₀H₂. Since we used 10% enriched ¹³C powder, three split pairs of peaks are discernible (e.g., see bottom trace). These satellites show splitting of ~262, ~51, or ~7 Hz due to coupling with a nuclear spin of ¹³C, and are associated with different isotopomers having different orders in the isotopes within a carbon chain. The split pair for the adjacent ¹H¹³C moiety is not very much reduced, implying that solvent molecules donate hydrogen or proton rather than fragments of hydrocarbon during the formation upon laser ablation in acetonitrile.

Corresponding Author: Tomonari Wakabayashi
 E-mail: wakaba@chem.kindai.ac.jp
 Tel. 06-6730-5880 (ex. 4101) / FAX 06-6723-2721

Production of Atomic Nitrogen-Doped Fullerene N@C₆₀ by Ion Bombardment

○Masahito Kinoshita and Tomonari Wakabayashi*

Department of Chemistry, Kinki University, Higashi-Osaka 577-8502, Japan

We have improved the production efficiency for N@C₆₀ by precise control of deposition rate and by increased ion current. A schematic view of the apparatus is shown in Fig. 1. Nitrogen gas was discharged in an induction coil supplied by 500 W radio-frequencies (RF). Positively charged ions (cations) generated in the plasma were accelerated by a static field toward a metal mesh on the entrance of a negatively biased cylindrical electrode. Solid C₆₀ (powder) was sublimed in a crucible heated up to ~420°C and the molecules emanated from the crucible were deposited on inner surfaces of the electrode where the molecules were bombarded with the cations. In order to increase the current of the cations, distance between an opening of the coil and the entrance of the electrode was reduced to ~4 cm. The pressure of the nitrogen gas was lowered down to 2.5 Pa to avoid collisions with neutral molecules and the attraction field was strengthened by increasing the bias for the electrode down to -80 V. The ion current achieved was more than 10 mA. Typically, a few tens of milligrams of C₆₀ (powder) was loaded in the crucible, then sublimed and bombarded for an hour.

Figure 2 shows ESR spectra of N@C₆₀ produced from a single experiment. In addition to a triplet for ¹⁴N@C₆₀, a doublet for isotopic ¹⁵N@C₆₀ was clearly observed for the natural abundance of 0.4% for ¹⁵N.

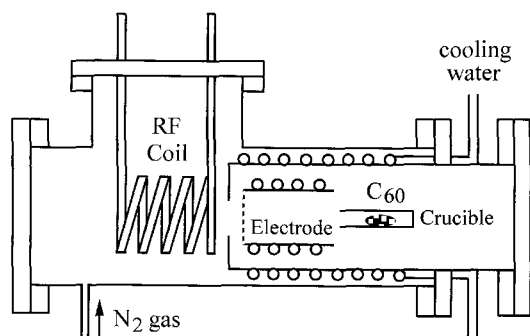
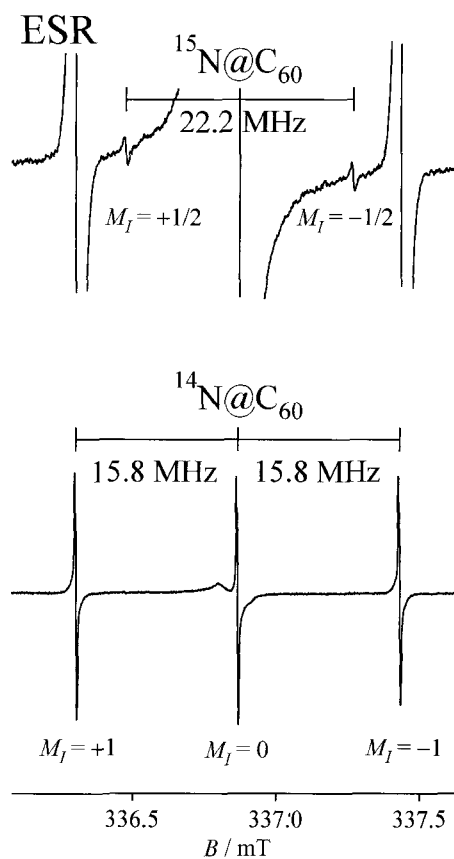


Figure 1 (above). Schematic view of the apparatus for the production of N@C₆₀.

Figure 2 (right). ESR spectra of N@C₆₀ produced upon a single experiment with ion bombardment for about 1 hour. The triplet is a hyperfine structure with $I = 1$ of ¹⁴N@C₆₀ (96.6%), while the doublet with $I = 1/2$ of ¹⁵N@C₆₀ (0.4%)



Corresponding Author: Tomonari Wakabayashi

E-mail: wakaba@chem.kindai.ac.jp

Tel. 06-6730-5880 (ex. 4101) / **FAX** 06-6723-2721

Computational Study on the Stone-Wales Transformation of non-IPR C₆₀ Fullerenes

Jun Li, Ting Ren, Xiang Zhao*

*Institute for Chemical Physics and Department of Chemistry,
Xi'an Jiaotong University, Xi'an 710049, P. R. China*

Hybrid Hartree-Fock density functional theories (B3LYP) have been applied to study the Stone-Wales transformation^[1] of non-IPR fullerenes C₆₀ (#1809) to yield five C₆₀ isomers with three or four adjacent pentagons (#1757, #1789, #1804, #1806, #1807). The results show that the transition states (TS) and reaction pathways could be identified for the rearrangement from C₆₀-C_{2v} (#1809) to the other five isomers C₆₀-C_S (#1757), C₆₀-C₂ (#1789), C₆₀-C_S (#1804), C₆₀-C₂ (#1806), C₆₀-C₂ (#1807) on the C₆₀ potential energy surface (PES). We found that all of these five transition states have C₂ molecular point group symmetry with the two migrating carbon atoms remaining close to the fullerene surface (figure 1), namely, the reaction path are all concerted 90° rotation of a C₂ unit. Another kind of possible TS with a carbene-like structure, proposed by Bettinger *et al.* which exists in the Stone-Wales transformation from C₆₀-I_h to C₆₀-C_{2v}^[2] does not exist as a stationary point with the density functional calculations here. Furthermore, Our investigation of the pathway using intrinsic reaction coordinate computation indicate that there are no intermediate steps along the Stone-Wales transformation pathway, namely, the carbene intermediate which was found by Murry, *et al.*^[3] along the stepwise reaction path could not be found here.

These reaction paths are found to have nearly identical energy requirements. As for the forward reactions, the barriers are from 160.61 kcal/mol to 173.03 kcal/mol; for the reverse reactions, the barriers are from 128.17 kcal/mol to 146.61 kcal/mol. The reaction barriers are summarized in Table 1. The detailed analysis of reaction pathway is discussed^[4] as well.

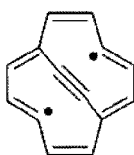


Figure 1. The TS Fragment for the reaction with two migrating carbon atoms remaining close to the fullerene surface.

Table 1: Barriers (in kcal/mol) of the Stone-Wales Transformation for non-IPR C₆₀ fullerenes at B3LYP/6-31G(d) Level.

Reactant	Products	E^a (forward)	E^a (reverse)
C ₆₀ -C _{2v} -1809	C ₆₀ -C _S -1757	173.03	128.17
	C ₆₀ -C ₂ -1789	161.55	129.18
	C ₆₀ -C _S -1804	160.61	141.66
	C ₆₀ -C ₂ -1806	168.14	129.89
	C ₆₀ -C ₂ -1807	169.74	128.81

[1] Stone, A. J.; Wales, D. J. *Chem. Phys. Lett.* **1986**, *128*, 501.

[2] Bettinger, H. F.; Yakobson, B. I.; Scuseria, G. E. *J. Am. Chem. Soc.* **2003**, *125*, 5572.

[3] Murry, R. L.; Strout, D. L.; Odom, G. K.; Scuseria, G. E. *Nature* **1993**, *366*, 665.

[4] Manuscript in preparation

Corresponding author: X. Zhao,

Email: xzhao@mail.xjtu.edu.cn; Fax: +86-29-82668559

Laser-merging experiments of C_{60}^- stored in an electrostatic ion storage ring

○H. Shiromaru¹, M. Goto¹, T. Kodama¹, J. Matsumoto¹, Y. Achiba¹,
T. Majima², H. Tanuma², T. Azuma², A.E.K. Sunden³, K.Hansen³

¹*Department of Chemistry, Tokyo Metropolitan University, Japan*

²*Department of Physics, Tokyo Metropolitan University, Japan*

³*Department of Physics, University of Gothenburg, 41296 Gothenburg, Sweden*

An electrostatic ion storage ring (E-ring) is a powerful device for the study of large molecular ions since ion storage conditions are independent of the ion masses at a given beam energy. So far, several studies on the fullerene ions have been reported by the group of ELISA, the world first E-ring [1]. An E-ring constructed in Tokyo Metropolitan University, TMU E-ring, is the third one, of which the schematic view is shown in Fig. 1. In the present study, we apply laser spectroscopy combined with ion storage techniques to “hot” C_{60} anions under radiative cooling to find, or to confirm the absence of, the structural isomers (namely non-IPR C_{60}), and to derive the cooling rate.

The purified IPR C_{60} was ionized by laser desorption without cooling gases, which in general produces high-temperature ions. The C_{60}^- was stored in the TMU E-ring, where the internal energy of anions was gradually dissipated by emitting IR photons. As a “fingerprint” of the IPR C_{60}^- , vis/near-IR excitation spectra were measured by detecting neutral species produced by photoabsorption. The detailed procedure of spectroscopic measurements is reported elsewhere [2].

The excitation spectrum of C_{60}^- is shown in Fig. 2. The broad band is naturally assigned to the hot IPR C_{60}^- . Although the signature of the non-IPR C_{60}^- was surveyed with the aid of ab initio calculations, signals of the non-IPR C_{60}^- have not so far been identified. The radiative cooling rate was derived from the storage time dependence of the decay signals of photoexcited anions.

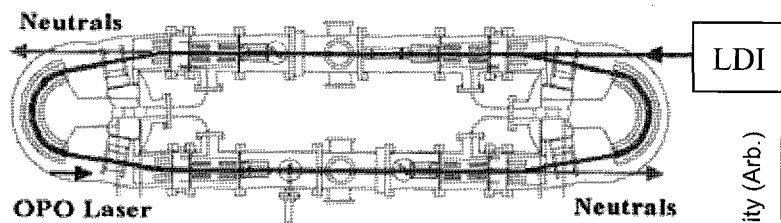


Fig. 1 Schematic view of TMU E-ring.

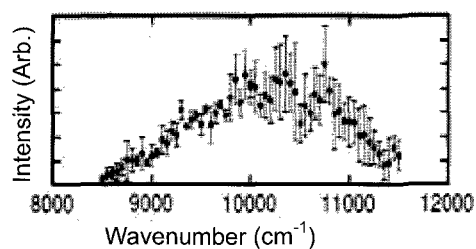


Fig. 2 Excitation spectrum of C_{60}^- .

[1] For example, S. Tomita et al. PRL94 053002 ('05).

[2] M. Goto et al., CPL 460, 46 ('08).

Corresponding Author: Haruo Shiromaru

TEL: +81-42-677-1111, FAX: +81-42-677-2525, E-mail: shiromaru-haruo@tmu.ac.jp

Si Doping into Densely-Aligned Carbon Nanotube Films on SiC

T. Maruyama¹, K. Yoshida², W. Norimatsu¹, M. Kusunoki^{1,2}

¹ Nagoya University, Nagoya, Japan

² Japan Fine Ceramics Center, Nagoya, Japan

maruyama.takehiro@e.mbox.nagoya-u.ac.jp

Carbon nanotube (CNT) has attracted a great attention for various applications based on its specific properties since its discovery. However, applying CNTs to nanodevices, it is important to control their electrical properties as a semiconductor. Theoretical calculation indicates the possibility that when another element is inserted into the CNT lattice, CNTs would exchange its physical and electrical properties dramatically. [1] And some groups reported about characterization of doped CNTs with some kinds of elements. [2]

We have reported that well-aligned CNTs are formed all over the SiC surface by selecting evaporation of Si atoms due to surface decomposition of SiC in vacuum at high temperature.[3] Here we report the results about Si-doping of the aligned CNT films formed by the SiC surface decomposition, using a conversion method aimed to control its electric property.

Firstly, CNTs 230 nm long oriented on SiC substrates were prepared by heating SiC(000 $\bar{1}$) surface to 1700 °C and held at the temperature for 0.5 h. (Figure 1) These were located with SiO₂ and C powders in carbon crucible. The crucible was heated to 1500-1600 °C and held at these temperatures for 0.5 h in vacuum around 3.0 x 10⁻⁴ Torr in the electronic furnace. The microstructure observation and EELS analysis were carried out using TEM (JEOL 2010-DM, 200kV) and EF-TEM (tecnaï 30F, 300kV).

Figure 2 shows Si element mappings of the CNT films (a) before and (b) after heat treatment at 1500 °C by EELS. These

results revealed that a little amount of Si atoms were doped into the pure CNTs without any change of CNT morphology. After treatment over 1515 °C, SiC single crystals started to grow at the CNT caps having orientation relationship with the CNT axis direction.

References

1. R. J. Baierle, Solange. B. Fagan, R. Mota, Antonio J. R. da Silva, A. Fazzio Phys. Rev. B, 64 (2001) 085413.
2. X. H. Sun, C. P. Li, W. K. Wong, N. B. Wong, C. S. Lee, S. T. Lee, B. K. Teo, J. Am. Chem. Soc., 124 (2002) 14464.
3. M. Kusunoki, T. Suzuki, T. Hirayama and N. Shibata, Appl. Phys., Lett. 77 (2000) 531.

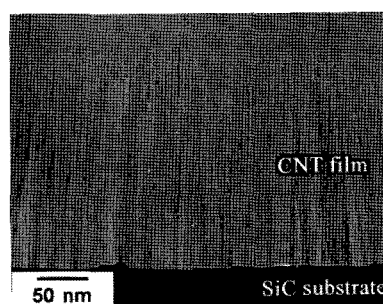


Fig. 1 Well-aligned CNT film on SiC(000 $\bar{1}$)

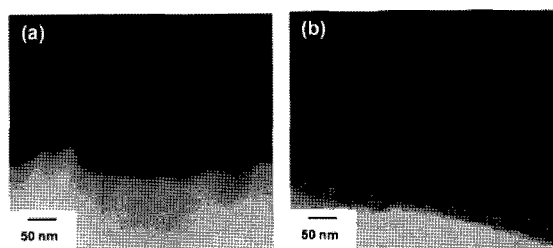


Fig. 2 Si element mappings of the CNT film (a) before and (b) after heat treatment.

Optical spectroscopic characterization of vertically aligned single-walled carbon nanotubes

○Erik Einarsson¹, Rong Xiang¹, Theerapol Thurakitseree¹, Zhengyi Zhang^{1,2},
Yoichi Murakami^{1,3}, Junichiro Shiomi¹, Shigeo Maruyama¹

¹*Department of Mechanical Engineering, The University of Tokyo, Tokyo 113-8656, Japan*

²*Department of Mechanical Engineering, Columbia University, New York, NY 10025, USA*

³*Department of Chemical System Engineering, The University of Tokyo,
Tokyo 113-8656, Japan*

Vertically aligned arrays of single-walled carbon nanotubes (SWNTs) were synthesized on both silicon and quartz substrates by the alcohol catalytic CVD method [1,2] using a wide range of catalyst concentrations. The influence of the various concentrations on the produced SWNTs was investigated by UV-Vis-NIR optical absorption and resonance Raman spectroscopy. The average diameter of the SWNTs was found to be dependent on both the relative and absolute catalyst amounts, as well as the substrate material. In the case of quartz, excess Mo was correlated with a decrease in SWNT diameter, but the absence of Mo typically resulted in no SWNT growth. On silicon (covered by an oxide layer), small-diameter SWNTs were obtained in the absence of Mo and for very low Co concentrations. Considering these findings, we investigate the role of the substrate in affecting the catalyst formation.

The overall morphology of the array was also investigated using the same spectroscopic methods. We find that the average diameter tends to increase during growth of vertically aligned SWNTs. This effect was clear in both optical absorption and resonance Raman spectra, where in the latter case an ultra-narrow-band Top Notch™ filter was employed to clearly observe low-frequency RBM peaks. The array morphology and the origin of anisotropic RBM peaks [3] was also investigated by polarization-dependent resonance Raman spectroscopy.

[1] S. Maruyama, R. Kojima, Y. Miyauchi, S. Chiashi, M. Kohno, *Chem. Phys. Lett.* **360** (2002) 229.

[2] Y. Murakami, S. Chiashi, Y. Miyauchi, M. Hu, M. Ogura, T. Okubo, S. Maruyama, *Chem. Phys. Lett.* **385** (2004) 298.

[3] Y. Murakami, S. Chiashi, E. Einarsson, S. Maruyama, *Phys. Rev. B* **71** (2005) 085403.

Corresponding Author: Shigeo Maruyama

TEL: +81-3-5841-6421, FAX: +81-3-5841-6983, E-mail: maruyama@photon.t.u-tokyo.ac.jp

Low Temperature Growth of Single-Walled Carbon Nanotubes by High Vacuum ACCVD Method

○Yohei Yamamoto, Hiroto Okabe, Taiki Inoue, Erik Einarsson, Makoto Watanabe,
and Shigeo Maruyama

Department of Mechanical Engineering, The University of Tokyo, Tokyo 113-8656, Japan

Single-walled carbon nanotubes (SWNTs) are one of the most promising materials for various novel applications. Currently, the alcohol catalytic chemical vapor deposition (ACCVD) method [1] is widely used to obtain high quality SWNTs such as vertically aligned SWNT films with small amounts of defects and impurities [2]. Recently, Shiokawa *et al.* [3] reported that SWNTs were grown at low temperature (~ 550 °C) and at low pressure of less than 0.1 Pa using the ACCVD method. Such CVD conditions are considered to be advantageous for growing small-diameter SWNTs with well controlled growth speed, which would give us valuable insights toward the control of SWNT chiralities. The purpose of present study is to clarify the growth mechanism of SWNTs through investigating SWNTs grown under well-defined high-vacuum environment.

Specifically, we have developed a high-vacuum CVD system that allows us to control the feedstock gas pressure as well as the reaction temperature accurately. We successfully synthesized SWNTs under various temperatures and pressures, and analyzed the obtained samples by resonant Raman spectroscopy (Fig. 1). From this, we found that the optimum synthesis temperature decreases as the ethanol vapor pressure decreases. We characterized thereby synthesized SWNTs by TEM (Fig. 2), SEM and AFM, showing that SWNTs with small diameter are preferably synthesized by the proposed approach that utilizes the low pressure and high vacuum conditions.

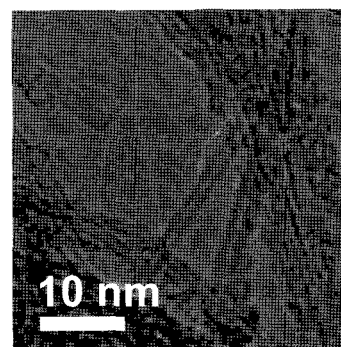
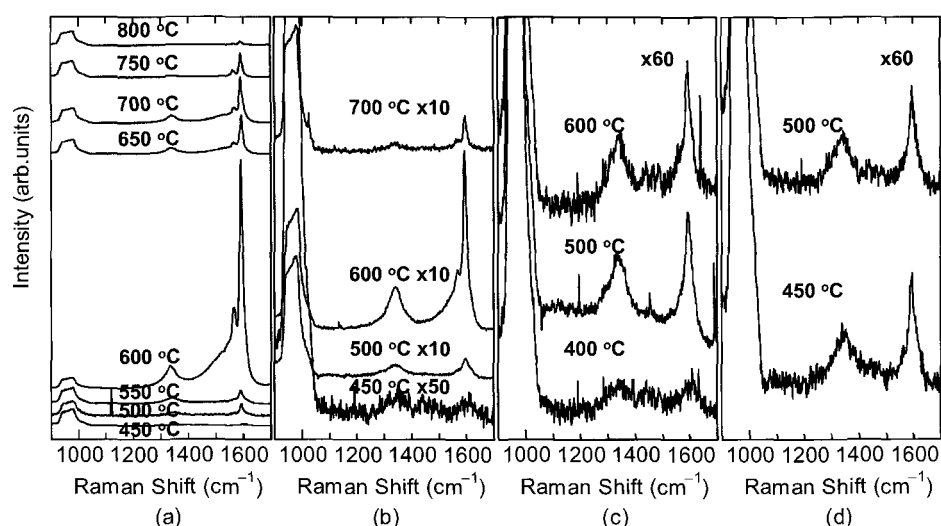


Fig.2 TEM image of SWNTs synthesized at 10 Pa and 600 °C for 30 min.

Fig.1 Raman spectra of SWNTs grown at different ethanol vapor pressures of (a) 10, (b) 1, (c) 1×10^{-2} , (d) 1×10^{-3} Pa. The CVD temperature is shown for each spectrum. The excitation wavelength was 488 nm.

- [1] S. Maruyama, R. Kojima, Y. Miyauchi, S. Chiashi, M. Kohno, *Chem. Phys. Lett.*, **360** (2002) 229.
 [2] Y. Murakami, S. Chiashi, Y. Miyauchi, M. Hu, M. Ogura, T. Okubo, S. Maruyama, *Chem. Phys. Lett.*, **385** (2004) 298.
 [3] T. Shiokawa, P. H. Zhang, M. Suzuki, K. Ishibashi, *Jpn. J. Appl. Phys.*, **45** (2006) L605.

Corresponding Author: Shigeo Maruyama

TEL: +81-3-5841-6421, FAX: +81-3-5841-6408, E-mail: maruyama@photon.t.u-tokyo.ac.jp

Selective Isolation of (6,5) Carbon Nanotubes by Density Gradient Ultracentrifugation

○Pei Zhao¹, Yoichi Murakami^{1,2}, Rong Xiang¹, Erik Einarsson¹, Junichiro Shiomi¹, Shigeo Maruyama¹

¹Department of Mechanical Engineering, The University of Tokyo

²Department of Chemical System Engineering, The University of Tokyo

We present a protocol to selectively isolate single-walled carbon nanotubes (SWNTs) with a chirality of (6,5) using density gradient ultracentrifugation (DGU)^[1]. Starting with SWNTs synthesized by the alcohol catalytic chemical vapor deposition (ACCVD) method, we used *sodium deoxycholate* (DOC), *sodium dodecyl sulfate* (SDS) and *sodium cholate* (SC) as co-surfactant encapsulating agents^[2] to separate (6,5) SWNTs. The optical absorbance spectra and photoluminescence excitation (PLE) map (Fig. 1) show that the resulting sample contained a high relative purity of (6,5) SWNTs, but other chiralities were still present at low concentrations. After this initial separation, we refined the selectivity by iteration using the same DGU conditions. Evaluation by PLE showed an increasing concentration of (6,5) SWNTs after each iteration. The final (rightmost) PLE map shown in Fig. 1, showing isolation of (6,5) SWNTs, was obtained after three iterations. This illustrates the potential for complete isolation by DGU, and we believe that by further refinement of this process similar results can be obtained in a single step.

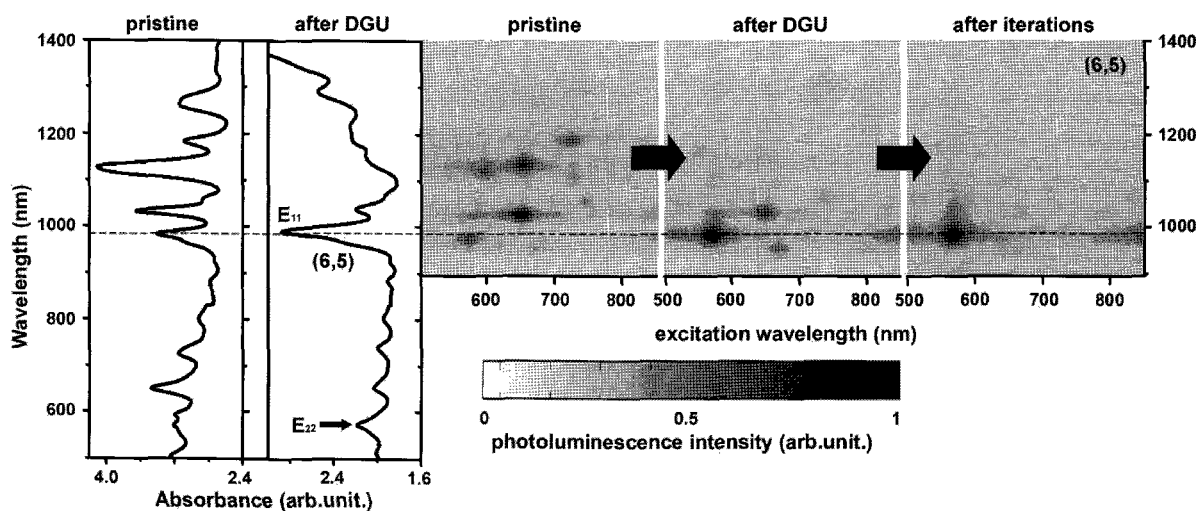


Figure 1: Optical absorbance spectra (left) and photoluminescence excitation maps (right) showing selective isolation of (6,5) SWNTs by iterated density gradient ultracentrifugation of ACCVD SWNTs.

[1] M. Arnold, A. Green, J. Hulvat, Stupp and M. Hersam. *Nat. Nanotechnol.* **1**, 60 (2006)

[2] K. Yanagi, Y. Miyata and H. Kataura, *Appl. Phys. Express* **1**, 034003 (2008)

Corresponding Author: Shigeo Maruyama

TEL: +81-3-5841-6421, FAX: +81-3-5841-6983, E-mail: maruyama@photon.t.u-tokyo.ac.jp

Laser Fluence Effect on the Chirality Characteristics of Individually Dispersed Single-walled Carbon Nanotube in Aqueous Solution with Pulsed OPO Laser Irradiation

○Isamu Tajima, Akira Kumazawa, Katsumi Uchida, Tadahiro Ishii, and Hirofumi Yajima*

*Department of Applied Chemistry, Faculty of Science, Tokyo University of Science
12-1 Funagawara-machi, Shinjyuku-ku, Tokyo 162-0826, Japan*

In the previous reports, we have proposed a new selective separation method for metallic (m-) and semiconducting (s-) single-walled carbon nanotubes (SWNTs) with nanosecond pulsed optical parametric oscillator (OPO) laser, choosing adequate excitation wavelength for the resonance absorption of individually dispersed SWNTs-NaDDBS (dodecylbenzenesulfonic acid sodium salt) solutions. As a result with high fluence OPO laser, choosing laser wavelength corresponding to typical absorption peaks in m-SWNTs first transition region (M_{11}), and s-SWNTs first and second transition band regions (S_{22} , S_{11}), respectively, the following findings and suggestion were obtained from the spectroscopic studies with UV-vis-NIR absorption and resonance Raman scattering spectra, and the structural studies with DLS and AFM: (1) The laser irradiation in M_{11} region gave rise to the bleaching of the m- and s-SWNTs, accompanied by a large structural collapse. On the other hand, the laser irradiation in S_{11} region, in particular S_{22} region, resulted in the removal of s-SWNTs as well as the M_{11} laser irradiation, but the peaks in the M_{11} region remained unchanged; (2) The efficiencies of the laser irradiation at either side wavelength (485 or 533 nm in M_{11} region and 690 or 768 nm in S_{22} region) for the chiral peak (510nm in M_{11} region and 730nm in S_{22} region) were greater than that at the main chiral peak; (3) Two species of contributions for energy migration processes, that is, photo-relaxation and thermal-relaxation are multiply involved in the energy conversion for the SWNTs excited with the laser irradiation. In the S_{22} irradiation, the photo-relaxation (photoluminescence) process is predominated for the resonance excitation of a chiral SWNT, whereas the thermal-relaxation process is predominated for the excitation at the wavelengths deviated from the chiral peak, accompanied by the collapse of SWNTs due to huge temperature rise. On the other hand, the collapse of SWNTs induced by the M_{11} irradiation would be concerned with the thermal-relaxation process through π -plasmon absorption, regardless of excitation wavelengths. Consequently, the laser irradiation in S_{22} region is suggested to be involved in the activation and excitation of merely the s-SWNTs, and to bring about the destabilization and/or destruction of the dispersed s-SWNTs through photo-thermal conversion process.

In order to gain better information with respect to the OPO laser efficiencies for the selective separation of either m- or s-SWNTs, the laser fluence effect on the chirality characteristics of the SWNTs has been scrutinized, including the effect of the SWNTs concentration. The detailed results will be discussed in *the F-NT Symposium*.

*Corresponding Author: Hirofumi Yajima

TEL: +81-3-5228-8705, FAX: +81-3-5261-4631, E-mail: yajima@rs.kagu.tus.ac.jp

Low-temperature growth of carbon nanotubes from acetylene

Takashi Shirai¹ and Suguru Noda^{1,*}

¹ Dept. of Chemical System Engineering, The University of Tokyo, Tokyo 113-8656, Japan

Low-temperature growth of carbon nanotubes (CNTs) on substrates is important to realize direct implementation of CNT devices such as CNT-interconnects [1]. Previous studies including chemical vapor deposition (CVD) assisted either by plasma or hot-wire imply that C_2H_2 is the key precursor. We performed a parametric study of CNT growth from C_2H_2 for a range of C_2H_2 pressures and growth temperatures.

Catalysts were prepared by sputter-deposition of 1.0-nm-Co/ 5-nm-TiN [1] on SiO_2/Si substrate followed by thermal annealing at 800 °C for 10 min under a H_2 flow at 10 mTorr. CNTs were grown in a tubular hot-wall CVD reactor by flowing a C_2H_2/Ar flow at a constant total pressure of 10 Torr. C_2H_2 partial pressure ranged between 1-100 mTorr and temperature ranged between 400-600 °C. Figure 1 shows the CNT growth curves at 550 °C. At low C_2H_2 pressures of 1 and 10 mTorr, CNT grew at a constant growth rate, while at higher pressures of 40 and 80 mTorr, CNT growth rate showed an exponential decay [2]. Figure 2 showed CNT morphologies at 550 °C. At a low C_2H_2 pressure of 10 mTorr, CNTs were straight and vertically aligned, while at a high pressure of 80 mTorr, CNTs grew randomly. Excess C_2H_2 feeding caused catalyst deactivation, and decreased number density of growing CNTs resulted in randomly oriented growth.

To grow CNT vertically and straightly at a low temperature, C_2H_2 pressure should be kept below a certain level such that the incorporation rate of C_2H_2 into catalyst does not exceed the segregation rate of CNTs from catalyst. Growth window, i.e. C_2H_2 partial pressure vs. temperature, will be presented.

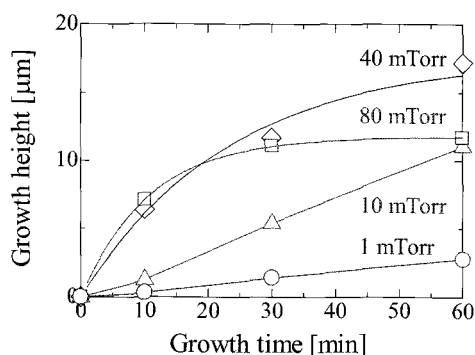


Fig. 1 CNT growth curves at 550 °C, 10 Torr with different C_2H_2 pressures.

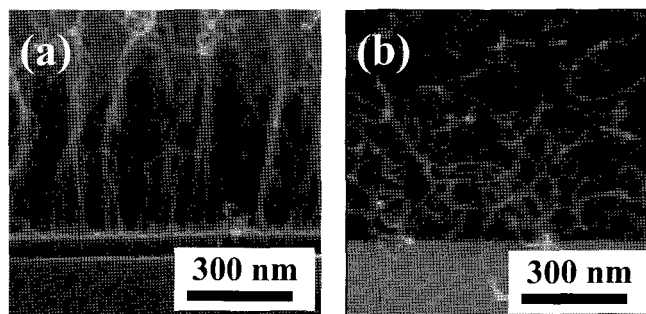


Fig. 2 Cross-sectional SEM images showing CNT morphologies grown at C_2H_2 pressures of (a) 10 mTorr and (b) 80 mTorr for 30 min.

[1] S. Sato, et al., Chem. Phys. Lett. **402**, 149 (2005).

[2] S. Maruyama, et al., Chem. Phys. Lett. **403**, 320 (2005).

*Corresponding Author: Suguru Noda

TEL: +81-3-5841-7330, FAX: +81-3-5841-7332, E-mail: noda@chemsys.t.u-tokyo.ac.jp

Progress in Separation of Metallic and Semiconducting Carbon Nanotubes Using Agarose Gel

○Takeshi Tanaka¹, Hehua Jin¹, Yasumitsu Miyata¹, Shunjiro Fujii¹, Hiroshi Suga¹,
Yasuhisa Naitoh¹, Takeo Minari¹, Tetsuhiko Miyadera¹, Kazuhito Tsukagoshi¹,
and Hiromichi Kataura^{1,2}

¹Nanotechnology Research Institute, National Institute of Advanced Industrial Science and Technology (AIST), Tsukuba, Ibaraki 305-8562, Japan

²JST, CREST, Kawaguchi, Saitama, 332-0012, Japan

Single wall carbon nanotubes (SWCNTs) have attracted a great deal of attention towards versatile applications, especially in the field of electronics, such as field effect transistor (FET). However, as-produced SWCNTs always contain both metallic and semiconducting SWCNTs, which is one of the most crucial problems preventing useful application of SWCNTs. Previously, we reported novel separation methods of metallic and semiconducting SWCNTs using agarose gel with electric field (gel electrophoresis)¹ and without electric field². In this presentation, we report our recent progress in the separation using agarose gel.

Raman spectroscopic analysis was performed with pristine and separated HiPco SWCNTs (Fig. 1). From the Raman data, the metallic/semiconducting (MS) separation was reconfirmed. When sodium tetradecyl sulfate was used in place of sodium dodecyl sulfate (SDS), the MS separation was observed to some extent. The performance of FETs made with separated semiconducting SWCNTs was much better than that of unseparated SWCNTs, namely, most of the semiconducting devices (94%) displayed a high on/off ratio of more than 10^4 , while all of the unseparated devices displayed less on/off ratio than 10^4 . We will also report the MS separation of CoMoCAT SWCNTs. This study was supported by the industrial technology research grant program of the New Energy and Industrial Technology Development Organization (NEDO) of Japan.

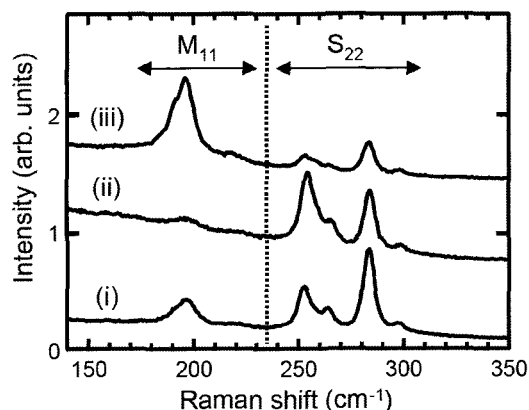


Fig. 1. Raman spectra of (i) pristine, (ii) semiconductor-enriched, and (iii) metal-enriched HiPco samples at 633 nm laser excitation. The spectra were shifted vertically for clarity.

[1] T. Tanaka et al., *Appl. Phys. Express* 2008, **1**, 114001.

[2] T. Tanaka et al., The 35th Fullerene-Nanotubes General Symposium, 2008, 2-4 (p53).

Corresponding Author: T. Tanaka

Tel: +81-29-861-2903, Fax: +81-29-861-2786, E-mail: tanaka-t@aist.go.jp

Influence of Laser Power on the Formation of SWNTs by Laser Ablation

○Masaomi Teshiba and Tomonari Wakabayashi*

Department of Chemistry, Kinki University, Higashi-Osaka 577-8502, Japan

Laser ablation is known for one of the methods for producing single-wall carbon nanotubes (SWNTs). It has advantageous features not only for high purity but also for diameter control for as-grown SWNTs [1]. The process in laser ablation can be controlled by experimental parameters such as temperature of the furnace, pressure and flow rate of the carrier gas, and so on. In this work, we studied influence of the laser power on the purity for as-grown samples by focusing on the issues for avoiding formation of undesired amorphous carbon that covers the surface of SWNTs.

A pellet of Metal/carbon composite (Ni/Co/C or Rh/Pt/C) was ablated by laser pulses (Nd:YAG 1064 nm, 5 ns, 10 Hz) in an argon gas flow under constant pressure of 70 kPa and elevated furnace temperature of 1100°C. Samples were prepared under different conditions for the laser power in a range of 150-900 mJ/pulse (0.2-1.2 GW/cm²) and then characterized by Raman spectroscopy and by field-emission scanning electron microscopy (FE-SEM). As the laser power increased, diameter distribution is broadened as revealed by RBM patterns in the Raman spectra (Fig. 1). The FE-SEM images showed that the amount of carbon particles increased relatively to that of SWNTs, especially for those prepared under the higher laser-power conditions. In the poster, we will discuss on the mechanism for laser ablation under the experimental conditions.

[1] H. Kataura, Y. Kumazawa, Y. Maniwa, Y. Ohtsuka, R. Sen, S. Suzuki, Y. Achiba, *Carbon* **38**, 1691 (2000).

Corresponding Author: Tomonari Wakabayashi
E-mail: wakaba@chem.kindai.ac.jp
Tel. 06-6730-5880 (ex. 4101) / FAX 06-6723-2721

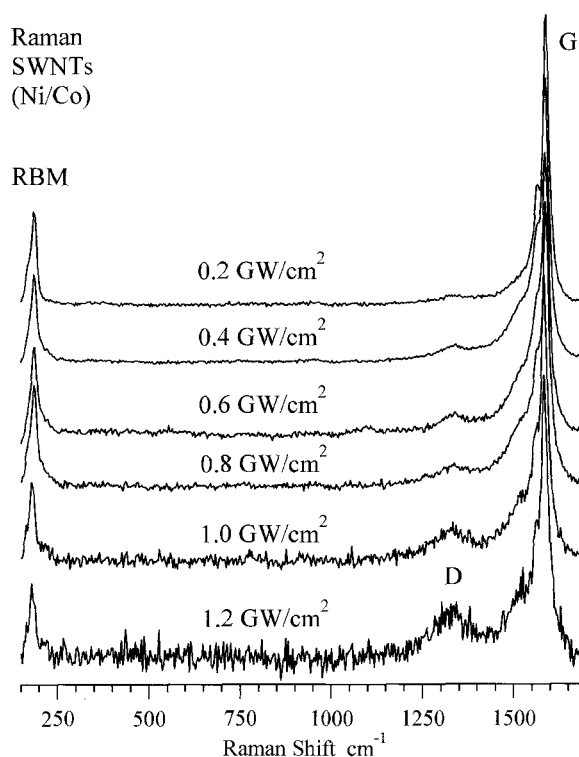


Figure 1. Laser power dependence in the Raman spectra (excitation at 532 nm, ~90 mW) for SWNTs produced by laser ablation (catalyst Ni/Co, furnace temperature 1100°C, ablation by Nd:YAG 1064 nm).

Synthesis of Thin Carbon Nanocoils by Fe-Sn Catalyst Supported on Zeolite

○M. Yokota¹, Y. Suda¹, S. Oke¹, H. Takikawa¹, Y. Fujimura²
T. Yamaura², S. Itoh², H. Ue³, M. Morioki⁴

¹ *Department of Electrical and Electronic Engineering, Toyohashi University of Technology*

² *Research and Development Center, Futaba Corporation.*

³ *Fuji Research Laboratory, Tokai Carbon Co., Ltd.*

⁴ *Fundamental Research Department, Toho Gas Co., Ltd.*

Carbon nanocoil (CNC) is a material of carbon fiber with helical shape. CNCs are synthesized by chemical vapor deposition using a composite catalyst, Fe-Sn. Fig. 1(a) shows CNC synthesized using the composite catalyst, which was made from Fe micro particles mixed in Sn solution. The CNC coil diameters were about 0.5-1.0 μm . It was reported that a coil diameter was proportional to the catalyst particle size [1]. In this study, Catalyst metals were supported on zeolite to obtain smaller particles. The catalyst was prepared by the solution of Fe and Sn pure powder dissolved in hydrochloric acid with zeolite. While the solution was dried in an electrical furnace, the composite metal was supported on zeolite surface. The catalyst on zeolite was placed on a quartz boat at the center of a quartz-made reaction tube. The reaction temperature, the gas flow rates of nitrogen as a dilution gas and acetylene as a source gas, and the reaction time were 700°C, 1000 sccm, 50 sccm, and 10 min, respectively. CNCs synthesized with zeolite were shown in Fig. 1(b). The CNC coil diameters were about 40-80 nm. The coil diameter was thinner on a scale of about one to ten than before.

This work has been partly supported by the Outstanding Research Project of the Research Center for Future Technology, Toyohashi University of Technology (TUT); the Research Project of the Venture Business Laboratory(TUT); Global COE Program "Frontiers of Intelligent Sensing" from the Ministry of Education, Culture, Sports, Science and Technology (MEXT); The Japan Society for the Promotion of Science (JSPS), Core University Programs (JSPS-KOSEF program in the field of "R&D of Advanced Semiconductor"; JSPS-CAS program in the field of "Plasma and Nuclear Fusion"); and Grant-in-Aid for Scientific Research from the MEXT.

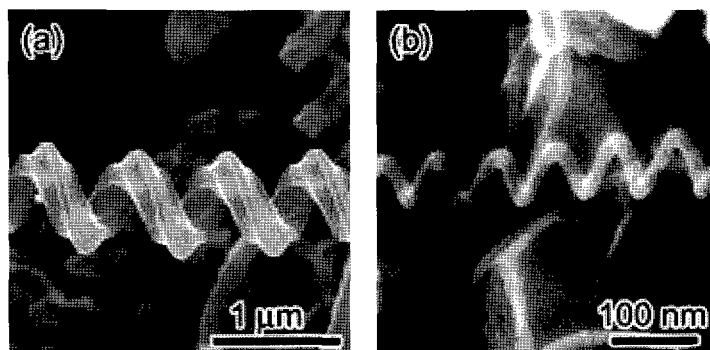


Fig. 1. SEM images of CNCs grown from Fe-Sn catalyst. The catalyst was made from (a) Fe micro particle with Sn solution and (b) Fe and Sn powder dissolved in HCl with zeolite.

Reference [1] S. Hokushin, L. Pan and Y. Nakayama: Jpn. J. Appl. Phys. 46 (2007) 5383

Corresponding Author: Yoshiyuki Suda

E-mail: suda@eee.tut.ac.jp, Tel: +81-532-44-6726

Chirality Selective Separation for Single-walled Carbon Nanotube with Density Gradient Ultracentrifugation

Yoshiya Kaminosono, Katsumi Uchida, Tadahiro Ishii, and Hirofumi Yajima*

*Department of Applied Chemistry, Faculty of Science, Tokyo University of Science
12-1 Funagawara-machi, Shinjyuku-ku, Tokyo 162-0826, Japan*

Chirality separations for single-walled carbon nanotubes (SWNTs) have attracted a great deal of attention for their practical and advanced applications. We have attempted the development of chirality selective separations method with density gradient ultracentrifugation (DGU). In the present study, the individually dispersed HiPco SWNTs in only carboxymethylcellulose (CMC) solution or the mixed solution of CMC and sodiumdodecylsulfate (SDS) was prepared by ultrasonication treatment for 180 min in an ice bath at about 20 W power, following ultracentrifugation treatment at 163,000 g for 1h. In DGU experiments, the density gradient ($d=1\sim 1.4$) was prepared by adding 60 % iodixanol to 20 mM tris (hydroxyl methyl) aminomethane buffer solution, following ultracentrifugation treatment at 175,000 g. Optical measurements revealed that semiconducting SWNTs was concentrated in the SDS and CMC mixed systems, whereas metallic SWNTs was concentrated in the CMC systems. This method is expected to be promising for the chirality selective separations.

Corresponding Author: Hirofumi Yajima

TEL: +81-3-3260-4272(ext.5760), FAX: +81-3-5261-4631, E-mail: yajima@rs.kagu.tus.ac.jp

Effect of Water Vapor on Structure of Single-Walled Carbon Nanotubes

○Naoki Yoshihara,¹ Hiroki Ago,^{*1,2,3} and Masaharu Tsuji^{1,2}

¹Graduate School of Engineering Sciences, Kyushu University, Fukuoka 816-8580, Japan

²Institute for Materials Chemistry and Engineering, Kyushu University, Japan

³PRESTO-JST, Japan

Water-assisted chemical vapor deposition (CVD), called super-growth, has attracted a great interest as a high yield growth method of single-walled carbon nanotubes (SWNTs) [1]. We studied chemistry of water-assisted SWNT growth over Fe/MgO catalyst and found that water vapor removed amorphous carbon primary based on chemical reaction, $C + H_2O \rightarrow CO + H_2$ [2]. We also found that the introduction of water vapor extends the catalyst lifetime but does not alter activation energy for the nanotube growth [2].

Effect of water vapor on the SWNT structure is also interesting. The water vapor introduced in chemical vapor deposition (CVD) may preferentially oxidize small-diameter SWNTs, because they are energetically less stable than large-diameter nanotubes. Here, we investigated the effect of water vapor on the diameter and chirality of SWNTs grown over the Fe/MgO catalyst by using Raman and photoluminescence (PL) spectroscopies.

Figure 1 compares the RBM spectra of nanotubes, which indicate effect of water vapor.

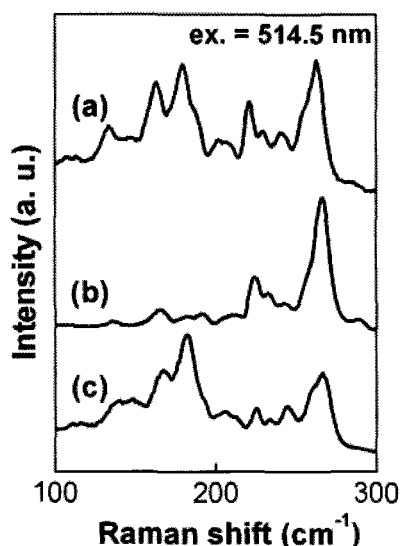


Fig. 1 RBM spectra of SWNTs synthesized by water-free CVD (a), water-assisted CVD (b), and thermal annealing of as-synthesized nanotubes in Ar-H₂O flow (c).

We synthesized SWNTs at 750 °C under a mixed flow of CH₄ (20%) and Ar with 350 ccm. The water vapor was introduced by passing 1 ccm of Ar gas through water vessel. Interestingly, we found that the SWNTs grown by water-assisted CVD (Fig. 1b) showed a narrower diameter distribution than those grown without water vapor (Fig. 1a). The SWNTs with small diameter (< 1 nm) were preferentially formed by the water-assisted CVD. Post-synthesis heat-treatment with water vapor for the SWNTs grown by water-free CVD resulted in selective oxidation of small-diameter SWNTs (Fig. 1c).

It is likely that the observed effect of water vapor during CVD on the SWNT diameter (Fig. 1b) reflects the change in distribution of catalyst particle size. This might be related with suppression of thermal aggregation of the metal catalyst reported very recently [3]. We will also show difference observed for the PL from the SWNTs grown by water-assisted and water-free CVD.

References

- [1] K. Hata, D. N. Futaba, K. Mizuno, T. Namai, M. Yumura, S. Iijima, *Science*, **306**, 1362 (2004).
- [2] N. Yoshihara, H. Ago, M. Tsuji, *J. Phys. Chem. C*, **111**, 11577 (2007).
- [3] P. B. Amama, C. L. Pint, L. McJilton, S. M. Kim, E. A. Stach, P. T. Murray, R. H. Hauge, B. Maruyama, *Nano Lett.*, ASAP article (2008).

Corresponding Author: Hiroki Ago (Tel&Fax: +81-92-583-7817, E-mail: ago@cm.kyushu-u.ac.jp)

Dip-pen nanolithography for CNTs patterning

○Naoko Kayumi¹, Tsuyohiko Fujigaya¹ and Naotoshi Nakashima^{1,2}

¹Department of Applied Chemistry, Graduate School of Engineering, Kyushu University,
Fukuoka 819-0395, Japan

²JST-CREST, 5 Sanbancho, Chiyoda-ku, Tokyo 102-0075, Japan

Carbon nanotubes (CNTs) have remarkable properties such as high electric conductivity, thermal conductivity and mechanical strength. The electric properties of CNTs, ranging from semiconducting to metallic, make them excellent candidate materials for novel nanoelectronic devices. However, the large difficulty in positioning of CNTs on Si substrate hinders the development of CNTs nanoelectronic circuit.

Dip-pen nanolithography (DPN, **Fig. 1**) is a versatile and powerful tool to transport materials to a substrate with high resolution as well as positional selectivity using an “ink”-coated atomic force microscope (AFM) tip [1].

In this study, we utilize this technique to position CNTs catalyst on desired position and size, where the metal salt was used as an ink for CNTs fabrication. **Fig. 2** shows AFM image of pattern of Co-acetate (II) $4\text{H}_2\text{O}$ generated by DPN (deposition time: 10 s, 23.2°C, 54 %RH). CNTs growth was carried out by alcohol catalytic chemical vapor deposition (ACCVD) method.

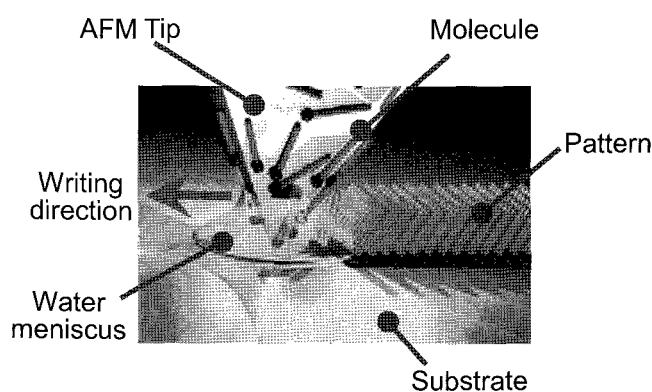


Fig. 1 Schematic image of DPN.

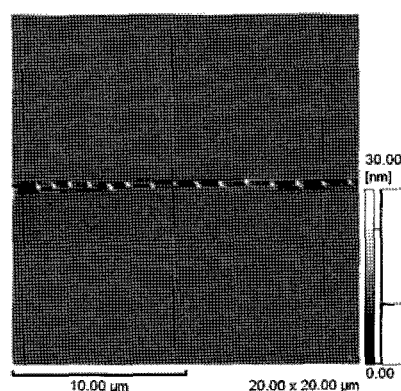


Fig. 2 AFM image of the Co (II) pattern generated by DPN.

[1] R. D. Piner, J. Zhu, F. Xu, S. Hong, C. A. Mirkin, *Science*, **283**, 661 (1999).

Corresponding Author: Tsuyohiko Fujigaya

TEL & FAX: +81-92-802-2842 E-mail: fujigaya-tcm@mail.cstm.kyushu-u.ac.jp

TiC formation for metal contact with carbon composite structures consisting of nanotubes and graphene multi-layers

○Daiyu Kondo¹, Shintaro Sato¹, Mizuhisa Nihei¹, Eiji Ikenaga², Masaaki Kobata²,
Jung Jin Kim², Keisuke Kobayashi² and Yuji Awano¹

¹*Nanotechnology Research Center, Fujitsu Laboratories Ltd., 10-1 Morinosato-Wakamiya, Atsugi 243-0197, Japan*

²*Japan Synchrotron Radiation Research Institute/SPring-8, 1-1-1 Kouto Sayo-cho Sayo-gun, Hyogo 679-5198, Japan*

We previously reported on a novel carbon structure composed of graphene multi-layers and aligned multi-walled carbon nanotubes (MWNTs) [1], which is clearly different from usual vertically-aligned MWNTs [2]. This unique structure has graphene multi-layers spontaneously formed on the top of aligned MWNTs. To apply the composite to electronic devices, it is important to realize good electrical and thermal contact between the composite and the metal electrodes. In this work, we have investigated the electronic structures of the interface between the composite and the metal electrodes by using hard x-ray photoemission spectroscopy (PES). The PES measurements were performed at the BL47XU in the SPring-8.

The composite was obtained by chemical vapor deposition (CVD). As the carbon source, a mixture of acetylene and argon gases was introduced into the CVD chamber. The substrate temperature was 510 °C. Details of the CVD process were shown elsewhere [1]. Figure 1 shows C 1s core level spectra of (a) the composite and (b) the composite with the metal electrodes (Ti films) by hard x-ray PES. The PES spectra indicate that the titanium carbide (TiC) was formed at the interface, although the Ti film was partly oxidized. On the other hand, the Ti film with the usual MWNTs was mostly oxidized (not shown). Taking into account the fact that TiC is known to form ohmic contact with nanotubes, the result indicates that the composite has better electrical contact with the metal electrodes. We believe that the better contact is mainly caused by the flatness of the top of the composite structure. The details will be discussed in the presentation. The authors thank Dr. N. Yokoyama, Fellow of Fujitsu Laboratories Ltd. for his support and useful suggestions.

[1] D. Kondo *et al.*, APEX 1 (2008) 074073.

[2] S. Sato *et al.*, Chem. Phys. Lett. 402 (2005) 149.

Corresponding Author: Daiyu Kondo

E-mail: kondo.daiyu@jp.fujitsu.com

Tel&Fax: +81-46-250-8234&+81-46-250-8844

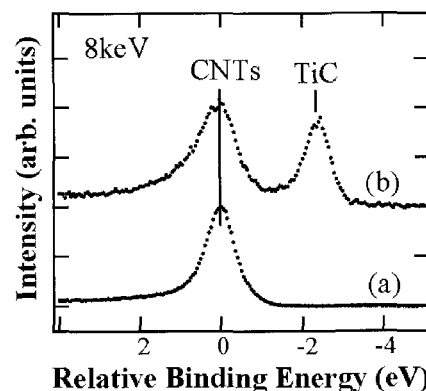


Figure 1 C 1s core level spectra of (a) the composite and (b) the composite with Ti films.

Theoretical Study on the Growth of Single Walled Carbon Nanotube (SWNT)

Jingshuang Dang, Weiwei Wang, Xiang Zhao*

*Institute for Chemical Physics and Department of Chemistry,
Xi'an Jiaotong University, Xi'an 710049, P. R. China*

The growth of armchair and zigzag SWNTs has been studied by PM3 quantum chemical method, with "H-closing" method in order to eliminate the boundary effect on one side of the structure. Taking (6, 6) SWNTs as a target model, the changing of the bond length between the C_2 group and the structure have been studied to simulate the departure process of C_2 group from the hexagon, which is the inverse process of C_2 addition process.

According to the potential energy data in each period of C_2 departure process, with the increase of the bond length between the C_2 group and the structure, a stable pentagon intermediate is formed in the reaction path. It shows that during the process of C_2 departure, the two C-C bonds don't break simultaneously but with one bond breaking at first and forming a pentagon intermediate. So the C_2 addition process of SWNTs should be recognized as follows: as C_2 group getting close to the molecule from infinity, first a relatively stable pentagon intermediate is formed, and then a stable hexagon. Supposing a layer of pentagons are formed, the spatial configuration of SWNTs will bend to finish the capping process of SWNTs.

The change of potential energy during the separation of a hexagon of growing (9, 0) SWNTs was also studied. Our results show that the formation of hexagon pair needs a pentagon-heptagon pair as an intermediate and a decagon as TS. So an assumption is put forward: as for a (n,0) SWNTs, if n is even, pentagons are formed by the addition of C_2 at first, and then heptagons are generated between two adjacent pentagons by C_2 addition. Pentagon-heptagon pairs rearrange and generate hexagon pairs. And if n is odd, pentagon-heptagon pairs are produced continuously at first, but as lack of dangling bonds, the last pentagon-heptagon pairs will add C_2 at the side of the first pentagon and generate a hexagon. Finally the last heptagon is formed by means of C_2 addition between the pentagon and hexagon. The detailed discussion will be presented, too.

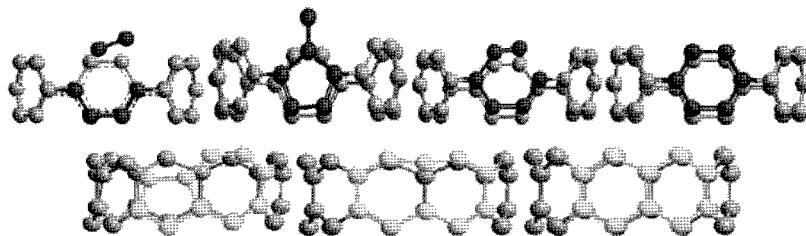


Fig.1 The process of C_2 addition of armchair (upper) and zigzag (nether) SWNTs

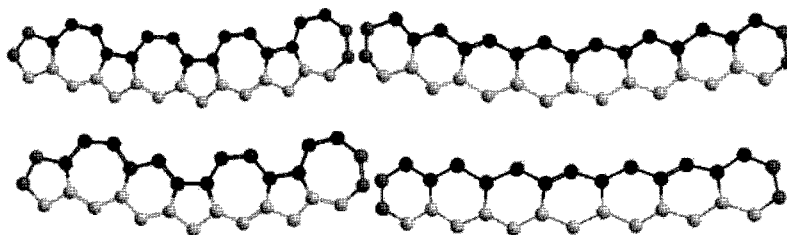


Fig.2 The C_2 addition and rearrangement of (n,0) SWNTs when n is even (upper) or odd (nether)

Corresponding author: X. Zhao,

Email: xzhao@mail.xjtu.edu.cn; Fax: +86-29-82668559

Analysis of Fe Catalyst Behavior on Al/SiO₂/Si Substrate for CNT Growth Using Mössbauer Spectroscopy

Hisayoshi Oshima¹, Tomohiro Shimazu¹, Milan Siry¹ and Ko Mibu²

¹Research Laboratories, DENSO CORPORATION

500-1 Minamiyama, Komenoki, Nisshin-shi, Aichi 470-0111, Japan

²Graduate School of Engineering, Nagoya Institute of Technology

Showa-ku, Nagoya 466-8555, Japan

Use of aluminum or alumina for a catalyst embedding layer and addition of water vapor in chemical vapor deposition (CVD) ambient are an excellent method to obtain long vertical aligned carbon nanotube (CNT) films.[1] However, there are few reports describing interactions between aluminum and catalysts.[2] One of the reasons is a difficulty to detect catalyst signals using standard analytical instruments such as XPS, because catalysts are covered with CNT and/or carbon.

In this study, we employed conversion electron Mössbauer spectroscopy [3] for an analysis of Fe chemical states from deposition of Fe to the end of CNT growth. The detection depth of Mössbauer spectroscopy is about 10 times deeper than XPS.

Samples for the investigation were prepared as follows. Al and ⁵⁷Fe were deposited on a thermally oxidized Si substrate by an evaporator. Film thickness of Al and ⁵⁷Fe were 15 nm and 5 nm, respectively. CNTs were grown at 1113 K under C₂H₄ gas flow with an addition of H₂ and water vapor. Heat treatment of a substrate was also performed using the growth tube at 1113 K under atmospheric pressure of flowing Ar gas for 5 min.

As-deposited ⁵⁷Fe was identified as α -Fe (Fig.1a). After annealing, α -Fe peaks became very weak and non-magnetic phase appeared (Fig.1b). However, α -Fe peaks came back with Fe₃C peaks after CNT growth (Fig.1c-d). This strange behavior of Fe could be explained by considering the results of SEM observation (not shown). Fe once reacts with Al to form non-magnetic Fe-Al alloy at the heating up stage, and then Fe segregates on the surface and at the Al₂O₃/SiO₂ interface during a formation of Al₂O₃ by the oxidation of Al and Fe-Al alloy in hydrogen and water vapor mixture gases. Fe on the surface would act as CNT growth catalysts and that at the interface would stayed passively as α -Fe.

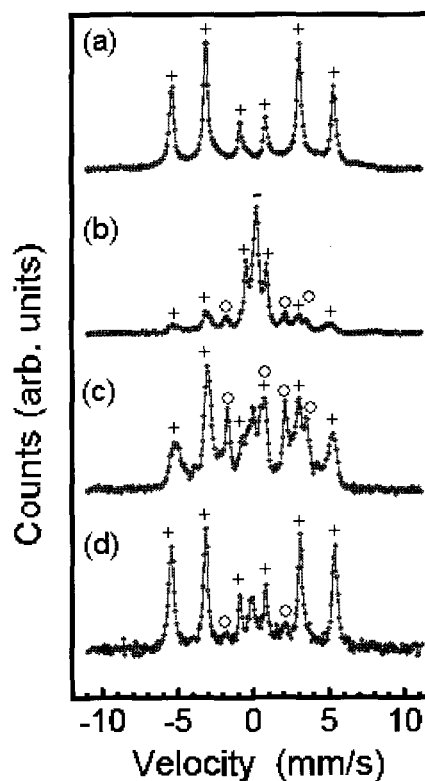


Fig.1 Mössbauer spectra of ⁵⁷Fe, (a); as-deposited on an Al/SiO₂/Si substrate, (b); heat treated at CVD temperature in Ar, (c); CNT growth for 3 min, (d); CNT growth for 60 min. (+); α -Fe, (o);Fe₃C, (-);Fe-Al alloy.

References: [1] K. Hata et al., *Science* **306**, 1362 (2004). [2] A. Okita et al., *Jpn. J. Appl. Phys.* **45**, 8323 (2006). [3] P. Coquay et al., *J. Appl. Phys.* **92**, 1286 (2002)

Corresponding Author: Hisayoshi Oshima

E-mail: hoosima@rlab.denso.co.jp Tel.: +81-561-75-1860 Fax.: +81-561-75-1193

Diameter control of single-walled carbon nanotubes grown by diffusion plasma CVD

○S. Kuroda, T. Kato, T. Kaneko, and R. Hatakeyama

Department of Electronic Engineering, Tohoku University, Sendai 980-8579, Japan

Single-walled carbon nanotubes (SWNTs) are nano carbon materials each consisting of a single graphene sheet. Since they have great and unique electrical properties, a carbon nanotube field effect transistor (CNT-FET) is expected to be a critical component of next-generation nano electronic devices. In order to realize the practical use of the CNT-FET, however, it is an inevitable issue to precisely control SWNT structures including tube diameter, length, chirality, alignment, and so on. Based on this back ground, we investigate effects of several parameters such as radio frequency (RF; 13.56 MHz) power and gas pressure on the chirality and diameter distribution of SWNTs with diffusion plasma CVD [1]. The mixture of methane and hydrogen gas is used as a carbon source. The pressure range and the RF power are varied from 20 Pa to 800 Pa and from 40 W to 300 W, respectively. The SWNTs production is carried out on a Fe 0.3 nm /Al₂O₃ 20 nm /Ag substrate that is heated and set underneath a lower discharge-electrode called an anode. The chirality distribution of as-grown SWNTs is analyzed with photoluminescence (PL) spectroscopy [2]. Figure 1 illustrates the photoluminescence-excitation (PLE) map of SWNTs produced by the diffusion plasma CVD method as a function of RF power. The results show that the small diameter SWNTs tend to increase with an increase in the RF power. This fact indicates that it might be possible to control the chirality or diameter distribution of SWNTs by precisely adjusting the plasma parameters.

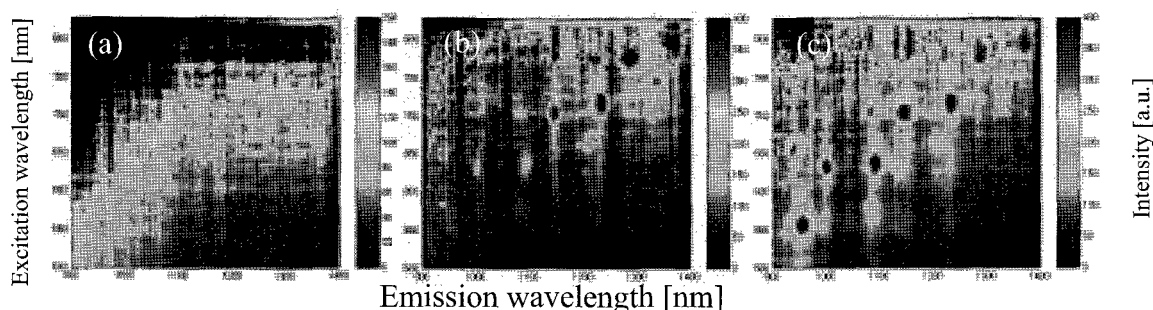


Fig. 1: PLE map of as-grown SWNTs. (a) 80 W, (b) 200 W, (c) 300 W.

[1] T. Kato and R. Hatakeyama, *Appl. Phys. Lett.* **92**, 031502 (2008).

[2] T. Kato and R. Hatakeyama, *J. Am. Chem. Soc.* **130**, 8101 (2008).

Corresponding Author: Shunsuke. Kuroda

TEL: +81-22-795-7046, FAX: +81-22-263-9225, E-mail: kuroda@plasma.ecei.tohoku.ac.jp

Comparison of thermal and plasma CVD for the growth of single-walled carbon nanotubes from nonmagnetic nanoparticles

○Z. Ghorannevis, T. Kato, T. Kaneko, and R. Hatakeyama

Department of Electrical Engineering, Tohoku University, Sendai 980-8579, Japan

The unique properties of single-walled carbon nanotubes (SWNTs) have motivated intense researches in the fabrication of electronic components, field emission sources, and hydrogen storage devices. Certain carbon nanotube (CNT) applications require specific dimensions and different levels of homogeneity (e.g. diameter, length, reactivity, crystallinity, purity, and chirality). Since the composition and morphology of catalyst nanoparticles are critical in determining the structure, length, and yield of nanotubes, different methods and catalysts include the superior possibility for the detailed structure control of CNTs. Up to now, the majority of works reporting CNTs synthesis focused only on iron family catalysts such as Fe, Co, and Ni. Recently it has been reported that nonmagnetic catalysts also play a significant role in the growth of SWNTs with thermal chemical vapor deposition (TCVD) [1]. This indicates that further detailed adjustments of SWNT structures might be possible with the combination of various growth methods and such novel catalysts.

We have demonstrated the growth of CNTs from nonmagnetic catalysts such as Au, Ag, and Pt with different two chemical vapor deposition (CVD) methods. In the case of TCVD, high quality SWNTs can be grown from various kinds of nonmagnetic catalysts. On the other hand, plasma chemical vapor deposition (PCVD) [2-4] can realize only poorly crystallized multi-walled CNT growth. Through the systematic investigation of hydrogen effects on the growth of CNTs with TCVD, it is found that the catalytic activity of nonmagnetic catalyst is fairly sensitive to hydrogen atoms and molecules. Slight addition of hydrogen gas causes a significant decrease in the amount of SWNTs. On the other hand, the hydrogen plays a positive role in the growth of SWNTs with the magnetic catalysts. In general, the surface cleaning by etching out hydrocarbons is known as a major role of hydrogen in the growth of CNTs. The adsorption ability of hydrocarbons in nonmagnetic particles is also known to be fairly low compared with that of magnetic catalyst. These two facts can explain the difference of hydrogen effect between the magnetic and nonmagnetic catalysts, i.e. positive and negative etching effects, for the growth of SWNTs, respectively.

[1] D. Takagi, Y. Homma, H. Hibino, S. Suzuki, and Y. Kobayashi, *Nano Lett.*, **6**, 2642 (2006).

[2] T. Kato, G-H. Jeong, T. Hirata, R. Hatakeyama, K. Tohji, and K. Motomiya, *Chem. Phys. Lett.*, **381**, 422 (2003).

[3] T. Kato, R. Hatakeyama, and K. Tohji, *Nanotechnol.*, **17**, 2223 (2006).

[4] T. Kato and R. Hatakeyama, *Appl. Phys. Lett.*, **92**, 031502 (2008).

Corresponding Author: Zohreh Ghorannevis

TEL: +81-22-795-7046, FAX: +81-22-263-9225, E-mail: Zohreh@plasma.ecei.tohoku.ac.jp

Effect of Al Oxide Buffer Layer on SWNT Growth at Low Temperature in Alcohol Gas Source Method in High Vacuum

○Yoshihiro Mizutani, Kuninori Sato,
*Takahiro Maruyama and Shigeya Naritsuka

*Department of Materials Science and Engineering, Meijo University,
1-501 Shiogamaguchi, Tempaku, Nagoya 468-8502, Japan*

Carbon nanotubes (CNTs) have been anticipated for application in a lot of future nanodevices. However, to fabricate devices compatible with conventional LSI, the current growth temperature is too high. Recently, we reported SWNT growth by alcohol gas source method in an ultra-high vacuum (UHV) chamber [1]. This growth technique enables SWNT growth at low temperature. However, the yield of grown SWNTs is not sufficient. In this study, we attempted to increase the yield of SWNTs in low temperature growth using Al oxide buffer layer and investigated the mechanism.

SiO₂/Si and Al₂O_x/SiO₂/Si were used as substrates. Al₂O_x buffer layers were formed by Al deposition (thickness: 30 nm) using a pulsed arc plasma gun in a UHV chamber, followed by exposure to the air. Co (thickness: 0.1 nm) was deposited by an e-beam evaporator on both substrates, on which SWNTs were grown. The growth temperature was 400°C, and ethanol gas pressure was 1.0×10⁻⁴ Pa. The samples were characterized by scanning electron microscopy (SEM) and Raman spectroscopy.

Fig. 1 shows Raman spectra measured using Kr laser (568.2 nm) for the grown SWNTs. Compared to the sample without the buffer layer, G band intensity increased for the sample grown with the buffer layer. In the RBM region, each peak intensity increased by inserting the buffer layer. Raman results measured by various excitation energies showed that the intensities of peaks in the lower wavenumber region were especially enhanced by the buffer layer, which suggests that the catalyst nanoparticles of larger size were activated.

This work was supported by the MEXT through the Nanotechnology Network Project and Grant-in-Aid for Scientific Research(C) #17560015. A part of the Raman measurements was performed in collaboration with the Institute of Molecular Science.

References

- [1] K. Tanioku et al., *Diam. Relat. Mater.*
Diamond Relat. Mater. 17 (2008) 589.

Corresponding Author: Takahiro Maruyama

E-mail: takamaru@ccmfs.meijo-u.ac.jp

Tel: +81-52-838-2386, **Fax:** +81-52-832-1172

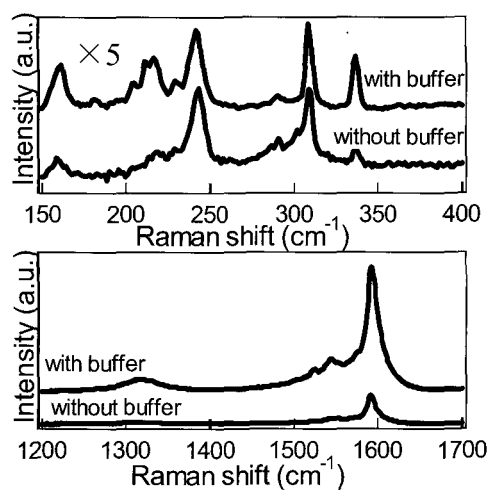


Fig1

Synthesis of DWNTs using arc discharge by adjusting gas pressure

○K. Kato¹, H. Wang¹, X. Zhao², S. Inoue¹ and Y. Ando¹

¹*Department of Materials Science & Engineering, Meijo University, Japan*

²*Department of Physics, Shanghai University, China*

Double-walled carbon nanotubes (DWNTs) has the simplest structure of MWNTs, which consists of two layers of an inner layer and outer layer. It is well known that, when DWNT is synthesized by arc discharge, sulfur is used as a promoter [1]. Sulfur has the effect of expanding the diameter of CNTs. In this study, we controlled a diameter of CNTs only by adjusting a gas pressure without using sulfur, and synthesized DWNT.

In this study, we use only iron as a catalyst and added 1at % in the anode. As the cathode a pure carbon rod was used. The Ar-H₂ mixture gas was used as the atmospheric gas, and the mixing ratio was 6:4[2]. The arc discharge was done under the gas pressure of 200 Torr, 350 Torr, and 500 Torr. After the production of DWNTs, as-grown DWNTs was purified by the following procedures: (i) air oxidation at 500°C for 1 hour, (ii) HCl treatment for 1day, (iii) vacuum heating under 10⁻⁵ Torr at 1500°C for 2 hours. The characterization was performed by high resolution transmission electron microscopy (HRTEM) [in Fig.1], field emission [in Fig.2], Raman spectroscopy and thermo gravimetric analysis (TGA).

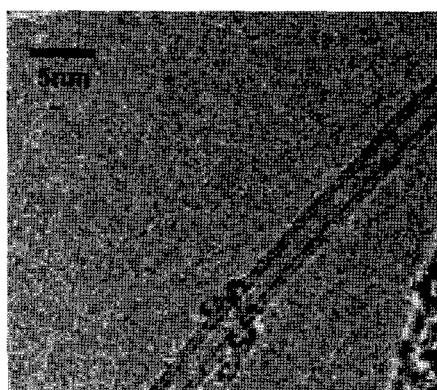


Fig. 1 HRTEM image of DWNTs
Produced in 500 Torr

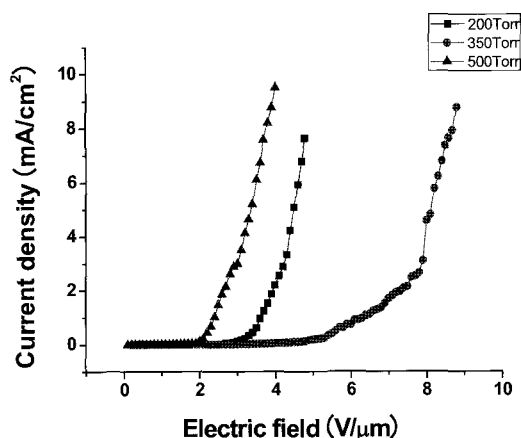


Fig. 2 Field emission properties of
DWNTs for different pressure

[1] Y. Saito et al., *J. phys. Chem. B.*, **107** (2003) 931.

[2] X. Zhao et al., *Chem. Phys. Lett.*, **373** (2003) 266.

Corresponding Author: Katsuhiko Kato

E-mail: m0734008@ccmailg.meijo-u.ac.jp

Tel: +81-(0)52-838-2409 **Fax:** +81-(0)52-832-1170

Purification of Single-walled Carbon Nanotubes Generated with Arc-burning Apparatus by Utilizing Mono-dispersion Technique

○Shinzo Suzuki¹, Kazuto Hara¹, Takuya Fujita¹, Takashi Mizusawa¹,
Toshiya Okazaki², and Yohji Achiba³

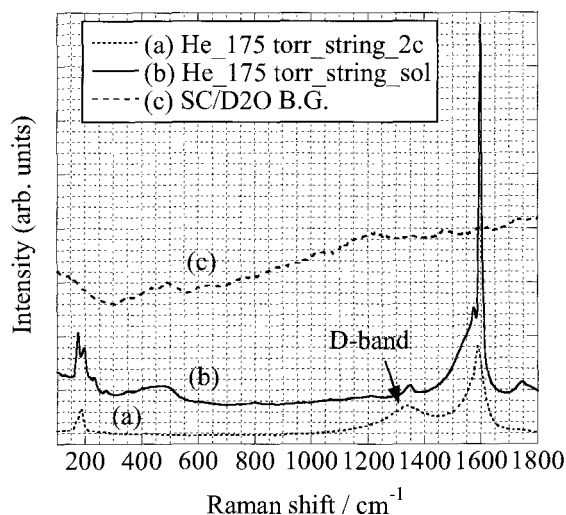
¹*Department of Physics, Kyoto Sangyo University, Kyoto 603-8555, Japan*

²*Nanotube Research Center., AIST, Tsukuba 305-8565, Japan*

³*Department of Chemistry, Tokyo Metropolitan University, Tokyo 192-0397, Japan*

Single-walled carbon nanotubes (SWNTs) generated by using arc-burning apparatus in nitrogen and helium atmosphere, were mono-dispersed in sodium cholate (SC) solution, respectively. Although raw soot generated with arc-burning in helium atmosphere includes larger amount of carbon impurities than that generated in nitrogen atmosphere, it was found that SWNTs made in helium atmosphere were as well mono-dispersed in SC solution as those SWNTs made in nitrogen atmosphere.

Figure 1 shows typical Raman spectra of SWNTs made in helium atmosphere as (a) raw solid material, and (b) mono-dispersed material in SC / D₂O solution (1 wt%). As a reference, (c) Raman background signal of SC / D₂O solution without SWNTs is also included in the figure. Figure 1 indicates that, despite that the Raman spectrum of raw solid material (a) clearly shows D-band structure (indicated by an arrow) corresponding to carbon impurities, this band can hardly be seen in the spectrum of mono-dispersed solution (b).



The possibility of enrichment of pure SWNTs in the soot including lesser amount of SWNTs and larger amount of carbon impurities, by applying mono-dispersion in the surfactant solution and density-gradient ultra-centrifugation is also discussed.

[1] S. Suzuki, T. Mizusawa, T. Okazaki, and Y. Achiba, *Eur. Phys. J. D*, in press.

[2] Y. Makita, S. Suzuki, H. Kataura, and Y. Achiba, *Eur. Phys. J. D*, **34**, 287(2005).

Corresponding Author: Shinzo Suzuki

TEL: +81-75-705-1631, FAX: +81-75-705-1640, E-mail: suzukish@cc.kyoto-su.ac.jp

Measurement of Cohesion Process of Carbon-Clusters by the Mie-Scattering Method in Gravity-free Arc-Synthesis of Nanotubes

○Tetsu Mieno¹, Tan Guodong¹, Shu Usuba², Kazunori Koga³, Masaharu Shiratani³

¹Department of Physics, Shizuoka University, Ooya, Suruga-ku, Shizuoka 422-8529, Japan

²AIST, Higashi, Tsukuba, 305-8561, Japan

³Graduate School of Info. Sci. & Electric Eng., Kyusyu University, Fukuoka, 819-0395, Japan

Single walled carbon nanotubes (SWNTs) are produced by the arc-sublimation method, where strong heat convection of He gas flows up the sublimated carbon atoms, and the cooling time and the reaction time are limited. Under the gravity-free and convection-free condition, carbon atoms slowly diffuse and the cooling time is much longer, which would make defect-free and longer SWNTs. [1] Previously, we have successfully produced SWNTs under zero-gravity and the effect was clear. [1] Now, we want to make clear the production process and cohesion process of carbon clusters. Therefore, we utilized the Mie-scattering method.

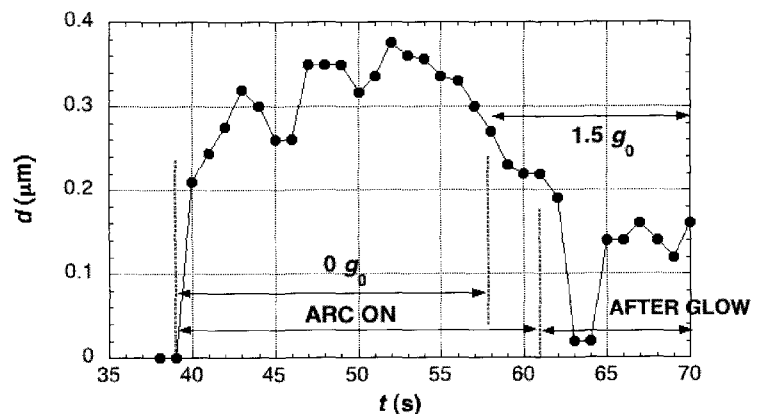
A metal reactor, 6.5 inch diam., 270 mm high (volume of 1.8 L) is used. A pulse-modulated green laser ($\lambda = 532$ nm) is penetrated from the bottom side to the top side through the center of the arc plasma. Along the laser axis (z axis), scattered lights with scattered angles of 15 deg. and 90 deg. are detected and averaged by using lock-in amplifiers. Figure 1 shows time variation of the estimated cluster size from the scattered signal-ratio, where $p(\text{He}) = 25$ kPa, discharge current of 40 A and $z = 2$ cm from the arc center. [2] Under zero-gravity, the diameter of carbon clusters increases to about 0.5 micro-m, and it decreases under 1.5 G . Under the ground gravity, the heat-convection strongly influences the cluster growth. These results support the theoretical prediction. We are planning to make more precise Mie-scattering method to obtain good-quality carbon-clusters.

[1] T. Mieno & M. Takeguchi, J. Appl. Phys. **99** (2006)104301.

[2] C. F. Bohren & D. R. Huffman, "Absorption and Scattering of Light by Small Particle", John Wiley Sons, 1983.

Corresponding Author: Tetsu Mieno, TEL & FAX: +81-54-238-4750, E-mail: sptmien@ipc.shizuoka.ac.jp

Fig. 1 Time variation of the cluster size under gravity-free condition.



Open and Closed Edges of Graphene Layers

*Zheng Liu¹, Kazu Suenaga¹, Peter J. F. Harris², Sumio Iijima¹

¹*Nanotube Research Center, National Institute of Advanced Industrial Science and Technology (AIST), Tsukuba 305-8565 Japan*

²*Centre for Advanced Microscopy, J.J. Thomson Physical Laboratory, University of Reading, Whiteknights, Reading RG6 6AF, UK*

Graphene, a single layer sheet of graphite, is the basic structural element of all other graphitic materials such as graphite, carbon nanotubes and fullerenes. The potential applications in condensed matter physics and electronics have boosted interest in graphene especially in the structure and properties of its edges [1]. Recent studies indeed clarified the unconventional electronic features of graphene not only the monolayer but also the bilayer graphene sheet [2-12]. Folding of monolayer and bilayer graphene, i.e. closed edges, were also studied by using the transmission electron microscope (TEM) [7,13,14], however, no confirming evidence for the presence of open edges has been so far provided. Neither has the actual edge structure of graphene ever been atomically revealed.

In this study, we report direct imaging of the edges of thermally treated graphite and show the evidence for a coexistence of closed and open edges in graphene. A high-resolution transmission electron microscope (HR-TEM) was operated at 120kV with a point resolution better than 0.106 nm. The method for determination of monolayer or more than one layer graphene sheets is established. Bilayer graphene with AA stacking has been carefully distinguished from a monolayer graphene by means of a series of tilting experiments. Open edge structures with carbon dangling bonds can be found only in a local area where the closed (folding) edge is partially broken [15].

References

- [1]. T. Enoki, Y. Kobayashi, and K. Fukui, *International Reviews in Physical Chemistry*, **26**, 609 (2007).
- [2]. K. S. Novoselov, A. K. Geim, S. V. Morozov, D. Jiang, Y. Zhang, S. V. Dubonos, I. V. Grigorieva, and A. A. Firsov, *Science* **306**, 666 (2004).
- [3]. K. S. Novoselov, A. K. Geim, S. V. Morozov, D. Jiang, M. I. Katsnelson, I. V. Grigorieva, S. V. Dubonos, and A. A. Firsov, *Nature* **438**, 197 (2005).
- [4]. C. L. Kane and E. J. Mele, *Phys. Rev. Lett.* **95**, 226801 (2005).
- [5]. T. Ohta, A. Bostwisch, T. Seyller, K. Horn, and E. Rotenberg, *Science* **313**, 951 (2006).
- [6]. K. S. Novoselov, Z. Jiang, Y. Zhang, S. V. Morozov, H. L. Stormer, U. Zeitler, J. C. Maan, G. S. Boebinger, P. Kim, and A. K. Geim, *Science* **315**, 1379 (2007).
- [7]. J. C. Meyer, A. K. Geim, M. I. Katsnelson, K. S. Novoselov, T. J. Booth, and S. Roth, *Nature* **446**, 60 (2007).
- [8]. E. V. Castro, K. S. Novoselov, S. V. Morozov, N. M. R. Peres, J. M. B. Lopes dos Santos, and J. Nilsson, *Phys. Rev. Lett.* **99**, 216802 (2007).
- [9]. R. Dillenschneider, and J. H. Han, *Phys. Rev. B* **78**, 045401 (2008).
- [10]. B. Sahu, H. Min, A. H. MacDonald, and S. K. Banerjee, *Phys. Rev. B* **78**, 045404 (2008).
- [11]. E. V. Castro, N. M. R. Peres, J. M. B. Lopes dos Santos, A. H. Castro Neto, and F. Guinea, *Phys. Rev. Lett.* **100**, 026802 (2008).
- [12]. Y. Barlas, R. Côté, K. Nomura, and A. H. MacDonald, *Phys. Rev. Lett.* **101**, 097601 (2008).
- [13]. Y. Kobayashi, K. Fukui, T. Enoki, K. Kusakabe, and Y. Kaburagi, *Phys. Rev. B* **71**, 193406 (2005).
- [14]. Y. Kobayashi, K. Fukui, T. Enoki, and K. Kusakabe, *Phys. Rev. B* **73**, 125415 (2006).
- [15]. Z. Liu, K. Suenaga, P. J. F. Harris, S. Iijima, *Phys. Rev. Lett.* **102**, 015501 (2009).

Corresponding Author: Zheng Liu

E-mail: liu-z@aist.go.jp

Tel: 029-861-2514

Fax: 029-861-4806

New Carbon Thin Film Growth on YSZ (111) by Very High Temperature Surface Pyrolysis of C₆₀

○Takuya Noguchi, Toshihiro Shimada, Akinori Hanzawa, Tetsuya Hasegawa

Department of Chemistry, The University of Tokyo, Tokyo 113-0033, Japan

Graphene has been attracting much interest after the discovery of micromechanical cleavage technique [1]. Since large area preparation is required for the application of the graphene, epitaxial growth on SiC single crystals by thermal desorption of Si is actively studied [2]. We have proposed the pyrolysis of molecular carbon sources on surfaces of refractory oxides for the preparation of graphene-related materials [3]. In this presentation we report new carbon thin films grown on yttria-stabilized zirconia (YSZ; Y_{0.07}Zr_{0.93}O₂) by pyrolysis of fullerene (C₆₀). In the experiment, C₆₀ was irradiated like molecular beam deposition onto YSZ (111) heated at 2170 K in vacuum chamber (~ 10⁻⁴ Pa). The films were characterized by AFM, X-ray diffraction (XRD) and Raman spectroscopy.

AFM images of the films deposited on the surface of YSZ (111) substrate are shown in Fig.1, in which hexagonal grains with the size of 500 nm were observed homogeneously on the surface. Raman spectra of the film showed that two peaks in G band (weak) and D band (broad), but no peaks characteristic to C₆₀ (1470 cm⁻¹ etc.) were observed. This result indicates that C₆₀ molecules were cracked on the surface of the substrate and an "amorphous" carbon film was formed. XRD and X-ray photoelectron spectroscopy analysis showed epitaxial growth of zirconium carbide underneath the carbon film. We will discuss the mechanism of the zirconium carbide formation and the origin of the hexagonal grain shape in the "amorphous" carbon film shown in Fig. 1.

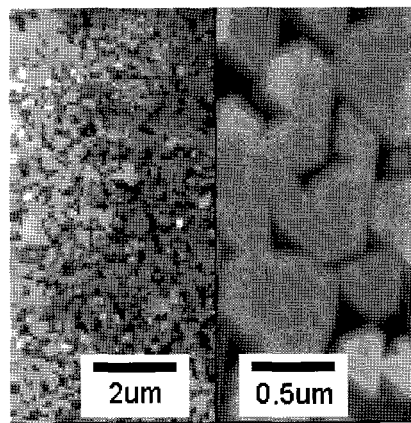


Fig. 1 AFM images of the carbon films on YSZ (111) surface.

- [1] K. S. Novoselov, A. K. Geim, S. V. Morozov, D. Jiang, Y. Zhang, S. V. Dubonos, I. V. Grigorieva, A. A. Firsov; *Science*, **306**, 666 (2004).
 [2] C. Berger, Z. Song, T. Li, X. Li, A. Y. Ogbazghi, R. Feng, Z. Dai, A. N. Marchenkov, E. H. Conrad, P. N. First, W. A. de Heer; *J. Phys. Chem. B* **108**, 19912 (2004).
 [3] T. Noguchi, T. Shimada, A. Hanzawa, T. Hasegawa: *submitted*.

Corresponding Author: Toshihiro Shimada

TEL/FAX: +81-3-5841-7595, E-mail: shimada@chem.s.u-tokyo.ac.jp

Temperature dependence of Raman spectra in epitaxial few-layer graphene on vicinal 6H-SiC

^oRyoji Naito¹, Susumu Kamoi¹, Hitoshi Kakehi¹, Noriyuki Hasuike¹, Kenji Kisoda², Hiroshi Harima¹, Kouhei Morita³, Satoru Tanaka³ and Akihiro Hashimoto⁴

¹Department of Electronics, Kyoto Institute of Technology, Kyoto 606-8585, Japan

²Physics Department, Wakayama University, Wakayama 640-8510, Japan

³Department of Quantum Applied Physics and Nuclear Engineering, Kyushu University, Fukuoka 819-0395, Japan

⁴Department of Electrical and Electronics Engineering, Fukui University, Fukui 910-8507, Japan

Graphene attracts much attention because it has remarkable electronic properties over existing materials such as silicon. Epitaxial growth of graphene on a silicon carbide substrate is an alternative way to obtain it instead of micro mechanical cleavage of highly oriented pyrolytic graphite (HOPG). However, the samples of the former method have to take into account the influence of the interaction from the substrate. Therefore, to elucidate the interaction, we have carried out Raman scattering experiments on few-layer graphene (FLG) grown on vicinal 6H-SiC substrates.

Epitaxial FLG was synthesized on vicinal 6H-SiC (0001) by surface decomposition. The substrate was inclined to [11-20] direction by 4 degree. The substrate was annealed at 1400 °C for 30 minutes under ultra-high vacuum. Raman scattering measurements were carried out under microscope from room temperature to 600 °C. The excitation wavelength was 532 nm.

Figure 1 shows Raman spectra from (a) FLG and the substrate, (b) the substrate, (c) their difference [(a)-(b)], and (d) HOPG. The G band of FLG clearly appears after taking difference between (a) and (b). The peak frequency is up-shifted about 15 cm⁻¹ from that of HOPG. Recalling that the peak frequency of FLG on SiO₂ is almost the same as that of HOPG [1], the up-shift of the present G band may suggest that the FLG suffers compressive strain from the SiC substrate. To demonstrate this, we compared temperature dependence of the G peak frequency between FLG and HOPG as shown in Fig.2. The solid lines are least-square fit to the measured points. The temperature gradient of FLG is larger than that of HOPG. In addition, linear thermal expansion coefficients between FLG and 6H-SiC are different. The FLG sample is exerted to compressive strain from the substrate in the cooling process from the growth temperature to room temperature.

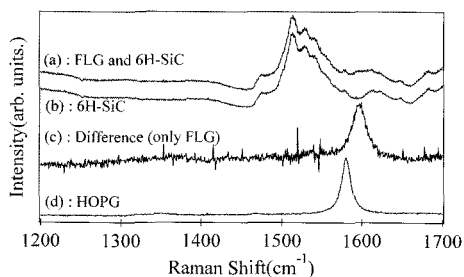


Fig.1 Raman spectra excited 532nm.
(a) : as-synthesized FLG, (b) : 6H-SiC,
(c) : difference of (a) and (b), (d) : HOPG

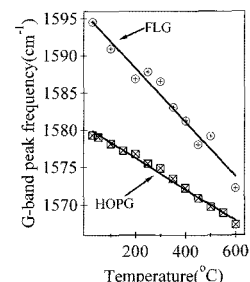


Fig.2 Temperature dependence of G-band peak frequencies.

[1] D. Graf *et al.*, Nano Lett. 7, 238 (2007)

Corresponding Author: R. Naito, TEL: +81-75-724-7421, E-mail: m7621018@edu.kit.ac.jp

Probing graphene-metal contacts in bilayer graphene nanoconstrictionY. Ujiie,¹ S. Motooka,¹ T. Morimoto,² D. K. Ferry,³ J. P. Bird,⁴ and Y. Ochiai¹¹Graduate School of Advanced Integration Science, Chiba University, 1-33 Yayoi, Inage, Chiba 263-8522, Japan.²Advanced Device Laboratory, RIKEN, 2-1 Hirosawa, Wako, Saitama 351-0918, Japan.³Department of Electrical Engineering and Center for Solid State Electronics Research, Arizona State University, Tempe, Arizona 85287-5706, USA.⁴Department of Electrical Engineering, University at Buffalo, The State University of New York, Buffalo, New York 14260-1920, USA.

Electrical transport in graphene is a rapidly expanding field of research, being strongly influenced by the linear energy spectrum and the chirality of the charge carriers. This material may have interesting applications as the base material for future carbon-based molecular electronics, however, a critical issue concerns the graphene-metal contact due to the generally complex interaction between organic materials and metals.

In this study, we report on the electrical transport in a metal-graphene-metal nanoconstriction device, from which we suggest that carrier injection at the graphene-metal interface is probably *not homogeneous*. At temperatures below a degree Kelvin, the conductance fluctuations in our device exhibit a quasi-periodic dependence across a wide range of magnetic field. The periodic nature is confirmed from the Fourier power spectrum of the fluctuations which consists of well-pronounced peaks at a few dominant frequencies. These results are in fact highly reminiscent of those reported previously in ballistic semiconductor quantum dots (QDs) which features quantum point contact (QPC) leads that are used to source and sink carriers to the QDs. We therefore suggest that the actual graphene-metal contact is inhomogeneous, also indicate the need to achieve a better understanding of the interfacial mechanisms that govern the injection of carriers from metal electrodes into graphene.

This work was supported by Grants-in-Aid for Scientific Research of the Japan Society for the Promotion of Science (JSPS) No. 19204030.

Reference:

Y. Ujiie, N. Yumoto, T. Morimoto, N. Aoki, and Y. Ochiai, “*Fractal behavior in graphene open quantum dot*”. J. Phys: Conf. Series, **109** 102035-1-4 (2008).

Edge States of ZigZag Boron Nitride Nanoribbons

○Fawei Zheng^{a,b}, Ken-ichi Sasaki^c, Riichiro Saito^{a1}, Wenhui Duan^b, and Bing-Lin Gu^b

^a*Department of Physics, Tohoku University, Japan*

^b*CASTU and Department of Physics, Tsinghua University, China*

^c*Department of Quantum Matter, Hiroshima University, Japan*

Single layer h-BN has been successfully fabricated on the surfaces of metals [1, 2]. From which, the BNNRs are expected to be produced. As graphene nanoribbons [3-6], the electronic and magnetic properties of BNNRs are very interesting to investigate theoretically [7-9].

We have studied the properties and their origins of BNNRs by using the tight-binding (TB) models [10]. In the present work, the TB parameters are obtained so as to reproduce the density functional calculation results. The analytical expressions of boron (nitrogen) edge states which appears near the zigzag edge of BNNRs are given. The edge states at B edge and N edge appears near the conduction energy bands bottom and the valence energy band top, respectively. The second nearest neighbor interaction and modification of the potential near the edge are found to be important to explain the dispersion of the edge states, which is similar to zigzag edge state of graphene nanoribbons [5, 6]. In this work, we also discuss the half metallicity for ZBNNR by considering the Hubbard type Coulomb interaction. Thus a possible spin-polarized current is expected especially for unterminated N edge with dangling bonds.

References

- [1] A. Nagashima, N. Tejima, Y. Gamou, T. Kawai, and C. Oshima, Phys. Rev. Lett. **75**, 3918 (1995).
- [2] M. Corso, T. Greber, and J. Osterwalder, Surf. Sci. **577**, L78 (2005).
- [3] K. Nakada, M. Fujita, G. Dresselhaus and M. S. Dresselhaus, Phys. Rev. B **54**, 17954 (1996).
- [4] Y.-W. Son, M. L. Cohen and S. G. Louie, Nature **446**, 342 (2007).
- [5] K. Sasaki, S. Murakami, R. Saito, and Y. Kawazoe, Phys. Rev. B **71**, 195401(2005).
- [6] K. Sasaki, S. Murakami and R. Saito, Appl. Phys. Lett. **59**, 113110 (2006).
- [7] J. Nakamura, T. Nitta, and A. Natori, Phys. Rev. B **72**, 205429 (2005).
- [8] F. Zheng, G. Zhou, Z. Liu, J. Wu, W. Duan, B.-L. Gu, and S. B. Zhang, Phys. Rev. B **78**, 205415 (2008).
- [9] F. Zheng, Z. Liu, J. Wu, W. Duan, and B.-L. Gu, Phys. Rev. B **78**, 085423 (2008).
- [10] F. Zheng, K. Sasaki, R. Saito, W. Duan, and B.-L. Gu, unpublished (2009)

¹Corresponding Author: Riichiro Saito, Tel: +81-22-795-7754, Fax: +81-22-795-6447,
Email: rsaito@flex.phys.tohoku.ac.jp.

Edge phonon of nano-graphite ribbons

○Masaru Furukawa¹, Zheng Fawei², Riichiri Saito¹

¹*Department of Physics, Tohoku University, Sendai 980-8587, Japan*

²*CASTU and Department of Physics, Tsinghua University, Chiana*

Nano-graphite ribbons have recently attracted intensive interest because of their potential applications in nano-size devices. In this study, we calculated phonon dispersions of nano-graphite ribbons by using the force constants models up to the 4th nearest neighbor interactions.[1] Especially we investigated the edge phonon states where amplitude are localized around zigzag and armchair edges. In the previous works they shows possible edge phonon mode for out-of-plane optic phonon(ω_{TO})[2][3] The edges are considered with and without termination of hydrogen atoms. By calculating amplitude of each vibration for Γ point phonon, we can recognize which vibration mode is edge localized phonon mode. We found edge localized mode of zigzag-ribbon around 1450cm^{-1} and that of armchair edges around 1530cm^{-1} . We will show the result comparing with numerical results by first principle calculation [4] and recent Raman measurement of single layer graphene [5]. We will also report at the corresponding Raman spectra which are relevant to the edge phonon of graphene.

Reference

- [1] R.Saito, T.Takeya and T.Kimura, Physical Review B **57** (1998), 4145.
- [2] Jian Zhou, Jinming Dong, Applied Physics Letters **91** (2007), 173108.
- [3] Masatsura Igami, Mitsutaka Fujita, Seiji Mizuno, Applied Surface Science **130-132** (1998), 870-875.
- [4] R.Saito, T.Takeya, T Kimura, G.Dresselhaus, M.S.Dresselhaus, Phys.Rev.B, **59** (1998), 2388.
- [5] W.Ren et al., unpublished.

Corresponding Author: Masaru Furukawa

TEL: 022-795-7754, FAX: +022-795-6447, E-mail: furukawa@flex.phys.tohoku.ac.jp

Ultra-fast structural change of graphite surface by pulse laser irradiation: A time-dependent first-principles approach

○Yoshiyuki Miyamoto

Nano Electronics Res. Labs, NEC, 34 Miyukigaoka, Tsukuba 305-8501, Japan

Structural deformation induced by pulse laser shot is a key phenomenon for fabricating materials with high melting temperatures. Recent experiments trying to change inter-layer distance of graphite with pulse laser shot [1,2] suggested initial contraction of inter-layer distance and later expansion. To understand such non-thermal processes theoretical treatment with use of extremely high-electronic temperature was made [3], however excited electrons were assumed to follow Boltzmann-type equation which works only in thermal equilibrium conditions..

To address the origin of structural change and to treat non-equilibrium electron dynamics, we have developed first-principles calculation scheme which monitors electron-ion dynamics in condensed matters under time-varying external electric field [4] based on numerical scheme [5] within the time-dependent density functional theory [6] and periodic boundary conditions using the plane-wave basis set. Then our simulation showed an expansion of the surface mono-graphene layer, while remaining layers sit at bulk positions. We expect the conditions of our simulation deviate from those in experiments [1,2] but give an new way to massively produce single-layer graphene sheets.

All calculations were performed by using the Earth Simulator.

- [1] F. Carbone et al, *Phys. Rev. Lett.* **100**, 035501 (2008).
- [2] R. K. Raman, et al., *Phys. Rev. Lett.* **101**, 077401 (2008).
- [3] H. O.Jeschke et al., *Phys. Rev. Lett.* **87**, 015003 (2001).
- [4] Y. Miyamoto and H. Zhang, *Phys. Rev.* **B77**, 165123 (2008).
- [5] O. Sugnio and Y. Miyamoto, *Phys. Rev.* **B59**, 2579 (1999); **B66** 089901(E) (2001).
- [6] E. Runge and E. K. U. Gross, *Phys. Rev. Lett.* **52**, 997 (1984).

Corresponding Author: Yoshiyuki Miyamoto

TEL: +81-29-850-1586, FAX: +81-29-856-6136, E-mail: y-miyamoto@ce.jp.nec.com

Detailed Structure Analysis of Carbon Nanohorns

Michiko Irie¹, Ryota Yuge², Sumio Iijima^{1,2}, and Masako Yudasaka¹

¹*Nanotube Research Center, National Institute of Advanced Science and Technology (AIST),
Central 5, 1-1-1 Higashi, Tsukuba, 305-8565, Japan*

²*NEC, 34 Miyukigaoka, Tsukuba 305-8501, Japan*

Single-wall carbon nanohorns (SWNHs) are single-graphene tubules, and it is estimated that they have diameters of 2-5 nm and length of about 40-50 nm from the transmission electron microscopy observation. SWNHs assemble and form spherical aggregates with diameters of about 80-100 nm. Since the aggregate is dense and the SWNH structures are not uniform, it is difficult to reveal the details of the assembly manner of SWNHs. We show in this report advanced thermogravimetric data of SWNH and SWNH with holes opened (SWNHox) and their analysis results.

SWNH was produced by CO₂ laser ablation of graphite, and SWNHox was prepared by “slow combustion” of SWNHs heated up to 400°C or higher at a temperature increase rate of 1°C/min in air. Thermogravimetric analyses (TGA) of SWNH and SWNHox were carried out in O₂ with a dynamic temperature mode in which the temperature increase rate was controlled according to the weight decrease rate. TGA of SWNH showed a major weight decrease at about 550°C, and additionally, a new one at about 570°C (Fig. 1). From TEM observation, we found that the 550°C component corresponded to the combustion of SWNH tubules, while the latter, the combustion of graphene-based aggregates, so called, petal-aggregates. From the analysis of the TGA profiles of SWNH and SWNHox, the weight ratio of the SWNH tubules and the petal-aggregates were estimated to be about 60 and 35%, respectively.

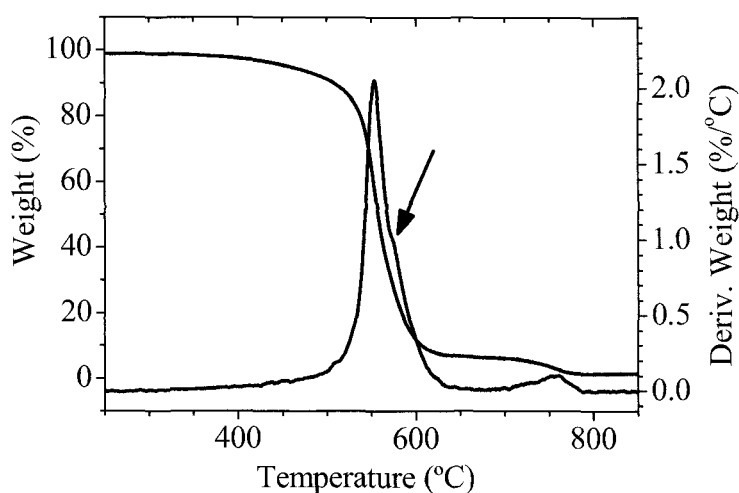


Fig. 1 TGA of SWNH. An arrow indicates a newly found weight decrease due to the combustion of petal-like parts of SWNH aggregates.

Corresponding Author: M. Yudasaka

TEL: +81-29-861-4818, FAX: +81-29-861-6290

E-mail: m-yudasaka@aist.go.jp

Isolating Individual Single-Wall Carbon Nanohorns From Their Aggregate

○Minfang Zhang¹, Sumio Iijima^{1,2,3}, Masako Yudasaka^{1,2}

¹*Nanotube Research Center, AIST, Tsukuba 305-8565*

²*NEC, Tsukuba 305-8501*

³*Department of Materials Science and Engineering, Meijo University, Nagoya 468-8502*

Applications of single-wall carbon nanohorns (SWNH) [1] to drug delivery system, fuel cell, and gas adsorption have been studied and they are found to be potentially useful due to their unique structures. SWNHs have diameters of about 2-5 nm and lengths of about 30-50 nm, and about 2000 of SWNHs form a spherical aggregate with diameters of about 80-120 nm. It is thought that the small size aggregate or individual nanohorns should be more useful in the drug delivery system for long blood circulation time and excretion from the animal bodies. However, separation of individual SWNHs so far has not been achieved due to the strong van der Waals interaction between each nanohorns. In this report, we show that separation of small-sized aggregate and even obtaining individual SWNHs from the 100-nm SWNH aggregate is possible by applying a combined process: oxidation, sonication and sucrose gradient centrifugation.

Firstly, as-grown SWNHs was oxidized (SWNHox) by air combustion from room temperature to 450°C with a heating rate of 1°C/min [2]. Then SWNHox were mixed with aqueous solution of sodium cholate (SC, 2 mg/ml) by sonication (~300W, 1.5 h). The obtained SWNH-SC dispersion was centrifuged through sucrose gradient solution (sucrose concentrations: bottom, 30%; middle, 10%; top, 5%) for 1-6 hours with centrifugal force of 4600g. After centrifuge, SWNHs separated into four zones of SC solution and sucrose solutions. The measurements by dynamic light scattering (DLS) showed that SWNHs in different zones have different sizes. When the centrifuge time was about 5 hours, the particle sizes of SWNHs were 30-40, 50-70, and 80-130 nm from top, middle, and below zones. The TEM observation showed that SWNHs isolated in top zone was individual SWNHs and small bud-type aggregate of SWNHs. We also checked as-grown SWNHs without oxidation by same process of sonication and centrifuge. We found that the as-grown SWNHs could not be separated into the individual SWNHs. This indicated that individual SWNHs and small aggregate SWNHs were produced through the process of oxidation, sonication in SC solution and separated by sucrose gradient centrifuge.

[1] S. Iijima, M. Yudasaka, R. Yamada, S. Bandow, K. Suenaga, F. Kokai, K. Takahashi, *Chem. Phys. Lett.*, **309**, 165–170 (1999).

[2] J. Fan, M. Yudasaka, J. Miyawaki, K. Ajima, K. Murata, and S. Iijima, *J. Phys. Chem. B*, **110**, 1587 (2006).

Corresponding Author: Zhang, Yudasaka

TEL&FAX: +81-29-861-6290 E-mail: m-zhang@aist.go.jp, m-yudasaka@aist.go.jp

Plugs Formed by Hydrogen Peroxide Treatment at Holes of Carbon Nanohorns

O Jianxun Xu,¹ Minfang Zhang,² Sumio Iijima,^{1,2} Masako Yudasaka²

¹ *Meijo University, 1-501 Shiogamaguchi, Tenpaku-ku, Nagoya 468-8502, Japan*

² *Nanotube Research Center, National Institute of Advanced Science and Technology (AIST), Central 5, 1-1-1 Higashi, Tsukuba, 305-8565, Japan*

We previously reported that oxidation with hydrogen peroxide at 70-80°C opened holes of single wall carbon nanohorns (SWNH) with abundant oxygenated groups such as carboxylic groups at the hole edges. We show in this report that “plugs” were formed at the holes when the hole-opened SWNH (SWNHox) was treated with hydrogen peroxide at room temperature, and at the same time, hydrocarbons and/or those with oxygenated groups as well as H₂O₂ solutions were confined inside SWNHox.

SWNHs were first oxidized by heating at 1°C/min in air up to 500°C, and further treated with H₂O₂ at room temperature for different periods with or without light irradiation. So-oxidized SWNH (SWNHox) showed abnormal phenomena. In the measurements of temperature programmed mass spectra (TPD-MS), various fragments were burst at about 190°C. The emitted fragments were H₂O, CO, CO₂, hydrocarbons, oxygenated hydrocarbons, and others. Quantities of the emitted fragments increased with the increase of H₂O₂ treatment periods (15 min. 2%; 45 min. 13%). Coinciding with TPD-MS results, IR spectra of SWNHox treated with H₂O₂ for 45 minutes showed broad peaks at 1050 and 1400 cm⁻¹. The former is likely to correspond to C-C and C-O stretching modes and, the latter, C-H or O-H bending modes.

Xylene adsorption by SWNHox decreased with the H₂O₂ treatment period (15 min. 0.29 g/g; 45 min. 0.14 g/g). The decreased xylene adsorption quantity of SWNHox recovered after the 190°C burst. By grinding the SWNHox for 2h, the fragment quantity emitted at 190°C in TPD-MS considerably decreased.

These results suggest that the plugs were formed at the holes of SWNHox during the H₂O₂ treatment, and the plug is stable up to 190°C. In the plug formation, hydrocarbons and/or those with oxygenated groups as well as H₂O₂ solutions were confined inside SWNHox. The plugs are probably made of oxygen-containing hydrocarbons, which will be discussed in the presentation.

Contact: m-yudasaka@aist.go.jp

Epitaxial growth and electronic characterization of Mg-doped C₆₀

Masato Natori, Nobuaki Kojima, Hidetoshi Suzuki and Masafumi Yamaguchi
Toyota Technological Institute, 2-12-1 Hisakata Tenpaku, Nagoya 468-8511, Japan

C₆₀ solids have been known as high resistive semiconductor materials. For organic solar cell applications, such high resistivity is one of the reasons of low charge transport efficiency in a C₆₀ acceptor layer. Impurity doping in organic semiconductor can increase conductivity, and control band profile at the interface between organic/metal or organic/organic materials. Mg is one of the promising materials for guest metal showing semiconductor property. In experimentally, it was reported that the conversion efficiency of C₆₀/MEH-PPV organic cells was significantly improved by the automatically Mg-doping in a C₆₀ layer during the Mg electrode deposition [1, 2]. However, the detailed discussion of semiconductor properties of Mg-doped C₆₀ films has not been reported yet.

The electric conduction of organic materials is also affected by the crystal quality. It has been observed the band conduction mechanism in organic single-crystal materials, while the amorphous one shows the hopping conduction mechanism. Therefore, to investigate the essential electric conductivity behaviors, the well-crystalline film is required.

In this paper, we investigate the epitaxial growth of Mg-doped C₆₀ films to obtain the well-crystalline films, and electric properties of the epitaxial Mg-doped C₆₀ films compared with micro-crystalline and/or amorphous Mg-doped C₆₀ films on glass substrate.

C₆₀ and Mg-doped C₆₀ films were grown on mica (001) and quartz glass substrates by molecular beam epitaxy (MBE). Mg composition was controlled by the beam flux ratio of C₆₀/Mg sources. The Mg/C₆₀ composition was confirmed by X-ray photoelectron spectroscopy (XPS). Crystal quality and orientations were investigated by X-ray diffraction (XRD) measurements.

Figure 1 shows the XRD patterns of Mg-doped C₆₀ (Mg/C₆₀ ratio = 0.6) films on glass and mica (001) substrates. For Mg-doped C₆₀ films on glass, the observed diffraction peaks correspond with polycrystalline C₆₀ phase with fcc lattice, though these diffraction peaks are quite weak and broad. In contrast, Mg-doped C₆₀ films on mica (001) shows only sharp (111)-related diffraction peaks, suggesting good crystal quality. Furthermore, the pole figure measurement of XRD indicates that Mg-doped C₆₀ films are grown epitaxially on mica (001) in the low Mg concentration region (Mg/C₆₀ ratio < 1).

Figure 2 shows Mg concentration dependence of the conductivity in comparison between glass and mica substrates. The conductivity increases with increasing Mg concentration, and besides well-crystalline films on mica (001) show much higher conductivity than glass substrate. It is considered that such significant increase is caused by the drastic improvement of crystal quality realized by epitaxial growth.

References

- [1] R.P.Gupta and M.Gupta: *Physica C*, **219**, pp21-25 (1994)
- [2] M.Chikamatsu *et al.*: *Appl. Phys. Lett.*, **84**, pp127-129 (2004)

Corresponding Author: Masato Natori

E-mail: sd08427@toyota-ti.ac.jp

Tel&Fax: +81-52-809-1877, +81-52-809-1879

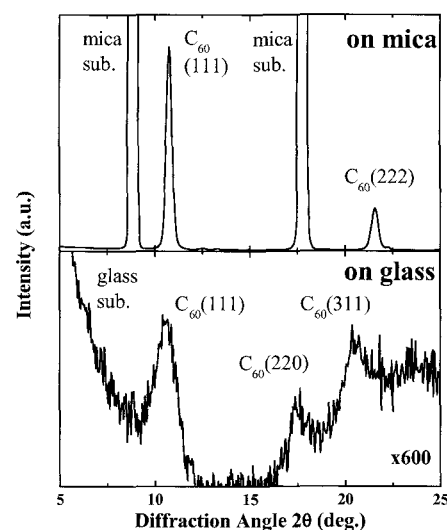


Fig.1. XRD patterns of Mg-doped C₆₀ (Mg/C₆₀ ratio = 0.6) films on mica and glass substrates.

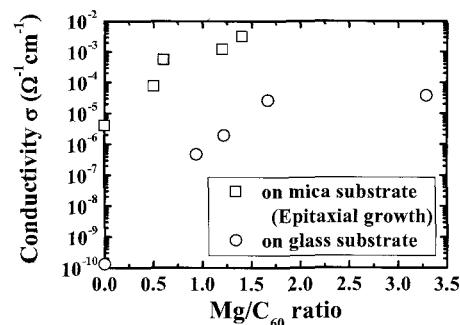


Fig.2. Mg concentration dependence of the conductivity in comparison between glass and mica substrates.

Pressure-Induced Structural Phase Transition of Solid C_{60}

○Yuichiro Yamagami and Susumu Saito

*Department of Physics, Tokyo Institute of Technology
2-12-1 Oh-okayama, Meguro-ku, Tokyo 152-8551, Japan*

It is well known that solid C_{60} is a molecular crystal, *i.e.*, C_{60} molecules form solid via the van der Waals interaction (fcc C_{60}). However, from the experiments by Rao *et al.* and Iwasa *et al.*, it is found that fcc C_{60} transforms into the polymer phase by light or external pressure. Moreover, it is also found from the *complementary* research by Núñez-Regueiro *et al.* and Xu *et al.* that the crystalline polymer phase can be synthesized under the particular pressure conditions. As a structure of such a crystalline polymer phase, three structures have been clarified so far, namely one-dimensional orthorhombic, two-dimensional (2D) ‘tetragonal’ (orthorhombic), and 2D rhombohedral phases. However, recently, the single crystal samples of two kinds of three-dimensional (3D) C_{60} polymer phases (orthorhombic phase [1] and cubic phase [2]) are synthesized from 2D orthorhombic phase and fcc C_{60} under 15 GPa, respectively, and are now of high interest.

In the present work, we perform the tight-binding molecular dynamics (TBMD) simulation of simple-cubic (sc) C_{60} , which is the low-temperature phase of fcc C_{60} , in order to investigate its pressure-induced structural phase transition. As for external pressure, we use two values of 10 and 20 GPa. Interestingly, results of the TBMD simulation at both pressure values are found to be the same, cubic 3D C_{60} polymer (Fig. 1(a)) with its lattice constant very close to the experimental value. Theoretical and experimental values are 12.15 and 11.93 Å, respectively. However, its internal structure is rather different from the experimentally proposed structural model [2]. In the experimental model, the translation symmetry is face-centered cubic, whereas in the obtained structure, the translation symmetry is primitive cubic. As for the electronic structure, this C_{60} polymer structure is estimated to be semiconductor with an energy gap of about 2 eV from the calculation using the tight-binding model. In the presentation, we will also discuss the details of this cubic 3D-polymer geometry optimized by the density functional theory within the local density approximation (LDA) as well as the electronic structure calculated by LDA.

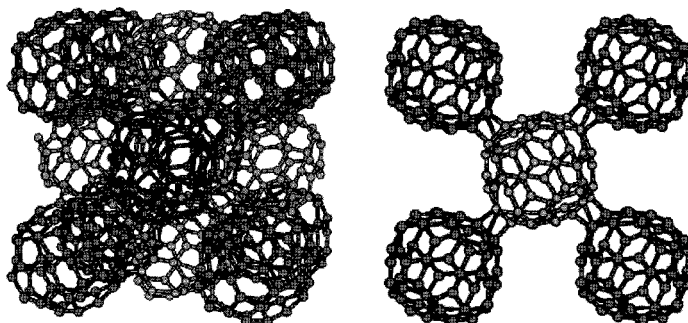


Figure 1: (a) cubic three-dimensional C_{60} polymer. (b) C_{60} units on (001) plane.

- [1] S. Yamanaka, A. Kubo, K. Inumaru, K. Komaguchi, N. S. Kini, T. Inoue, and T. Irifune, *Phys. Rev. Lett.* **96**, 076602 (2006).
 [2] S. Yamanaka, N. S. Kini, A. Kubo, S. Jida, and H. Kuramoto, *J. Am. Chem. Soc.* **130**, 4304 (2008).

Corresponding Author: Yuichiro Yamagami

TEL: +81-03-5734-2386, FAX: +81-03-5734-2739, E-mail: yamagami@stat.phys.titech.ac.jp

Electronic transport properties of photo-irradiated C₆₀○Y.Chiba¹, H.Tsuji¹, M.Ueno¹, Shih-Ren Chen^{1,2}, N.Aoki¹, and Y.Ochiai¹*1) Chiba University, Yayoi, Inage-Ku, Chiba 263-8522, Japan**2) Southern Taiwan University, Tainan, Taiwan*

Recently, one of the attractive topics in fullerene research is polymerization of C₆₀ molecules. Since the first report in 1993, several kinds of polymerization methods have been proposed. However, most of them have not examined the electronic transport properties of C₆₀ polymers so far.

We have, therefore, investigated the effect of photo irradiation on the electronic transport properties of C₆₀ thin film and fullerene nanowhisker (FNW) that is monocrystalline wire of C₆₀. It was confirmed by investigating the field-effect transistor (FET) characteristics. Furthermore, the morphology of photo-irradiated C₆₀ thin film was confirmed by scanning electron microscope (SEM) inspection.

In our previous research, it was clarified that the electrodes for the top contact blocked off the UV-light and polymerization was obstructed underneath the electrodes. Therefore this C₆₀ FETs were fabricated with a bottom-contact configuration. From *I-V* characteristics at several back-gate voltages (V_G), it has been confirmed that the source-drain current (I_{SD}) and the field-effect mobility (μ) decrease by about one order of magnitude after the irradiation. However, the threshold-voltage (V_T) determined at I_{SD} - V_G curves was lowered from 12 V to 2 V by photo-irradiation. Furthermore, the photo-irradiated C₆₀ FET shows clear FET characteristics after exposing ambient atmosphere. Although, the I_{SD} value is decreased three or four order of magnitude, it showed a response by the back gate operation.

About FNWs FET, the value of I_{SD} and μ declined by photo irradiation. In addition, the cracks were observed as well as our previous case of the C₆₀ thin film. However, the cracks were not observed at some FNWs of thick diameter. Therefore, it seems that the effect of the photo irradiation depends on the diameter of FNW.

Corresponding Author: Y.Chiba

E-mail:ochiai@faculty.chiba-u.ac.jp

Tel.043-290-3428, Fax.043-290-3427

Assembling behaviors of [70]fullerene on addition of aliphatic diamines

○Ken-ichi Matsuoka¹, Tsuyoshi Akiyama^{1,2}, and Sunao Yamada^{1,2,3}

¹*Department of Materials Physics and Chemistry, Graduate School of Engineering,
Kyushu University, 744 Moto-oka, Nishi-ku, Fukuoka 819-0395, Japan*

²*Department of Applied Chemistry, Faculty of Engineering, Kyushu University,
744 Moto-oka, Nishi-ku, Fukuoka 819-0395, Japan*

³*Center for Future Chemistry, Kyushu University, 744 Moto-oka, Nishi-ku, Fukuoka
819-0395, Japan*

Assembling molecular components into specific structure, shape and texture is an important and challenging issue in basic science to develop functionalities and technological applications. Fullerenes have attracted much attention because of their physical properties and wide range of applications. Besides these facts, their spherical molecular structure and rich chemistry make themselves intriguing building blocks for functional architectures. Accordingly, wide varieties of fullerene-based assemblies have been prepared [1]. We report herein the unique assembling phenomena of C₇₀ through the interaction with linear aliphatic diamines.

Primary and secondary aliphatic amines are known to add readily to fullerene via single electron transfer process [2]. When C₇₀ was treated with aliphatic diamine species such as 1,2-diaminoethane and 1,3-diaminopropane, rhombic dodecahedral particles with (sub)micrometer size were selectively formed. We found that the resultant particles were dominantly composed of the complex species of C₇₀ and diamines, but not fullerene-aliphatic amine adducts. We further investigated the aliphatic amine (guest) exchange behavior with other amines inside of C₇₀ assemblies and found that the C₇₀ framework shrinks or expands to accommodate smaller or larger amine species.

[1] For example: a) T. Nakanishi, T. Michinobu, K. Yoshida, N. Shirahata, K. Ariga, H. Möhwald, D. G. Kurth, *Adv. Mater.* **20**, 443 (2008). b) M. Sathish, K. Miyazawa, *J. Am. Chem. Soc.* **129**, 13816 (2007).

[2] G.P. Miller, *C. R. Chimie* **6**, 952 (2006).

[3] K. Matsuoka, S. Matsumura, T. Akiyama, S. Yamada, *Chem. Lett.* **38**, 932 (2008).

Corresponding Author: Tsuyoshi Akiyama

TEL: +81-92-802-2816, FAX: +81-92-802-2815, E-mail: t-akitcm@mbox.nc.kyushu-u.ac.jp

Length growth measurement of C₆₀ fullerene nanowhiskers

○Kayoko Hotta and Kun'ichi Miyazawa

*Fullerene Engineering Group, Advanced Nano Materials Laboratory,
National Institute for Materials Science, Tsukuba, 305-0044, Japan*

The growth mechanism of C₆₀ nanowhiskers (C₆₀NWs) is investigated. The C₆₀NWs were prepared by the liquid-liquid interfacial precipitation method (LLIP method) [1, 2], where toluene was used as a good solvent and isopropyl alcohol (IPA) as a poor solvent for C₆₀.

In this study, the growth of C₆₀NWs in various conditions is investigated to know the growth mechanism by using optical microscopy (Nikon ECLIPSE ME600) and scanning electron microscopy (SEM, JEOL JSM-6700F).

Various volume ratios of C₆₀-saturated toluene solution and IPA were examined and the volume ratios were set to be 1:9, 1:7, 1:5, 1:3, 1:1, 3:1, 5:1, 7:1 and 9:1. The average length and diameter of C₆₀NWs were measured 24 h after the start of the synthesis at 20°C. The length growth of C₆₀NWs changed depending on the volume ratio of solvents. The most uniform C₆₀NWs with similar diameter and morphology were synthesized when the solvent volume ratio of 1:1 was used. For the solutions with the solvent volume ratios of 3:1, 5:1, 7:1 and 9:1, C₆₀NWs were not formed.

To investigate the effect of water contained in IPA, distilled water was added to IPA, where the solvent volume ratio of the C₆₀-saturated toluene solution and IPA was 1:1. The water contents in IPA were set to be 0, 0.4, 0.6, 0.9, 1.3, 2.5, 3.8, 5.0, 6.3, 7.5, 8.7, 9.9, 11.2 and 12.4 mass %. The average length and diameter of C₆₀NWs were measured 24 h after the start of synthesis at 20°C. The length of C₆₀NWs was observed to change depending on the water content in IPA. When the concentration of water in IPA was less than 2.5 %, a small addition of water promoted the length growth of C₆₀NWs. The average diameter of C₆₀NWs, however, remained constant. When IPA added with an excess amount of water was used, C₆₀NWs were not synthesized, although granular bulk C₆₀ crystals appeared.

[1] K. Miyazawa, A. Obayashi and M. Kuwabara, *J. Am. Ceram. Soc.* **84** 3037 (2001)

[2] K. Miyazawa, Y. Kuwasaki, A. Obayashi and M. Kuwabara, *J. Mater. Res.* **17** 83 (2002)

Corresponding Author: Kayoko Hotta

TEL: +81-29-860-4667, FAX: +81-29-860-4667, E-mail: HOTTA.Kayoko@nims.go.jp

Internalization of Fullerene Nanowhiskers by PMA-treated THP-1 Cells

○Shin-ichi Nudejima¹, Kun'ichi Miyazawa¹,
Junko Okuda-Shimazaki² and Akiyoshi Taniguchi²

¹Fullerene Engineering Group, Advanced Nano Materials Laboratory,
National Institute for Materials Science (NIMS), Tsukuba 305-0044, Japan

²Advanced Medical Material Group, Biomaterials Center, NIMS, Tsukuba 305-0044, Japan

Fullerene nanowhiskers (FNWs) can be synthesized by the liquid-liquid interfacial precipitation method [1]. FNWs are composed of the fullerene molecules that are usually bonded via van der Waals forces and expected to have various application fields such as low dimensional semiconductors, field emission tips, nanoprobe for microdevices, fiber-reinforced nanocomposites, composite elements for lubrication, and so on.

FNWs have a needle-like morphology that resembles asbestos. Public concern have raised that carbon nanotubes (CNTs) may cause asbestos-like damage in health and environment owing to their needle-like morphology and strong mechanical properties like asbestos in spite of their enormous potentials of wide applications in various fields. Recently, an asbestos-like pathogenic behavior associated with CNTs indicated a structure-activity relationship based on length, to which asbestos and other pathogenic fibers conform [2]. For this reason, it is imperative to evaluate the biological impacts of FNWs before practical applications of them can be developed.

Macrophages are one of the immune system cells and defend the host against the foreign substances in a nonspecific manner during the early phase of infection. THP-1 is a human acute monocytic leukemia cell line and it is well known that the THP-1 cells are induced to differentiate into macrophage-like cells when treated with phorbol 12-myristate 13-acetate [3].

Macrophages recognize, internalise and digest foreign substances and the uptake of them depends on their size and surface properties [4]. C₆₀ is also phagocytized by macrophages [5] and the uptake rate of C₆₀ is lower than that of graphite particles [6]. It is important to investigate the phagocytosis of C₆₀NWs to evaluate the biological impacts of them. We located the position of C₆₀NWs among the macrophage-like cells three-dimensionally with differential interference contrast and confocal laser microscope and observed a time dependent manner of increased uptake of C₆₀NWs by the cells.

Part of this work was supported by NIMS Center for Nanotechnology Network.

- [1] K.Miyazawa, Y.Kuwasaki, A.Obayashi and M.Kuwabara, *J.Mater.Res.*, **17** [1], 83 (2002).
- [2] C.A.Poland, R.Duffin, I.Kinloch, A.Maynard, W.A.H.Wallace, A.Seaton, V.Stone, S.Brown, W.Macnee and K.Donaldson, *Nature Nanotechnol.*, **3**, 423 (2008).
- [3] S.Tsuchiya, Y.Kobayashi, Y.Goto, H.Okumura, S.Nakae, T.Konno and K.Tada, *Cancer Research*, **42**, 1530 (1982).
- [4] Y.Tabata and Y.Ikada, *Biomaterials*, **9**, 356 (1988).
- [5] A.E.Porter, K.Muller, J.Skepper, P.Midgley, M.Welland, *Acta Biomaterialia*, **2**, 409 (2006).
- [6] S.Fiorito, A.Serafino, F.Andreola, P.Bernier, *Carbon*, **44**, 1100 (2006).

Corresponding Author: Shin-ichi Nudejima

TEL: +81-29-851-3354 (EXT: 8463), FAX: +81+29-860-4667, E-mail: NUDEJIMA.Shinichi@nims.go.jp

Water-Dispersible Fullerene Whisker

○Yasuhiko Fujita, Yutaka Takaguchi

Graduate School of Environmental Science, Okayama University, Okayama 700-8530, Japan

As concern is raised for the potential environmental impact of nanostructured materials, there has been considerable interest in water dispersion of C₆₀ nanoparticles. Although fullerenes are hydrophobic carbon allotropes and not at all soluble in water, the nanoparticles of them remain dispersed in water even without the aid of a dispersant such as surfactants.[1] This is in marked contrast to carbon nanotubes, which requires dispersing agents to form stable dispersions in water. Recently, we have reported stable water dispersion of single walled carbon nanotubes (SWNTs) via formation of supramolecular nanocomposite using fullerodendron.[2] Meanwhile, fibrous fullerene nanowhiskers, which are made of C₆₀ or C₇₀ and have submicron diameters and lengths of more than 100 μm, have attracted many attention because of their unique properties and applications.[3] However, as in the case of SWNTs, stable dispersions of fullerene nanowhiskers in water without dispersant have never been reported. This paper describes easy fabrication of water-dispersible fullerene whiskers upon irradiation by a fluorescent lamp.

C₆₀ nanowhiskers obtained by reprecipitation method were irradiated by a fluorescent lamp for 40 hours in a stirring solution of toluene/2-propanol. After the filtration, nanowhiskers could be dispersed in ion-exchanged water (Figure 1b). It is confirmed by IR, Raman, XRD, and SEM observation (Figure 1a) that the structure of fullerene nanowhiskers was not changed upon photoirradiation. However, obvious anionic charge on the surface of the whisker was observed by zeta potential measurement.

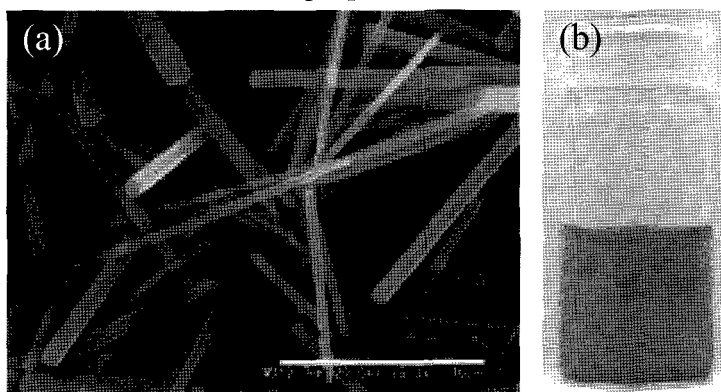


Figure 1. (a) SEM images of fullerene whisker, and (b) photograph of water dispersed fullerene whisker.

[1] Deguchi, S.; Mukai, S.; Tsudome, M.; Horikoshi, K., *Adv. Mater.* **2006**, 18, 729.

[2] Takaguchi, Y.; Tamura, M.; Sako, Y.; Yanagimoto, Y.; Tsuboi, S.; Uchida, T.; Shimamura, K.; Kimura, S.; Wakahara, T.; Maeda, Y.; Akasaka, T., *Chem. Lett.* **2005**, 34, 1608.

[3] Minato, J.; Miyazawa, K., *Carbon* **2005**, 43, 2837.

Corresponding Author: Yutaka Takaguchi

TEL: +81-86-251-8903, FAX: +81-86-251-8903, E-mail: yutaka@cc.okayama-u.ac.jp

Transmission Electron Microscopy Observation of Cross-Sectional Structure of C₆₀ Nanofibers

○Ryoei Kato and Kun'ichi Miyazawa

National institute for Materials Science, Tsukuba, Ibaraki, 305-0044, Japan

The liquid-liquid interfacial precipitation method is effectively used to create fullerene nanofibers, i.e. nanowhiskers[1] and nanotubes[2], composed of fullerene molecules such C₆₀, C₇₀ and their derivatives.

The as-prepared solvated C₆₀ nanofibers have hexagonal structures, before losing solvent molecules by drying, while the C₆₀ nanofibers turn to a face-centered cubic structures, after drying in air. These behaviors show the C₆₀ nanofibers can take various crystallographic structures depending on the amount of contained solvent molecules and also suggest that the bonding states of C₆₀ molecules change depending on their crystallographic structure.

On the other hand, the C₆₀ nanotubes have a tubular structure. It was suggested that the hollow structure was formed through a dissolution of the inner part in their growth process.

These mechanisms of structural change of fullerene nanofibers have not been understood in detail. We observed the cross-sections of C₆₀ nanofibers to understand the structural change mechanism of C₆₀ nanofibers.

The C₆₀ nanofibers were fabricated by the liquid-liquid interfacial precipitation method, where a pyridine solution saturated with C₆₀ irradiated by visible light or ultraviolet light was used. The C₆₀ nanofibers dispersed in isopropyl alcohol were collected by use of a pipette and embedded into a polyvinyl alcohol mold. Thin slices were obtained by using a focused ion beam system or an ultramicrotome with a diamond knife.

We observed the cross-sectional morphology and structure of C₆₀ nanofibers by transmission electron microscopy.

[1] K. Miyazawa, A. Obayashi, and M. Kuwabara, *J. Am. Ceram. Soc.*, **84**, 3037 (2001)

[2] K. Miyazawa, J. Minato, T. Yoshii, M. Fujino and T. Suga, *J. Mater. Res.*, **20**, 3, 688-695 (2005)

Corresponding Author: Ryoei Kato

Tel: +81-029-851-3354 ext. 8462, Fax: +81-029-860-4667, E-mail: KATO.Ryoei@nims.go.jp

Insulating behavior of Cs_3C_{60} at ambient pressure as probed by optical reflectivity measurements

○Takumi Takano¹, Alexey Y. Ganin², Yasuhiro Takabayashi³,
Matthew J. Rosseinsky², Kosmas Prassides³, Yoshihiro Iwasa^{1,4}

¹*Institute for Materials Research, Tohoku University, Sendai 980-8577, Japan*

²*Department of Chemistry, University of Liverpool, Liverpool L69 7ZD, UK*

³*Department of Chemistry, University of Durham, Durham DH1 3LE, UK*

⁴*CREST, Japan Science and Technology Corporation, Kawaguchi 332-0012, Japan*

The discovery of superconductivity in alkali-metal (A) intercalated $A_x\text{C}_{60}$ has led to a broad class of superconductors of composition $A_3\text{C}_{60}$ (fcc) with superconducting critical temperature, T_c , up to 33 K in $\text{RbCs}_2\text{C}_{60}$ at ambient pressure [1]. Recently, A. Y. Ganin *et al.* succeeded in the synthesis of Cs_3C_{60} with high crystallinity, which adopts the A15 structure based on body-centered cubic (bcc) packing of the C_{60}^{3-} anions, and demonstrated the non-superconducting-to-superconducting transition with high pressure condition of about 3 kbar without any indication of structural transition, and the bulk superconductivity of $T_c \sim 38$ K at 12 kbar, which is the highest T_c value of any molecular-based systems [2]. Consequently, the great attention for the material has been reinforced. However, because of the difficulty in synthesis and the extreme air-sensitivity of Cs_3C_{60} , even basic information of the electronic properties of the material is still insufficient thus far; for example, there is no experimental evidence to explain the electronic state of Cs_3C_{60} at ambient pressure (metal? or insulator?), and how it transforms into the superconducting state with the application of pressure.

In this presentation, we carried out the optical reflectivity measurements for a compressed-pellet sample of Cs_3C_{60} in the room temperature to identify the ambient pressure non-superconducting electronic state of the material. In the figure, the optical conductivity spectra derived via Kramers-Kronig transformation are plotted for $A_3\text{C}_{60}$ (A : K, Rb, Cs) samples. In sharp contrast to the spectra for K_3C_{60} and Rb_3C_{60} [3], that for Cs_3C_{60} exhibits an obvious insulating behavior. Additionally, no indication of Jahn-Teller effect has also been detected. These results indicate that the pressure-induced superconductivity of Cs_3C_{60} can be attributed to Mott-Hubbard insulator-metal transition.

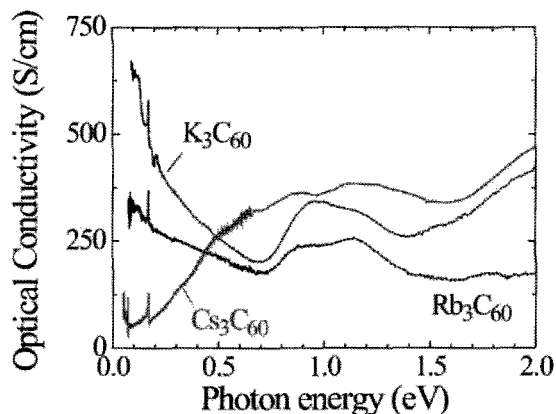


Fig.: Optical conductivity of Cs_3C_{60} , K_3C_{60} [3], and Rb_3C_{60} [3].

[1] K. Tanigaki *et al.*, *Nature* **352**, 222 (1991).

[2] A. Y. Ganin *et al.*, *Nature Materials*, **7**, 367 (2008).

[3] Y. Iwasa *et al.*, *Phys. Rev. B* **51**, 3678 (1995).

Corresponding Author: Takumi Takano

TEL: +81-22-215-2032, FAX: +81-22-215-2031, E-mail: takano@imr.tohoku.ac.jp

発表索引
Author Index

Author Index

～A～

Achiba, Yohji 2P-40, 3-3, 3P-20
 Ago, Hiroki 3-6, 3P-11
 Akaike, Kouki 2-5
 Akasaka, Takeshi 1P-11, 1P-32, 2-3,
 2P-22
 Akiyama, Tsuyoshi 3P-35
 Amaratunga, Gehan A.J. 2P-5
 Ando, Yoshinori 2P-6, 3P-19
 Aoki, N. 1P-6, 3P-34
 Aoki, Yuusuke 2-4
 Aoyagi, Shinobu 1P-23
 Arsawang, Uthumporn 1P-1
 Asaka, Koji 2P-10, 2P-14
 Atake, Tooru 2-7
 Awano, Yuji 1-8, 2-15, 3P-13
 Azuma, T. 2P-40

～B～

Bandow, Shunji 1P-18
 Berthe, Maxime 1P-2
 Bird, J. P. 1P-6, 3P-25

～C～

Chen, Shih-Ren 3P-34
 Chen, Shimou 1P-29
 Chiashi, Shohei 1-1
 Chiba, Y. 3P-34
 Chiu, Chien-Chao 2P-16

～D～

Dang, Jingshuang 3P-14
 Dresselhaus, Mildred S. 1P-17
 Dresselhaus, Gene 1P-17
 Duan, Wenhui 3P-26

～E～

Ebine, Yuta 1P-2
 Eguchi, T. 1-6, 1P-9, 1P-20
 Einarsson, Erik 2P-15, 3-5, 3P-2, 3P-3,
 3P-4
 Endo, Hiroki 1P-18

Endo, Morinobu 1-7
 Endoh, Shigehisa 2-1, 2-2
 Enoki, Toshiaki 2-13

～F～

Feng, Ye 2P-7
 Ferry, D. K. 3P-25
 Fueno, Hiroyuki 1P-36
 Fujigaya, Tsuyohiko 1-17, 1-18, 2P-19,
 3P-1
 Fujii, Motoo 2P-12
 Fujii, Shunjiro 1-15, 3P-7
 Fujii, Tatsuo 2P-9
 Fujita, Katsuhide 2-1, 2-2
 Fujita, Takuya 3P-20
 Fujita, Yasuhiko 3P-38
 Fujiwara, Yuji 2-12
 Fujumura, Youhei 3P-9
 Fukai, Hirofumi 3-7
 Fukumar, Takahiro 1-17
 Fukuzono, Kazuyuki 2P-5
 Furuichi, Koji 2P-18
 Furukawa, Masaru 3P-27
 Futaba, Don N 1-16

～G～

Ganin, Alexey Y. 3P-40
 Ghorannevis, Zohreh 3P-17
 Ghosh, Kaushik 2P-6
 Goto, M. 2P-40
 Gu, Bing-Lin 3P-26
 Guodong, Tan 3P-21

～H～

Haba, Eisuke 2P-20
 Hakamatsuka, Mari 1P-10
 Hanabusa, Yohei 2P-24
 Hanashima, Tateki 1-1
 Hannongbua, Supot 1P-1
 Hansen, K. 2P-40
 Hanzawa, Akinori 3P-23
 Hara, Hironori 1P-37

Hara,Kazuto	3P-20	Imahori,Hiroshi	3S-4
Hara,Tomoko	1-7	Inoue,Akihito	3-3
Harada,Keitaro	1P-25	Inoue,Sakae	2P-6, 3P-19
Harima,Hiroshi	1P-7, 3P-24	Inoue,Taiki	3P-3
Harris,Peter J. F.	3P-22	Irie,Michiko	3P-29
Haruyama,J.	1-6, 1P-9, 1P-20	Irlé,Stephan	1P-37, 2P-23
Hasegawa,Kei	3-7	Ishii,Fumiyuki	2-14
Hasegawa,Tadashi	1P-11	Ishii,Juntaro	1-16
Hasegawa,Tetsuya	3P-23	Ishii,Tadahiro	3P-5
Hasegawa,Y.	1-6, 1P-9, 1P-20	Ishikawa,Kei	1-9
Hashimoto,Akihiro	3P-24	Ishimaru,K.	1-8
Hasuike,Noriyuki	1P-7, 3P-24	Ishitsuka,Midori O.	2-3
Hata,Kenji	1-16	Issiki,Toshiyuki	1P-7
Hatakeyama,Rikizo	1-14, 1P-15, 1P-28, 2P-24, 3P-16, 3P-17	Itami,Kenichiro	2P-33
Hatori,T.	1P-6	Ito,Shigeo	3P-9
Hayamizu,Yuhei	1-16	Ito,Yasuhiro	2-4, 2P-25, 2P-36
HAYASHI,Takuya	1-7	Ito,Yoichi	2P-5
Hayashi,Yasuhiko	2P-5	Iwahashi,Hitoshi	2-1, 2-2
Heguri,Satoshi	1P-38	Iwamoto,Masachika	2P-25
Hibino,Norihito	2P-13	Iwasa,Yoshihiro	3P-40
Higo,Junki	1P-11	Iwasaki,T.	1-8
Hino,Shojun	2-4	Iye,Y.	1-6, 1P-9, 1P-20
Hirana,Yasuhiko	1-11	Izu,Yoshifumi	1P-24
Hirofumi,Yajima	3P-10	Izumi,Noriko	2P-25
Hirotsu,Yu	1P-15	~J~	
Ho,Dean	2-16	Jang,Bongyong	2P-5
Homma,Yoshikazu	1-1	Jin,Hehua	1-15, 3P-7
Hong,Sung Kyu	2P-28, 2P-35		
Horie,Masanori	2-1, 2-2	~K~	
Hotta,Kayoko	3P-36	Takehi,Hitoshi	1P-7, 3P-24
Huang,Houjin	2-16	Kaminosono,Yoshiya	3P-10
Hujita,Hideki	2P-1	Kamoi,Susumu	3P-24
Hwang,Sung Ho	2P-28, 2P-35	Kanai,Kaname	2-5
~I~		Kaneko,Shiori	2P-2
Iijima,Sumio	1-5, 1P-18, 3-4, 3P-22, 3P-29, 3P-30, 3P-31	kaneko,Toshiro	1-14, 1P-15, 2P-24, 3P-16 3P-17
Iijima,Yuki	1P-27	Kanemitsu,Yoshihiko	1-3
Iizuka,M.	1-8	Kang,Dongchul	1P-10
Ikenaga,Eiji	3P-13	Kasama,Yasuhiko	2P-24, 2P-26
Ikeuchi,Ryouta	2P-9	Katagiri,Yoji	1P-33
Imai,Tomohito	1P-40	Kataura,Hiromichi	1-15, 2P-7, 3-8, 3P-7
Imazu,Naoki	1P-27, 2P-36	Kato,Haruhisa	2-1, 2-2
		Kato,Haruo	2P-1

Kato,K.	3P-19	Kohno,Masamichi	2P-12
Kato,Koichiro	1P-8	Kojima,Kenichi	1P-10
Kato,Masaru	1P-16	Kojima,Nobuaki	3P-32
Kato,Ryoei	3P-39	Kokai,Fumio	1P-33, 1P-40, 2-12
Kato,Takaaki	1P-11	Komatsu,Koichi	2-7
Kato,Tatsuhisa	1P-31	Kondo,Daiyu	2-15, 3P-13
Kato,Toshiaki	1P-28, 3P-16, 3P-17	Koretsune,Takashi	1P-3
Kato,Yoshitaka	1P-36	Korobov,Michail	2-16
Kato,Yuichi	3-1	Koshio,Akira	1P-33, 1P-40, 2-12
Kawachi,Kazuhiko	2P-26	Kubozono,Yoshihiro	2P-26
Kawai,Takazumi	1-13, 2-11	Kuga,Hidenori	2P-22
Kawaji,Hitoshi	2-7	Kumagai,Susumu	2P-27
Kawarada,H.	1-8	Kumashiro,Ryotaro	2-7
Kayumi,Naoko	3P-12	Kumazawa,Akira	3P-5
Kazachenko,Victor	1P-34	Kurihara,Hiroki	2-3
Kida,M.	1P-6	Kuroda,Shunsuke	3P-16
Kikuchi,Yosuke	2P-26	Kusano,Yoshikazu	2P-10
Kim,Do-Hyun	2P-21	Kusunoki,Michiko	2P-1, 3P-1
Kim,Dong Young	3-7		
Kim,Jung Jin	3P-13	～L～	
Kim,Jung Mi	2P-35	Lacher,Sebastian	2P-32
KIM,Yoong-Ahm	1-7	Lee,Jeong Ho	2P-28, 2P-35
Kimata,Nozomu	1P-38	Li,Chang-Zhi	2P-31
Kinoshita,Masahito	2P-38	Li,Jun	2P-39
Kinugasa,Shinichi	2-1	Li,Yongfeng	1-14
Kishi,Naoki	2P-5	Li,Zhenhua	2P-6
Kishida,Hideo	1-16	Liu,Huarong	2P-8
Kishimoto,Shigeru	1P-19	Liu,Zheng	3P-22
Kisoda,Kenji	1P-7, 3P-24	Lu,Jing	1P-11
Kitamura,Hiroshi	1P-35, 2P-27		
Kitaura,Ryo	1P-23, 1P-27, 1P-29, 2-10, 2P-36	～M～	
Kito,Hironobu	2-12	Maeda,Yutaka	1P-11
Ko,Weon Bae	2P-28, 2P-35	Majima,T.	2P-40
Kobata,Masaaki	3P-13	Majima,Yutaka	2P-25
Kobayashi,Keisuke	3P-13	Maki,Hideyuki	2P-13
Kobayashi,Keita	2-10	Maniwa,Yutaka	1P-25, 1P-26
Kobayashi,Mototada	1P-38	Maruyama,Shigeo	1-2, 1-9, 1P-24, 2P-15, 2P-1 3-2, 3-5, 3P-2, 3P-3, 3P-4
Kobayashi,Yoshihiro	2P-13	Maruyama,Takahiro	2P-6, 3P-18
Kobayashi,Yuki	2P-4	Maruyama,Takehiro	3P-1
Kodama,T.	2P-40	Matsuda,Kazunari	1-3
Kodama,Takeshi	3-3	Matsuda,Kazuyuki	1P-25
Koga,Kazunori	3P-21	Matsudaira,M.	1-6, 1P-20
Kohama,Yoshimitsu	2-7	Matsuishi,Kiyoto	2P-7

Matsumoto,Hidetoshi	2P-5	Nakamura,Ayako	2-1, 2-2
Matsumoto,J.	2P-40	Nakamura,Eiichi	2P-30, 2P-31, 2P-32
Matsunaga,Ryusuke	1-3	Nakamura,Hisashi	1P-25
Matsuo,Keiko	2P-32	Nakamura,J.	1-6, 1P-20
Matsuo,Teppeï	2P-17	Nakamura,Y.	1P-6
Matsuo,Yutaka	2P-30, 2P-31, 2P-32	Nakanishi,Junko	2-1, 2-2
Matsuoka,Ken-ichi	3P-35	Nakano,Hiroyuki	2-12
Mibu,Ko	3P-15	Nakashima,Naotoshi	1-11, 1-17, 1-18, 2P-19, 3-1, 3P-12
Mieno,Tetsu	1P-34, 3P-21	Nakayama,Takashi	3-3
Mikmai,Fuminori	1P-26	Nambo,Masakazu	2P-33
Minari,Takeo	1-15, 3P-7	Naritsuka,Shigeya	3P-18
Mitobe,Ryota	1-1	Natori,Masato	3P-32
Miyadera,Tetsuhiko	1-15, 3P-7	Nihei,Mizuhisa	1-8, 2-15, 3P-13
Miyamoto,Yoshiyuki	1-13, 3P-28	Niidome,Yasuro	3-1
Miyata,Yasumitsu	1-15, 2P-7, 3-8, 3P-7	Nikawa,Hidehumi	2P-22
Miyazaki,Koji	1-9	Nishibori,Eiji	1P-23
Miyazaki,Takafumi	2-4	Nishide,Daisuke	3-8
Miyazawa,Kun'ichi	2S-2, 3P-39, 3P-36, 3P-37	Nishimura,Fumio	1-10, 1P-21
Mizorogi,Naomi	2-3, 2P-22	Nishimura,Toshifumi	2P-2, 2P-3
Mizuguchi,Yoshikazu	1P-5	Nishimura,Yasuhiro	2-13
Mizuno,Kohei	1-16	Nishio,Keiko	2-1, 2-2
Mizusawa,Takashi	3P-20	Nishio,Koji	1P-7
Mizutani,Takashi	1P-19	Nishio,T.	1-6, 1P-9, 1P-20
Mizutani,Yoshihiro	3P-18	Noda,Suguru	1S-1, 2P-18, 2P-20, 3-2, 3-7, 3P-6
Mori,Susumu	2P-33	Noguchi,Takuya	3P-23
Morimatsu,Takeshi	2P-12	Norimatsu,Wataru	3P-1
Morimoto,T.	3P-25	Nudejima,Shin-ichi	3P-37
Morimoto,Tatsuro	1-18		
Morioki,Masakatsu	3P-9	～O～	
Morita,Kouhei	3P-24	Ochiai,Y.	1P-6, 3P-25, 3P-34
Moroe,Shogo	2P-12	Ogata,Terihiko	2-8
Morokuma,Keiji	2P-23	Ohashi,Kazunori	1P-27, 2P-36
Moteki,Takahiko	3-2	Ohfuchi,Mari	3-9
Motooka,S.	3P-25	Ohno,Katsuma	2P-27
Murakami,Yoichi	3-2, 3P-2, 3P-4	Ohno,Masatomi	1P-35, 2P-27
Muramoto,Yoshitaka	1-7	Ohno,Yutaka	1P-19
Murata,Yasujiro	2-7	Ohyama,Yasuyuki	2P-27
～N～		Okabe,Hiroto	3P-3
Nagase,Shigeru	1P-11, 2-3, 2P-22	Okada,Susumu	1-4, 1-12, 1P-22, 2-11
Naito,Ryoji	1P-7, 3P-24	Okamoto,Minoru	2P-19
Naitoh,Yasuhisa	1-15, 3P-7	Okawa,Jun	2P-15
Nakahara,Hitoshi	2P-8, 2P-10, 2P-14	Okazaki,Toshiya	3-3, 3P-20
Nakahara,Katsumasa	2P-30		

Oke, Shinichiro	3P-9	Sakamoto, Shingo	2P-2, 2P-3
Okigawa, Yuki	1P-19	Sakata, Makoto	1P-23
Okimoto, Haruya	2-4, 2P-25	Sakurai, Masahiro	1P-4
Okubo, Tatsuya	3-2	Sano, H.	1-6, 1P-9, 1P-20
Okuda, Koji	1P-30	Sano, Masahito	2P-4
Okuda-Shimazaki, Junko	3P-37	Saraswati, Teguh Endah	2P-36
Omote, Kenji	2P-26, 2P-24	Sasaki, Kenich	1P-17, 1P-13, 3P-26
Onishi, Yuki	3-3	Sato, Hideki	2-12
Ono, Yoshihiro	2P-26	Sato, Kentaro	1-2
Onoe, Jun	2-6	Sato, Kuninori	3P-18
Ooba, Takuma	2P-26	Sato, Motohiro	1P-14
Oohara, Wataru	1P-28	Sato, Shintaro	1-8, 2-15, 3P-13
Orofeo, Carlo M.	3-6	Sato, Tetsuya	2P-13
Osada, Ryoichi	1P-31	Sawa, Hiroshi	1P-23, 2-7
Osawa, Eiji	2-16	Sawada, Keisuke	2-14
Osawa, Toshio	3-7	Seki, Kazuhiko	2-5
Oshima, Hisayoshi	3P-15	Sekido, Masaru	1P-35, 2P-27
Otani, Minoru	1-12	Shibata, Noriyoshi	2P-1
Ouchi, Yukio	2-5	Shiga, Takuma	1P-12
		Shigekawa, Hidemi	1P-2
～P～		Shima, Hiroyuki	1P-14
Park, Jin Sung	1P-17	Shima, Hiroyuki	2-6
Prassides, Kosmas	3P-40	Shimada, Toshihiro	3P-23
		Shimazu, Tomohiro	3P-15
～R～		Shimizu, T.	1-6, 1P-9, 1P-20
R. Hernandez, Eduardo	1P-12	Shimizu, Tetsuhiro	1P-28
Rachi, Takeshi	2-7	Shinohara, Hisanori	1P-23, 1P-27, 1P-29, 2-4, 2-10, 2P-25, 2P-36
Rao, A. M.	1-6, 1P-9, 1P-20		
Razanau, Ihar	1P-34	Shinohara, Naohide	2-1, 2-2
Ren, Ting	2P-39	Shiomi, Junichiro	1-2, 1-9, 1P-24, 2P-15, 2P-17, 3-5, 3P-2, 3P-4
Reppert, J.	1-6, 1P-9, 1P-20		
Rosseinsky, Matthew J.	3P-40	Shirai, Takashi	3P-6
Rozhkova, Natalia	2-16	Shiratani, Masaharu	3P-21
		Shiratori, Yosuke	2P-18
～S～		Shiromaru, H.	2P-40
Saengsawang, Oraphan	1P-1	Shukla, Bikau	1-5, 3-4
Saikawa, Mao	2-9, 2P-37	Siry, Milan	3P-15
Saito, Mineo	2-14	Suda, Yoshiyuki	3P-9
Saito, Riichiro	1-2, 1P-13, 1P-17, 3P-26	Suenaga, Kazu	3P-22
Saito, Susumu	1P-3, 1P-4, 1P-8, 3P-33	Suga, Hiroshi	1-15, 3P-7
Saito, Takeshi	1-5, 3-4	Sugai, Toshiki	1P-39
Saito, Yahachi	2P-8, 2P-10, 2P-14	Sugihara, Kunihiro	2P-1
Saitou, Daisuke	2P-27	Sugime, Hisashi	3-7
Sakamoto, Aiko	2P-32	Sugimoto, Shigeyuki	2P-1

Sumii,Ryohei	2-4	Thurakitseree,Theerapol	3P-2
Sumitomo,Koji	1P-2	Togashi,Y.	1P-6
Sunden,A.E.K.	2P-40	Tojo,Tomohiro	1-7
Suzuki,Hidetoshi	3P-32	Tokumoto,Youji	2-4
Suzuki,Satoru	1P-2, 2P-13	Tokunaga,Ken	2P-34
Suzuki,Shinzo	2P-12, 3P-20	Tokunaga,Tomoharu	2P-5
		Tominaga,Masato	2P-2, 2P-3
～T～		Tsuchiya,Takahiro	1P-11, 2-3
Tachibana,Masaru	1P-10	Tsuda,Shunsuke	1P-5
Tajima,Isamu	3P-5	Tsugawa,Naoki	2P-29
Takabayashi,Yasuhiro	2P-26, 3P-40	Tsuji,H.	3P-34
Takada,Jun	2P-9	Tsuji,Masaharu	3-6, 3P-11
Takagi,Yoshiteru	1-4	Tsukagoshi,Kazuhito	1-15, 3P-7
Takaguchi,Yutaka	2P-9, 2P-11, 2P-29, 3P-38	Tsutsui,Akira	2P-11
Takahashi,Nobuhiro	2P-29		
Takahashi,Toru	1P-12, 1P-21	～U～	
Takahiro,Yamamoto	1-10	Ubukata,Masa-aki	1P-30
Takai,Kazuyuki	2-13	Uchida,Katsumi	3P-5, 3P-10
Takano,Takumi	3P-40	Uchida,Tetsuya	2P-9
Takano,Yoshihiko	1P-5	Ue,Hitoshi	3P-9
Takata,Yasuyuki	2P-12	Ueda,Kazuyuki	2P-16
Takeda,Mitsuhiro	2P-27	Uemura,Sashiro	2P-8
Takeuchi,Hisato	1P-35	Ueno,M.	3P-34
Takeuchi,Osamu	1P-2	Ujiiie,Y.	3P-25
Takeuchi,T.	1-8	Umemoto,Hisashi	2-4, 2P-25
Takikawa,Hirofumi	3P-9	Usuba,Shu	3P-21
Tanaka,Kazuyoshi	1P-36		
Tanaka,Michiko	2-11	～W～	
Tanaka,Saburo	1-9	Wada,Yoriko	1P-30, 1P-31, 2-9
Tanaka,Satoru	3P-24	Wakabayashi,Katsunori	1P-13
Tanaka,Takeshi	1-15, 3-8, 3P-7	Wakabayashi,Tomonari	1P-30, 1P-31, 2-9, 2P-37, 2P-38, 3P-8
Tanaka,Yasuhiko	1-11		
Tanemura,Masaki	2P-5	Waki,Keiko	2P-21
Tango,Yuta	1P-40	Wang,Huafeng	2P-6, 3P-19
Tanigaki,Katsumi	2-7	Wang,Jian	2P-23
Taniguchi,Akiyoshi	3P-37	Wang,Weiwei	3P-14
Taniguchi,Isao	2P-2, 2P-3	Watanabe,Kazuyuki	1-10, 1P-12, 1P-21
Taninaka,Atsushi	1P-2	Watanabe,Makoto	3P-3
Tanioka,Akihiko	2P-5	Watanabe,Tohru	1P-5
Tanuma,H.	2P-40	Watari,Fumio	3S-5
Tatamitani,Yoshio	2-8		
Tejima,Syogo	1P-25	～X～	
Teshiba,Masaomi	3P-8	Xiang,Rong	3-5, 3P-2, 3P-4
Thompho,Somphob	1P-1	Xu,Jianxun	3P-31

~Y~

Yamada,Sunao	3P-35
Yamada,Takeshi	1P-30
Yamagami,Yuichiro	3P-33
Yamaguchi,Hiroyuki	2P-2
Yamaguchi,Masafumi	3P-32
Yamaguchi,Takahide	1P-5
Yamamoto,Kazunor	1P-32
Yamamoto,Nobuyuki	2P-1
Yamamoto,Tatsuhiko	1P-16
Yamamoto,Yohei	3P-3
Yamasaki,Takayuki	1P-40
Yamashita,Fuyuko	2P-26
Yamashita,Tetsuya	2P-14
Yamaura,Tatsuo	3P-9
Yamazaki,Yuko	2-3
Yamana,Shuichi	2S-3
Yanagi,Kazuhiro	3-8
Yasuda,Satoshi	1-16
Yasutake,Yuhsuke	2P-25
Yokomae,Takuya	1-7
Yokota,Masashi	3P-9
Yokoyama,D.	1-8
Yoon,Shinsook	2P-28, 2P-35
Yoshida,Kenta	3P-1
Yoshida,Shoji	1P-2
Yoshida,Yasukazu	2-1, 2-2
Yoshihara,Naoki	3-6, 3P-11
Yoshimura,Masamichi	2P-16
Yoshioka,Hideo	2-6
Yoza,Kenji	2P-22
Yudasaka,Masako	3S-6, 3P-29, 3P-30, 3P-31
Yuge,Ryota	3P-29
Yuito,I.	1-8
Yumura,Motoo	1-5, 1-16, 3-4

~Z~

Zdenek,Slanina	2P-22
Zhang,Minfang	3P-30, 3P-31
Zhang,Zhengyi	3P-2
Zhao,Pei	3P-4
Zhao,X.	3P-19
Zhao,Xiang	2P-39, 3P-14
Zheng,Fawei	3P-26, 3P-27

複写される方へ

フラーレン・ナノチューブ学会は、有限責任中間法人 学術著作権協会（学著協）に複写に関する権利委託をしていますので、本誌に掲載された著作物を複写したい方は、学著協より許諾を受けて複写して下さい。

但し、社団法人日本複写権センター（学著協より複写に関する権利を再委託）と包括複写許諾契約を締結されている企業の社員による社内利用目的の複写はその必要はありません。（※社外頒布用の複写は許諾が必要です。）

権利委託先：有限会社中間法人 学術著作権協会

〒107-0052 東京都港区赤坂 9-6-41 乃木坂ビル 3階

電話：03-3475-5618 FAX：03-3475-5619 E-Mail：info@jaacc.jp

注意：複写以外の許諾（著作物転載・翻訳等）は、学著会では扱っていませんので、直接、フラーレン・ナノチューブ学会へご連絡下さい。

Notice for Photocopying

If you wish to photocopy any work of this publication, you have to get permission from the following organization to which licensing of copyright clearance is delegated by the copyright owner.

<All users except those in USA>

Japan Academic Association for Copyright Clearance, Inc. (JAACC)

6-41 Akasaka 9-chome, Minato-ku, Tokyo 107-0052 Japan

TEL：81-3-3475-5618

FAX：81-3-3475-5619 E-Mail：info@jaacc.jp

<Users e in USA>

Copyright Clearance Center, Inc.

222 Rosewood Drive, Danvers, MA 01923 USA

Phone：1-978-750-8400 FAX：1-978-646-8600

2009年3月2日発行

第36回フラーレン・ナノチューブ総合シンポジウム 講演要旨集

<フラーレン・ナノチューブ学会>

〒464-8602 愛知県名古屋市千種区不老町
名古屋大学大学院理学研究科 物質理学専攻
篠原研究室内

Tel：052-789-5948

Fax：052-747-6442

E-mail：fullerene@nano.chem.nagoya-u.ac.jp

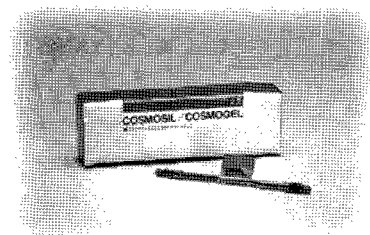
URL：http://fullerene-jp.org

印刷 / 製本 (有) イヅミ印刷所



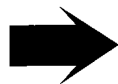
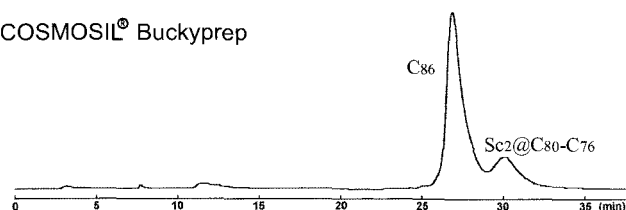
COSMOSIL[®] Buckyprep-M

今まで分離できなかった
金属内包フラーレンが分離可能！！

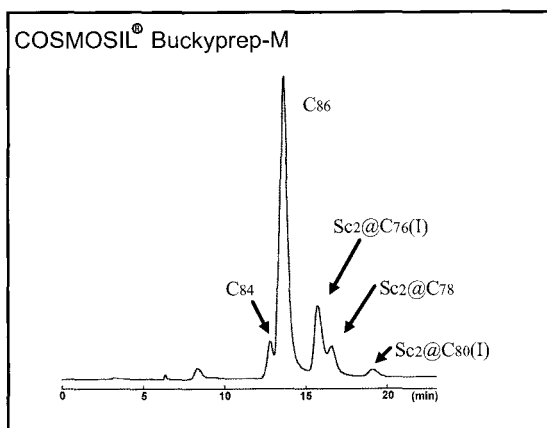


■分析例

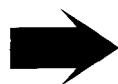
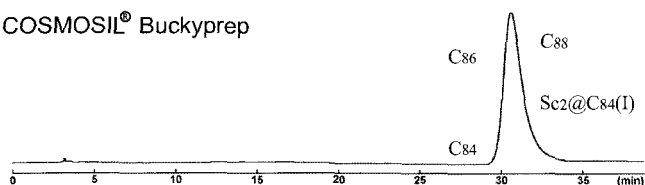
COSMOSIL[®] Buckyprep



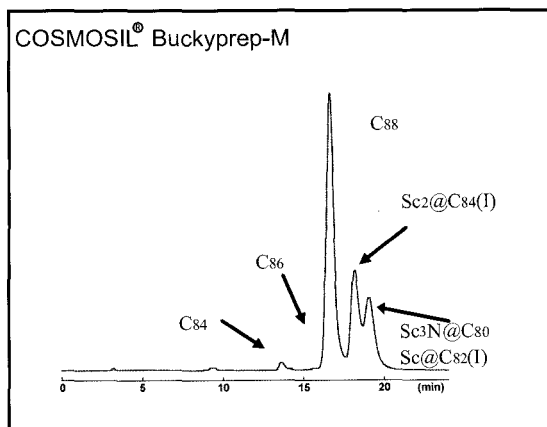
COSMOSIL[®] Buckyprep-M



COSMOSIL[®] Buckyprep



COSMOSIL[®] Buckyprep-M



分析条件

カラムサイズ：4.6mm I.D. × 250mm, 移動相：トルエン, 流速：1.0 ml/min, 温度：30°C, 検出：UV312

資料提供：名古屋大学 大学院理学研究科物質理学専攻 篠原 久典教授

■その他COSMOSIL[®] フラーレン関連カラム

フラーレン分離のスタンダードカラム



COSMOSIL[®] Buckyprep

C₆₀, C₇₀等の大量分取に



COSMOSIL[®] PBB

詳しい情報はWeb siteをご覧ください。

ナカライテスク株式会社

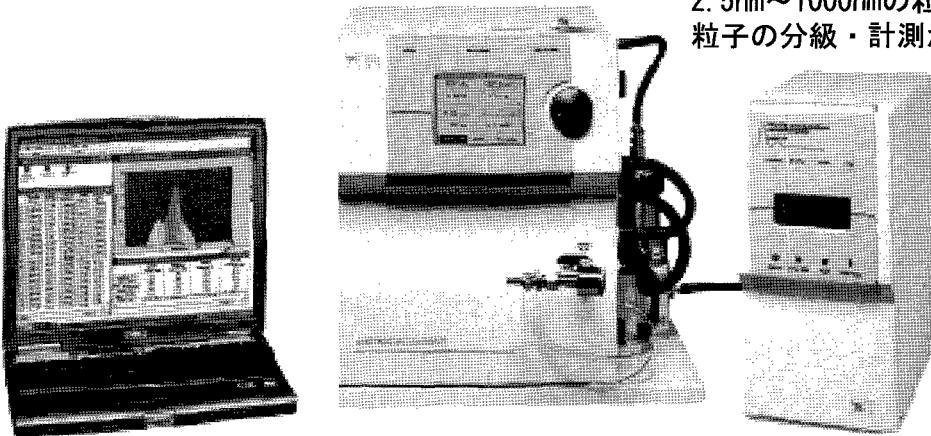
〒604-0855 京都市中京区二条通烏丸西入東玉屋町498

価格・納期のご照会 フリーダイヤル 0120-489-552
製品に関するご照会 TEL: 075-211-2703 FAX: 075-211-2673

Web site : <http://www.nacalai.co.jp>

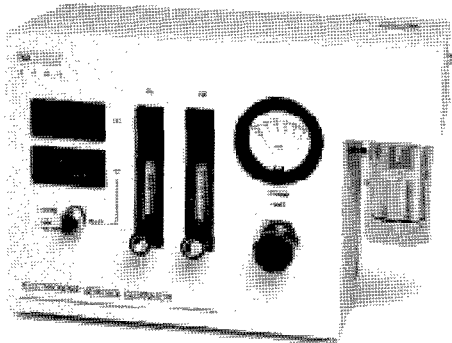
エアロゾルの計測・分析に

SMPS 3936シリーズ
2.5nm~1000nmの粒径範囲で
粒子の分級・計測が可能

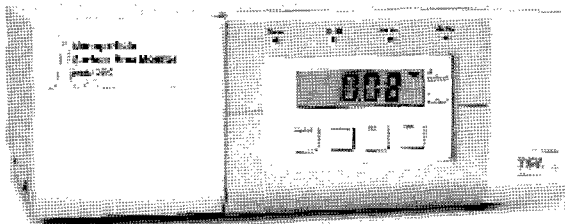
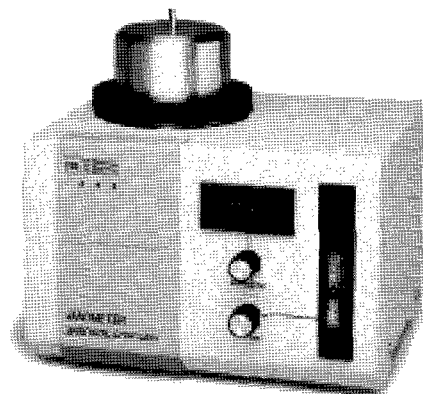


最高のラインナップとサポートを

エレクトロスプレー 3480
最小粒子径3nmでの発生が可能



ナノ粒子サンプラー 3089
2~100nmの帯電粒子を捕集



ナノ粒子表面積モニター 3550
気管支や肺胞に沈着する粒子表面積に
対応したデータを提供

*** CPG校正サービスも御提供**
一部製品にまだ対応出来ないものも有ります

Dylec 東京ダイレック株式会社 URL: <http://www.t-dylec.net/> Email: info@tokyo-dylec.co.jp

東京本社 〒160-0014 東京都新宿区内藤町1内藤町ビルディング

TEL: 03-3355-3632 FAX: 03-3353-6895

本社分室 〒151-0051 東京都渋谷区千駄ヶ谷1-33-5 千駄ヶ谷パークスクエア1階

TEL: 03-5367-0891 FAX: 03-5367-0892

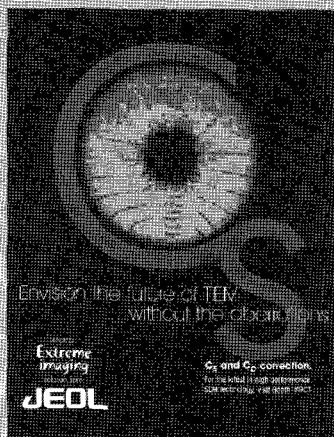
つくば営業所 〒305-0035 茨城県つくば市松代4-9-26-101

TEL: 0298-50-3056 FAX: 0298-50-3058

西日本営業所 〒601-8027 京都府京都市南区東九条御霊町53-4-4F

TEL: 075-672-3266 FAX: 075-672-3276

収差補正 (Cs) レンズで 世界最高性能の電子顕微鏡



JEM-2100F フィールドエミッション電子顕微鏡

次世代超高性能電子顕微鏡

レンズの球面収差を補正することにより、分解能を飛躍的に向上させた次世代超高性能収差補正装置（球面収差補正形電子レンズ）を、電子光学技術で高い技術を誇るドイツのCEOS社との共同開発により完成させ、最新のTEMに導入しました。

主な特長

照射系（コンデンサ）レンズの収差補正により、非常に細い電子ビームが形成され、走査透過電子顕微鏡（STEM）の分解能や元素分析などを行う際の空間分解能が飛躍的に向上

対物レンズの収差補正により、点分解能が0.12nmまで向上し、フリッジが解消され、高精度での微小結晶界面などの特定が可能



お問い合わせは、電子光学機器営業本部 (E0販促グループ) ☎042(528)3353

JEOL
Serving Advanced Technology

日本電子株式会社

本社・昭島製作所 〒196-8558 東京都昭島市武蔵野3-1-2 ☎(042)543-1111
営業統括本部 〒190-0012 東京都立川市曙町2-8-3 新鈴春ビル3F ☎(042)528-3381
札幌 (011) 726-9680・仙台 (022) 222-3324・横浜 (029) 856-3220・東京 (042) 528-3211・横浜 (045) 474-2181
名古屋 (052) 581-1406・大阪 (06) 6304-3941・広島 (082) 221-2500・福岡 (092) 411-2381

<http://www.jeol.co.jp/>



波長可変チタンサファイアレーザー 3900S

- 優れた操作性とメンテナンス性、高い変換効率を実現
- 高い安定性を実現し、675~1100nmの超広帯域発振が可能
- フラレン・ナノチューブの分光用光源として最適



【主な仕様】

平均入力：5Wおよび10W

発振波長域：700-1000nm(5W励起)/675-1100nm(10W励起)

線幅：40GHz以下(1GHz以下のオプション有り)

ノイズ：1%以下

安定性：3%以下

空間モード：TEM₀₀

 Spectra-Physics.

A Division of Newport Corporation

スペクトラ・フィジックス株式会社

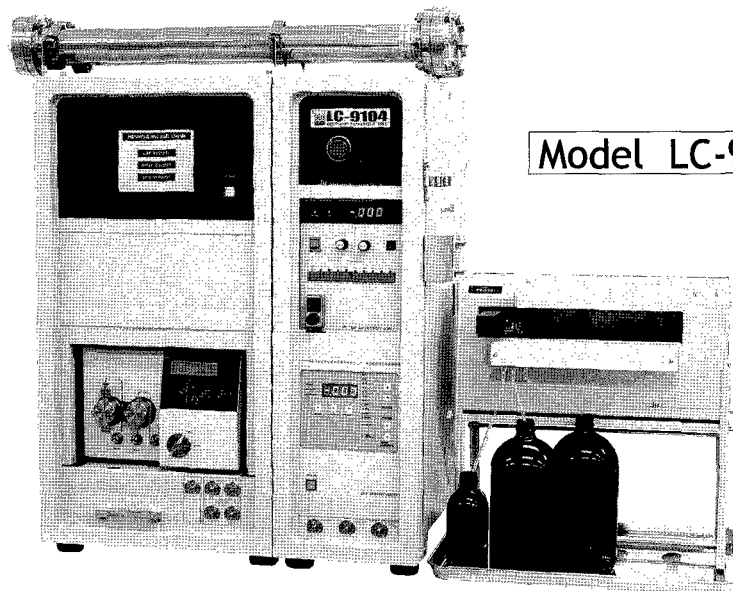
本社 〒153-0061 東京都目黒区中目黒4-6-1 大和中目黒ビル TEL(03)3794-5511 FAX(03)3794-5510
大阪支社 〒550-0005 大阪府大阪市西区西本町3-1-43 西本町ソーラービル TEL(06)4390-6770 FAX(06)4390-2760

MAKE LIGHT | MANAGE LIGHT | MEASURE LIGHT

製品情報・お問い合わせは <http://www.spectra-physics.jp>

リサイクル分取HPLCはJAIのLC-9000シリーズ!

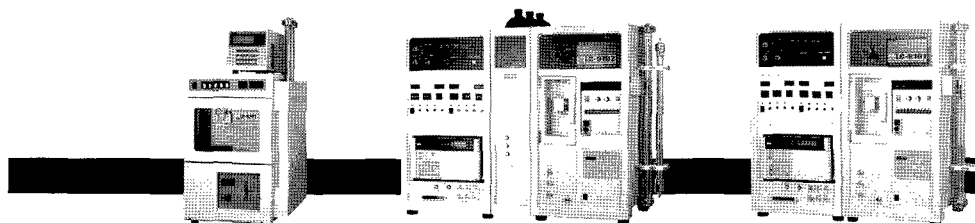
Recycling Preparative HPLC



Model LC-9104

◆LC-9104 大量分取モデル

専用のGPCカラム(40 φ×600 mm)を装着すれば、試料処理量は、LC-9101型の約4倍。試料注入から分取まで自動化されています。また、ODS・シリカカラムなど、大量分取用カラムの性能を最大限に引き出す装置設計がなされています。



◆LC-9201/LC-9204
コンパクトモデル

分離分取に定評のあるLC-9101型の高い性能を受継ぎながら、サイズをコンパクトにし、省スペース化と低価格化を実現しました。

◆LC-9102/9103
グラジエントモデル

グラジエントとリサイクルがワンタッチで切替えられます。

◆LC-9101
標準モデル

専用のGPCカラム(20 φ×600 mm)を装着すれば、分離能を落とすことなく、常時300 mgを注入することができます。

—— 高分子分析の未来と取り組む! ——

分取LCに関する
新連携認定企業

JAI 日本分析工業株式会社

URL: <http://www.jai.co.jp/> E-mail: sales-1@jai.co.jp

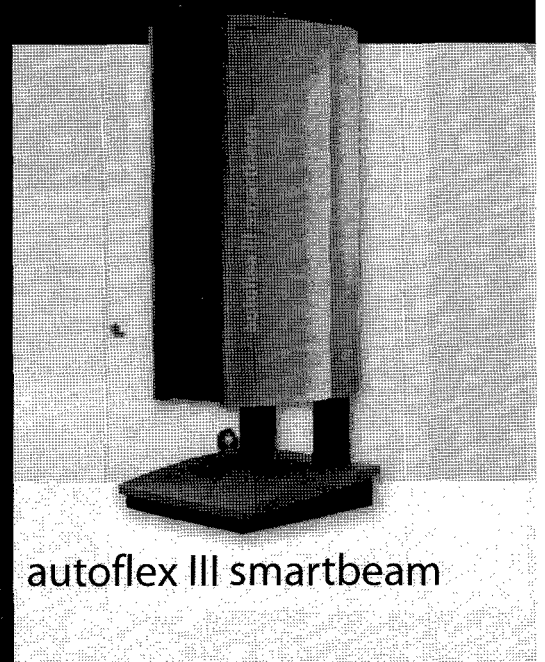
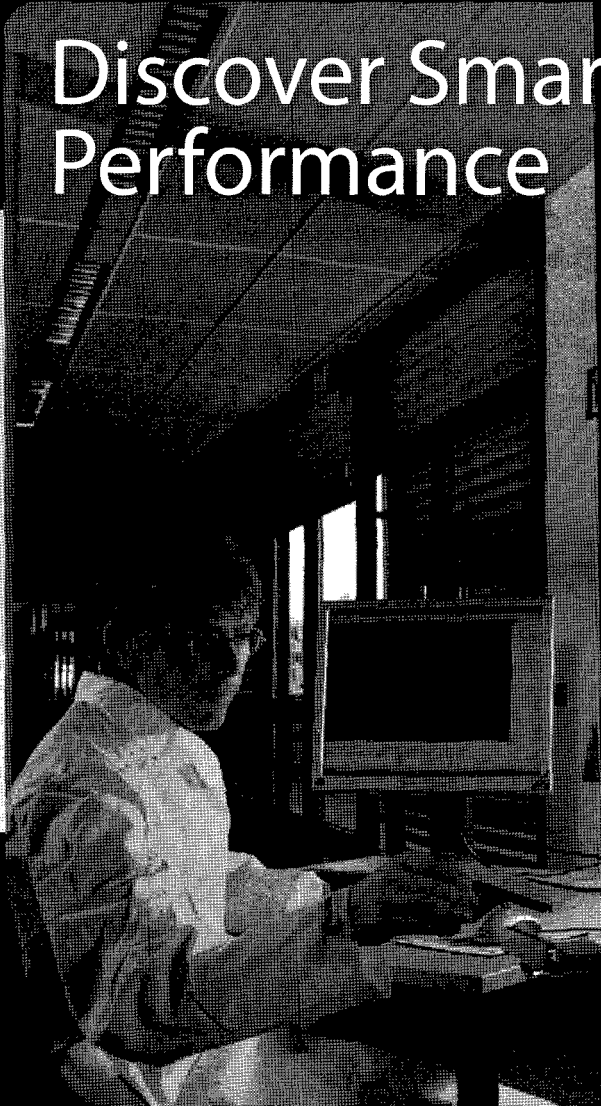
ISO9001/14001取得

□本社・工場: 〒190-1213 東京都西多摩郡瑞穂町武蔵208 TEL 042-557-2331 FAX 042-557-1892
□大阪営業所: 〒532-0002 大阪市淀川区東三国5-13-8-303 TEL 06-6393-8511 FAX 06-6393-8525
□名古屋営業所: 〒465-0025 愛知県名古屋市名東区上社3-609-3D TEL 052-709-5400 FAX 052-709-5403



Bruker Daltonics

Discover Smart Performance



autoflex III smartbeam

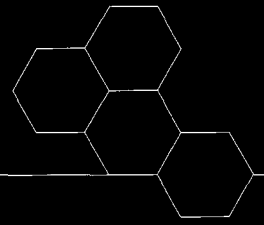
smartbeam レーザーテクノロジー
PANIによる広範囲での質量分解能
最高の質量精度
バイオマーカー探索、MALDIイメージング
および成功率の高いプロテオミクスのため
のクラスリーディング

スマートな性能とスマートなイメージをご覧ください。
革新的なマスペクトロメトリーは、信頼性が高く次世代の定性・定量的なタンパク質の
同定、高分解なMALDIイメージング、さらにはバイオマーカー探索を可能にします。
特許のsmartbeam™ レーザーテクノロジーは、いかなる定性・定量プロテオミクスの
プロジェクトにおいても非常に優れた性能を発揮します。

<http://www.bruker.co.jp/daltonics> をご訪問ください。

think forward

MALDI-TOF/TOF MS

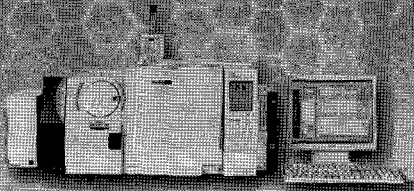


Best for Our Customers

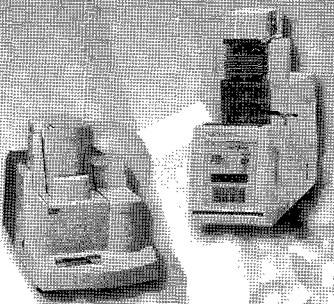
～すべてはお客様のために～ を合言葉にナノテク新材料における最高のソリューションを提供します。

1 微量測定

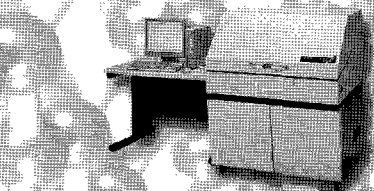
① 熱分解生成物・発生ガスの分析
 ガスクロマトグラフ質量分析計
 GCMS-QP2010 Plus



① 微量CNTの純度・熱特性評価
 ② CNTの結晶性と耐熱性の評価
 ミクロ熱重量測定装置
 TGA-50
 TG/DTA同時測定装置
 DTG-60/60H



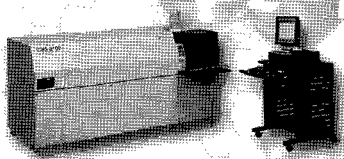
①② CNTの紫外可視近赤外吸収スペクトル測定
 紫外可視近赤外分光光度計
 SolidSpec-3700
 紫外可視近赤外分光光度計
 UV-3600



② CNTの密度測定
 乾式自動密度計
 アキュピック II 1340シリーズ



② 触媒元素の測定
 ツインシーケンシャル形ICP発光分析装置
 ICPS-8100



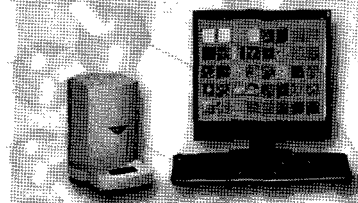
2 純度



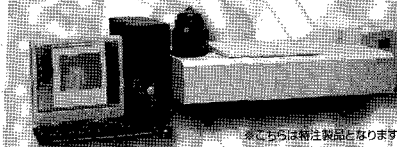
②③ 直径測定
 ②③ 結晶性と耐熱性の評価
 ラマン分光光度計
 Holo-Probe モニタリングシステム



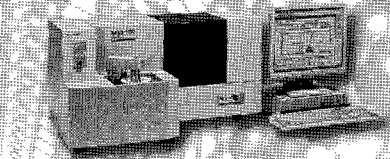
③④ あらゆるナノテク材料を観察・測定
 ナノサーチ顕微鏡
 SFT-3500



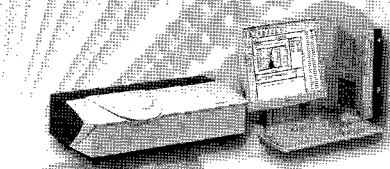
③④ 直径測定
 ③④ 精製前後の観察
 ③④ CNTとポリマーコンポジット試料の観察
 走査型プローブ顕微鏡
 SPM-9600



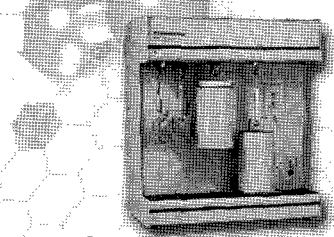
⑤ SWNTの近赤外PL 3次元分布測定
 近赤外フォトルミネッセンス測定システム
 NIR-PL System



⑥ 分散・凝集過程評価
 ナノ粒子径分布測定装置
 SALD-7100



⑥ 独自のIG法によるシングルナノ領域の粒子径評価
 シングルナノ粒子径測定装置
 IG-1000



⑥ 比表面積と吸着特性
 マイクロメディックス
 高速比表面積/細孔分布測定装置
 アサップ2020シリーズ

nanotech
 SHIMADZU

Total solutions for the future of nanotechnology

株式会社 島津製作所

分析計測事業部 マーケティング部 セールスプロモーションG
 〒604-8511 京都市中京区西ノ京桑原町1
 TEL075-823-1468 FAX075-823-1380 <http://www.shimadzu.co.jp>

株式会社 マシナックス

代表取締役 佐野隆治

〒454-0856 名古屋市中川区小碓通 2-6

TEL 052-654-5021(代) FAX 052-654-5125

HP <http://www.mashinax.jp/>

メール mashinax@sf.starcat.ne.jp

菱田商店会社案内

オフィス家具

メーカー(既製品) オカムラ・コクヨ・プラス等
木製家具 好みにあわせて作ります

室内装飾

ブラインド 立川・日米
カーテン・カーペット スミノエ・サンゲツ・タジマ等
床仕上げ フリーアクセス・Pタイル・ロンリウム等
クロス ルノン・サンゲツ等
間仕切り 各種パーテーション

学校関連

黒板・ホワイトボード・掲示板
実験台・薬品棚・吊棚
既製品から特注品まで、もちろん取り付けます。

(有)菱田 商店

名古屋市緑区浦里4-207

Tel 891-8125

Fax 891-3957

高機能、簡単操作がかつてない 測定環境を実現 多目的な Raman series です。

NRS-3000シリーズは、操作性の向上を実現しました。試料のセットからオートアライメントなどの装置の最適化、測定までをスピーディーに行えます。また、低波数測定ユニットへの切替えもボタンひとつで行えます。測定結果の解析には、データベース機能を用い簡単検索、ジャスコキャンバスを用いた簡単レポート作成機能があります。ラマン分析の可能性を大幅に広げました。



Laser Raman Spectrophotometer

レーザラマン分光光度計

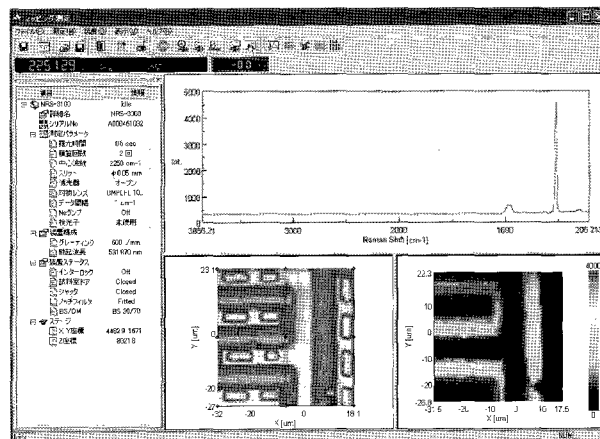
NRS-3000 series

NRS-3100/3200/3300

● 特 長

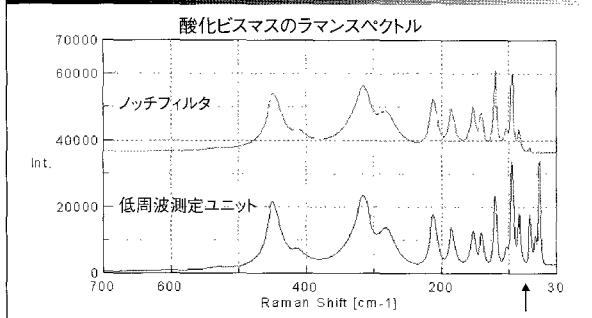
- ▶ ユーザーフレンドリーな操作性を実現
- ▶ ダイレクトドライブ方式のモノクロメータと高性能ノッチフィルタの組合わせにより、高い波数精度・再現性と高感度化を実現
- ▶ グレーティングを最大3枚搭載でき、多様な測定に対応
- ▶ レーザを最大6台まで搭載可能
- ▶ 日本分光独自のSRI機能 (SRI: Spacial Resolution Image) によりPCモニター上で試料像とアパーチャ像およびレーザービームを同時観察
- ▶ コンフォーカル光学系により深さ方向の測定が可能
- ▶ イメージング測定に対応可能
- ▶ オートアライメント機能によりシステムの安定性を追及
- ▶ レーザ放射安全基準Class1の安全性を確保
- ▶ スペクトル検索プログラムおよびデータベース、解析プログラムを標準搭載

● シリコンパターンのマッピング測定例



マッピング測定で機能と操作性が向上しました。画像情報をもとに測定者が画像上でマウスを使って、測定エリアを指定できます。また、測定中のデータを色分け図で表示することで測定結果をリアルタイムで確認することができます。

低波数測定ユニットの測定例



低波数測定ユニットは、無機物などの格子振動低波数域を精度よく測定する場合に有効になります。

JASCO は日本分光株式会社の登録商標です。

光と技術で未来を見つめる

日本分光

JASCO 日本分光株式会社

〒192-8537 東京都八王子市石川町2967-5
PHONE 042 (646) 4111 (代表)
FAX 042 (646) 4120
URL : http://www.jasco.co.jp/

北海道S-C 011(741)5285
北日本S-C 022(748)1040
筑波S-C 029(857)5721
東京S-C 03(3294)0341
西東京S-C 042(646)7001

神奈川S-C 045(989)1711
名古屋S-C 052(452)2671
大阪S-C 06(6312)9173
広島S-C 082(238)4011
九州S-C 092(588)1931

ISO 14001
ISO 9001
JSA
JIS Q 9001
JIS Q 9002
JIS Q 9003
JIS Q 9004
JIS Q 9005
JIS Q 9006
JIS Q 9007
JIS Q 9008
JIS Q 9009
JIS Q 9010
JIS Q 9011
JIS Q 9012
JIS Q 9013
JIS Q 9014
JIS Q 9015
JIS Q 9016
JIS Q 9017
JIS Q 9018
JIS Q 9019
JIS Q 9020
JIS Q 9021
JIS Q 9022
JIS Q 9023
JIS Q 9024
JIS Q 9025
JIS Q 9026
JIS Q 9027
JIS Q 9028
JIS Q 9029
JIS Q 9030
JIS Q 9031
JIS Q 9032
JIS Q 9033
JIS Q 9034
JIS Q 9035
JIS Q 9036
JIS Q 9037
JIS Q 9038
JIS Q 9039
JIS Q 9040
JIS Q 9041
JIS Q 9042
JIS Q 9043
JIS Q 9044
JIS Q 9045
JIS Q 9046
JIS Q 9047
JIS Q 9048
JIS Q 9049
JIS Q 9050
JIS Q 9051
JIS Q 9052
JIS Q 9053
JIS Q 9054
JIS Q 9055
JIS Q 9056
JIS Q 9057
JIS Q 9058
JIS Q 9059
JIS Q 9060
JIS Q 9061
JIS Q 9062
JIS Q 9063
JIS Q 9064
JIS Q 9065
JIS Q 9066
JIS Q 9067
JIS Q 9068
JIS Q 9069
JIS Q 9070
JIS Q 9071
JIS Q 9072
JIS Q 9073
JIS Q 9074
JIS Q 9075
JIS Q 9076
JIS Q 9077
JIS Q 9078
JIS Q 9079
JIS Q 9080
JIS Q 9081
JIS Q 9082
JIS Q 9083
JIS Q 9084
JIS Q 9085
JIS Q 9086
JIS Q 9087
JIS Q 9088
JIS Q 9089
JIS Q 9090
JIS Q 9091
JIS Q 9092
JIS Q 9093
JIS Q 9094
JIS Q 9095
JIS Q 9096
JIS Q 9097
JIS Q 9098
JIS Q 9099

地球の一員として私たちの責任

私たちは無限の可能性を秘めた炭素に魅せられ、理想の品質を追求し研究開発を重ねてきました。今や炭素の可能性は飛躍的に拡がり、エネルギー、環境など最先端テクノロジー分野にも幅広く採用されています。

これからも創造力を磨き続け、画期的な製品開発により社会に貢献できる企業を目指して、私たちの挑戦は続きます。



TOYO TANSO
Inspiration for Innovation

東洋炭素株式会社

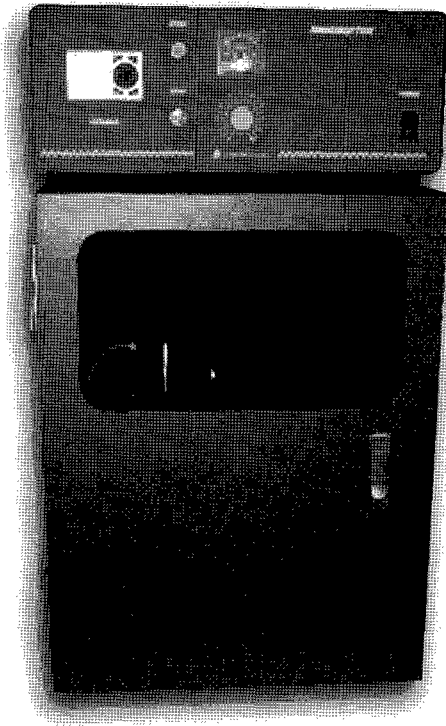
本社 〒530-0001 大阪市北区梅田3-3-10 梅田ダイビル10F Tel 06-6451-2114 Fax 06-6451-2186 www.toyotanso.co.jp

超音波破碎・分散装置

分散に最適!!

NANORUPTOR®

MODEL NR-350



特長

- 各種ナノ粒子(カーボンナノチューブ、フラーレン、ナノダイヤモンド等)の分散処理に最適。
- 最大超音波出力 350 W の強力パワー。
- 丸形超音波処理槽の採用により分散の高効率化を実現。
- 密閉条件でのサンプル処理が可能。
- コンタミがありません。
- 高性能消音箱付属。
- デジタルタイマーによりきめ細かい時間設定が可能です。
- 冷却ファン及び専用回路の採用により長時間運転が可能。

NR-350仕様表

品番	NR-350
品名	密閉式超音波分散装置 Nanoruptor
超音波周波数	20 kHz
超音波出力	～ 350 W 可変
電源	100 V、50/60 Hz、5.5 A
最低設置スペース概寸	300 (W) × 400 (D) × 680 (H) mm
発振ユニット概寸	400 (W) × 260 (D) × 160 (H) mm
処理ユニット概寸	170 (W) × 160 (D) × 270 (H) mm
消音箱概寸	300 (W) × 400 (D) × 520 (H) mm
NR-350 全体重量	36 Kg
ランタイマー	0 ～ 99 分 59 秒、デジタル
インターバルタイマー (ON)	0 ～ 99.99 秒、デジタル
インターバルタイマー (OFF)	0 ～ 99.99 秒、デジタル
処理本数	1 本 (50 mL)
付属品	消音箱、電源ケーブル、接続ケーブル、排水ポンプ、取り扱い説明書、ユーザー登録カード
備考	NR-350 は機器のみです。別途処理量に応じたアクセサリ (ギヤ-板+チップ) をお買い求め下さい。

メーカー略号：TOS

品名	品番	包装	希望販売価格
超音波密閉式分散装置 Nanoruptor®	NR-350	1 UNIT	¥1,950,000

*アクセサリユニットは含みません

別売品 使用可能チューブ：マルエム社製 50 mL ねじ口試験管

メーカー略号：TOS

品名	品番	包装	希望販売価格
50 mL チューブ用チップ	MM-50WS	1 SET*	¥54,000
ギヤ-板	NG350-50	1 PC	¥9,000

*50 mL 専用共振棒 1 本入りセット。ギヤ-板は別売品。



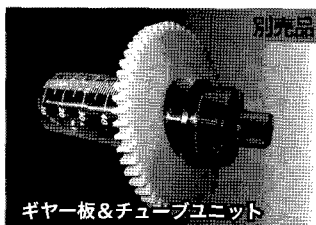
丸形超音波処理槽

丸形超音波処理槽の採用により分散の高効率化を実現。



冷却ファン

冷却ファン及び専用回路の採用により長時間運転が可能。



別売品

ギヤ-板 (品番：NG-350-50)、50 mL 専用共振棒 1 本入りセット (品番：MM-50WS)

ギヤ-板&チューブユニット

販売元

製造元



コスモ・バイオ株式会社

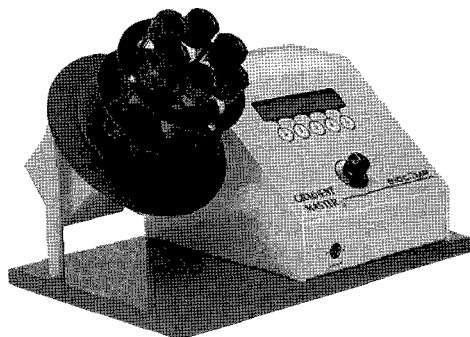


東湘電機株式会社

密度勾配遠心用装置

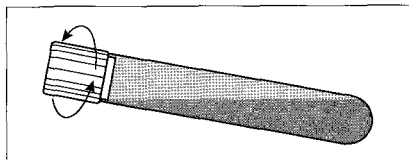
グラジェント・マスター

107-201M



■ 価格 ¥710,000(本体のみ)~

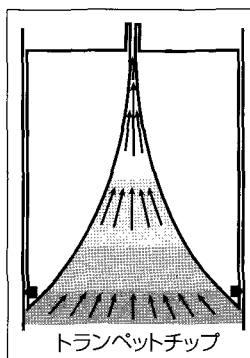
パテントである「Tilted tube rotation」の技法を使用して、短時間に、一度に6本の遠心チューブ内に、希望するグラジェントが作成できます。付属のマーカブロックを用いて、チューブの下半分に希望するSolutionのBottom%溶液を入れ、上半分にTop%溶液を入れ、あとはDisplayに従って、2~3回ボタンを押すだけ! 誰にでも容易に再現性の良いリニアグラジェントが作成できます。



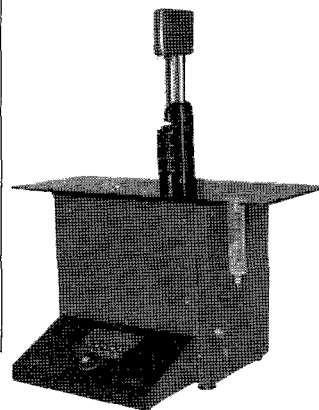
Tilted tube rotation

ピストン・グラジェント・フラクショネーター 152-001

パテントである「Trumpet Tip」を用い、チューブ内に形成されたバンド(目に見えても、見えなくても)を上から順番に、水平に、上下のグラジェントとコンタミ無く、分離回収することができます。またair、rinse機構により、非常に狭い巾のバンド(通常は0.3mm巾以上も回収可能です。カーボンナノチューブの分離、精製には最適です。(Arnold et al, 2006, Nature Nanotechnology, 1:60)



トランベットチップ

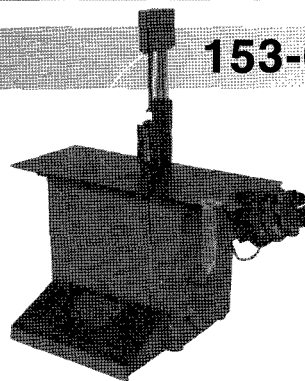


■ 価格 ¥1,960,000(本体のみ)~

グラジェント・ステーション

153-001

グラジェント・マスターとピストン・グラジェント・フラクショネーターを一体化した省スペースタイプです。



■ 価格 ¥2,600,000(本体のみ)~

● 詳細については下記にお問合せ下さい。



日本総代理店

エスケーバイオ・インターナショナル株式会社

〒113-0033 東京都文京区本郷3-41-9

TEL 03-5689-9888 FAX 03-5689-9890

E-mail: info@skbio.co.jp

超遠心機による単層CNTの分離(2)

※CNT:Carbon Nano Tubes

CNTは炭素でできた円筒状の物質で、電極あるいは半導体材料などで驚異の新素材として注目を集めています。また、単層CNTには構造の違いにより金属としての性質を持つCNTと半導体としての性質を持つCNTが存在します。そして、その分離を超遠心機による密度勾配遠心法により行うことができます。

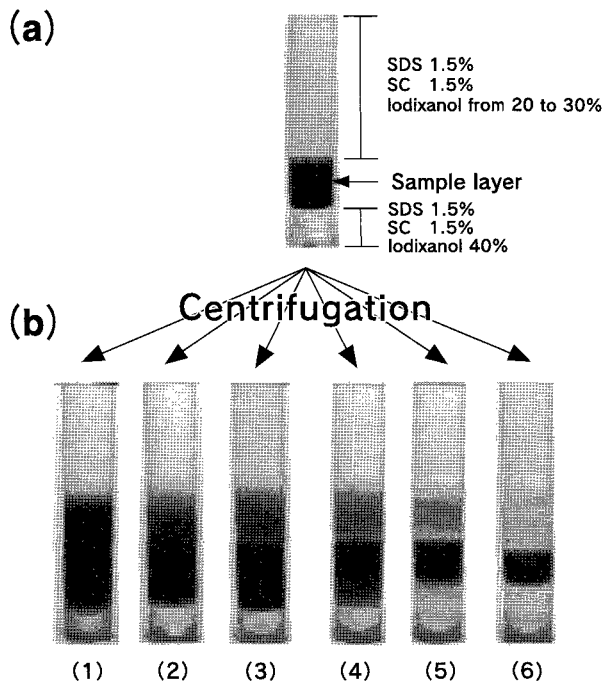


Fig.1. Pictures of centrifuge tubes (a) before and (b) after centrifugations in LV nanotubes. The concentration of iodixanol in a sample layer was 30%. The concentrations of surfactants in the centrifuge tube (except the sample layer) were set to be SDS 1.5%, SC 1.5%. Those concentrations in the sample layer were (1) SDS 1.5%, SC 1.5%, (2) DOC 0.25%, SDS 1.5%, SC 1.5%, (3) DOC 0.5%, SDS 1.5%, SC 1.5%, (4) DOC 0.5%, SDS 1.0%, SC 1.0%, (5) DOC 0.5%, SDS 0.5%, SC 0.5%, and (6) DOC 0.5%

本結果は試料に含まれる界面活性剤の組成により金属性CNTの分離状況が変化することを示しています。(詳細は下記の参考文献を参照ください。)

(参考文献)

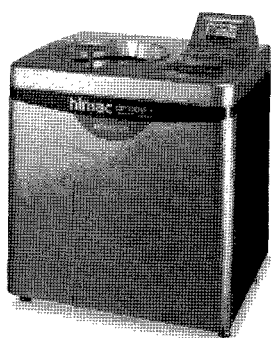
Yanagi, K.; Miyata, Y.; Kataura, H. Appl. Phys. Express **2008**, *1*, 034003-034005.
Yanagi, K.; Iitsuka, T.; Fujii, S.; Kataura, H. J. Phys. Chem. C **2008**, *112*, 18889-18894.

単層CNT分離システム

(システム構成)

・日立工機(株)製

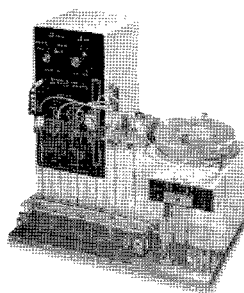
- (1) CP100WX形分離用超遠心機
- (2) P40ST形シングロータ
- (3) DGF-U形密度勾配フラクシヨネータ



CP100WX



P40ST



DGF-U

この分離を日立工機(株)製分離用超遠心機CP-WXシリーズにて行うことができます。

また、遠心後の試料の分画にはDGF-U形密度勾配フラクシヨネータを使用すると便利です。

皆様のご研究にお役立てください。

遠心分離条件の例

- ・使用ロータ: P40ST (文献と同等のシングロータ)
- ・回転速度: 40,000rpm (284,000 xg (max.))
- ・遠心管: 13PAチューブ
- ・時間: 約18時間
- ・密度勾配液: Iodixanol

【製造・販売・保守】

日立工機株式会社

URL <http://www.hitachi-koki.co.jp/himac/>

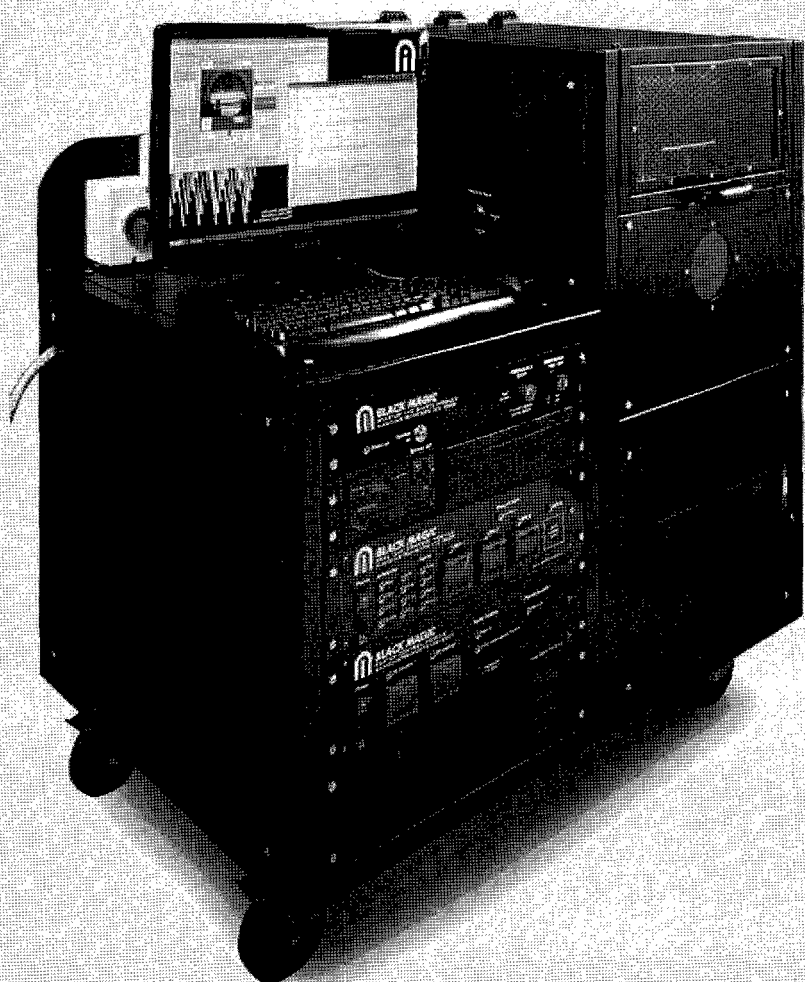
日立遠心機お客様相談センター

0120-024125

受付時間 9:00~12:00 / 13:00~17:00 (土・日・祝日・弊社休業日除く)

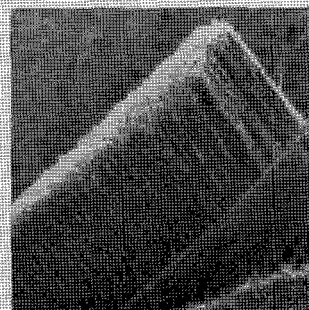
CVDのリーディングカンパニー
アイクストロン社の
CNT成膜装置

- 小片から300mmウェハまで
- CVDとPECVDの2モード

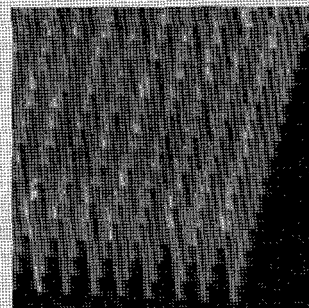


AIXTRON

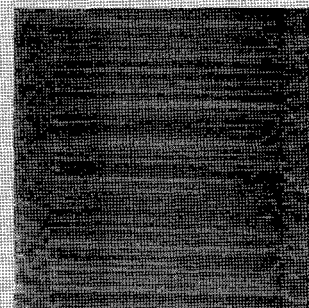
Your results -



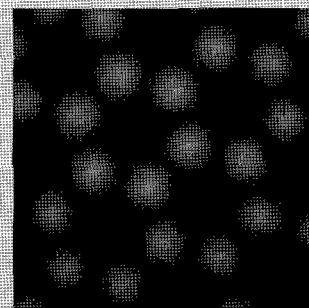
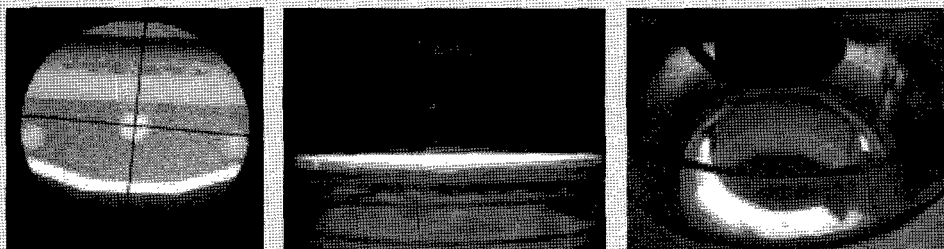
Dense CNT



Vertical CNT



Horizontal SWCNT



Graphene

アイクストロン株式会社
〒140-0001 東京都品川区北品川1-8-11ダヴィンチ品川II 9F
TEL: 03-5781-0931 FAX: 03-5781-0940 <http://www.aixtron.com>

科学分析のご相談・ご依頼は UBE科学分析センターへ!

まずは、ホームページへ、どうぞ
<http://www.ube-ind.co.jp/usal>

検索サイトにて

UBE科学

検索

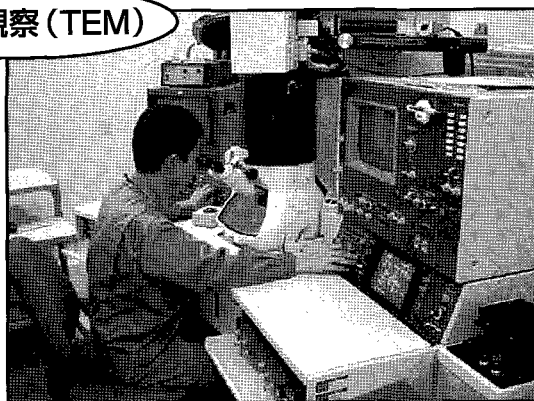


迅速に・精緻に・確実に

分析業務

- ☆組成分析と構造解析
- ☆形態観察と物性評価
- ☆表面・局所の超微小分析
- ☆超微量分析
- ☆安全性試験

形態観察 (TEM)



ご相談窓口	電話番号	FAX番号
東日本・関東地区	東京営業部 03-5419-6333	03-5419-6334
	千葉営業所 0436-23-5155	0436-23-5449
関西地区	大阪営業部 06-6346-2853	06-6346-1763
西日本地区	西部営業部 0836-31-6568	0836-31-6601

ユービーイー

株式会社UBE科学分析センター

<http://www.ube-ind.co.jp/usal>

— フロンティア出版のナノテクノロジー・ナノマテリアルシリーズ —

自己組織化ナノマテリアル

— フロントランナー85人が語るナノテクノロジーの新潮流 —

企画：理化学研究所 フロンティア研究システム
時空間機能材料研究グループ
監修：国武豊喜(北九州市立大学/理化学研究所)
編集幹事：下村政嗣(北海道大学/理化学研究所)
山口智彦(産業技術総合研究所)
■体裁/B5判・392頁 ■価格/57,750円(税込)

有機・無機・金属ナノチューブ

— 非カーボンナノチューブ系の最新技術と応用展開 —

編集：清水敏美(産業技術総合研究所)
木島 剛(宮崎大学)
■体裁/B5判・330頁 ■価格/57,750円(税込)

ナノ粒子の創製と応用展開

編集：米澤 徹(東京大学)
■体裁/B5判・322頁 ■価格/57,750円(税込)

ナノコンポジットマテリアル

— 金属・セラミック・ポリマー3大物質のナノコンポジット —

編集：井上明久(東北大学)
■体裁/B5判・363頁 ■価格/52,500円(税込)

ナノオプティクス・ナノフォトニクスのすべて

— ナノ光技術の基礎から実用まで —

監修：河田 聡(大阪大学/理化学研究所)
編集：梅田倫弘(東京農工大学)
川田善正(静岡大学)
羽根一博(東北大学)
■体裁/B5判・352頁 ■価格/57,750円(税込)

MEMS/NEMSの最先端技術と応用展開

編集：前田龍太郎(産業技術総合研究所)
澤田廉士(九州大学)
青柳桂一(マイクロマシンセンター)
■体裁/B5判・285頁 ■価格/52,500円(税込)

ナノインプリントの最新技術と装置・材料・応用

— ナノインプリント技術の最先端と拓がる用途 —

編集：平井義彦(大阪府立大学)
■体裁/B5判・330頁 ■価格/57,750円(税込)

ナノバイオエンジニアリングマテリアル

— バイオインターフェイス・ナノバイオプロセッシング

・バイオコンジュゲーション・バイオマトリックス —

監修：石原一彦(東京大学)
■体裁/B5判・350頁 ■価格/52,500円(税込)



フロンティア出版

〒110-0012 東京都台東区竜泉1-21-18 TEL:03-6802-1640 FAX:03-6802-1641 E-mail: info@frontier-books.com

<http://www.frontier-books.com>

溶液中の粒子のナノレベル微細化・分散に

BRANSON 超音波ホモジナイザー

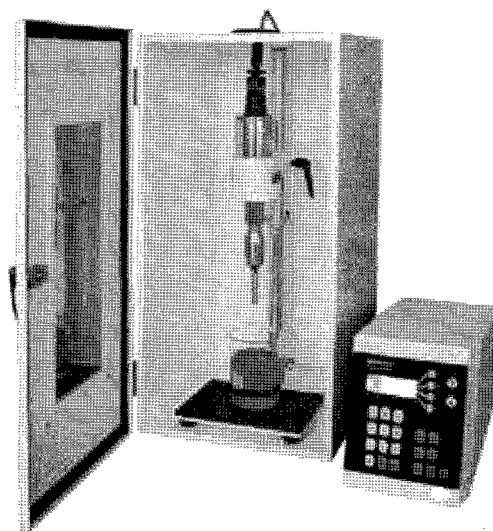
ホーン先端部の振幅の安定性を、より高めた Advance タイプ になりました。

近年のナノテクノロジーの発展及び粉体関連技術の向上により、より微細な粒子に対する乳化分散処理の要望が増えてまいりました。

超音波ホモジナイザーを使用し、均質な乳化分散処理を行い、安定させることにより製品の機能は向上します。

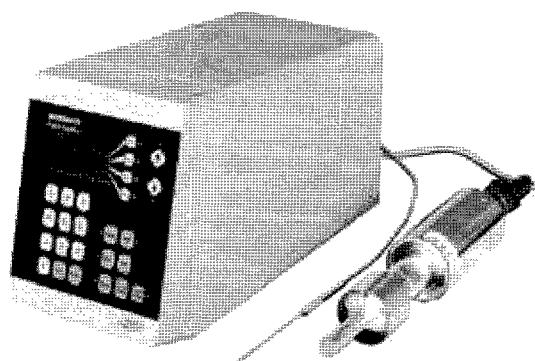
ブランソン社では 20kHz 機と、40kHz 機の 2 タイプを用意しております。

1 次粒子の凝集力にも拠りますが、20kHz 機では 100nm 程度までの分散力があります。40kHz 機は、さらに細かいレベルで分散ができる可能性があります。



20KHz 超音波ホモジナイザー
BRANSON SONIFIER シリーズ

高周波 40KHz 超音波ホモジナイザー
BRANSON SLPe シリーズ



ブランソン社の製品は、ホーン先端部の振幅の安定性が高く、強力なキャビテーションが得られ、効率良く、再現性の高い分散処理が行えます。

主なアプリケーション

分散

カーボンナノチューブ 有機顔料 無機顔料 セラミック セメント 感光体 記録材料
磁性粉 粉末冶金 酸化鉄 金属酸化物 シリカ アルミナ カーボンブラック
ポリマー ラテックス 製紙 ファンデーション
研磨剤 電池 フィラー 光触媒 触媒 ワクチン 体外診断薬 歯磨き粉 シャンプー
半導体 電子基盤 液晶 貴金属 金属 宝石 タイヤ 発酵菌類 その他

乳化

エマルジョン製剤 農薬 トナー ラテックス 界面活性剤 クリーム 乳液 クリーム 等

株式会社 **セントラル** 科学貿易

本社：111-0052 東京都台東区柳橋 1-8-1
Tel 03-5820-1500 Fax 03-5820-1515
URL <http://www.cscjp.co.jp/>

大阪支店：Tel 06-6325-3171 Fax 06-6325-5180
福岡営業所：Tel 092-482-4000 Fax 092-482-3797
札幌出張所：Tel 011-764-3611 Fax 011-764-3612

進化する売れ筋ナノテク材料

弊社取扱いナノテク材料群

フラーレン材料群

【60】【70】【84】PCBMフラーレン

bis【60】PCBMフラーレン

高次フラーレン(C76,C78,C84)

水溶性フラーレン

C60(OH)6, C60(OH)22-26, C60(OH)24,

C60(OH)18-22(O-K+)4フラーノール

アミノ酪酸フラーレン誘導体

アミノカブロン酸フラーレン

ビスマロン酸エチルフラーレン

C13安定同位体置換フラーレン

Gd@C82金属内包フラーレン

La@C82金属内包フラーレン

Ce@C82金属内包フラーレン

Sc3N@C80内包フラーレン

Anti-HIVフラーレン

C60F36, C60F48, C60Br24フラーレン

カーボンナノチューブ

高純度多層カーボンナノチューブ

高純度単層カーボンナノチューブ

水溶性ナノチューブ

SWNT-COOH, SWNT-NH₂, SWNT-PEG, SWNT-SH

MWNT-COOH, MWNT-NH₂, MWNT-PEG, MWNT-SH

大口径カーボンナノチューブ

2層構造カーボンナノチューブ

カーボンナノチューブ・フィルム【Cu, Si, Ni, Graphite】

カーボンナノチューブ・カソード【Cu, Si】

金ナノ微粒子

金ナノ微粒子, 0.01%金, 2~50nm

Dextranコート, 0.01%金, 10~50nm

PEGコート, 0.01%金, 10~50nm

Biotinラベル, 0.01%金, 5~50nm

Streptavidinラベル, 0.01%金, 5~50nm

その他銀ナノ微粒子

希少価値金属(レアメタル)

ニッケル, コバルト, フェロクロム, フェロマンガニウム, フェロバナジウム, 亜鉛, チタン, スズ, アンチモン, タングステン

電気製造精密メッシュ

金, 銅, ニッケル, 透過率(36~98%), 標準サイズ279×279mm

ナノ微粒子群

1. 元素材料

Ag, Al, Au, Bi, B, C, Co, Cr, Cu, Fe, In,
Mo, Ni, Pd, Pt, Si, Ti, W, Zn

2. 非酸化物ナノ化合物

AlN, B₄C, BN, GaP, InP, LaB₆, MoS₂, Si₃N₄,
TaN, TiC, TiC_{1-x}N_x, TiN, WC, WC/Co, YbF₃

3. 酸化物

Al₂O₃, Al(OH)₃, B₂O₃, BaCO₃, BaSO₄, BaTiO₃, CeO₂, CoFe₂O₄, Co_{0.5}Zn_{0.5}Fe₂O₄, CoO, Co₃O₄, CrO₃,
CsH₂PO₄, CuO, Dy₂O₃, Er₂O₃, Eu₂O₃, Fe₂O₃, Fe₃O₄, Gd₂O₃, HfO₂, In₂O₃, In(OH)₃:SnO₂, La₂O₃,
Li₄Ti₅O₁₂, MgAl₂O₄, MgO, Mg(OH)₂, Mn₂O₃, MoO₃, Nd₂O₃, NiFe₂O₄, Ni_{0.5}Zn_{0.5}Fe₂O₄, NiO, Ni₂O₃,
Pr₆O₁₁, Sb₂O₃, SiO₂, Sm₂O₃, SnO₂, SrAl₁₂O₁₉, SrCO₃, SrFe₁₂O₁₉, Tb₄O₇, TiO₂, VO, V₂O₃, V₂O₅,
WO₃, YAG, YAG/Ce, YAG/Nd, Y₂O₃, ZnFe₂O₄, ZnO, ZrO₂, ZrO₂/Y₂O₃, ZrO₂/CaO, ZrO₂/CeO₂



株式会社 ATR

Advanced Technology Research

〒270-0021 千葉県松戸市小金原 7-10-25

TEL : 047-394-2112 FAX : 047-394-2100

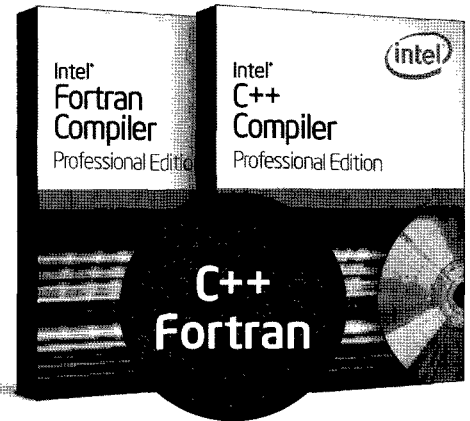
Mail : sales@atr-atr.co.jp Web : atr-atr.co.jp

インテル® コンパイラー 11.0

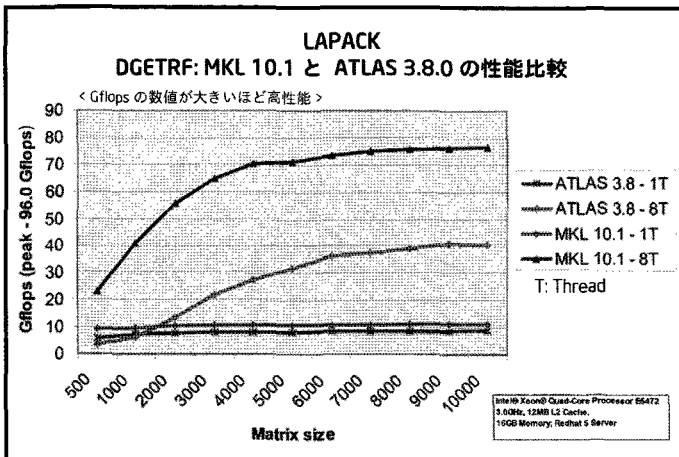
日本語版 新発売

インテル® コンパイラーは、シミュレーション解析用プログラム等を高速化することで研究の効率化を支援します。

- ✓ インテル® Core™ i7 プロセッサに対応
- ✓ OpenMP* 3.0 対応、自動ベクトル化 / 並列化機能
- ✓ BLAS/LAPACK を高速化し、さらに強化したインテル® MKL ライブラリー をバンドル



Windows*/Linux*/Mac OS*



他にも以下の性能向上が確認されています。

- ・タッドコア インテル® Xeon® プロセッサ 5300 番台で (Z.OGEMM が最大 50% 向上 (32 ビット))
- ・インテル® Core® i7 プロセッサで SGEMM が 50% 向上 (64 ビット)

- サイエンス・テクノロジー分野の研究、開発に最適!
- 研究機関、企業での実績多数!

お客様の声

「私の研究では 10 万円程度の連立 1 次方程式を数万回繰り返し解く作業に帰着させます。インテルのコンパイラーを用いれば、gcc に比べて格段に実行時間が減らせますので、大変役に立っています。」

国立大学 工学部 情報工学科 殿

画像パターンマッチング処理にてインテル® コンパイラーを使用した場合、評価アルゴリズムの速度が約 30% 向上しました。

大手 宇宙情報システム開発会社 殿

製品の詳細に関するお問い合わせ先

XLSOFT エクセルソフト 株式会社

www.xlssoft.com/intel/
Tel: 03-5440-7875

11.0 ベンチマークを公開!
圧倒的なスピードをご確認ください。

ご購入に関するお問い合わせ先

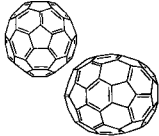
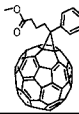
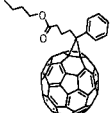
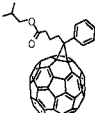
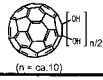
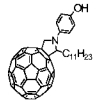
HPC システムズ株式会社
www.hpc.co.jp
TEL: 03-3599-3652

株式会社 HPC ソリューションズ
www.hpc-sol.co.jp
TEL: 03-5640-7858

HPC テクノロジーズ株式会社
www.hpc-technologies.co.jp
TEL: 03-6410-6070

住商情報システム株式会社
www.clubscs.com
TEL: 03-5859-3011

こちらからもご購入いただけます。 www.xlssoft.com/intel/purchase

銘柄		分子構造	純度(HPLC面積%、代表値)	取扱数量
nanom purple フラーレンC60	ST		99	10g以上
	TL		99.5	5g以上
	SU		99.5/昇華精製品	2g以上
	SUH		99.9/昇華精製品	1g以上
nanom orange フラーレンC70	ST		97	1g以上
	SU		98/昇華精製品	0.5g以上
nanom mix 混合フラーレン	ST		C60、C70、その他高次フラーレンの混合物 ST-FはSTの微粒化品	50g以上
銘柄		分子構造	純度(HPLC面積%、代表値)	取扱数量
nanom spectra E100 PCBM (phenyl C61-butyl acid methyl ester)			99	1g以上
nanom spectra E200 PCBNB (phenyl C61-butyl acid n-butyl ester)			99	1g以上
nanom spectra E210 PCBIB (phenyl C61-butyl acid i-butyl ester)			99	1g以上
nanom spectra E110 C70PCBM (phenyl C71-butyl acid methyl ester)		 主成分	99 (異性体トータル) 位置異性体の混合物	0.5g以上
銘柄		分子構造	内容	取扱数量
nanom spectra D100 水酸化フラーレン		 (n = ca. 10)	C ₆₀ OH _n n=10を主成分とする混合物	2g以上
nanom spectra A100 水素化フラーレン		 (n = ca. 30)	C ₆₀ H _n n=30を主成分とする混合物	2g以上
nanom spectra G100			純度(HPLC面積%、代表値) 99	1g以上

2008年11月1日現在

銘柄、取扱数量等は予告無く変更する場合がございます。予めご了承下さい。

当社製品は、下記2社から購入いただけます。詳細は直接お問い合わせください。

- ・関東化学株式会社 試薬事業本部
〒103-0023 東京都中央区日本橋本町3-11-5 TEL:03-3663-7631 FAX:03-3667-8277
<http://www.kanto.co.jp> E-mail:reag-info@gms.kanto.co.jp
- ・第一実業株式会社 新事業推進室【担当: 鎰広(カギヒロ)】
〒102-0084 東京都千代田区二番町11-19 TEL:03-5214-8579 FAX:03-5214-8501

<本資料に関するお問い合わせ先>
フロンティアカーボン株式会社 営業販売センター【担当: 梶原】
〒806-0004 福岡県北九州市八幡西区黒崎城石1-1 (移転いたしました)
TEL:093-643-4400 FAX:093-643-4401 <http://www.f-carbon.com>
※弊社へのお問い合わせはHPよりお願いいたします。

